I. Mokhun, Yu. Viktorovska, Yu. Galushko

OPTICAL APPROACHES IN INFORMATION TECHNOLOGY

ВСТУП

One of the main problems of modern information devices is the increase in the speed of calculations, information processing, and the speed of its transmission. In this direction, great progress has certainly been made, which is primarily associated with the improvement of electronic components of such systems. At the same time, as you know, there are fundamental physical limitations to the characteristics of electronic components, which set certain limits in weight, size, performance, the number of parallel transmission channels, etc.

In addition, the main focus in the development of information systems is aimed at the use of classic digital processors, the action of which is based on the so-called von Neiman architecture, which in one form or another involves a sequence of elementary operations. Naturally, modern computers have both a high speed of information processing (for example, when using multi-core processors), and ultra-high accuracy of calculating the final result (for example, 32 decimal places).

At the same time, despite such impressive characteristics of use, computers have an auxiliary character aimed at performing calculations (unloading the human brain), which have little to do with final fundamental decisions.

As you know, the principles of the human brain are built on completely different algorithms, namely the algorithms of the so-called neural networks (NM), which are generally not digital, but analog computers. Elements of such systems are indiscriminating associative storage devices. The final system response is probabilisive.

Naturally, recently neural network technologies with the use of traditional computers have been paid a lot of attention. In this direction, the attempt to apply a large number of parallel processors faces the same fundamental physical limitations of electronic systems, which ultimately limits the number of neurons in NM, the number of images stored, etc. Such restrictions play a fundamental role in the creation of artificial intelligence systems, the effective work of which is associated with the number of acts of "training" of NM, which directly depends on the number of neurons.

It is this situation that encourages the search for new ways of implementing NM, for example, the use of optical technologies. After all, the use of optics makes it possible to form neural networks with the number of neurons, which is 3-4 orders of order more than in electronic analogues. At the same time, the speed of information processing in NM is limited only by the speed of light propagation.

That is why, in our opinion, the prospects for the development of optical NM (even in the distant future) do not cause any doubts.

It should be noted that the development of relevant optical analog computers is not limited to neural networks. Such computers can be effectively used in solving highly specialized tasks, for example, when analyzing the spectra of signals, the characteristics of which are rigidly set, the recognition of a certain class of images for which certain restrictions are performed, for example, by scale, angle, image

class, etc. The use of such specialized processors for a certain class of tasks can lead to a significant reduction in time costs, the cost of manufacturing devices, etc.

Finally, the use of optical technologies in modern communication has virtually no alternative.

It is in modern systems and networks of telecommunications that fiber optic transmission lines (VOLP) and fiber optic transmission systems (WOSP) have found the widest application. On their basis, both main lines are laid and communication systems are built, as well as lines and local communication systems. Fiber optic transmission lines are increasingly a dream for the formation of local computing networks, etc. It should be noted that today in Ukraine most of the main communication lines have already been built on the basis of fiber optic communication lines (FIS). Fiber cable gradually begins to replace the old copper and for inter-station joints in regional centers and large cities of our country.

The natural question arises, why exactly did THE FIPS, which are built on the basis of glass fibers, find such wide distribution in different areas of telecommunication networks?

A simple and short answer to such a question may be as follows. Glass, which is an optically transparent medium, is the most promising medium for transmitting information signal. To date, systems have already been created and implemented in the production of SSOs with a transmission speed of up to 40 Gbps.

All of the above directly affects the questions and their scope set forth in the manual.

In the manual, yay is not a specialized monograph, but only reveals to the reader certain directions of application of optical technologies, which are more fully and detailed in other sources.

The purpose of the manual is to try to interest the student in the relevant optical directions and to provide the basic knowledge and concepts necessary when familiar with the issues of the use of optical technologies in information technology.

The basis of this manual is an attempt to simply and clearly lay out the physical and theoretical basics of optical technologies in information technology. It should be noted that when presenting theoretical material, the manual was overloaded with deep and detailed mathematical presentations. For example, the physical processes in the wave drive are considered in detail only for a flat wave, since the main regularities are preserved for cylindrical fibers.

Physicists of the active elements of integral optics are also presented very briefly, given that individual elements are considered in detail in other professional sources.

The issues of fiber optic lines and components of fiber optic transmission systems are presented in the most detail. Additionally, the emphasis is placed on the practical aspects of the use of SSROs, the regulation of their characteristics, which is based on the relevant RECOMMENDATIONS of ITU-T.

The manual contains general issues of optical field formation, spatial (optical) implementation of Fourier transformation, correlation, convolution, since it is optical systems (and integral-optical as well) that make it possible to perform them relatively simply and build analog processors in which such operations are basic. The methods of signal processing that can be implemented in the planar version are

considered.

A significant part of the manual is occupied by the principles of operation of systems with open atmospheric communication channels, which, in our opinion, have wide prospects for application in the future.

1. OPTICAL SIGNAL AND ITS DISTRIBUTION

1.1. Basic equations

Electromagnetic wave (EMW) can be uniquely described by establishing the dependence of electrical and magnetic field vectors in space and time.

1.1.1. Maxwell equation

According to [1-3], Maxwell equations have the form of:

$$rot\vec{H} - \frac{1}{c}\frac{\partial \vec{D}}{\partial t} = \frac{4\pi}{c}\vec{j}; \qquad (1.1.)$$

$$rot\vec{E} - \frac{1}{c}\frac{\partial \vec{B}}{\partial t} = 0; \qquad (1.2)$$

$$div\vec{D} = 4\pi\rho ; \qquad (1.3)$$

$$div\vec{B} = 0 \quad , \qquad (1.4)$$

where $\vec{E}, \vec{H}$ – *vectors of electrical and magnetic intensity of electromagnetic field;* $\vec{D}, \vec{B}$ – *vectors of electrical and magnetic induction;* $\vec{j}$ – *electric current density;* ρ – *electric charge density.*

In a free space $\vec{j}, \rho$=0. $\vec{D}, \vec{B}$ – take into account the impact of the environment.

1.1.2. Material equations

If $\vec{j}$= 0, then there are only two such equations:

$$\begin{cases} \varepsilon\vec{E} = \vec{D} \\ \mu\vec{H} = \vec{B} \end{cases}, \qquad (1.5)$$

де ε, μ – dielectric and magnetic permeability, respectively.

1.1.3. Wave equation

From equations (1.1-1.4) follows:

$$\nabla^2\vec{E} - \frac{\varepsilon\mu}{c^2}\frac{\partial^2\vec{E}}{\partial^2 t} = 0, \qquad (1.6)$$

$$\nabla^2\vec{H} - \frac{\varepsilon\mu}{c^2}\frac{\partial^2\vec{H}}{\partial^2 t} = 0. \qquad (1.7)$$

Wave propagation speed, respectively $v = \frac{c}{\sqrt{\varepsilon\mu}}$.

It is known [1-3] that one of the main optical characteristics of any medium is the refractive index, which is associated with dielectric and magnetic permeability:

$$\sqrt{\varepsilon\mu} = n. \qquad (1.8)$$

And since for a transparent environment (it is mainly paramagnetics) $\mu \approx 1$, то $\sqrt{\varepsilon} = n$.

Як наслідок,

$$\nabla^2\vec{E} - \frac{1}{v^2}\frac{\partial^2\vec{E}}{\partial^2 t} = 0. \qquad (1.9)$$

Accordingly, for vacuum

$$\nabla^2\vec{E} - \frac{1}{c^2}\frac{\partial^2\vec{E}}{\partial^2 t} = 0. \qquad (1.10)$$

Add that in a homogeneous environment in an area that is free of currents and charges, equality (1.9, 1.10) is performed for each Cartesian component of the electromagnetic field $\vec{E}$.

Consider some scalar field. If the field is homogeneously polarized, then this approximation is fair. At the same time, we will assume that the paraxial approximation is performed. Then the tension of the electric field can be recorded in the form of:

$$E(\vec{r},t) = A(\vec{r})\cos[\omega t + \varphi(\vec{r}) + kz]. \tag{1.11}$$

where $\omega = 2\pi\nu$ – circular frequency; ν – oscillation frequency; $\varphi(\vec{r})$ – spatial phase that determines the shape of the front wave; $A(\vec{r}) > 0$ – field amplitude module; $k = \frac{2\pi}{\lambda} = \frac{\omega}{c}$ – wave number; λ – wavelength of radiation.

Although there are no physically substantiated objections to equality to the amplitude module at some point in space, we will consider it strictly more than zero. But the case of the zero amplitude module is interesting and corresponds to the whole class of special waves, the so-called waves with the singular phase, or optical vortices [1-4]. Surfaces for which the condition is met $\varphi(\vec{r}) = const$, are called the surface of a flat phase, or wave surfaces, or the front of the wave.

Equality (1.11) can be rewritten as:

$$E(\vec{r},t) = Re[U(\vec{r})\exp(\omega t + kz)], \tag{1.12}$$

where $U(\vec{r}) = A(\vec{r})\exp[j\varphi(\vec{r})]$ – complex field amplitude.

It can be shown that for a complex amplitude of a field that actually exists, equality is performed (Laplace equation):

$$\nabla^2 U + n^2 k^2 U = 0. \tag{1.13}$$

Or for vacuum

$$\nabla^2 U + k^2 U = 0. \tag{1.14}$$

The equation (1.13, 1.14), as well as the equation (1.9, 1.10), is also sometimes called wave equations.

1.2. Change of wave phase when it spreads
1.2.1. Phase latency

Consider some wave of general appearance falling on the porch (see Figure 1.1). Determine what phase difference occurs when the wave spreads further to the plane x_1 from dots 1_0 and 2_0. Move the rays from these points to the points 1_1 and 2_1 plane x_1 shown curved l_1 and l_2 respectively. In general, the fracture factor of the medium in which the wave spreads is a function of three coordinates.
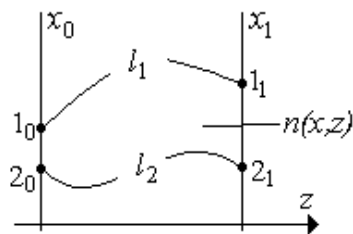
Fig. 1.1

Then the phase raid along the distribution tractory is described by the expression:

$$\Phi_m = k \int_{m_0}^{m_1} n(l_s)dl, \tag{1.15}$$

where $m=0,1$, $s=1,2$.

In case, when $n=const$ (1.15) transform to form:

$$\Phi_m = knl_s = kl_{s\,\text{опт}}, \tag{1.16}$$

where $l_{s\,\text{опт}} = nl_s$ – so-called optical length.

1.2.2. Phase latency caused by a thin optical element

The optimum element is thin (Fig. 1.2), when passing through the element is possible to neglectby shifting the beam from the point (4) to the point (3), that is, the value of such displacement goes to zero. Here and further for simplicity we will consider a one-dimensional case. Then the phase latency entered by such an element can be calculated by the following expression:

$$\Phi(x_0) = k(n_0 l_{12} + n l_{24}) \qquad (1.17)$$

Fig. 1.2

In general, a thin element in addition to the phase also modulos the amplitude and can be described using a complex pass rate:

$$H(x_0) = A(x_0)\exp[j\Phi(x_0)] . \qquad (1.18)$$

Then the field is directly behind the item $U_{(+)}$ described by the expression:

$$U_{(+)} = U_{(-)}H(x_0). \qquad (1.19)$$
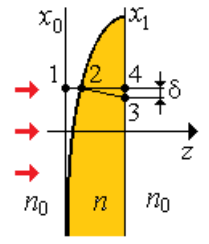
1.2.3. Phase latency caused by thin collecting lens
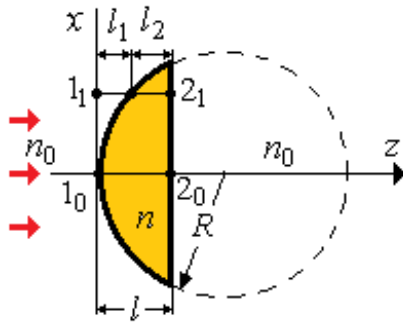
To determine the phase delay caused by the lens (see Figure 1.3), it is enough to calculate the difference in the phases that the wave acquires along the segment $1_0 2_0$ (lens center) and any segment $1_1 2_1$ [5,6].

The phase that the wave acquires along the segment $1_0 2_0$, is equal:

$$\Phi_0 = knl. \qquad (1.20)$$

Рис. 1.3

The phase that the wave acquires along the section of the track $1_1 2_1$, is equal:

$$\Phi_1 = k(n_0 l_1 + n l_2) = k\{n_0 z(x_{1_1}) + n[l - z(x_{1_1})]\}. \qquad (1.21)$$

Function can be obtained from the equation of the circle $z(x)$ $x^2 + (z - R)^2 = R^2$. One of the solutions to this equation is:

$$z = R - \sqrt{R^2 - x^2} \approx \frac{x^2}{2R}. \qquad (1.22)$$

Accordingly, the phase difference is described by the expression:

$$\Delta\Phi = \Phi_1 - \Phi_0 = \frac{kn_0}{2f}, \qquad (1.23)$$

де $f = \dfrac{R}{n/(n_0 - 1)}$ – focal length of the lens.

Thus, due to the fact that the thin collecting lens does not modulo wave amplitudes, it can be considered as a transmission:

$$L(x) = \exp(-j\frac{kn_0}{2f}x^2). \qquad (1.24)$$

1.2.4. Special (singully) wave structures

Let us turn to the expression (1.11). As we can see from the expression, the strict requirement to be met is the requirement that the wave amplitude module $A(\vec{r})$ must be strictly more than zero. At the same time, if at some point in the field this value acquires a zero value, then the wave for which it is performed satisfies the Maxwell equation (1.1-1.4), the wave equation (1.6), etc. In other words, nothing denies the existence of such a wave. Complex amplitude of such a wave U satisfies the Laplace

equation (1.13,1.14).

Recall that the solution of this equation is any analytical function, the simplest of them:

$$U = x \pm jy, \tag{1.25}$$

which exactly equals zero at a point $x, y = 0$.

If (1.25) write down in traditional form:

$$U = \rho e^{\pm j\Phi}, \tag{1.26}$$

where $\rho = \sqrt{x^2 + y^2}$ – amplitude module and $\pm\Phi = \pm arctan\frac{y}{x}$ – phase component, which is determined by spatial coordinates. As follows from (1.26), the amplitude module of such a wave really goes to 0, and the phase is not defined provided that the $x, y \to 0$. In other words, at the point of $x = 0, y = 0$ there is singulity of the phase. This wave structure was called the dislocation of the wave front or optical vortices [3;7].

It is worth noting that such light beams, due to the properties of our space, have increased stability (comparable to ordinary beams, for example, Gaussic) to physical perturbations of various types, which can be used in communication systems with an atmospheric communication channel. The application of such wave structures in the information technology will be discussed below (see section 20).

2. CONCEPT OF INTEGRATED TRANSFORMATION, SIGNAL SPECTRA ANALYSIS AND SIGNAL FILTRATION [5,6,8-11]

2.1. Receiving signal images. Purpose. Spectrum analysis

In mathematics, many types of function transformations are known, which in most cases are reduced to obtaining certain integrals that depend on one or more parameters. From a practical point of view, the signal is put in line with some function, which depends on the time or spatial coordinates. As a result of the conversion, we get an image of the signal, which in most cases is called the signal spectrum. The question arises, why do you want to perform a rather complex mathematical operation on the signal? What does she give? If the system that performs the conversion does not interfere and performs the conversion in full, then the amount of information in the signal and image is the same. It would seem that there is no point in such an operation, if not one however! The information present in the signal is provided in an image in another form, which may be more convenient for its analysis. Moreover, sometimes the so-called filtration can be applied to the image, an operation that significantly changes the original image and allows you to get rid of redundancy in the signal, get rid of interference, etc.

The most commonly used conversion in signal processing and analysis is the Fourier transformation.

2.1.1. Fourier Transformation

Before entering the definition of Fourier transformation, we note that in connection the signal value (voltage, current, etc.) is set, as a rule, as a function of time. In other words, we have amplitude-time signal representation.

Let's have four harmonic signals of the same amplitude, the frequencies of which are 10, 25, 50 and 100 Hz. Such a signal, as you know, can be recorded in the form of

$$x(t) = a\cos(\omega t + \varphi_0), \tag{2.1}$$

where a – signal amplitude; $\omega = 2\pi\vartheta$ – circular frequency; ϑ –"normal" frequency; $\varphi_0 = \omega t_0$ – initial signal phase, which is determined by the moment the signal transmission starts t_0.

Naturally, the signals of such a sufficiently simple structure are very easy to distinguish from each other. At the same time, the sum of such signals

$$x(t) = \cos(2\pi 10t) + \cos(2\pi 25t) + \cos(2\pi 50t) + \cos(2\pi 100t), \tag{2.2}$$

provided in Fig. 2. 2.1, much more complex and no longer subject to such simple analysis.
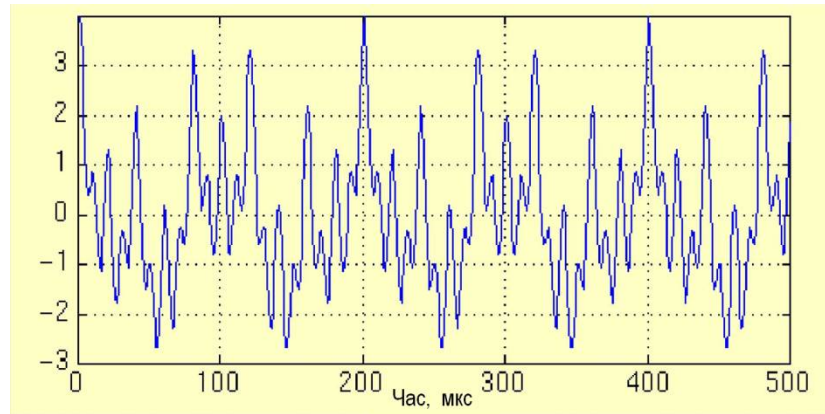
Fig. 2.1

We will introduce the definition of integral Fourier transformation. Under Fourier signal image $f(t)$ we will understand this expression:
$$\Im(\omega) = \frac{1}{2\pi} \int_{-\infty}^{\infty} f(t) \exp(-j\omega t)\, dt, \qquad (2.3)$$
де $\omega = 2\pi\vartheta$ – circular frequency, ϑ – normal frequency.

Fourier transformations will also be denoted by the following expressions:
$$f(t) \xrightarrow{\Im} \Im(\omega), \Im(\omega) = \Im\{f(t)\}. \qquad (2.4)$$

The Fourier transformation is inverse, meaning that fourier transformations can also be considered, which also binds the signal and its image:
$$f(x) = \int_{-\infty}^{\infty} \Im(\omega) \exp(j\omega t)\, d\omega, \qquad (2.5)$$

or
$$\Im(\omega) \xrightarrow{\Im^{-1}} f(t), f(t) = \Im^{-1}\{\Im(\omega)\}. \qquad (2.6)$$

Signal Fourier image is often referred to as the representation of the signal in the frequency plane, or simply the frequency representation of the signal.

Here are some examples (with precision to $1/2\pi$) Fourier image:

Table 2.1 Examples of Fourier image features

$f(t)$	$\Im(\omega)$
1	$\delta(\omega)$
$\delta(t)$	1
$\exp(j\omega_0 t)$	$\delta(\omega - \omega_0)$
$a + b\cos(\omega_0 t)$	$a\delta(\omega) + \dfrac{b}{2}\delta(\omega - \omega_0) + \dfrac{b}{2}\delta(\omega - \omega_0)$
$P_a(t)$	$a\,sinc\left(\dfrac{a\omega}{2\pi}\right)$

Here in the table
$$P_a(t) = \begin{cases} 1, & |t| \leq \frac{a}{2} \\ 0, & \text{в р. інт.} \end{cases}, \qquad (2.7)$$
$$sinc(t) = \frac{\sin \pi t}{\pi t}, \qquad (2.8)$$

$\delta(t)$ – delta function. Under this function we mean this value:

$$\delta(t) = \begin{cases} 1, & t = 0 \\ 0, & t \neq 0 \end{cases}, \qquad (2.9)$$

which is graphically displayed in Fig. 2.2.
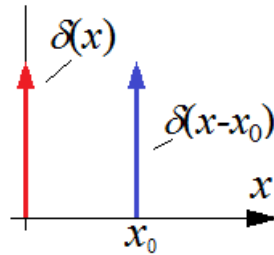
Fig.2.2

According to the table (the third row), Fourier image of the harmonious signal is graphically shown in Fig. 2.3.
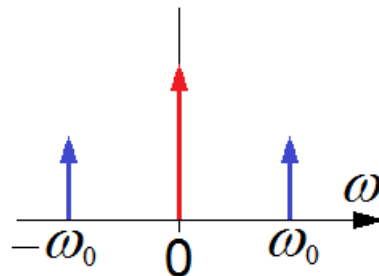
Fig.2.3

As we can see from the figure, Fourier's image of a harmonious signal, or, in other words, its frequency representation is characterized by the following:

1. In the Fourier image there are three sharp bursts:

1st at zero frequency corresponds to the constant component of the signal;

2nd and 3rd symmetrical bursts located at points $+$ and $-\omega_0$. At the same time $\omega_0 = 2\pi\vartheta_0$, that is, the localization of bursts is determined by the frequency of the harmonious signal.

2. Note that bursts in points $+$ and $-\omega_0$ absolutely identical. In general, it can be argued: *for valid signals, parts of the image that correspond to positive and negative frequencies are the same.*

That is why for real signals it is enough to consider (analyze) signal images only for positive ω.

2.1.2. Some Fourier properties
Here are some important Properties of Fourier Conversion:
1. *Fourier transformation linearity*

$$a_1 f_1 + a_2 f_2 + \ldots + a_n f_n \xrightarrow{\Im} a_1 \Im_1 + a_2 \Im_2 + \ldots + a_n \Im_n, \qquad (2.10)$$

де $\Im_n$ – Fourier images of functions f_n respectively; a_n – coefficients

For a signal in which f_n – harmonic components, such coefficients are real and positive and determine the value of the contribution of this component to the signal.

2. Offset theorem

$$\exp(j\omega a)\,\Im(\omega) = \frac{1}{2\pi}\int_{-\infty}^{\infty} f(t-a)\exp(-j\omega t)\,dt, \qquad (2.11)$$

where $\Im(\omega)$ – Fourier image of an unsaled signal; a – offset amount
or

$$f(t-a) \xrightarrow{\Im} \exp(j\omega a)\,\Im(\omega), \qquad (2.12)$$

that is, the Fourier image of the shifted function differs from the image of an exponential multiplier that is not moved to the exponential $\exp(j\omega a)$.

Note, if we consider the value of $M(\omega) = |\Im(\omega)|^2$, which in connection is called the signal spectrum, the following values for the shifted and unslated signal are exactly the same.

3. Scale theorem

$$\frac{1}{a}\Im\left(\frac{\omega}{a}\right) = \frac{1}{2\pi}\int_{-\infty}^{\infty} f(at)\exp(-j\omega t)\,dt, \qquad (2.13)$$

where $\Im(\omega)$ – Fourier image of an unsealed signal; a – zoom factor.

Another entry in this theorem is:

$$(at) \xrightarrow{\Im} \frac{1}{a}\Im\left(\frac{\omega}{a}\right), \qquad (2.14)$$

4. *Derivative of the signal expressed through its Fourier image:*

$$\frac{df(t)}{dt} = j\int_{-\infty}^{\infty} \omega\Im(\omega)\exp(j\omega t)\,d\omega. \qquad (2.15)$$

2.2. Convoluted. Signal Blur
Under the convoluted two functions $f_1(t)$ and $f_2(t)$ understand expression:

$$\psi(\tau) = f_1 \otimes f_2 = \int_{-\infty}^{\infty} f_1(t)\,f_2(\tau - t)dt. \qquad (2.16)$$

In Fourier-transformation theory, the so-called convoluted theorem is formulated, which has the form:

$$f_1 f_2 \xrightarrow{\Im} \Im_1 \otimes \Im_2$$
$$\Im_1 \otimes \Im_2 \xrightarrow{\Im^{-1}} f_1 f_2 \qquad (2.17)$$
$$f_1 \otimes f_2 \xrightarrow{\Im} \Im_1 \Im_2$$
$$\Im_1 \Im_2 \xrightarrow{\Im^{-1}} f_1 \otimes f_2$$

The essence of these ratios is as follows. For example, the first expression reads: Fourier image from the product of two functions is equal to the convoluted two Fourier images.

Here is another important aspect of:

$$f \otimes \delta = \int_{-\infty}^{\infty} f(t)\,\delta(\tau - t)dt = f(\tau). \qquad (2.18)$$

Recall the geometric content of the convolution of real functions. Its essence is

very easy to understand from the figures. 2.4. In fact, convoluting is the area of mutual overlapping of functions $f_1(t)$ and $f_2(t)$. In Fig. 2. 2.4, b shows a rectangular pulse convoluted width a.
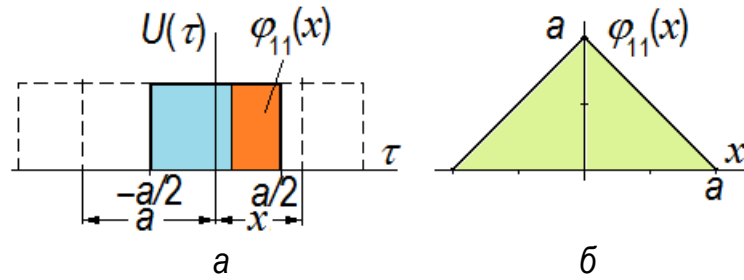
Fig. 2.4

As you can see, the width of the convoluted is twice the width of the pulse itself. This is a common consequence of.

This fact follows an equally important consequence. The smallest convolution structural element is larger than the width of the smallest element of the collapse function. In other words, the signal $f_1(t)$, minimized with some function $f_2(t)$(e.g. rectangular pulse width a), err and loses the fine structure. At the same time, the smallest element of the converted signal $f_1 \otimes f_2$ becomes no more small than the double width of the function $f_2(t)$.
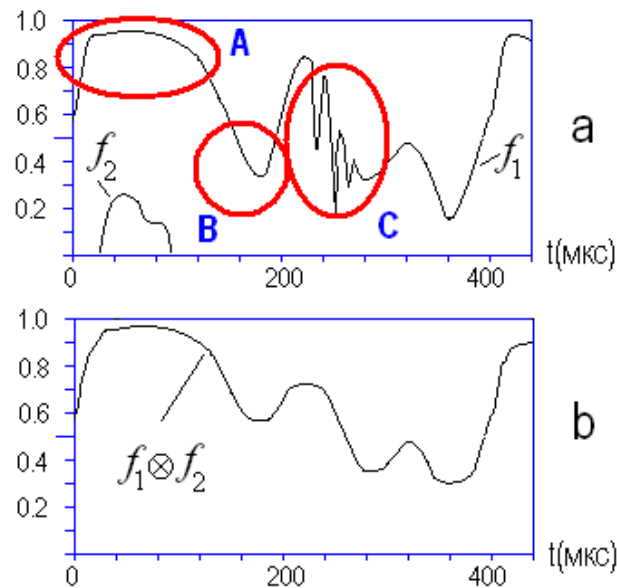
Fig. 2.5.

This fact is illustrated by Figure 2.5. As you can see, the fine structure of the signal disappears (C region of Figure A). Changes but maintains the structure of the function $f_1(t)$ in type B, where the transverse dimensions of the elements of the order of the width of the function $f_2(t)$ and only in the regions of type A, the structure of the converted signal remains almost the same as in the signal $f_1(t)$.

Note that only when the signal is minimized with an infinitely narrow function (δ- function) does not change the signal (see ratio 2.18)

Let's return to harmonious signals with different frequencies. At the same time, we will assume that they are the same amplitude and exist for a certain period of time Δt.

The spectra of such signals (positive frequencies only) are shown in Fig. 2. 2.6. Lower picture - zoomed in copy of the top picture. As you can see, each signal corresponds to a surge, the position of which is determined by its frequency. The width of the splash depends on the duration of the signal Δt. The more Δt, the heer width of the splash. Naturally, the magnitude of the surge depends on the signal amplitude.

Now consider the spectrum of the sum of these signals, specified in accordance with the ratio 2.2, and shown in Figure 2.1.
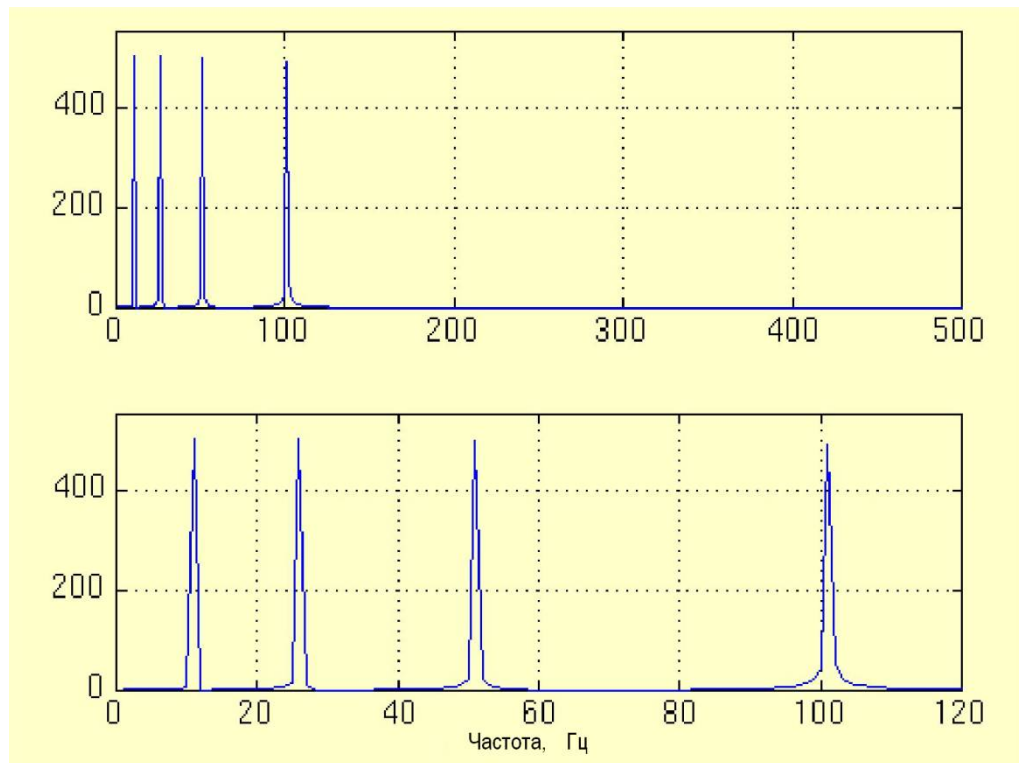
Fig. 2.7

Naturally, due to the fourier-transformation linearity, four bursts will also be observed in places that correspond to each frequency, and the picture of the signal spectrum is almost the same as in the previous case.

Such bursts are quite simply identified both by size and location. As a result, we can make an unambiguous conclusion about the contribution of each harmonious component to the initial signal. Moreover, sometimes there is simply no alternative to spectral signal analysis. For example, it is known that the so-called imitators can quite accurately "fake" a language that belongs to another person. If the qualification of the simulator is high, then very often it is impossible to distinguish who owns this or that fragment of the sound message. At the same time, the spectra of these audio messages differ dramatically.

Once again we note that, unlike rice. 2.3. in the frequency area, bursts corresponding to the different frequency components of the signal, due to the linearity of fourier-transformation and the limited time of its existence will be depicted not infinitely narrow bursts of the same intensity, but similar to as shown in the figure.

This expansion of bursts occurs as a result of the fact that the first ratio of the expression (2.17) is performed and the fact that the convolution operation leads to smoothing and signal expansion.

Indeed, let Fourier-like signal $f(t) \overset{\Im}{\to} \tilde{\Im}(\omega)$. Then Fourier image of a time-limited signal (at interval length Δt) may look like this:

$$\Im(\omega) \sim \int_{-\infty}^{\infty} P_{\Delta t}(t) f(t) \exp(-j\omega t)\, dt. \tag{2.19}$$

According to 2.17, we have

$$\Im(\omega) \sim \Im_p(\omega) \otimes \tilde{\Im}(\omega), \tag{2.20}$$

where $\Im_p(\omega) = \Delta t\, sinc(\frac{\Delta t \omega}{2\pi})$.

From 2.20 it follows that the more Δt, the more time-limited signal image approaches $\tilde{\Im}(\omega)$, because $\Im_p(\omega)$ is approaching δ-functions. Conversely, the shorter the amount of time when a signal exists the more it smooths out $\Im(\omega)$. Finally, when the time interval becomes very small, that is, $\Delta t \to \delta$, $\Im(\omega)$ degenerates into a function with a constant amplitude, since the Fourier image from the δ-функції is a unit. In other words, absolutely all signal information is lost.

Now consider two cases:

1. The signal is the sum of four signals (5, 10, 25 and 50 Hz) that are transmitted simultaneously (Fig. 2.8, a) during the time interval Δt_1, starting from the moment of time t_0:

$$x_1(t) = P_{\Delta t_0}[t - (t_0 + \frac{\Delta t_0}{2})] \times$$
$$\times [\cos(2\pi 5t) + \cos(2\pi 10t) + \cos(2\pi 25t) + \cos(2\pi 50t)] \tag{2.21}$$

The spectrum of this signal is given in Fig. 2. 2.8, b.

2. Harmonic signals of the same frequency, but each of them is transmitted in its own period of time

$$x_2(t) = P_{\Delta t_1}(t - \frac{\Delta t_1}{2})\cos(2\pi 5t) +$$
$$+ P_{\Delta t_2}[t - (\Delta t_1 + \frac{\Delta t_2}{2})]\cos(2\pi 10t) + \tag{2.22}$$
$$+ P_{\Delta t_3}[t - (\Delta t_1 + \Delta t_2 + \frac{\Delta t_3}{2})]\cos(2\pi 25t) +$$
$$+ P_{\Delta t_4}[t - (\Delta t_1 + \Delta t_2 + \Delta t_3 + \frac{\Delta t_4}{2})]\cos(2\pi 50t)$$

Such a signal can be similar to the one shown in Fig. 2. 2.9, a. The spectrum of this signal is given in Fig. 2. 2.9, b.

a

b

Fig. 2.8

a

b
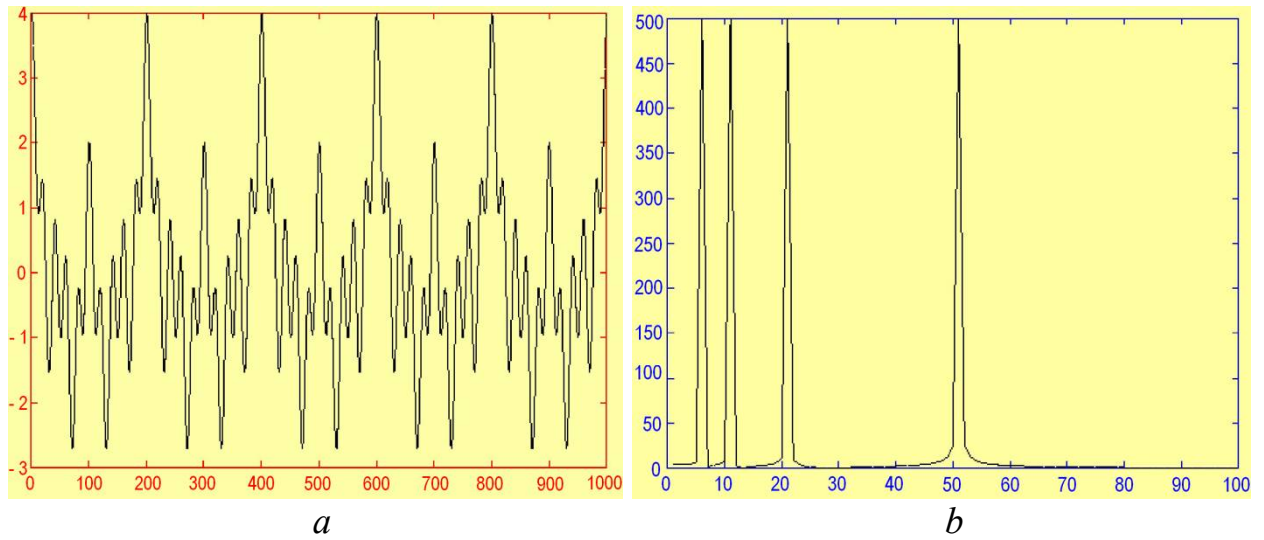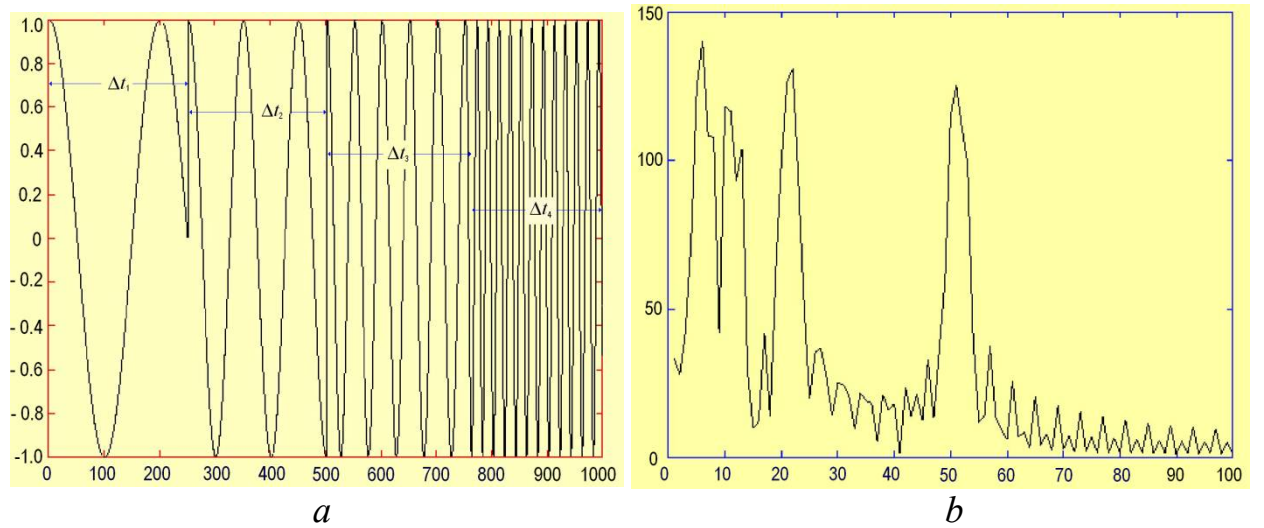
Fig. 2.9

As we can see from the figures 2.8 and 2.9, and in the first and second cases, the corresponding highs are observed at the points of frequency axis of 5, 10, 25 and 50 Hz. In other words, the characteristic features of the spectra of two different signals are the same. Moreover, if the time during which there is each harmonic signal with different frequencies Δt_1 the same as in the previous case Δt_0, as a result of, What's for Fourier Transformation an offset theorem is performed and this transformation is linear, it can be argued that the width and intensity of the bursts are the same.

In other words, the spectra of signals that we take for example and consist of four harmonious, almost the same regardless of the location of their harmonious components relative to the axis of time.

What really differs between these two signals? -The answer is simple. The first of them is stationary, that is, a signal whose characteristics do not change in time. The second does not meet this criterion. In the first period of time, a signal is transmitted with a minimum frequency, which then changes to the average and then to a high.

What is the reason that the two spectra are very similar? The answer is as follows.

At Fourier-transformation of the signal there is a change in the signal representation – the transition from amplitude-time to amplitude-frequency. In other words, by integrating by t and limitless integral boundaries in expression 2.3 there is a complete loss of information about the time behavior of the signal.

Hence the conclusion: it is obvious that Fourier transformation can be effectively applied primarily to stationary signals. To analyze non-existent signals, there must be another transformation that does not lose information about the change of signal in time.

2.3. Window Fourier Transformation

One of the ways that allows you to somehow remove the problem of loss of information about the behavior of the signal in time is the use of the so-called Fourier window transformation [8].

Imagine that in general, a non-stop signal can be divided into areas within which there is no change in the characteristics of the signal. If we return to our example (Fig. 2.9, a), the signal is stationary in periods of 0-250 mcs, 250-500 mcs, 500-750 mcs and 750-1000 mcs.

Then if we implement Fourier transformations for such stationary areas, we get an image that, firstly, like the usual Fourier transformation, will carry information about the frequency components of the signal. Secondly, for different areas of stationaryness, the spectra will be different. Therefore, we additionally have information about the time behavior of the signal.

Such an algorithm can be implemented by entering a certain window function, which is characterized by a certain width and moves in time along the signal. Mathematically, this operation can be written as follows:

$$\Im_{win}(\tau, \omega) = \frac{1}{2\pi} \int_{-\infty}^{\infty} f(t)\, s^*(\tau - t) \exp(-j\omega t)\, dt, \qquad (2.23)$$

where $s(t)$ – window function

The window function can be of different appearances (see Figure 2.10)
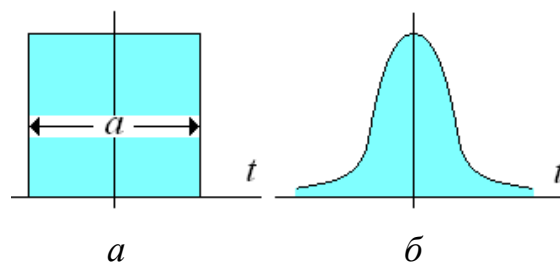
Fig. 2.10
a – rectangular pulse window function;
б –"Gaussid" window function.

Apply the VPF to the signal shown in Fig. 2. 2.9, a. Let the width of the window be commensurate with the interval of time during which there is each harmonious signal. Then we get a result similar to the one shown in Fig. 2. 2.11, which shows not only positive, but also negative frequencies.
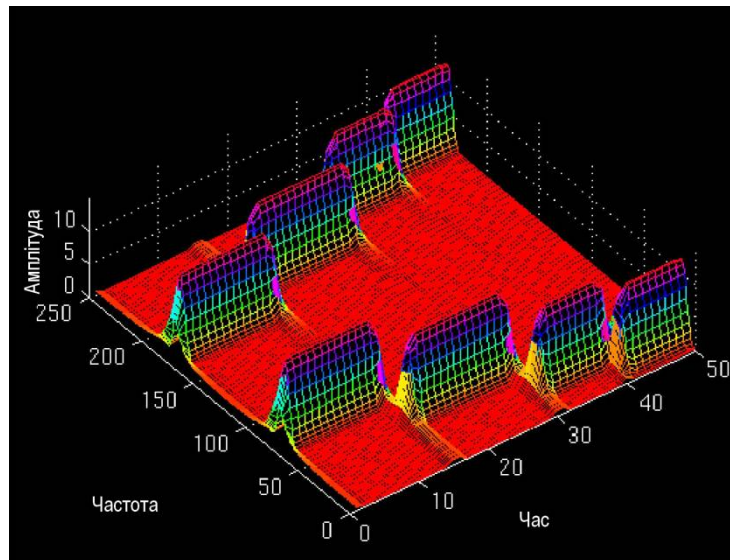
тут треба переклад на картинці
Fig. 2.11

So, it would seem that the problem is solved. Indeed, four bursts indicate the presence of four frequency components in the signal, and their different localization along the time axis makes it possible to establish when such components appear. In other words, VFP provides frequency-time signal conversion.

However, the AFP does not allow to get an image in which the resolution in frequency and time would be equally high. For VFP, you can get a high resolution by frequency, but in this case information about the time behavior of the signal is lost and vice versa, high resolution in time leads to loss of information about the frequency components of the signal. Something similar to Heisenberg's uncertainty ratio in quantum mechanics works.

Let's try to explain it. Obviously, the resolution of the image depends on the width of the window function. The smaller the width of this function, the higher the resolution.

We will reduce the width of the window function. Accordingly, in the time representation, we have:

$$\tilde{x}(t,\tau) = f(t)s^*(\tau - t). \tag{2.24}$$

According to the convoluted theorm, the VPF can be depicted as

$$\mathfrak{I}_{win}(\tau,\omega) = \mathfrak{I}(\omega) \otimes \mathfrak{I}_s(\omega), \tag{2.25}$$

where $\mathfrak{I}(\omega)$ and $\mathfrak{I}_s(\omega)$ – Fourier images of the signal and window function, respectively. Then, as indicated in paragraph 2.2, the smaller the width of the window $s^*(t)$ (limit case $s^*(t) = \delta(t)$), the "wider" Fourier image of this function and the more "emanating" the signal image, that is, information about the frequency components of the signal is lost.

a

б
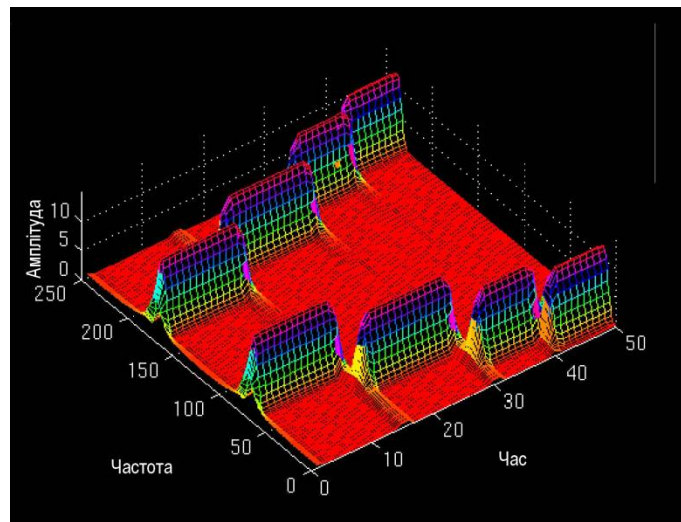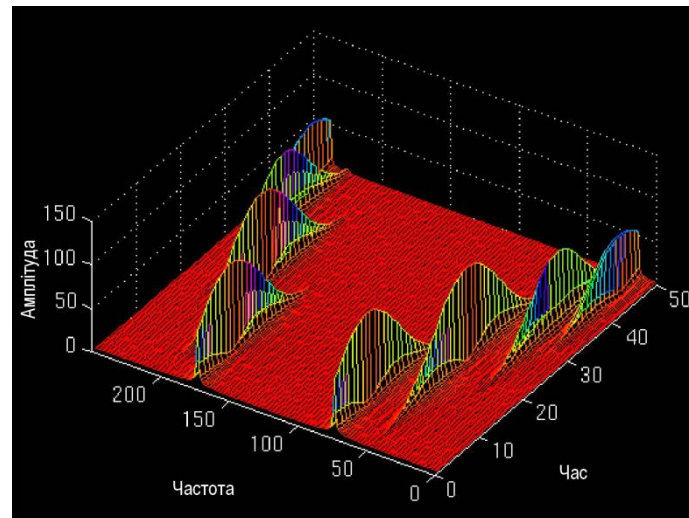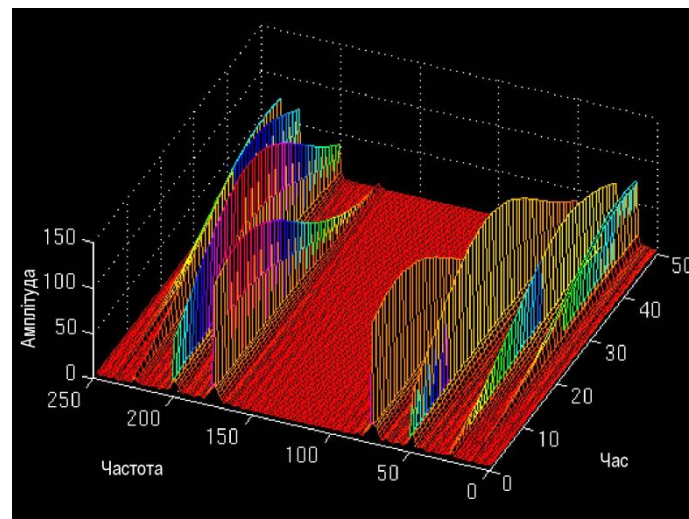
Тут треба переклад на картинці
Fig. 2.12. VPF for the signal shown in fig. 2. 2.9,
and for different widths of the window function
.

a – Smallest window function width; *b* – «middle» window function width; *в* – largest window
function width

Exactly the same when increasing the width $s^*(t)$ (limiting case width limitless)

information about the time behavior of the signal is lost. This fact is illustrated by Fig. 2. 2.12, which displays images of a signal consisting of four harmonious signals for windows of different widths.

As you can see from the pictures, as the window width increases, the image resolution increases in frequency, but the resolution decreases in time. From the figure it is almost impossible to determine the beginning of the moments when the signal frequency change begins.

2.4. Concept of wavelet transformation [8,9,11]

To some extent, the problem of simultaneous high resolution, both frequency and time, can be solved by the so-called wavelet conversion.

By definition, continuous wavelet conversion can be written as

$$WL(\tau, s) = \Psi(\tau, s) = \frac{1}{\sqrt{|s|}} \int_{-\infty}^{\infty} f(t)\psi^* \left(\frac{t-\tau}{s}\right) dt, \qquad (2.26)$$

where $\psi(t)$ – conversion function called mother wavelet; s – copyer scale or simply scale.

The word "wavelet" can be translated as "small wave". The word "small" is understood as the fact that such a window function has a final width. The word wave indicates that a window function is an oscillation function. The term maternal means that the width-different window functions used in the transformation are born from the same basic function – the mother wavelet.
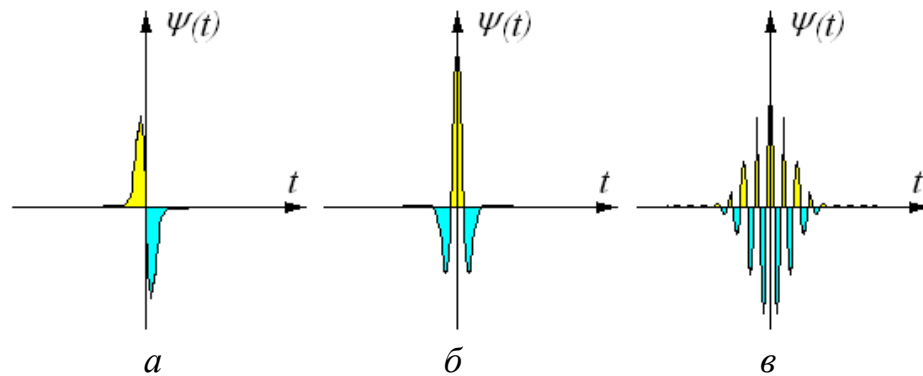
Fig. 2.13

а – Wave-wavelet; б – *MHAT*-wavelet (Mexican Hat); в – Wavelet Morle

Wavelets can be of different configurations (see Figure 2.13). The main requirement for a wayalet is:

$$\int_{-\infty}^{\infty} \psi(t)dt = 0. \qquad (2.27)$$

Since wavelet is a oscillation function near zero, the geometric interpretation of expression 2.27 means that the area of areas limited by positive and negative areas of wavelet is the same.
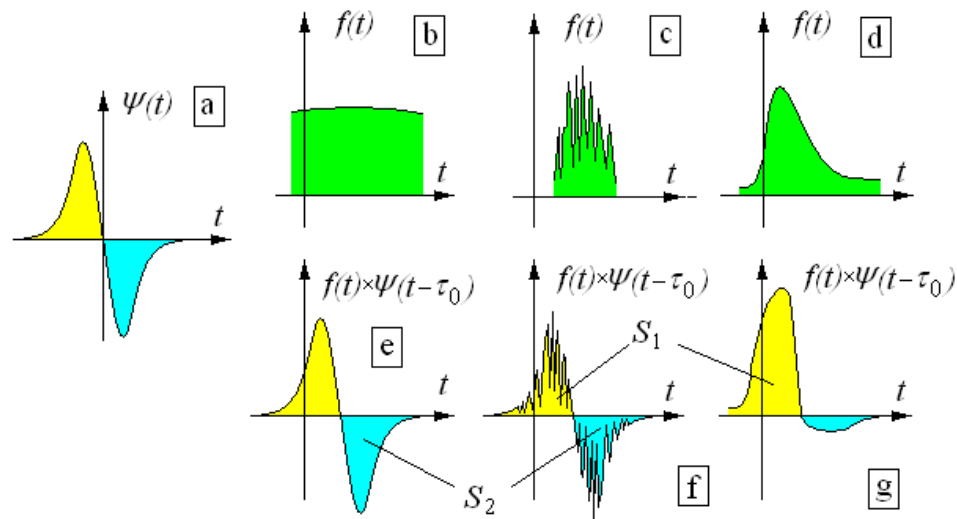
Fig. 2.14. To explain the idea of wavelet analysis

a – wavelet of a certain scale; b-d – signal areas with different flucation scales; b – signal area where the characteristic duration of the signal element is much greater than the wavelet width; c – signal area, where the characteristic duration of the signal element is much less than the wavelet width; d – wavelet width is measured in size with a signal element; e-g – wavelet multiplication results by signal with different fluculation scale; S_1, S_2 – positive and negative area of multiplication result.

It should be noted that to solve a specific signal analysis problem, there is an optimal wavelet configuration, the choice of which is far from simple.

If you pay attention to the definition of wavelet transformation, you can see that the wavelet image is a function of scale. Setting s Can be either more or less than one, i.e. the window function is compressed or expanded according to the s. In other words, for each point in time there is a whole set of images obtained for different s. Thanks to this wavelet transformation allows you to analyze in detail the behavior of the signal in time.

Let's try to explain the idea of wavelet transformation, based on the following considerations. According to the definition of wavelet transformation, to calculate the image, it is necessary to carry out such operations:

1. Select the magnitude of the scale s. Note that the calculation of the image begins with the value of s=1. Further, the value of s changes both toward more units ("narrow" wavelets) and towards s less than one ("wide" wavelets).

2. Offset wavelet with scale s to a specific τ.

3. Multiply the window function and signal. Naturally, a certain value of the product can be expected only in the interval comparable to the wavelet width.

4. Integrate Product.

Let us have a mother wavelet, similar to the one shown in Fig. 2. 2.14, but also for a certain τ_0 this wavelet occupies a position relative to the signal as shown in Fig. 2. 2.14, b. Since in the area in the area τ_0 the signal is almost constant, then we have the result of multiplying the window function by a signal similar to the figure shown. 2.14, e. Naturally, in this case, the integration result is approaching zero. The value of "positive" areas $S_1 S_1$ approximately equal to the value of "negative" areas S_2.

We will get a similar result in the case when the wavelet is shifted to the signal area, where it has a structure smaller in scale than a wavelet (see Figure 2.14, *c*).

And only if the wavelet is in the neighborhood of the point where the signal has a fluctuation scale close to the width of the window function, the result of integration will be significantly different from zero. Thus, the difference from zero image at a certain point τ for a certain value s indicates that this is where the signal has a flucation with a similar scale.

We will demonstrate the effectiveness of the waylet transformation on the example of a signal in Fig. 2. 2.15. This signal is non-stationary, but at different intervals of time it is possible to allocate stationary areas where the signal frequency is constant:

1st section – 30 Hz (0-300 mcs),
2nd section – 20 Hz (300-600 mcs),
3rd section – 10 Hz (600-800 mcs),
4th section – 5 Hz (800-1000 mcs).
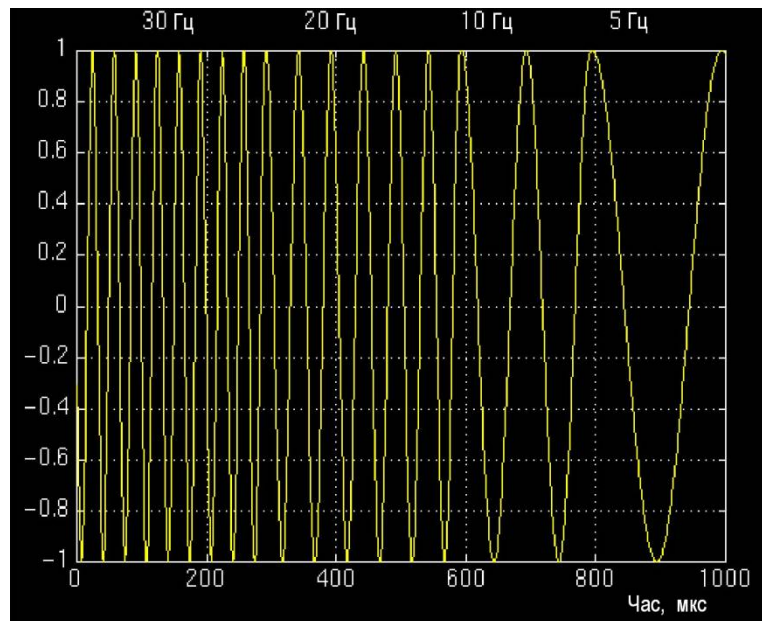
тут треба переклад

Fig. 2.15. Non-stationary signal consisting of four stationary sections with frequencies of 30 Hz (0-300 mcs), 20 Hz (300-600 mcs), 10 Hz (600-800 mcs) and 5 Hz (800-1000 mcs)

In general, the large-scale wavelet-transformation parameter cannot be directly associated with frequency. Nevertheless, it can be argued – the smaller the signal structure, the higher the frequencies are present in the signal. Naturally, for a set of harmonious signals that do not overlap in time (signal in Fig. 2.15), the analogy between the scale of signal flucation and its frequency is complete. In fact, the scale of signal flucation is equal to half of the period of the harmonious signal. Or otherwise, the scale is inversely proportional to frequency. So, analyzing the wavelet image of such a signal, we can draw an unambiguous conclusion not only about the stationaryness (or non-stationaryness) of the signal at certain intervals of time, but

also about the change in the scale of its flucations, that is, the change in frequency.

This conclusion is confirmed by Fig. 2. 2.16 on which wavelet image of the signal in question is provided
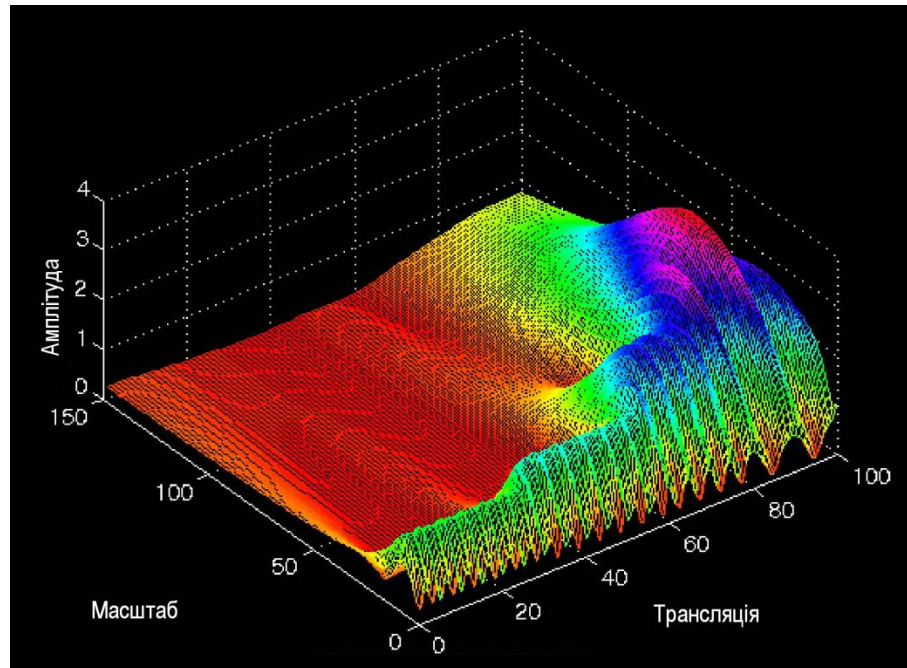
Треба переклад

Fig. 2.16. Wavelet image of the signal depicted in Fig. 2. 2.15
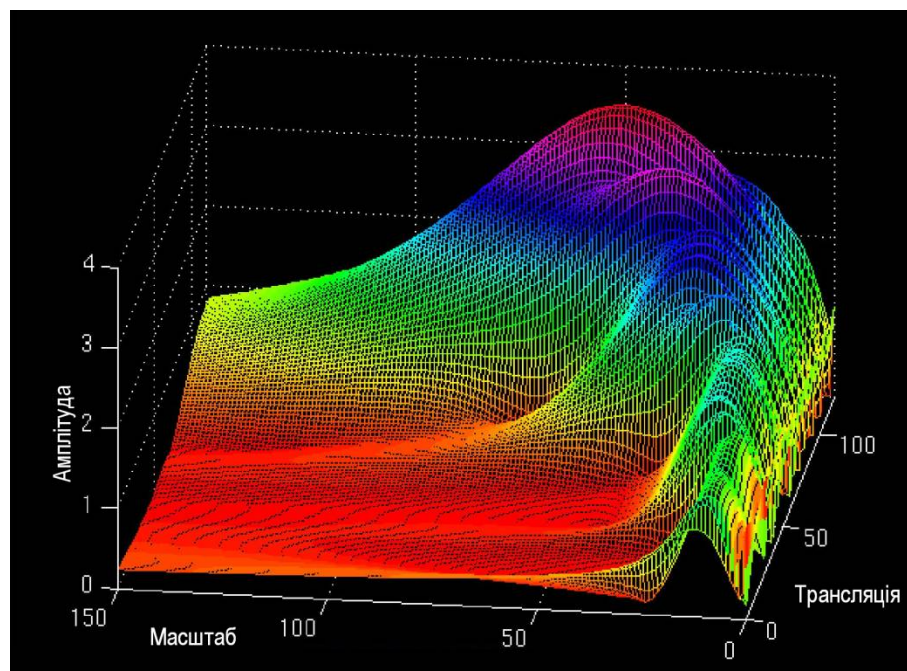
Треба переклад

Fig. 2.17

In Fig. 2. 2.17. the same wavelet image depicted from a different angle is provided.

Note that the offset τ (in the figure – broadcast) may be associated with the time.
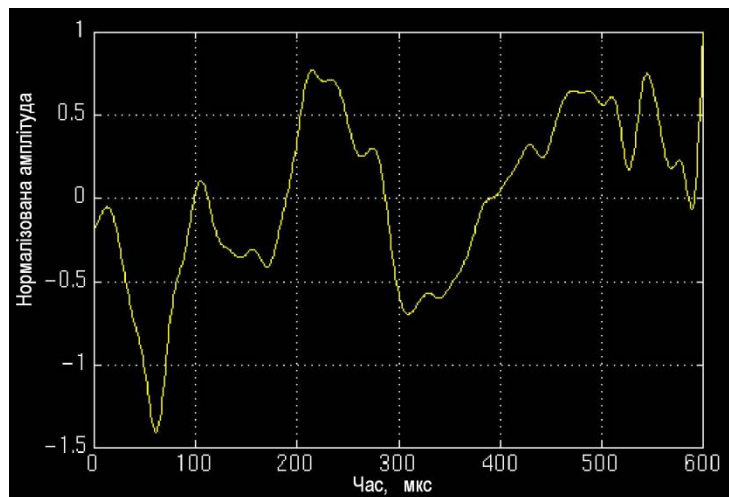
Fig. 2.18
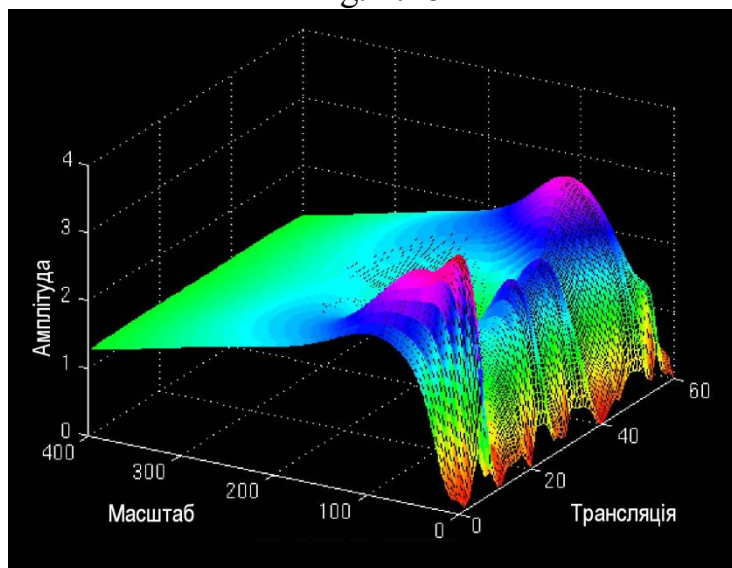
Fig. 2.19
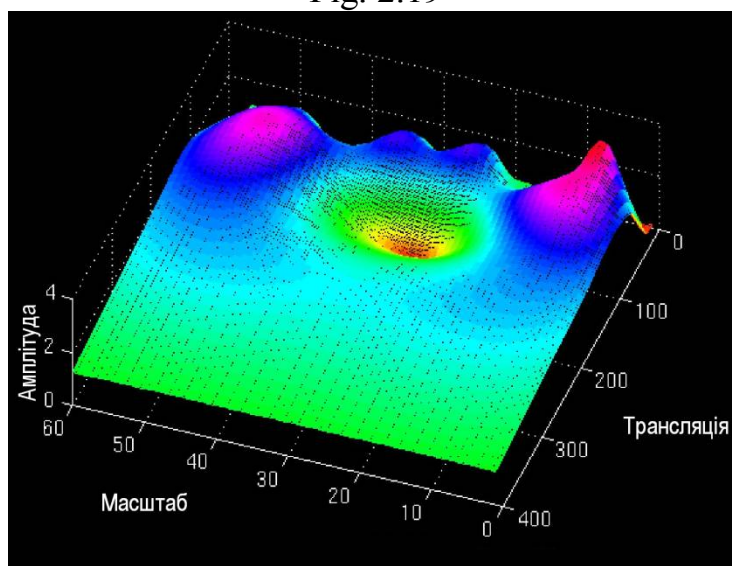
Fig. 2.20
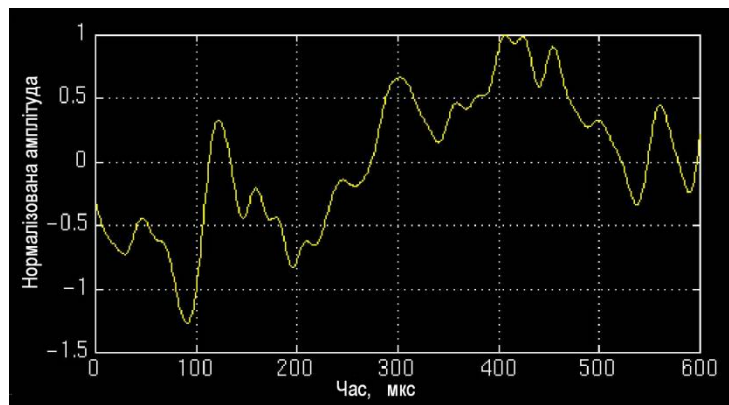
Fig. 2.21
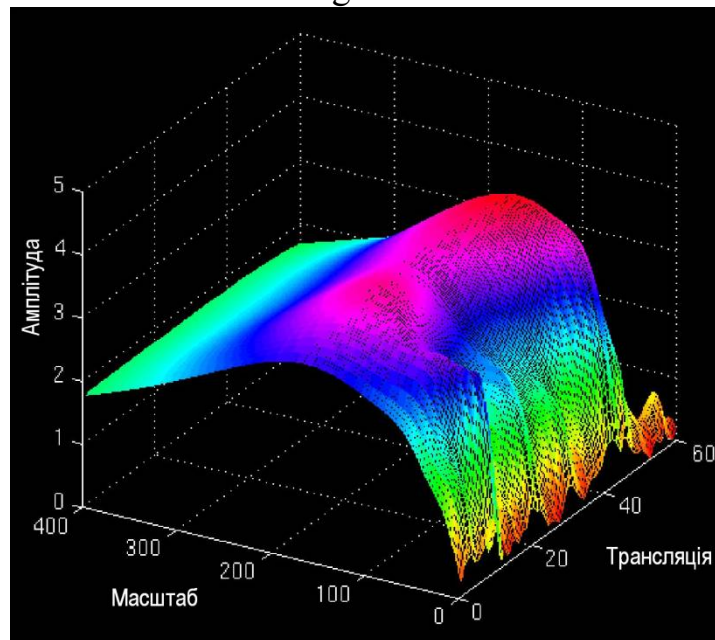
Fig. 2.22
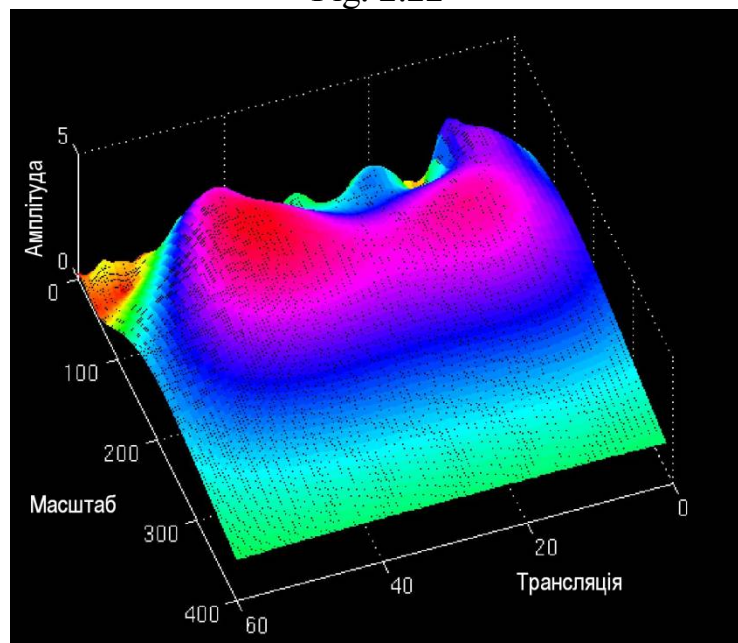
Fig. 2.23

Тут скрізь треба переклади

From the figures it is clearly visible that at first in the signal there are the smallest scales of flucation (high frequency), which increase and reach a maximum at the end of the existence of the signal (frequency 5 Hz).

Note that wavelet transformation, which we considered as an "alternative" of OFP, is not devoid of shortcomings. For example, different time resolutions for different levels of flucation.

Accordingly, for a relatively complete analysis of the signal, it is desirable to apply all three transformations considered by us: Fourier transformation, OFP, and wavelet transformation.

Here is an example of the real application of wavelet transformation.

In Fig. 2. 2.18 a certain medical characteristic of a healthy person is presented. Wavelet image of this signal illustrates Fig. 2. 2.19 and Fig. 2.20 (wavelet image from a different angle).

As can be seen from figures 2.19 and 2.20, in the field of "medium scale" wavelet image characteristics of a healthy person has a pronounced gap.

In Fig. 2. 2.21 a characteristic of a person with Alzheimer's disease is given. In Fig. 2. 2.22 and 2.23 wavelet images are given.

It should be noted that comparing figures 2.18 and 2.19, it is difficult to draw conclusions about differences in medical characteristics. However, as clearly follows from figures 2.19, 2.20 and 2.22, 2.23, a sick person in wavelet image does not have a gap in the field of "medium scale". In other words, in this case, it is wavelet transformation that gives us the opportunity to unequivocally establish a diagnosis of the disease.

2.5. The concept of signal filtration [4-6]

It is worth noting that the signal filtration operation is usually carried out in the case when the signal is provided in frequency representation. In general, the signal filtration process can be presented in the form of such a chain:

1. $f(t) \xrightarrow{\Im} \Im(\omega)$ – signal transformation to frequency representation.

2. $\widetilde{\Im}(\omega) = H(\omega)\Im(\omega)$ – Multiplication of Fourier signal image by filtering function (direct filtration).

3. $\widetilde{\Im}(\omega) \xrightarrow{\Im^{-1}} \tilde{f}(t)$ – inverse of Fourier transformation, transformation of the filtered image into a time representation (obtaining a filtered signal).

2.6. Some examples filtering
2.6.1. Filtering of additive interference

It is known that the signal with additive interference can be recorded in the form of

$$x(t) = f(t) + s_A(t), \tag{2.28}$$

where $s_A(t)$ – additive interference

So let's perform the first operation, get Fourier's image from $x(t)$. Thanks to the fourier-transformation linearity, we have:

$$\Im_x(\omega) = \Im(\omega) + S_A(\omega), \tag{2.29}$$

where $\Im(\omega)$ та $S_A(\omega)$ – Fourier images of signal and interference, respectively
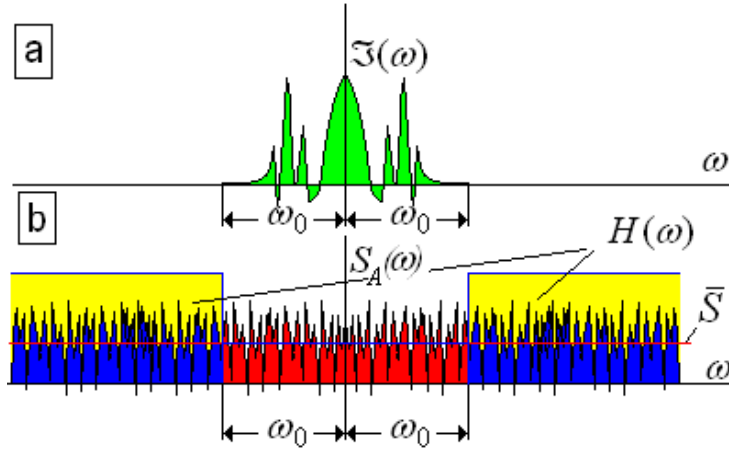
Fig. 2.24

It should be noted that, as a rule, the Fourier signal image occupies a frequency band much smaller than the interference (see Figure 2.24). In Fig. 2. rice. 2.24, b provided a spectrum of interference, the so-called "white" noise, which is characterized by a constant average level of intensity $\bar{S}$ for all frequencies from $-$ to $+$ limitlessness. Consequently, all noise energy is evenly distributed along the entire frequency axis. However, the signal energy is concentrated at a fairly small interval (compared to the band that the interference takes) $2\omega_0$. Accordingly, if you apply a simple band filter

$$H(\omega) \begin{cases} 1, & |\omega| \leq \omega_0 \\ 0, & \text{в р. інт.} \end{cases}, \tag{2.30}$$

which has a single pass in frequency interval $-\omega_0, \omega_0$ and zero passing outside this interval, the lion's share of the interference energy will be cut off.

Accordingly, after the inverse of Fourier transformation, we have a signal that approaches the unspoined signal

$$\tilde{x}(t) \to f(t). \tag{2.31}$$

2.6.2. Filtering cartoon interference

Let us have a signal with multiple interference:

$$x(t) = s_M(t)f(t). \tag{2.32}$$

It is absolutely clear that simple filtration will not be possible to get rid of such a hindrion, since Fourier's image from $x(t)$ there is nothing but a convoluted:

$$\Im_x(\omega) = S_A(\omega) \otimes \Im(\omega). \tag{2.33}$$

So, before proceeding to the filtration procedure, we will do another additional operation – logarithm of the signal. Then instead of (2.32) we have

$$\ln[x(t)] = \ln[f(t)] + \ln[s_M(t)]. \tag{2.34}$$

Such an operation is quite simple to perform if you pass the signal through a logarithmic amplifier. As we can see from 2.34, after logarithming, the multiplier interference turned into an additive.

Therefore, in the future, the main impact of such noise can be removed with a strip filter. Naturally, to get a signal that is approaching $f(t)$, at the last stage, the

filtered signal must be missed through the exponential amplifier that performs the operation inverse to logarithm $\exp[\tilde{x}(t)] \rightarrow f(t)$.

2.6.3. Filter a permanent component

Let us have a signal with some constant component or with a component that changes much slower than the signal:

$$x(t) = f(t) + a, \qquad (2.35)$$

Such a permanent "stand" is easy to get rid of with a filter that filters a very narrow strip in the low frequency area.

Indeed thanks to the linearity of Fourier's transformation of the Fourier image from $x(t)$ looks like:

$$\Im_x(\omega) = \Im(\omega) + A(\omega). \qquad (2.36)$$

At the same time, if the signal life was long enough, then $A(\omega) \rightarrow a\delta(\omega)$, since, as follows from Table 2.1, the Fourier image from a unit is a delta function. So, by applying a filter that filters a very narrow strip in the zero frequencies area (such filtration practically does not affect the signal itself), and by making the Fourier conversion inverse, you can get rid of the constant component in the signal.

2.6.4. Signal differentiation

The signal differentiation operation can also be performed by filtering it.

Let's turn to the expression (2.5) and differentiate the left and right parts by t.

We have

$$\frac{df}{dt} = \int_{-\infty}^{\infty} (j\omega)\Im(\omega)\exp(j\omega t)\,d\omega. \qquad (2.37)$$

This expression actually specifies the algorithm for the necessary filtering. First we get Fourier-like signal $\Im(\omega)$. At the next stage, we pass this image through a filter with the function of passing

$$H(\omega) = j\omega, \qquad (2.38)$$

so-called LCHM filter (filter with linearly modulated frequency).

After that, we perform the inverse of Fourier transformation and get the derivative from the signal.

In conclusion, we will analyze the consequences of such filtration for the signal of a given sequence of rectangular pulses (digital signal). In Fig. 2. 2.25 the signal itself and its derivative were provided. Since the geometric interpretation of the derivative is its association with the tangent of the tangent to the ogina signal, it is quite clear that on plot 1-2 the derivative has zero value. At point 2, she jumps to change her value from zero to $+\infty$. Then, by point 2, the derivative is zero again. That is, in the neighborhood of point 2, the derivative is equal to the delta function. Finally, at point 3, it has a magnitude $-\infty$. Or, in other words, in the neighborhood of point 3 derivative – negative delta function.
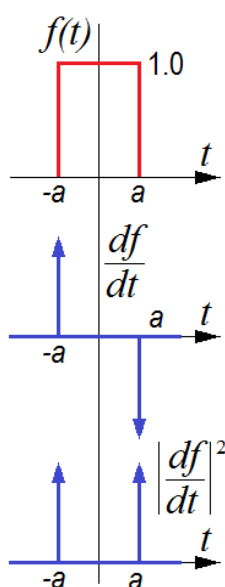
Consequently, the differentiation operation, which can be performed by frequency filtration when applied to a sequence of rectangular pulses, leads to the replacement of these pulses by a system of very short-time bursts that occur at the beginning and end of each rectangular pulse.

In Fig. 2. 2.26 an example of image differentiation is given. As you can see, such an operation applied to images characterized by constant brightness in certain regions and the level of which varies from area to region can be interpreted as opreation of edification.

а   *б*
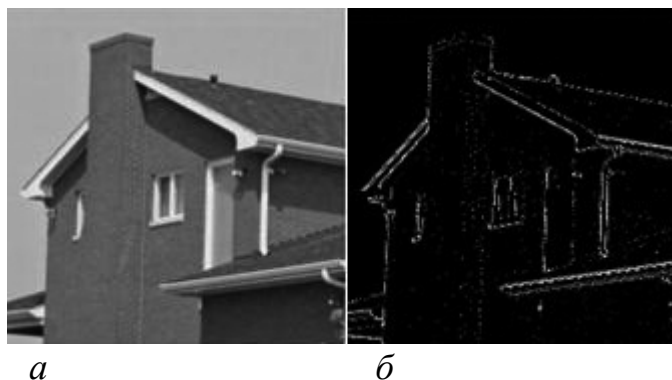
Рис. 2.26

a – original image; *б* – filter result

2.7. Optical wave propagation [1,5,6,9]
2.7.1. Optical wave propagation in free space
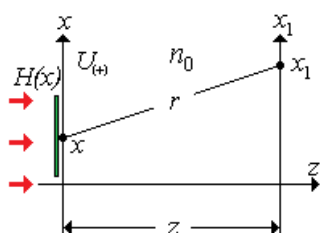
Let the unit in intensity flat wave (Fig. 2.27), which is distributed in an environment with a relapation rate n_0, lightens a thin crossbar with pass-through (generally complex) $H(x)$. According to (1.19) the field directly by transparent is equal to:

$$U_{(+)}(x) = H(x) = A(x)e^{j\Phi} \qquad (2.39)$$

Then we can assume that each field point by transparent is a point source with an amplitude module and a phase in accordance with the (2.39).

Select any point source located at the point x. A spherical wave spreads from such a point source, which is in the plane x_1 in one-dimensional case is described by a complex amplitude:

$$U_{ca} = \frac{1}{\sqrt{r}} H(x)\exp(jkn_0 r) \qquad (2.40)$$

where

$$r = \sqrt{z^2 + (x_1 - x)^2}. \qquad (2.41)$$

For a two-dimensional case, the multiplier $\frac{1}{\sqrt{r}}$ в (2.41) transformed into multiplier $\frac{1}{r}$.

Field at point x_1 is the result of interference of all such waves that came from the flatness of the x:

$$U(x_1) = \int_{-\infty}^{\infty} \frac{1}{\sqrt{r}} H(x) \exp(jkn_0 r)\, dx. \tag{2.42}$$

We will assume that the transverse dimensions of the transparant and the size of the area in the plane x_1, Where field analysis is carried out, small comparable to the distance z between planes x and x_1. Then r can be appeximated as:

$$r \approx z + \frac{(x_1 - x)^2}{2z}. \tag{2.43}$$

Add that amplitude multiplier $\frac{1}{\sqrt{r}}$ can be approximiated even more roughly $\frac{1}{\sqrt{r}} \approx \frac{1}{\sqrt{z}}$. Accordingly, the expression (2.42) will be rewrited as:

$$U(x_1) = \frac{1}{\sqrt{z}} \exp(jkn_0 z) \int_{-\infty}^{\infty} H(x) \exp[j\frac{kn_0}{2z}(x_1 - x)^2] dx. \tag{2.44}$$

An expression (2.44) is sometimes referred to as a Frenel transformation from a function $H(x)$. This expression describes the proliferation of a pro-government $H(x)$ waves in Fresnel diffraction area.

Let's make another approximation:

$$\frac{(x_1 - x)^2}{2z} = \frac{1}{2z}(x_1^2 + x^2) - \frac{1}{z}x_1 x \approx -\frac{1}{z}x_1 x. \tag{2.45}$$

Then (2.45) takes the form:

$$U(x_1) = \frac{1}{\sqrt{z}} \exp(jkn_0 z) \int_{-\infty}^{\infty} H(x)\exp(-jwx) dx, \tag{2.46}$$

where $w = \frac{kn_0}{z} x_1$. Expression (2.46) describes the propagation of a pro-pro-government $H(x)$ waves in the fraunhosphere diffraction area and are fourier transformations in coordinates $w = \frac{kn_0}{z} x_1$.

2.7.2. The implementation of fourier transformations in optics and in integral optics in particular [5,6]

Let the flat wave (Fig. 2.28) illuminate the $H(x)$. The field, respectively, $U_{1(+)}$ immediately after the transmission is equal to its skipping. Close to the transparant is a lens L with focal length f. After passing the lens, the field is described by a complex amplitude [5]:

Рис. 2.28

$$U_{2(+)} = H(x)L(x) =$$
$$= H(x)\exp(-j\frac{kn_0}{2f} x^2) \tag{2.47}$$

At some distance z, according to (1.24), the field is as follows:
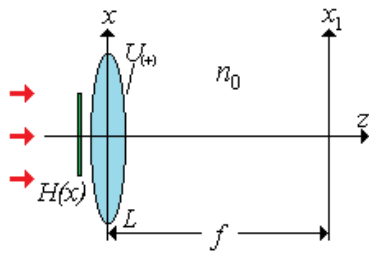
$$U(x_1) = \frac{1}{\sqrt{z}} \exp(jkn_0 z) \exp(j\frac{kn_0}{2z} x_1^2) \times$$
$$\times \int_{-\infty}^{\infty} H(x)\exp[j\frac{kn_0}{2z} x^2(\frac{1}{z} - \frac{1}{f})]\exp(-j\frac{kn_0}{z} x_1 x) \tag{2.48}$$

From (2.48) it follows that when $z=f$, $U(x_1)$ with precision quadratic phase multiplier precision $\exp(j\frac{kn_0}{2z} x_1^2)$ equals Fourier-insult from $H(x)$.

It can be shown [6] that if the pair is located at a distance of z_0 lens (or even behind it), field $U(x_1)$ also proportional to Fourier's insult from $H(x)$ and quadratic

phase multiplier, which disappears only when $z_0 = f$, i.e. when the crossbow is located in the front focal plane of the lens. But in any case, the intensity of the field in the plane x_1 always equals the power spectrum from $H(x)$

$$I(x) = \left| \Im\left(\frac{kn_0}{f} x_1\right) \right|^2. \qquad (1.49)$$

It is clear that the above ratios remain relevant for the systems of integral optics, and planar focusing elements implement one-dimensional Fourier transformation. But convolution and correlation operations, as follows from expressions (2.17), can be implemented on the basis of the Fourier multiplication and transformation operation.

2.8. Neural and neuro-like networks and their optical realization [12-15]
2.8.1. Structure of neural networks

The main purpose of the neural (or neuro-like) network (NM) is associated with the task of pattern recognition [12]. In this case, the associative principle of recognition is used, and the final decision on belonging a certain insult to a particular class, the answer to the question "YES" or "NO" is made on a probable basis. Based on this interpretation, in general, the algorithm of NM's work is reduced to comparison according to the associative features of the analyzed image with the image stored in NM. That is, to a certain extent, NM can be interpreted as an associative-storage device (AZP). When you submit an image (or part of it) to the entrance of such a filling station, it is compared with the image stored on the network, and an image (or signal corresponding to the image) is formed at its output, the closest to the input signal. Such actions of NM are possible only if a certain number of reference images corresponding to the class to which the input image belongs are pre-recorded in NM. The process of recording images in NM is called network training. So, the more images of this class are written to the network, the greater the likelihood of correct recognition of the input image.

In Fig. 2. 2.29, a depicts some

FIG. 2.29. To the structure of neuronal measures
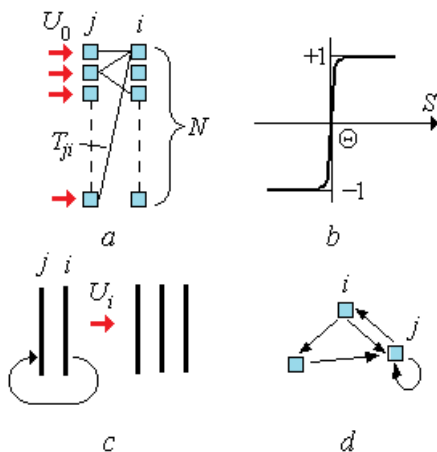
a – two NM layers with N elements in each layer; U_0 – вхідний сигнал; T_{ij} – link between elements of the first and second HM layer; b – diagram of the functioning of the element HM; c – layer structure HM; d – possible layer configuration HM

structure(network), which consists of layers of j and i, which, in turn, consist of N Items. Note that in general, each layer may have a different number of elements. Let such a network receive a signal:

$$U_0 = \sum_j^N U_j, \qquad (2.50)$$

where U_j – elementary signal entering the j element of the 1st layer.

Such a network will be called neural (or neuro-like) if the network has the following properties [14]:

1. Depending on the amount of input signal S the output signal (reaction) of an element (neuron) can take a value of only +1 or –1 (see Figure 2.29, b). In fact, the output signals (states) may be different or other levels of the output signal may be associated with them, for example, 0 and 1. In any case, the element is triggered as a threshold, that is, when the input signal is reached a certain value Θ the output signal of the element by jumping changes its value.

2. Input signal on the i element of the 2nd layer is determined by the ratio of

$$U_{0i} = \sum_{j=1}^{N} T_{ji} U_j(t), \tag{2.51}$$

where T_{ji} – determines the connection between neurons j and i first and second layers of HM.

Then the output signal from the i neuron may be as follows:

$$\begin{cases} U_i(t+1) = NL\{U_{0i}(t)\} = +1, & U_{0i} = \sum_{j=1}^{N} T_{ji} U_j(t) > \Theta \\ U_i(t+1) = NL\{U_{0i}(t)\} = -1, & U_{0i} = \sum_{j=1}^{N} T_{ji} U_j(t) \leq \Theta \end{cases}, \tag{2.52}$$

where $U_i(t+1)$ – conditional designation of the state of the element after the influence of the input signal on it, which indicates that there is a certain time of relaxation of the neuron;

NL – nonlinean operator, which provides a jump-like change in the output signal;

Θ – input signal threshold, which is usually the same for all neurons.

Based on the expression (2.52) and Figure 2.29, and the technical model of the neuron can be imagined as a specific device that contains:
- sumator that combines signals coming from the previous layer;
- *nonlinean operator;*
- distributor, which transmits the result of processing either to the next layer or to the output of the system through interconnection.

Note that it is possible when the output signal from the exit i layer is again fed to the entrance j-го, that is, a link of positive or negative feedback is formed (Fig. 2.29, p). In this case, the layers of the network stand out quite conditionally. In fact, such a division of NM into layers is not always possible, since the connections between neurons may be random in nature and, accordingly, the "architecture" of NM has the form similar to that shown in Fig. 2. 2.29, d.

2.8.2. The algorithm of the neural network. Hopfield algorithm

Before the learning process $T_{ji}=0$, that is, all links have zero value. So, for the functioning of the NM, it is necessary to set specific values for these links, that is, you need to perform a network training operation. The essence of this operation is that the network input is provided M (M- multiple learning) signals $U^{(m)}$. In this case, the value of an arbitrary relationship T_{ji} set according to the equation:

$$T_{ji} = \sum_{m=1}^{M} U_i^{(m)} U_j^{(m)}. \tag{2.53}$$

At the same time

$$\begin{cases} U_i^{(m)} U_j^{(m')} = +1 & U_i^{(m)} = U_j^{(m')} \\ U_i^{(m)} U_j^{(m')} = -1 & U_i^{(m)} \neq U_j^{(m')} \end{cases} . \tag{2.54}$$

Two situations are possible when submitting a NM signal to the input:

1. NM "rolls" to one of the images stored in its memory, that is, this image is generated at the output of the network.
2. NM goes into auto-prick mode, that is, a time-variable signal is formed at the output. The network "cannot" decide what image it is offered.

A signal is signaled to the network input $\widehat{U}^{m_0}(t)$. Then on the way out i layer NM formed signal:

$$\dot{U}_i^{m_0}(t+1) = NL\{\sum_{j=1}^N T_{ji}\, \widehat{U}_j^{m_0}(t)\}. \tag{2.55}$$

According to the equation (2.53) we have:

$$\dot{U}_i^{m_0}(t+1) = NL\{\sum_{j=1}^N \sum_{m=1}^M U_i^{(m)}\, U_j^{(m)}\, \widehat{U}_j^{m_0}(t)\}. \tag{2.56}$$

Let the image $\widehat{U}^{m_0}$ closest to image U^m, stored in network memory. Then

$$\dot{U}_i^{m_0}(t+1) = NL\{\sum_j^N U_i^{m_0} U_j^{m_0} \widehat{U}_j^{m_0} + \sum_{j=1}^N \sum_{m \neq m_0}^M U_i^{(m)}\, U_j^{(m)}\, \widehat{U}_j^{m_0}\}. \tag{2.57}$$

Let N_{m_0} – number of bits matching in images $\widehat{U}^{m_0}$ and U^m. Тоді (2.57) under conditions (2.54) is transformed to:

$$\dot{U}_i^{m_0}(t+1) = NL\{N_{m_0} U_i^{m_0} - (N - N_{m_0})U_i^{m_0} + \sum_{j=1}^N \sum_{m \neq m_0}^M [U_j^{(m)}\, \widehat{U}_j^{m_0}]U_i^{(m)}\} \tag{2.58}$$

or

$$\dot{U}_i^{m_0}(t+1) = NL\{(2N_{m_0} - N)U_i^{m_0} + \sum_{j=1}^N \sum_{m \neq m_0}^M [U_j^{(m)}\, \widehat{U}_j^{m_0}]U_i^{(m)}. \tag{2.59}$$

Second add-on in curly braces goes to zero because images $\widehat{U}^{m_0}$ and U^m is different. Accordingly, the quantities – and + units formed during multiplication $U_j^{(m)}$ and $\widehat{U}_j^{m_0}$, approximately equal according to statistics. The result of this addition to the output signal is insignificant and forms the so-called noise of the network.

The target value of an expression (2.59) depends on the ratio of $2N_{m_0}$ and N, as well as actions ("settings") of a nonlinean operator NL, the value of the threshold value Θ, which determines the transition of initial neurons to the state – or +1. Given this, it can be argued that when the signal is repeatedly $\dot{U}_i^{m_0}$ to the entrance of the network it or "rolls" to the image U^{m_0}, which will be formed at the NM output, or will be in a state of auto-pricking (will not be able to form at the output of any image stored in memory).

The second situation occurs when the threshold Θ is set unreasonably high. This leads to the fact that even with a large $2N_{m_0}$ and N ($2N_{m_0} - N \to 0$) at the output of the neuron is formed -1. At the same time, it is not optimal and the low threshold Θ, because in this case the NM will go to the wrong image.

Once again, we note that the quality (probability correctly) of image recognition is associated with the number of acts of network training M, that is, significantly depends on the number of images of one class stored in memory HM.

2.8.3. Prospects for the development of optical neural networks

It can be shown that the number of images that can be effectively written to the memory of the neutron network is determined by the ratio of:
$$M \approx 0{,}15N. \tag{2.60}$$
Consequently, the number of neurons in the network layer determines its power and resolution [15].

The number of incoming neurons NM is called the unification coefficient K_u. The number of outgoing neurons is called the branching coefficient K_s. Maximum number of relationships, respectively $K_{T\,max}$ between neurons equals $K_u K_s$. In the real case, the number of links K_T less than this value, since the network additionally implements so-called empty links ($T_{ji}=0$).

In most cases, for normal operation of the network K_o i K_p must have a value close to $10^3 \div 10^6$. Under
$$10^3 \div 10^6 < K_T < 10^6 \div 10^{12} \tag{2.61}$$
The literature knows [??] that the best electronically based NM variants have $K_T \sim < 10^3$. This fact is due to the fact that each neuron is a microprocessor of a certain type and, accordingly, each neuron needs program support, the main of which is the switching of the processed data. At the same time, processing time and energy costs increase catastrophically with an increase in the number of neurons in the network.

Taking into account the fact that the result of signal processing in NM is probabilist, the promising direction of their construction is the formation of a network as an analog processor, the elements of which work independently and autonomously, and the "switching" of output signals is carried out automatically. In this sense, the optical implementations of NM have indisputable advantages over other types of analog neural networks. These advantages are due to such considerations:

1. The input signal generated as a particular image may have an extremely large number of elements, which is limited only to the resolution of the optical system. It is this number that $n \times n$ determines the number of neurons in the layer (K_u, K_s) and can reach values $10^6 \div 10^8$ in three-dimensional and $n \sim 10^3 \div 10^4$ in planar variants.

2. In optical networks, a standard digit that determines the number of links $KT \sim n^3$(3D variant) and $KT \sim n^3$(planary version). So, the number of relationships that can be formed in a three-dimensional variant has a value $10^9 \div 10^{12}$ and in planar, respectively $10^{9/2} \div 10^6$.

3. The speed of signal processing in the optical network is limited only to the speed of light propagation through the optical system.

2.8.4. Implementation of optical neural networks
2.8.4.1. Optical neural network with processor core in the form of a non-stop hologram

Let the field be fed into the optical system (Fig. 2.30, a) U_0, which is conventionally divided into fields U_1 and U_2. Then in the focal plane of the lens L_1

a field is formed:

$$U(x_f) = \Im\{U_1 + U_2\} = \Im_1 + \Im_2, \qquad (2.62)$$

where $\Im_1, \Im_2$ – Fourier field images U_1 and U_2 respectively.
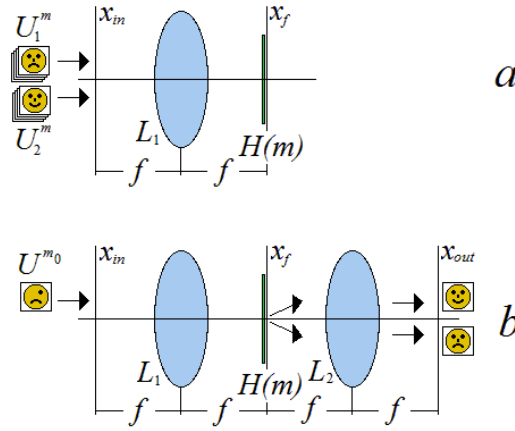
Fig. 2.30

Field intensity in plane x_f is described by the ratio of:

$$I(x_f) = |U(x_f)|^2 = |\Im_1|^2 + |\Im_2|^2 + \Im_1^*\Im_2 + \Im_1\Im_2^*. \qquad (2.63)$$

Let in the plane x_f placed photosensitive material (FCHM), the change of local parameters of which (for example, blackening) occurs in proportion to the intensity of the falling light. Then we can assume that in this plane the $H(x_f)$ with skipping $\sim I(x_f)$. Similarly, several intensity distributions corresponding to different input fields can be recorded per place. Therefore, in the end, the transmission of the pair can be described by the expression

$$H(x_f) = \sum_m^M I^{(m)} = \sum_m^M \{|\Im_1^m|^2 + |\Im_2^m|^2 + \Im_1^{m*}\Im_2^m + \Im_1^m\Im_2^{m*}\}. \qquad (2.64)$$

Such a transparant recording process can be described as the process of "learning" the system.

Let's outline a few more assumptions:

1. Input fields U_1^m and U_2^m have a relatively small structure.

2. Fields U_k^i and U_l^j completely different if $i \neq j$ and even $k=l$.

Then it is fair to

$$\begin{cases} \varphi_{kl} = U_k^i * U_l^j \to \delta(x_m), & \begin{cases} i = j \\ k = l. \end{cases} \\ \varphi_{kl} = U_k^i * U_l^j \to 0, & i \neq j \end{cases} \qquad (2.65)$$

Let the login of the system be submitted field U^{m_0} (Fig. 2.30, b), close to any image, for example U_1^m, recorded in the system. Then the correlation function

$$\varphi = U_1^m * U^{m_0} = \alpha\delta(x_m) \qquad (2.66)$$

where $\alpha < 1$, does not equal zero.

Field in plane x_ϕ described by the expression:

$$U(x_f) = \Im^{m_0} H(x_f) = (\Im^{m_0}\Im_1^{m*})\Im_1^m + (\Im^{m_0}\Im_1^{m*})\Im_2^m + R^{m,m_0}, \qquad (2.67)$$

where R^{m,m_0} combines all other add-ons.

We will arrange after the transaction $H(x_f)$ (Fig. 2.30, b), another optical cascade with lens L_2, distance from the transponthian by the focal length. Then

(indicating that there is no separation of the direct and inverse Fourier transformation) in its rear focal plane, the field is Fourier-image from the field $U(x_f)$:

$$U(x_{out}) = \Im\{(\Im^{m_0}\Im_1^{m*})\Im_1^m\} + \Im\{(\Im^{m_0}\Im_1^{m*})\Im_2^m\} + \Im\{R^{m,m_0}\}. \quad (2.68)$$

Each of the additions (2.68) is a Fourier transformation from the product of three functions and when applying fourier theorems about the conversion of the product of two functions and convolution theorems can be calculated according to the following scheme:

$$\Im\{(\Im_k\Im_p^*)\Im_q\} = \Im\{(\Im_k\Im_p^*)\}\otimes U_q = (U_k * U_p)\otimes U_q. \quad (2.69)$$

The result of such an operation for the third dowry in accordance with (2.65) goes to 0, since the so-called cross-correlation functions (correlation functions of different values (second ratio equation)) are obtained. This add-on generates system noise (similar to the second add-on in (2.67)). The 1st and 2nd add-ons form a field described by the expression:

$$U(x_m) = \alpha[\delta(x_m) \otimes U_1^m + \delta(x_m) \otimes U_2^m] + \text{noise}. \quad (2.70)$$

From here we get

$$U(x_m) = \alpha[U_1^m + U_2^m] + \text{noise}, \quad (2.71)$$

weakened in α repeatedly to show margins U_1^m and U_2^m. $U(x_{out})$ you can log on again using spatial-time modulators, a digital computer, and additional light separations. This will result in a corresponding redistribution of intensity between the U_1^m, U_2^m and noise component: the noise component will decrease. In addition, a nonlinean device can be installed at the system output, which will additionally ample the useful signal and reduce the noise component. Consequently, the action of such a system can be considered as an action similar to the action of a neutron network. Just like NM, a system with a non-stop hologram works like a filling station and rolls to a certain image recorded on a non-stop hologram.

2.8.4.2. Optical neural network with processor core as a coordinated filter

The field is fed to the optical system (Fig. 2.31, a) U_0, which is a set of fields U^m. Each subsequent input image is shifted in the input plane by a value Δ_m:

$$\Delta_m = (m - 1)\Delta. \tag{2.72}$$

From (2.72) it follows that the first input image is centered relative to the axis of the system.

Then the field U_0 looks like:

$$U_0 = \sum_m^M U^m[x_m - (m - 1)\Delta]. \tag{2.73}$$
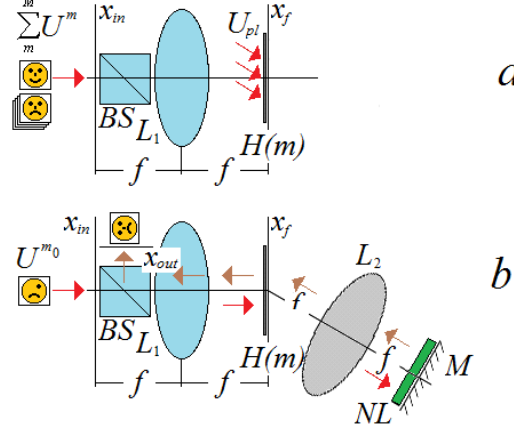
Fig. 2.31

Given the shear theorem, the field in the focal plane of the lens L_1 is opposed to the expression:

$$U(x_f) = \sum_m^M \exp\left\{-j\frac{k}{2f}(m - 1)\Delta x_f\right\}\Im^m. \tag{2.74}$$

Let in the plane x_f parallel beam is directed – flat wave P at an angle α to the system axis. In this case, the intensity distribution in this plane will have the form of:

$$I(x_f) = |U(x_f) + P|^2 = |U(x_f)|^2 + |P|^2 +$$
$$+ \sum_m^M \exp\left\{j\frac{k}{2f}(m - 1)\Delta x_f\right\}\mathcal{F}^{m*}\exp(jkx_f \sin\alpha) + \tag{2.75}$$
$$+ \sum_m^M \exp\left\{-j\frac{k}{2f}(m - 1)\Delta x_f\right\}\mathcal{F}^m\exp(-jkx_f \sin\alpha)$$

Next, there is a fixation of the resulting distribution on the photo carrier. So, as in the previous case, a kind of training operation is carried out, in which the set of images is recorded in the memory of the system.

Let the login of the system be submitted field U^{m_0} (Fig. 2.31, b), close to any image, for example U_1^m, recorded in the system. At the same time:

1. Image given centered relative to system axis.
2. The requirements for the fields formulated above are fulfilled, and as a result, the ratio of (2.65, 2.66).

Field in plane x_f described by the expression

$$U(x_f) = \Im^{m_0}H(x_f) =$$
$$= \Im^{m_0}\Im^{m*}\exp\left\{j\frac{k}{2f}(m - 1)\Delta x_f\right\}\exp(jkx_f \sin\alpha) + R^{m,m_0}, \tag{2.76}$$

where R^{m,m_0} combines all other add-ons.

The first add in (2.76) can be transformed to the view:
$$U_1 = \mathfrak{I}^{m_0}\mathfrak{I}^{m*}\exp(jk\delta_{m_0}x_f) \qquad (2.77)$$
where $\delta_{m_0} = \frac{1}{2f}(m_0 - 1)\Delta + \sin\alpha$.

Add after the transparant $H(x_f)$ (рис. 2.31, b) another optical cascade with lens L_2, which is located at the focal length of the, but its optical axle in direction coincides with the direction of distribution of the flat wave P. Then the exponent multiplier in (2.77) can be interpreted as the action of passing a prism-type transparant, which is set directly by $H(x_f)$ and which simply turns the recovered field to a certain angle, which is set by the inclination of a parallel beam P and image offset U^{m_0} in the initial field U_0. Then in a plane perpendicular to the optical axis of the cascade, the field will be described by an expression:

$$U(x_f) = \mathfrak{I}^{m_0}H(x_f) =$$
$$= \mathfrak{I}^{m_0}\mathfrak{I}^{m*}\exp\left\{j\frac{kx_f}{2f}(m-1)\Delta\right\}\exp(jkx_f\sin\alpha) + R^{m,m_0}. \qquad (2.78)$$

After the inverse of Fourier-transformation, the source field in the plane Z looks like:
$$U(Z) = \alpha\delta[Z - (m_0 - 1)\Delta] + \text{noise}. \qquad (2.79)$$

So, in this plane, a correlation peak (bright spot) is formed, shifted relative to zero position by the value corresponding to the reference image number.

It is in this plane that a mirror is installed that turns the beam in the opposite direction, and an additional nonlineable element NL. The transformation of the field that performs this element is qualitatively illustrated by Fig. 2.32.

Note that the expression (2.79) is executed only in a certain approximal. Consequently, the auto-correlation function has one or another thickness (Fig. 2.32, a) and is larger than the diameter of the optical cascade scattering spot with a lens L_2. Nonlinean action that a field falls on $U(Z)$, reduced to nonlinean increase in intensity $I(Z) = |U(Z)|^2$. The sensitivity curve of the NL element is given in Fig. 2.32, b.

Thus, after the action of the nonlineary element, the following signal changes occur:
1. The maximum signal intensity is amplated.
2. Narrows the width of the auto-correlation spot (to the size of the scattering spot, Fig. 2.32, c).
3. Almost disappears noise component.

Fig. 2.32 <mark>треба переклад</mark>

In this case, we can assume that at the point with the coordinate $x_{out} = (m_0 - 1)\Delta$ plane Z a point source appears, the radiation of which after passing the lens L_2 Forms a parallel beam, which in the plane x_f is described by a complex amplitude:
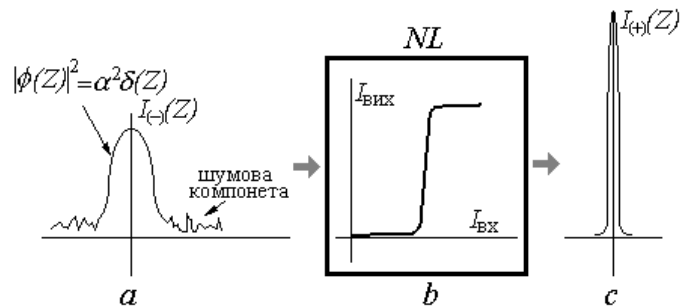
$$U_{pl}(x_f) = P\exp\left\{j\frac{k}{2f}(m_0 - 1)\Delta x_f\right\}. \tag{2.80}$$

Then the recovered from $H(x_f)$ field has the form:

$$U_r(x_f) = \Im^{m_0} + \sum_{m \neq m_0}^{M} \exp\left\{-j\frac{k}{2f}(m - m_0)\Delta x_f\right\}\mathcal{F}^m + R. \tag{2.81}$$

Accordingly, such a field after passing the light separator D will form an image on the axis of the system U^{m_0}.

2.8.4.3. Disadvantages and advantages of both systems
1. The second system is characterized by a lower noise level and keeps the reproduction of the associative image linear in intensity, even when using a nonlinear element.
2. The number of images stored on such a system is limited by the size of the input plane, while in the system with a non-stop hologram this restriction is absent.

3. BASICS OF INTEGRAL OPTICS [9,16,17]

3.1. Flat wave. General approach to the physics of wave propagation in wavelengths [9,16]

We will consider the flat wave, since it is for this case it is quite easy to get quite strict solutions of the corresponding wave equations. For the case of a cylindrical wave drive (optical fiber), this is not so easy to do. But the main physical patterns of optical wave propagation in optical fiber are almost the same as in flat wave water.

Consider the three-layer structure (Fig. 3.1). condition in progress $n_w > n_s > n_p$. Layers n_p, n_w, n_s (environments I, II and III respectively) conventionally we will call the cover layer, waver and lining, respectively.

All layers are infinite in plane x,z. Magnitude h – waveleg thickness. Layers n_p and n_s infinite thickness. So, if any reflections of light are possible in the system, they occur only at the boundaries of the environments n_p, n_w and n_w, n_s. Imagine that a flat wave is spreading in the direction z, the polarization of which coincides with the axis y (TE- wave). Choice TE-wave is not fundamental.
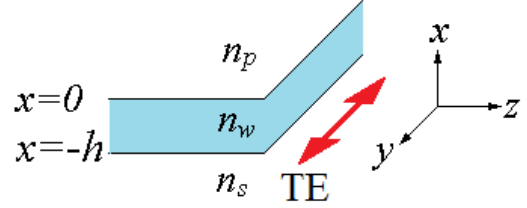
Рис. 3.1

You can consider the TM wave. Any other oscillation can be considered as a superposition of TE- and TM oscillations. The distribution constant that determines the rate at which the wave spreads in the wavelength is equal to β. Then the wave equation for such a wave has the form:

$$\nabla^2 E_y - \frac{n_i^2}{c^2}\frac{\partial^2 E_y}{\partial^2 t} = 0, \qquad (3.1)$$

where $i = p, w, s$, corresponds to the relature coefficient in each environment.

Accordingly, the solution (3.1) has the form of:

$$E_y = \tilde{U}_y(x)\exp[j(\omega t - \beta z)]. \qquad (3.2)$$

Naturally, in accordance with the law of energy conservation and intuitive requirement (a loose wave can only spread in wave waves) $\tilde{U}_y$ in general, will be written as follows:

$$\tilde{U}_y = \begin{cases} A\exp(-qx), & 0 \le x \le \infty \ \text{(I)} \\ B\cos(rx) + C\sin(rx), & -h \le x \le 0 \ \text{(II)} \\ D\exp[p(x+h)], & -\infty \le x \le -h \ \text{(III)} \end{cases} \qquad (3.3)$$

where A,B,C,D,q,r,p –Some constants. (3.3) states that there is some fluctuation in the wavelep, and in the cover layer and the linings of oscillations are sedentary according to exponential law. The speed of atering is determined by constant q,p.

Derivatives from $\tilde{U}_y$ in environments I, II, III determined by ratios:

$$\frac{\partial \tilde{U}_y}{\partial x} = \begin{cases} -qA\exp(-qx), & \text{(I)} \\ -rB\sin(rx) + rC\cos(rx), & \text{(II)}. \\ pD\exp[p(x+h)], & \text{(III)} \end{cases} \qquad (3.4)$$

Due to continuity $\tilde{U}_y$ and its derivative $\frac{\partial \tilde{U}_y}{\partial x}$ on the boundaries of environments n_p, n_w та n_w, n_s of (3.3) and (3.4) follows the following:

At $x = 0$ (the boundary of environment I and II):
$$\begin{cases} A = B \\ -qA = rC \end{cases},$$
respectively
$$A = B = -\frac{r}{q}C = C', C = -\frac{q}{r}C',. \tag{3.5}$$

At $x = -h$ (environment boundary II and III):
$$C'\cos(rh) - \frac{q}{r}\sin(rh) = D.$$

So, taking into account (3.5), (3.3) will be rewrited as:
$$\tilde{U}_y = \begin{cases} C'\exp(-qx), & 0 \le x \le \infty \ (\text{I}) \\ C'[\cos(rx) - \frac{q}{r}\sin(rx)], & -h \le x \le 0 \ (\text{II}) \\ C'[\cos(rh) - \frac{q}{r}\sin(rh)]\exp[p(x+h)], & -\infty \le x \le -h \ (\text{III}) \end{cases}. \tag{3.6}$$

Unlike (3.3), u (3.6) instead of four constants A,B,C,D(as it turned out, related) we have only one constant for all types of waves C', which can be ignored when rationing the amplitudes of these waves (for example, up to one).

Therefore, only the explicit appearance of constants is not clear q,r,p.

Recall that the operator ∇^2 in our case (if $\frac{\partial^2}{\partial y^2} = 0$) looks like $\nabla^2 = \frac{\partial^2}{\partial x^2} + \frac{\partial^2}{\partial z^2}$. Let's start (3.6) first in (3.2) and then in (3.1). Constant C' in all equations will be reduced. All exponential members will also be reduced, as $\frac{\partial \exp(t)}{\partial t} = \exp(t)$ and they are located both on the right and on the left side, all equations.

Therefore, for the region I we have:
$$q^2 - \beta^2 = -\frac{n_p^2}{c^2}\omega^2. \tag{3.7}$$

Given that $k = \frac{\omega}{c}$ (3.7) takes effect:

$$q = (\beta^2 - n_p^2 k^2)^{1/2}. \tag{3.8}$$

For scope II we have:

$$\frac{\partial}{\partial x} \sim -r\sin(rx) - \frac{q}{r}\cos(rx);$$
$$\frac{\partial^2}{\partial x^2} \sim -r^2[\cos(rx) - \frac{q}{r}\sin(rx)]; \tag{3.9}$$
$$\frac{\partial^2}{\partial z^2} \sim -(-j\beta)^2[\cos(rx) - \frac{q}{r}\sin(rx)];$$
$$\frac{\partial^2}{\partial t^2} \sim -(j\omega)^2[\cos(rx) - \frac{q}{r}\sin(rx)].$$

Where it comes from:
$$r = (n_w^2 k^2 - \beta^2)^{1/2}. \tag{3.10}$$

For region II, we have:
$$p = (\beta^2 - n_s^2 k^2)^{1/2}. \tag{3.11}$$

Consequently, with the accuracy of C' and β the field is defined in all three areas due to known parameters. At the same time, the constant C' can be ignored. It remains to determine only the explicit appearance of permanent distribution β.

From the condition of continuity of derivatives on the boundaries of the structure

environments when $x = -h$ з (3.4 і 3.6) we have a ratio for the first derivatives:

$$\tan(rh) = \frac{r}{r^2 - qp}(q + p) \qquad (3.12)$$

If in (3.12) substitute q,r,p(3.8,10,11), then (3.12) will be an equation from one unknown β. From this transcendental equation we see that wave propagation in the system is only possible for certain discrete β, that satisfy (3.12).

The equation (3.12) is called the dispersion equation of the waveleg. Waves corresponding to these β_m, called *wave-drive* mods.

For TM oscillations, a similar equation can be obtained:

$$\tan(rh) = \frac{r}{r^2 - \overline{qp}}(\bar{q} + \bar{p}), \qquad (3.13)$$

where $\bar{q} = \frac{n_w^2}{n_p^2}q$, $\bar{p} = \frac{n_w^2}{n_s^2}p$.

3.2. Opto-geometric approach to the physics of flat wave [9,17]
3.2.1. Variance waveleg equation

Again consider the three-layer structure (Fig. 3.2), for which the condition is met $n_w > n_s > n_p$.

Imagine that some flat wave spreads at an angle in the wavelets Θ_w to normal to the surface of the wavelet. Naturally, snellius invariant is performed:

$$\begin{cases} n_w \sin\Theta_w = n_p \sin\Theta_p \\ n_w \sin\Theta_w = n_s \sin\Theta_s \end{cases}, \qquad (3.14)$$

from where for the angle Θ_w we have:

Рис. 3.2

$$\begin{cases} \Theta_w = \sin^{-1}(\frac{n_p}{n_w}\sin\Theta_p) \\ \Theta_w = \sin^{-1}(\frac{n_s}{n_w}\sin\Theta_s) \end{cases}. \qquad (3.15)$$

The spread speed of any wave in the wave environment is the same for any wavelength Θ_w. But, if we consider the spread of the wave along the axis z, then its швидкість (константа розповсюдження) залежить від цього кута (для різних Θ_w we have different optical pathways and different phase latency in the interseading environments). The wave distribution constant can be described by the ratio:

$$\beta = kn_w\sin\Theta_w. \qquad (3.16)$$

Magnitude

$$n_f = n_w\sin\Theta_w \qquad (3.17)$$

is called an *effective relature indicator*.

For corners $\Theta_{wp} > \sin^{-1}\frac{n_p}{n_w}$ and $\Theta_{ws} > \sin^{-1}\frac{n_s}{n_w}$, as you know, there is a complete internal reflection. Consequently, the light wave that spreads at an angle $\Theta_w > \Theta_{wp}$ (because $\Theta_{wp} > \Theta_{ws}$) does not leave the wavelet medium. Note that when the wave bounces off the boundary of the partition, the wave acquires an additional phase shift (the so-called *Gaussian-Henchen amendment*):
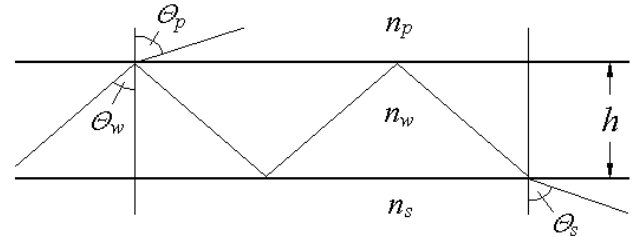
For TE-mode:

$$\tan \Phi_{wi} = \frac{(n_w^2 \sin^2 \Theta_w - n_i^2)^{1/2}}{n_w \cos \Theta_w}. \tag{3.18}$$

For TM-mode:

$$\tan \Phi_{wi} = \frac{n_w^2}{n_i^2} \frac{(n_w^2 \sin^2 \Theta_w - n_i^2)^{1/2}}{n_w \cos \Theta_w}. \tag{3.19}$$

where $i=p,s$.

The presence of such phase shifts in terms of geometric optics can be explained only in one way. The wave on the boundary of the partition is not reflected immediately, but is immersed by a certain distance into the medium bordering the wavelep (see Figure 3.3).

Fig. 3.3

Phase shifts in this case are determined by double optical l_{ps}.

From the conditions of complete internal reflection there are no physical restrictions on the angles under which the wave spreads in the wave. But:
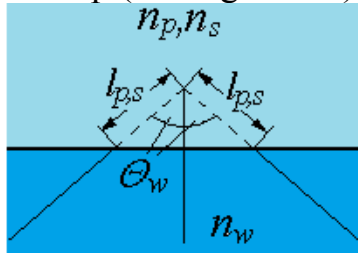
1. The wave that spreads in the wavelength is absolutely coherent, that is, the length and time of coherence are unlimited.

2. The front of the wave is also unlimited in space.

In this case, oscillations at any point of the wave is a superposition of an unlimited number of waves reflected from the boundaries of the wavelengths that interact with each other. These waves can reinforce each other or extinguish if spread in phase or antiphage. When the angles Θ_w such that the oscillations are ampled, they say that the condition of self-compliance is met.

Fig. 3.4

The condition of self-compliance is performed if the ratio is met (see Figure 3.4):

$$n_w(l_{1,2,3} - l_{1,2'}) = m\lambda \text{ або } kn_w(l_{1,2,3} - l_{1,2'}) = 2m\pi. \tag{3.20}$$

Note that (3.20) does not take into account delays that occur on the boundaries between environments.

From the figure it follows that:

$$l_{1,2,3} = \frac{2h}{\cos \Theta_w} \text{ та } l_{1,2'} = \frac{h}{\cos \Theta_w}(1 - \cos 2\Theta_w) \tag{3.21}$$

If we take into account the phase shifts that occur with complete internal reflection, then in the end the condition of self-compliance has this form:

$$2kn_w h\cos \Theta_w - 2\Phi_{w,s} - 2\Phi_{w,p} = 2m\pi. \tag{3.22}$$

The expression (3.22) as well as (3.12) is called a dispersion equation. This transcendental equation of solutions gives a set of angles Θ_w in interval $\sin^{-1}\frac{n_s}{n_w}, \frac{\pi}{2}$. This set of angles determines the angles of flat waves that can propaed in wavelengths, as well as their respective effective relapertion and distribution constants, i.e. determines the characteristics of wave-like mods.
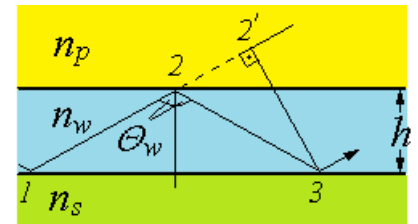
3.2.3. Effective wave weight thickness

As previously claimed, the wave that spreads in the wave dives into the media of the cover layer and lining. So, the layer in which the wave-like process occurs has a greater thickness than the geometric thickness of the wave layer. We will call the thickness of the wave structure h_f, in which 90 percent of the wave energy (standard criterion) is transmitted, the effective thickness of the wavelength. We will find this value.

Let's turn to Figure 3.5.
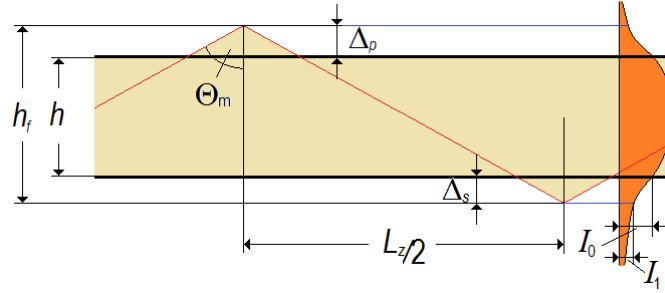
Fig. 3.5

We find the distance at which the intensity of te-wave in zones I and 3i decreases by 10 times. To do this, use the 1st and 3rd equations of the ratio (3.3). For simplicity, we will use a slightly different condition. Namely, we will assume that the amplitude of the field in zones I and III decreases in e times (the intensity drops about 8 times).

Consequently, the distances Δ_p and Δ_s can be found from the ratios:

$$\begin{cases} \widetilde{U}_p \sim \exp(-q\Delta_p) = e^{-1} \\ \widetilde{U}_s \sim \exp(-p\Delta_s) = e^{-1} \end{cases} \tag{3.23}$$

From (3.23) follows:

$$\begin{cases} \Delta_p = \dfrac{1}{q} = \dfrac{1}{k}(n_f^2 - n_p^2)^{-1/2} \\ \Delta_p = \dfrac{1}{p} = \dfrac{1}{k}(n_f^2 - n_s^2)^{-1/2} \end{cases} \tag{3.24}$$

$$h_f = h + \frac{1}{k}\left[\left(n_f^2 - n_p^2\right)^{-\frac{1}{2}} + \left(n_f^2 - n_s^2\right)^{-\frac{1}{2}}\right]. \tag{3.25}$$

Note that the values Δ_p and Δ_s, and as a result, the effective thickness of the h_f (as well as the corresponding modal characteristics) depend not only on the parameters of the substantive wavelength, the cover layer, but also on the wavelength ($\Delta_{p,s} \sim \lambda$).

Figure 3.6 shows the qualitative structure of oscillation types, which are implemented in a wave-like structure for different distribution constants. In accordance with the size of this constant, the fashions of the cover layer, substlets and wave-like mods are conditionally distinguished. Illustration shows when the graph graph of the substvo is greater than the graphing of the cover layer $(n_s > n_p)$.
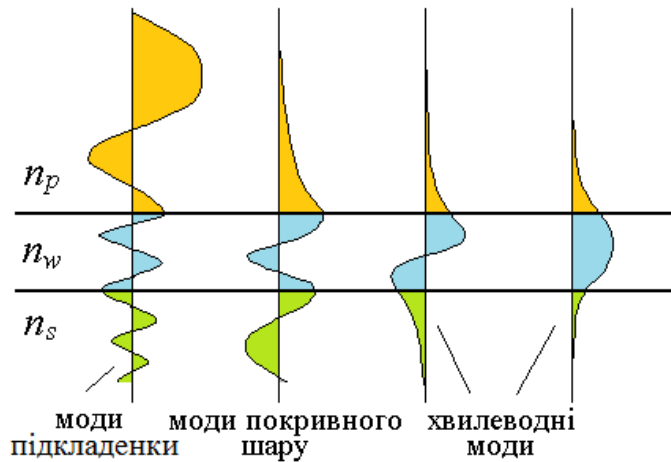
So, directly in the wavelets can exist only certain types of oscillations – wave-like fashions. The angles at which they propax are determined from the dispersion equation. In some ways, it can be argued that the process of wave propagation is zigzag in nature.

Fig. 3.6
Треба переклад

At the same time:

1. The smaller the fashion number, the greater the angle $\Theta_{w,s}$ it corresponds.

2. The smaller the fashion number, the less it plunges into the environment.

3. The larger the fashion number, the less powerful it is (if the wavelend absorption rate is small). Fashion with the number 0 is the main fashion and it is the most powerful.

3.2.4. Optical zigzag length

Using an opto-geometric approach, it can be assumed that the wave in the chilewater spreads zigzag, penetrating into the boundary of the environment at a distance Δ_p and Δ_s. Based on simple geometric considerations (see Figure 3.7) we have a length optical zigzag:
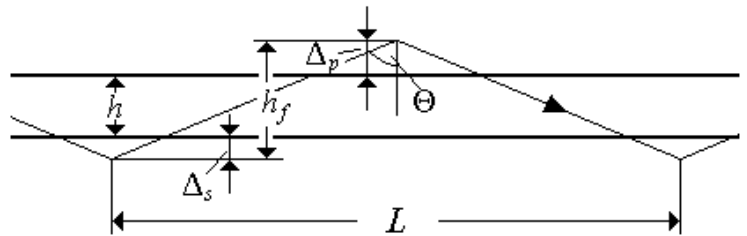
Рис. 3.7

$$L = 2h_f \tan \Theta \qquad (3.26)$$

Or given that $n_f = \sin \Theta_w$:

$$L = \frac{n_f}{(n_w^2 - n_f^2)^{1/2}} 2\left\{ h + \frac{1}{k}\left[\frac{1}{\left(n_f^2 - n_p^2\right)^{\frac{1}{2}}} + \frac{1}{\left(n_f^2 - n_s^2\right)^{\frac{1}{2}}} \right] \right\}. \qquad (3.27)$$

3.2.5. Кількість мод, які можуть розповсюджуватися у хвилеводі [18]

There are cases of symmetrical $(n_p = n_s)$ and asymmetric $(n_p \neq n_s)$ wave drive.

For the case of symmetric wave drive $(n_p = n_s = n)$:

$$M < \frac{2h}{\lambda}(n_w^2 - n^2)^{1/2} + 1. \tag{3.28}$$

For a very asymmetric wave ($n_s \gg n_p$):

$$M < 0.5 + \frac{2h}{\lambda}[2n_w(n_w - n_s)]^{1/2} \tag{3.29}$$

The question arises – can wave mods spread for any thickness of the wavelet? From the analysis of the dispersion equation, it follows that with an increase in the thickness of the wave, the number of mods increases. Another question is whether fashion will be distributed in a very thin wave ($h \to 0$)?

Let's turn to the equation (3.12):

$$\tan(rh) = \frac{r}{r^2 - qp}(q + p),$$

which is for small h transformed into an expression:

$$h \approx \frac{q+p}{r^2 - qp} \tag{3.30}$$

a) Symmetric wave. For a symmetric waver, it has the form:

$$h \approx \frac{2p}{r^2 - p^2} \tag{3.31}$$

Taking into account (3.10) and (3.11) we have

$$h = \frac{2(\sin^2\Theta_w - \frac{n_s^2}{n_w^2})^{1/2}}{kn_w(\cos^2\Theta_w - \sin^2\Theta_w + \frac{n_s^2}{n_w^2})} \tag{3.32}$$

From (3.32) it follows that for any thickness and wavelength λ(including when $h \to$

a   *б*   *в*

Рис. 3.8

0 there will be at least one wave-like fashion. Note that when $h \to 0$ $\sin\Theta_w \to \frac{n_s}{n_w}$. In other words (see Figure 3.8 a), the angle of fashion distribution approaches a critical angle Θ_{kr} (full internal reflection angle). Thus, with an increase in the thickness of the waveleod, the distribution angle of zero fashion increases (Fig. 3.8 b). Finally, at a certain frequency, the 1st fashion appears (Fig. 3.8 v) etc.
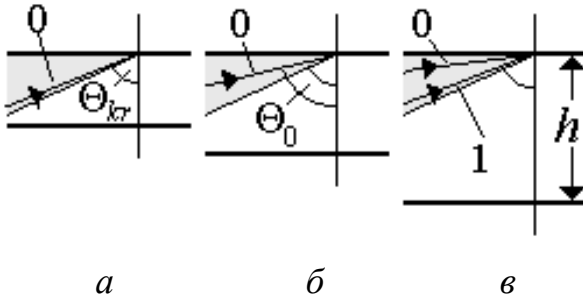
B) Asymmetric wave. For waves of this type of equation (3.31) will be converted to an expression:

$$h = \frac{1}{kn_w}\frac{(\sin^2\Theta_w - \frac{n_s^2}{n_w^2})^{1/2} + (\sin^2\Theta_w - \frac{n_p^2}{n_w^2})^{1/2}}{\cos^2\Theta_w - (\sin^2\Theta_w - \frac{n_s^2}{n_w^2})^{1/2}(\sin^2\Theta_w - \frac{n_p^2}{n_w^2})^{1/2}} \tag{3.33}$$

Naturally, with a decrease in the thickness of the waveleg h numerator (3.33) also decreases. However, the numerator never reaches zero because $n_s \ne n_p$. So there is some thickness h_{kr} asymmetric wavelength, such that for a given

wavelength λ in structures with a lower thickness, the wave-like process does not occur.

From the same expression it follows that there is a critical wavelength λ_{kr}, such that with an increase in λ and this thickness of the structure h wave-water process is also not observed.

Note that the minimum value of the numerator reaches when $\Theta_w = \Theta_{kr}$ (fulfillment of the condition of full internal reflection on the lower boundary):

$$(\sin^2\Theta_w - \frac{n_s^2}{n_w^2})^{1/2} = 0 \tag{3.34}$$

It is in this case that the 0th (main) waveleg fashion appears and the equation (3.33) takes the form:

$$\frac{h_{kr}}{\lambda_{kr}} \approx \frac{1}{2\pi} \frac{(n_s^2 - n_p^2)^{1/2}}{n_w^2 - n_s^2} \tag{3.35}$$

A ratio (3.35) can be used to assess h_{kr} and λ_{kr}.

Note that the smaller the thickness of the wave, the deeper the wave mods penetrate into the cover layer and lining environments. It is this fact that can explain the impossibility of the wave-draining process in a very thin asymmetric waveleg. Figuratively (not strictly) speaking, in such a structure, with very small h due to the asymmetric distribution of the field along the axis x maximum wave energy distribution ejected from the wavelet and the wave-water process stops.

3.2.6. The difference between the thyrization coefficients of the waveleg and the surrounding layers [18]

The question arises – what should be the difference between the thyrization coefficients in order for the wave-water process to form?

It is clear that for a symmetric wave for the existence of the main, 0th fashion, any difference between the relapor coefficients is enough. In general, for a symmetric waveleg, there is a ratio of:

$$\Delta n = n_w - n > \frac{m_0^2 \lambda^2}{4h^2(n_w + n)}, \tag{3.36}$$

where m_0 – maximum fashion number that can exist in wave water.

Similar ratios can be recorded for cases where the difference between relature indicators:

1. small $n_w \approx n$:

$$\Delta n = n_w - n > \frac{m_0^2 \lambda^2}{8h^2 n_w}, \tag{3.37}$$

2. and vice versa, a significant $n_w \gg n$:

$$\Delta n = n_w - n > \frac{m_0^2 \lambda^2}{4h^2 n_w}, \tag{3.38}$$

where $m_0 = 0,1,2, ...$ – wave mode number.

For asymmetric wave drive ($n_s \gg n_p$, $n_w \to n_s$) a similar condition has the form:

$$\Delta n = n_w - n_s > \frac{(2m_0 + 1)^2 \lambda^2}{32h^2 n_w} \tag{3.39}$$

You can make the following assessments: For asymmetric wavelengths, the thickness is close to the wavelength and n_w order 2 Δn is a value close to 0.01.

3.3. Real wave [19,20]

Consideration of the processes that occur in the wavewater system was carried out by us, based on the assumption that the wavelength is infinite, the material of the wave-water layer is absolutely transparent, and the boundaries between the environments are ideal.

We will now assume that:

1. Wavelegging absorption rate, although small, is not equal to 0;

2. Its final length;

3. Waveguide boundaries (for simplicity at least one) are promodulated by a weak sinusoidal grid with a certain period.

Note that the consideration of waveguid processes during the 3rd condition then makes it possible to move to a distorted boundary of the general type, since arbitrary modulation of the boundary can be considered as a superposition of sinusoidal laths with a certain distribution of depth and periods.

Let's turn to Figure 3.9. In order for the wavewater system to establish a field that does not depend on the z, we will send a flat wave with an amplitude from the cover layer to the grid A_0. Then a certain energy balance will be established in the system.

Since the wave-drive environment has a certain absorption, the relaut coefficient (including the effective relamination coefficient) becomes a complex value:

$$\tilde{n}_w = n_w + j\tau, \qquad (3.40)$$

where n_w – the actual part of the fracture indicator (directly "reflection index"), τ – absorption index.
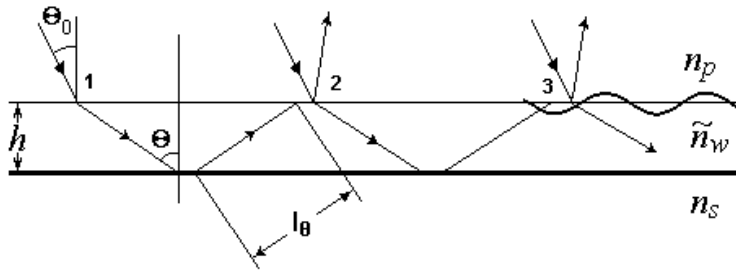
Рис. 3.9

You can show that if you τ not very large, wave-like properties of the structure and its parameters (mod spectrum, effective thickness, etc.) are determined by the value n_w.

Recall that in accordance with the law, Booger poured absorption on the amplitude of the wave is described by the ratio:

$$A(l) = A_0 e^{-l\tau}, \qquad (3.41)$$

where l – wavelength in the environment.

According to the grid formula, the diffraction angle is determined by the formula:

$$n_w \sin \Theta = n_p \sin \Theta_0 + \frac{m\lambda}{T}, \qquad (3.42)$$

where m – diffraction order number.

We will introduce a certain value – amplitude diffraction efficiency, which shows what the fate of the amplitude of the wave, which is held with a grid, is directed in the direction of a certain diffraction order. So, wave amplitude after interaction with the grid in the direction of m diffraction order is described by the expression:

$$A_m^i = A \begin{cases} T_m, \\ R_m, \end{cases} \tag{3.43}$$

where A – wave amplitude to interaction with the grid, $i=r,t$ confirms the reflected or missed wave formed after the diffraction of the initial wave on the grid.

T_m, R_m – amplitude diffraction efficiency of the grid for passing and reflecting, respectively.

So, we assume that at point 1 (the point of radiation input into the wavelength) before the interaction with the grid of the wave amplitude in the wavelength has a value A_0. After introduction to the wavelead, the complex amplitude is described by the formula:

$$U_1 = A_0 T_m, \tag{3.44}$$

At the same time, without losing the generality, we believe that the wave phase at point one is equal to 0, since the determining phase is not the absolute phase of oscillation, but the difference between the oscillations at different points. At point 2 before the interaction of the wave with the grid (after reflecting it from the lower boundary), the complex amplitude has the form:

$$U_{2(-)} \sim \tilde{\tau} A_0 T_m e^{j\Phi_m}, \tag{3.45}$$

where $\tilde{\tau} = \exp(-2\tau l_\Theta)$ – attenuation of the wave amplitude by spreading between points 1,2, $l_\Theta = \dfrac{h}{\cos\Theta}$, Φ_m – phase raid due to diffraction and interaction with the lower boundary. From expression $n_f = n_w \sin\Theta$ it follows that $\cos\Theta = \sqrt{1 - \dfrac{n_f^2}{n_w^2}}$.

Than

$$\tilde{\tau} = \exp(-\frac{2\tau h n_w}{\sqrt{n_w^2 - n_f^2}}). \tag{3.46}$$

At point 2, after interaction, the complex amplitude is determined by a number of factors:

1. Boosting the wave due to additional energy from the outside (from the cover layer).

2. Radiation output due to the diffraction of the wave into the cover layer T'_m.

3. Diffraction efficiency of the grille for reflection in the 0th order R_0.

4. Phase difference $\Delta\Phi_\Theta$ between the wave of feeding and the wave spreading in the wave.

Note that the difference phases $\Delta\Phi_\Theta$ equal to 0 if the direction of the wave diffraged from the cover layer and the wave spreading along the waveguid coincides with the direction of distribution of waveguine fashion (with the condition of self-compliance of the phase of waveguid fashion in points (1) and (2) the same).

The rest of the complex amplitude at point 2 is equal to:

$$U_{2(+)} = A_0 T_m (1 + \tilde{\tau} R_0 e^{j\Delta\Phi_\Theta}). \tag{3.47}$$

Accordingly, at point 3 we have:

$$U_{3(+)} = A_0 T_m (1 + \tilde{\tau} R_0 e^{j\Delta\Phi_\Theta} + \tilde{\tau}^2 R_0^2 e^{j2\Delta\Phi_\Theta}). \tag{3.48}$$

At point N:

$$U_{N(+)} = A_0 T_m \sum_{k=0}^{N} (\tilde{\tau} R_0 e^{j\Delta\Phi_\Theta})^k. \tag{3.49}$$

(3.49) is a geometric progression with an indicator of $\tilde{\tau} R_0 e^{j\Delta\Phi_\Theta}$ Module smaller

than one $(\tilde{\tau} R_0 < 1)$.

At $N \to \infty$ its sum can be calculated by the formula $s = \frac{a_0}{1-q}$. The resulting expression takes effect:

$$U = \frac{A_0 T_m}{1 - \tilde{\tau} R_0 e^{j\Delta\Phi_\Theta}}. \tag{3.50}$$

As noted above, $\Delta\Phi_\Theta = 0$ for Θ, which coincides with the direction on wave-water mods. Accordingly, the most unfavorable distribution conditions for the wave for which $\Delta\Phi_\Theta = \pi$ (assembly of waves in the antiphr phase). We will call such directions directions on antimodes.

Let's compare the amplitudes of waves that spread in directions to fashion and antimodes. Take into account the fact that $e^{j0} = 1$, i $e^{j\pi} = -1$. Then the relationship of such amplitudes will be described by the expression:

$$\gamma = \frac{U_m}{U_{am}} = \frac{1 + \tilde{\tau} R_0}{1 - \tilde{\tau} R_0}. \tag{3.51}$$

In the absence of a grid and absolute passing of the wavelet medium $\tilde{\tau} R_0 = 1$. Respectively $\gamma \to \infty$. So, indeed, in an infinitely long completely transparent waver with perfect edges, only wave-like fashions spread. At the same time, for $\tilde{\tau} R_0 = 0.95$ $\gamma = 39$, $\tilde{\tau} R_0 = 0.8$ $\gamma = 9$. In non-epidemiological wavelengths, all types of oscillations can exist, even oscillations that correspond to the spread of the wave in the most adverse directions. It can be shown that this statement is also true for wavelengths of the final length. Figure 2.3.2 shows the qualitative distribution of the amplitude for the first two wave drive modes for different values of the parameter $\tilde{\tau} R_0$.

Note that the distribution of the amplitude shown in Figure 3.10 is very similar to the corresponding distribution in the Fabry-Perot interferometer, depending on the reflecting coefficients of flat-parallel plates. From here it follows that a flat wave can be considered as a thin resonator with infinite walls. Or, on the contrary, to analyze the processes that occur in the Fabry-Perot interferometer, you can apply the modal approach of integral optics.
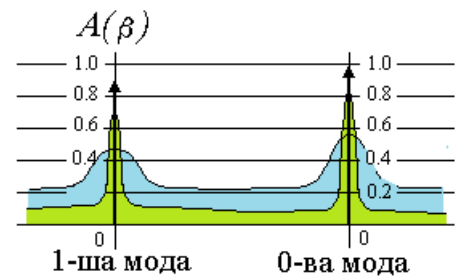
Fig. 3.10

Треба переклад

Note that in the case of the final wavelength length (even in the absence of absorption and distortion of boundaries), the spectrum of distribution of wavewater mods becomes similar to the spectrum shown in Fig. 2. 3.10. The emergence of this "expansion" of wave-water mods becomes clear if we take into account the fact that the condition of self-compliance (3.22) in practice is carried out with a certain accuracy, for example, according to Reley criterion, with accuracy to $\pm\pi/2$. Naturally, with a small wavelength, the number of zigzags carried out by wave-water fashion is also small. As a result, the variance equation is $\pm\pi/2$ is performed for a fairly wide angle interval $\Delta\Theta$. Given that the phase difference between waves that accurately spread in directions to wave-water mods and close angles will increase with an increase in the number of zigzags (increasing the length of the waveguode) it can be argued that the angle interval $\Delta\Theta$ for which there will be a significant intensity of waves will decrease and with infinitely long wavelength wavelength wavelength $J(\Theta)$ as an angle function Θ is converted to system δ-functions $\qquad (J(\Theta) \to \sum_{m=0} J_m \delta(\Theta - \Theta_m),$ characteristic of the ideal wave.

Let's make another remark. As stated above 0-th (main) fashion is the most powerful of the fashions that are distributed in wavewater. In the real integral-optical structure, this is not always the case. Very often it is made up in practice that the pass rate of the wave-water layer is much lower than the corresponding coefficients of the cover layer and substance (for example, air and optical glass). Recall that the fashion waver with a higher number plunges deeper into the environments that border the wave. Consequently, the proportion of energy carried by these mods inside the wavelet is lower than in the main fashion. Naturally, in the wavelenth with losses, such mode will be absorbed faster than modes with a higher number, and the most powerful will be modes, the parameters of which most coincide with the suffrage condition.

Fig. 3.11
Destruction of pulse shape in wave drive with modal dispersion
a – pulses (1) and (2) before passing the wave drive with significant dispersion,
b-c – pulse delays that are carried by different waver modes
d – blurring of the resulting impulse
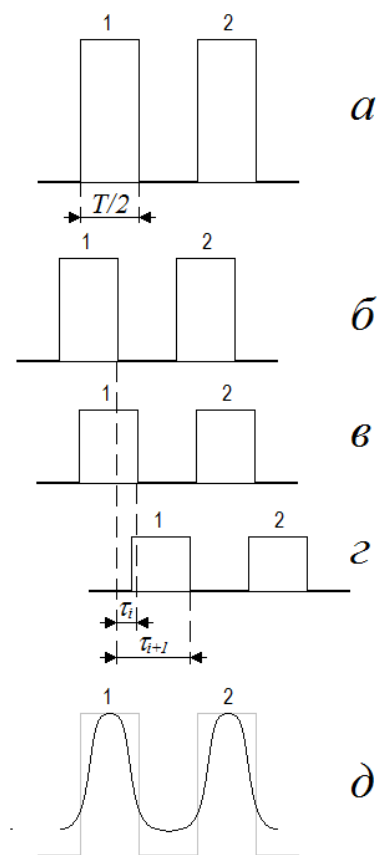
3.4. Дисперсія у хвилеводній системі

Most often, the phenomenon of dispersion in the waveguides system is considered in the optics of floodwaters, since it significantly affects the characteristics of the information transmitted by the fiber-optic channel. However, the physics of this phenomenon in the planar light is the same. So, consider this phenomenon for a planar wave. First of all, they share chromatic and intermodal (modal) dispersions.

3.4.1. Modal dispersion [9,21-27]

The phenomenon of modal dispersion is inherent in multimode waveguides. The geometric lengths of the paths along which different wavelength mods are distributed are different. In addition, different fashions delve differently into wave-blocking environments. This leads to the fact that each fashion has its own distribution constant. As a result, by the end of the optical track waves come at different times. In other words, there is a variance in the speeds (or phases) of wavelength mods.

If the wavelength length is insignificant, then the difference in delays in different modes can be neglected. Another situation arises in fiber-optic communication lines, the length of which can reach tens or even hundreds of kilometers. Then such time delays between modes become quite large compared to the period of change of the information signal. This leads to the destruction of the form of impulses that are transmitted through wave-water channels, since the information signal is carried by all wavelet modes (see Figure 3.11).

3.4.2. Chromatic dispersion [3,21-27]

Imagine that a polychromatic wave is spreading in the wave. This situation corresponds to the real case, since each radiation source has the final semi-wide radiation spectrum. The process of spreading such a wave can be considered as a process of propagation of a set of monochromatic waves. Naturally, each such wave spreads along the wavelength with its distribution constant, since this characteristic depends on the wavelength. In addition, the indicators of wavelength, substantive and cover layer environments depend on the wavelength. There is, the so-called phenomenon of dispersion of the entanglement indicator. Figure 3.12 shows the qualitative dependence of the fracture indicator on the frequency of light oscillations.
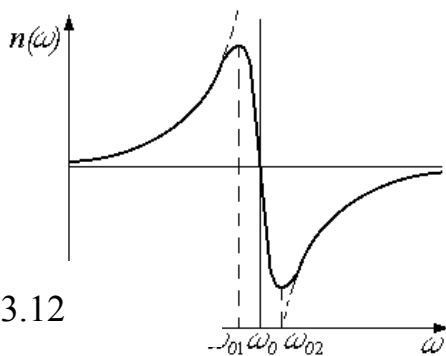
Рис. 3.12

Except for frequency intervals ω_{01}, ω_{02} relap rate increases with increasing frequency (decreases with wavelength increase). As you know, dependence of this type is called normal dispersion. In frequency interval ω_{01}, ω_{02} dispersion of the fracture indicator is called abnormal. In physics fiber optic communication lines addiction $n = f(\omega)$ called material chromatic dispersion. This name is introduced in order to distinguish this type of dispersion from others observed in wave-water systems.

Note that when analyzing the dispersion equation, we can conclude that in the case of polychromatic radiation in the wavelead, even in a monomode (in the traditional sense of this term), a set of monochromatic mods is distributed. Each such mode has its own distribution constant, which is determined by the fracture indicator for this wavelength and the condition of self-consolation (the angle of inclination to the plane of the wavelength). As a result, these waves at each wavelength have their own phase or, in other words, have different time delays at each point, which are determined by an effective reflective index. This phenomenon was called the

chromatic dispersion of the wavewater system. If the wavelength length is insignificant, then the difference in the delays of monochromatic waves resulting from the phenomenon of chromatic dispersion can in principle be neglected. However, over long distances, the time difference between waves of different lengths can be significant. This, as in the case of modal dispersion, leads to the destruction of impulses transmitted by wave-water channels (see Figure 3.11). This is especially true in modern communication, when the length of optical cables is measured in kilometers, and the frequency of the signal being transmitted is gigahertz. In SSRS, chromatic dispersion is, as usual, characterized by the coefficient of chromatic dispersion $D(\lambda)$ in units with dimension (ps/(nm km)), which determines the normalized (wavelength) signal delays arising for a given wavelength in a cable length of 1 km. On methods of reducing the effect of chromatic dispersion on the characteristics of signals transmitted through fiber, we will talk when studying the characteristics of modern lightguide.

3.4.3. Polarization variance [25,26]

Another type of dispersion can be considered in the wavewater system when considering polarizing effects. Indeed, as shown above, TE- and TM oscillations in waveleases are characterized by different dispersion equations. As a result, TE- and TM waves spreading in wavewater have different distribution constants. Imagine that a wave with elliptical polarization spreads in the wave. Such a wave can be represented as a superposition of TE- and TM waves. From this fact, it follows that the polarization state of the resulting wave will constantly change along the wavelength, since the phase difference between TE- and TM waves will constantly change due to different distribution constants. This phenomenon was called polarization dispersion. It should be noted that if such a wave transmits an information signal, then, as in previous cases, pulses at the output of the wave-water structure will be erode. However, we must take into account the fact that in fiber-optic communication lines the influence of polarization dispersion on the form of impulse is usually much less than the influence of modal and chromatic dispersions.

3.4.4. Waver with an optical track of limited length. Trace variance 3.4.4.1. Variance equation for wave drive with an optical track of limited length

We assume that the boundaries of the angle interval within which wave-water fashion can exist are determined by the level of fall-off of the wave intensity to half the maximum value of this value for the wave spreading at the optimal angle, which is the solution of the dispersion equation of the ideal waveguide.
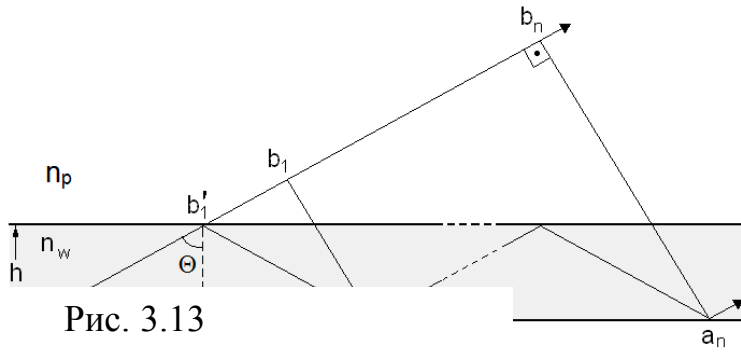
In this case, the deviation of the phase of a certain wave from the phase of the ideal wave will be considered insignificant if it does not exceed the relay criterion $\frac{\pi}{2}$.

Рис. 3.13

Again consider (Fig. 3.13) three-layer structure (with wave layer thickness h), for which the condition is met:

$$n_w > n_s > n_p. \tag{3.52}$$

where n_w, n_s, n_p – indicators of thyrization of the wave-watering layer, lining and cover screw, respectively.

Imagine that some flat wave spreads in the wavelet at an angle Θ_w to normal to the surface of the wavelet. At the same time, the wavelength length is such that the wave during distribution can make n «zigzags».

Naturally, as in the case of an ideal wave drive, a wave-water process can occur only in a situation where the condition of complete internal reflection on the lower boundary is met, since $n_s > n_p$:

$$\Theta_w > \Theta_{kr} = \sin^{-1}\frac{n_s}{n_w}. \tag{3.53}$$

Note that when the wave bounces off the boundary of the partition, the wave acquires each time, an additional phase shift (Gauss-Henchen correction, ratio (3.18) and (3.19)).

From the condition of complete internal reflection there are no physical restrictions on the angles at which the wave in the waveleg can spread, if $\Theta_w > \Theta_{kr}$. However:

1. The wave that spreads in the wavelength is absolutely coherent, that is, the length and time of coherence are not limited.

2. The front of the wave is also unlimited in space.

In this case, oscillations at any wavelength point are a superposition of an unlimited number, many times reflected from the boundaries of the wavelength of waves that interact with each other. These waves, as in the case of an ideal wavegud, can reinforce each other, or extinguish if distributed in phase or antiphage. When the angles Θ_w such that the oscillations are ampled, they say that the condition of self-compliance is met.

Note that unlike the ideal waveguod, where the analysis was carried out only for one zigzag, in our case it is necessary to consider all n zigzags.

Then the corresponding condition of self-compliance has the form (see Figure

3.13):
$$n_w\left[l_{ob_1'a_1} - l_{ob_n}\right] - 2\Phi_b/k = m\lambda, \text{ або } kn_w\left[l_{ob_1'a_1} - l_{ob_n}\right] - 2\Phi_b = 2m\pi, \quad (3.54)$$
where l_i – matching geometric lengths, Φ_b – the total phase shift that occurs with all wave reflections from the boundaries of the waveguage and inter limiting media, $m = 0.1,2 \dots ,$.

From the figure it follows that:
$$l_{ob_1'a_1} = \frac{2h}{\cos\Theta_w} \text{ и } l_{ob_n} = \frac{nh}{\cos\Theta_w}(1 - \cos 2\Theta_w). \quad (3.55)$$

If we take into account the phase shifts that occur with the single interaction of the wave with the edges, then in the rest the condition of self-coordination has this form:
$$n(2kn_w\cos\Theta_w - 2\Phi_{w,s} - 2\Phi_{w,p}) = 2m\pi. \quad (3.56)$$

Expression (3.56) And is a variance equation for a wave drive with an optical track of limited length. This is a transcendental equation whose solutions give a set of angles in intervals $\sin^{-1}\frac{n_s}{n_w} < \Theta_w < \pi/2$. This set of angles determines the angles of flat waves that can spread in the wavelength, as well as the corresponding effective relapation indicators and distribution constants, that is, determine the characteristics of waveguides mods.

Note that according to relay criterion, the phases of two waves are considered the same if their difference does not exceed $\pi/2$. Then the ratio (3.56) should also be performed within the same accuracy.

Based on this ratio (3.56) for a real wave drive with an optical track of limited length is transformed to the view:
$$n(2kn_w\cos\Theta_w - 2\Phi_{w,s} - 2\Phi_{w,p}) = 2m\pi \pm \delta. \quad (3.57)$$

Or by dividing the right and left parts into n and reassigned m/n on l we have
$$2kn_w\cos\Theta_w - 2\Phi_{w,s} - 2\Phi_{w,p} = 2l\pi \pm \frac{\delta}{2n}. \quad (3.58)$$
where $l=0,1,2, \dots ,$ n – number of zigzags carried out by the wave spreading at an angle Θ_w along the optical waveleg route, $\delta \leq \pi/2$ permissible phase error.

Note that the expression (3.58) is very similar to the dispersion equation of the ideal waveleg, with the exception of the last member. At $n \to \infty$ (3.58) transitions to the traditional dispersion equation.

Analyze the equation (3.58):

1. Obviously, the maximum deviation of the angles of distribution of the wave Θ_{1w} and Θ_{2w} from angles corresponding to wavewater mods Θ_l, resulting from the solution of the dispersion equation for the ideal wavelegum is achieved for phase error $\delta = \pm\pi/2$. Then the angle interval in which flat waves can exist can be defined as the difference of angles Θ_{1w} and Θ_{2w}:
$$\Delta\Theta_l = |\Theta_{1w} - \Theta_{2w}|. \quad (3.59)$$

2. Simply show that in this case, due to the interference addition, the intensity of waves with "limit" distribution angles Θ_{1w} and Θ_{2w} halved in matching fashion of the perfect wave.

3. Angle differences $\Delta\Theta_l = |\Theta_{1w} - \Theta_{2w}|$ can be matched by the difference between distribution constants:
$$\Delta\beta_l = kn_w|\sin\Theta_{1w} - \sin\Theta_{2w}|, \quad (3.50)$$
which leads to a phenomenon similar to modal dispersion. This phenomenon will be called trace dispersion.

4. Obviously, unlike modal dispersion, the effect that increases when the optical track length increases, the trace variance will affect the less, chim longer wavelength.

3.4.4.2. Assessment of the impact of trace variance

1. The analysis will be carried out for a wave-water layer of quartz glass (optical fiber). The erosion rate of the wavelet can be determined by the Sellmeyer formula [20].

$$\varepsilon = 1 + \frac{a_1\lambda^2}{\lambda^2-l_1^2} + \frac{a_2\lambda^2}{\lambda^2-l_2^2} + \frac{a_3\lambda^2}{\lambda^2-l_3^2} \tag{3.51}$$

where

$$a_1=0{,}69616630, \quad l_1=0{,}068404300,$$
$$a_2=0{,}40794260, \quad l_2=0{,}11624140,$$
$$a_3=0{,}89747940, \quad l_3=9{,}8961610.$$

2. The difference between reflection index of the kernel and shell Δn is the value of $0.001 - 0.01$.

3. As "test" fibers we will use standard fibers with a core diameter of 10 microns (single-mode fiber) and 50 microns (multimode fiber).

4. The wavelengths of radiation with which fiber is excited correspond to the so-called 1st, 2nd and 3rd transparency windows of standard quartz fiber. Under $\lambda=0.9$ mcm, $\lambda=1.33$ mcm i $\lambda=1.55$ mcm.

At the first stage, we will evaluate the "half-wide" angle interval, in which wave-water mods can spread in wavelets with a small length of the optical track. Such assessments can be useful in the design of optical integrated circuits (OIS).

Figure 3.14 illustrates the change in the angular interval in which waveguid mods in quartz multimode waveguids can be distributed if only one wave-water zigzag is carried out.

As you can see from the figure, the corner spacing $\Delta\Theta$ decreases by mary increasing fashion number. However, the length of the zigzag in fashion with different number is different. Chim is the smaller the fashion number, the greater the length of the zigzag.

Figure 3.15 illustrates the change of angular iteration $\Delta\Theta$ for different mods at the same length of the optical track of about 16 mm, for fiber with a core diameter of 50 microns. Wavelength of radiation $\lambda=0.9$ mcm.

Fig. 3.14. Half-wide angular range of wavewater mods for one wave-water zigzag in quartz multimode fiber. Kernel diameter 50 microns, $\lambda=1.55$ microns
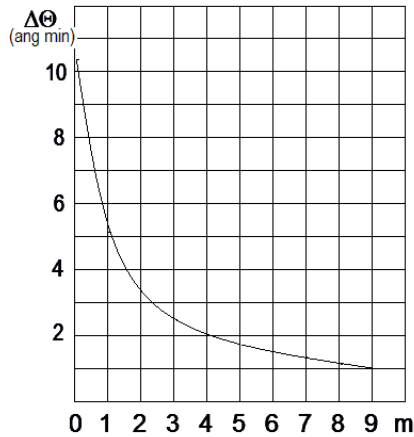
Fig. 3.15. Change the corner spacing $\Delta\Theta$ for different mods at the same length. The length is close to 16 mm. The diameter of the wave duct nucleus is 50 microns. Wavelength of radiation $\lambda=0.9$ mcm.

Naturally, a different number of zigzags are placed on the length of the waveguod, which correspond to different fashions. In particular, it is from this $\Delta\Theta$

decreases rapidly as the fashion number increases.

Figure 3.16 shows the change in size ΔΘ depending on the wavelength of radiation for the main fashion multimode waveguid and one wave zigzag.
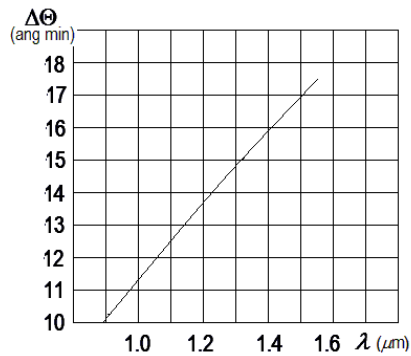
Fig. 3.16. Change ΔΘ depending on the wavelength of radiation for the main fashion multi-mod wave. One wave-water zigzag. Waver nucleus diametr 50 microns.

As we can see from the figure, with an increase in the wavelength of radiation ΔΘ grows almost linearly.

Given that integral optics are the theoretical basis of fiber optic communication lines, we will evaluate the effect of trace dispersion on signal transmission speed in relatively short fibers. Because the value of the ΔΘMuch less than the angular distance between mods, as a result, the effect of trace variance is much less than the effect of intermodal dispersion. That is why for ratings we will use a standard single-mode wave with a core diameter of 10 microns.

Time delays arising from the effects of chromatic dispersion for a radiation source with a spectral width of 2 nm were calculated for the leveling. The corresponding distribution constants were calculated from the solutions of equation 3.58 when changing the central wavelength to nm and under the condition $l, \delta = 0$.

The results of calculations are illustrated with Figure 3.17.
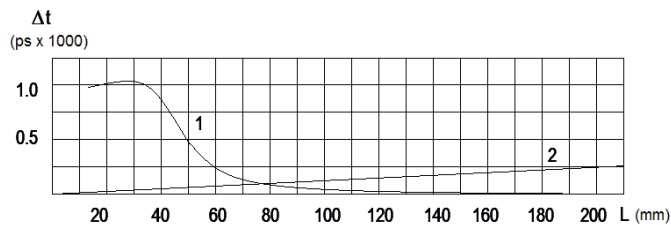
Rice. 3.17. Time delays that occur in fiber due to trace and chromatic dispersion. Fiber kernel diameter – 10 microns. λ=1.55 мкм. 1 – impact of trace dispersion; 2 – exposure to chromatic dispersion.

As we can see from the figure, unlike the time delay caused by chromatic dispersion, which increases linearly as the length of the optical track (curve 2) increases, the time delays caused by trace dispersion (curve 1) on optical tracks of more than 10 cm are reduced to almost zero.

At high transmission speeds, the effect of chromatic dispersion begins to appear on the lengths of communication lines that have a length of several kilometers.

It follows that trace variance practically does not affect the signal transmitted in fiber, and is relevant exclusively for integrated optics devices.

3.5. **Wave propagation in gradient wavelength** [9,28]

The dependence of the change in the thyrization rate along the intersection of the wavelen is called the profile of the thyrization indicator. Up to this point, the wavelets that were considered had clearly defined boundaries between the hilevod medium and the substantive, the chilevod and the cover layer. At the same time, it was assumed that the value of the fracture indicator within the same environment is
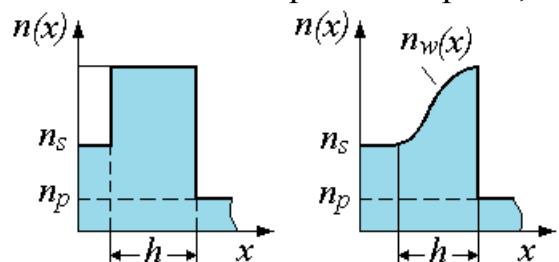
constant. Such wave-waterers, in particular, lighters are called wavelets with a stepped profile of the thyrization indicator (see Figure 3.17 a). However, most wavewater does not meet this assumption (see Figure 3.17 b). First, as a rule, there is no clear boundary between environments (in this case, on both boundaries. Secondly, there is often a change in the relaponsion rate within the same environment, in particular in the wave layer. Such wave wavess are called gradients.

Consider the features of wave propagation in gradient wavelength. A typical example of the behavior of the profile of the fracture indicator provided in Fig. 2.
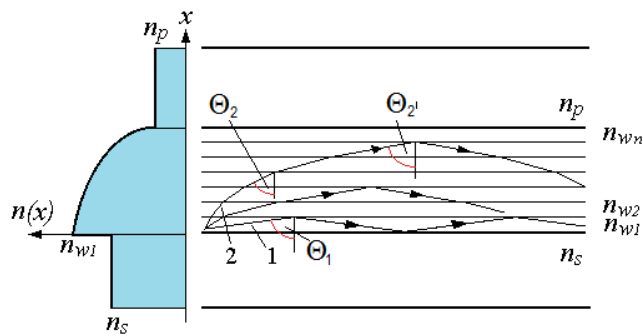
Fig. 3.18

3.18. Break the wave layer into infinitely thin layers, within which the value of the entrization indicator can be considered constant.

We will assume that several wave-like fashions can be distributed in wave-drive, in particular lower-order fashion (1) and higher-order fashion (2). Based on Snellius's invariant and the analysis of the profile behavior of the fracture indicator, it can be argued that for fashion (1) the condition of full internal reflection will occur for a layer that is located closer to the substrate than in the case of fashion distribution (2). This statement is true because for this fashion the "initial" distribution angle Θ_2(the angle between the normal to the wave front and the norm to the surface of the wave ovation) in a layer directly bordering the lining of a smaller angle Θ_1 for fashion (1). Accordingly, as follows from the figure, the difference between effective thicknesses for modes of higher and lower order of gradient wave is greater than in the case of a wave with a stepped profile of the entrization indicator. Figuratively speaking, in a gradient wave of fashion of the lower order "pressed" to the boundary of the wavelet and lining. Thus, lower-order wave mods are distributed through a layer of medium for which the average relamination rate is greater than the corresponding value calculated for the entire wave-o'-wave layer. Consequently, its spread rate in the wave-drive environment is less than the corresponding average speed. Therefore, despite the fact that the geometric path for such fashion is much smaller than for a similar value for higher-order fashions, it is possible to choose the profile of the relap indicator in such a way that at the end point of the fashion wave (1) and (2) will have the same time delays. Such considerations formed the basis for the development of optical fibers in which chromatic dispersion is minimized. However, this issue will be carefully considered when studying the physical characteristics of optical fibers.

3.6. Wave propagation in cylindrical wavelengths. [7-11]
3.6.1. Light-output transmission equation

Consider the fiber light output without loss of the two-layer structure, which is shown in Fig. 2. 3.19.

To describe the behavior of the electromagnetic field in the core ($0<r<r_w$) and in the shell ($a<r<b$) you need to use different functions. Based on the physical nature of the processes, functions inside the nucleus when r=0 must be final, and in the shell describe the falling field.

To determine the main parameters of lighters (critical frequency, distribution constants, etc.) we will use the main equations of electrodinums – Maxwell equation (1.1 – 1.4), which for dielectric wavers have the form [1,2]:

Рис. 3.19

$2r_w$ – light output core diameter, $2r_p$ – shell diameter

$$\begin{cases} \mathrm{rot}\vec{H} = j\omega\varepsilon\vec{E} \\ \mathrm{rot}\vec{E} = -j\omega\mu\vec{H} \\ \mathrm{div}\vec{H} = 0 \\ \mathrm{div}\vec{E} = 0 \end{cases}, \tag{3.52}$$

where ε, μ – dielectric and magnetic permainance, ω – circular frequency.

Maxwell's equations are fair to any coordinate system. For guide systems, these equations are most often used in the cylindrical coordinate system, here z which is directed along the optical axis of the light drive.

To solve engineering problems of electrodynamics, you need to know the longitudinal components of the fields E_z and H_z. They can be obtained as follows. Let's turn the first of Maxwell's equations into a look (take the rot from the left and right):

$$\mathrm{rotrot}\vec{H} = -j\omega\varepsilon\mathrm{rot}\vec{E}. \tag{3.53}$$

We will use the ratio [14]:

$$\mathrm{rotrot}\vec{H} = \mathrm{graddiv}\vec{H} - \nabla^2\vec{H}. \tag{3.54}$$

Then, given that $\mathrm{div}\vec{H}$ =0, we have

$$-\nabla^2\vec{H} = -j\omega\varepsilon(j\omega\mu\vec{H}) \text{ або } \nabla^2\vec{H} + \omega^2\varepsilon\mu\vec{H} = 0 \text{ або}$$

$$\nabla^2\vec{H} + k^2\vec{H} = 0, \tag{3.55}$$

where $k = \omega\sqrt{\varepsilon\mu}$ – wave number of light output.

Similarly, maxwell's second equation can be obtained

$$\nabla^2\vec{E} + k^2\vec{E} = 0. \tag{3.56}$$

It follows that the longitudinal electromagnetic components of vectors E_z and H_z satisfied with the equation

$$\begin{cases} \nabla^2 E_z + k^2 E_z = 0 \\ \nabla^2 H_z + k^2 H_z = 0 \end{cases}, \tag{3.57}$$

where ∇^2 – Laplace operator $\nabla^2 = \dfrac{\partial^2}{\partial x^2} + \dfrac{\partial^2}{\partial y^2} + \dfrac{\partial^2}{\partial z^2}$, or in the cylindrical coordinate system $\dfrac{\partial^2}{\partial r^2} + \dfrac{1}{r}\dfrac{\partial}{\partial r} + \dfrac{1}{r^2}\dfrac{\partial^2}{\partial \varphi^2} + \dfrac{\partial^2}{\partial z^2}$

Then for the longitudinal constituents E_z i H_z in the cylindrical coordinate system we get differential equations of the second order:

$$\begin{cases} \dfrac{\partial^2 E_z}{\partial r^2} + \dfrac{1}{r}\dfrac{\partial E_z}{\partial r} + \dfrac{1}{r^2}\dfrac{\partial^2 E_z}{\partial \varphi^2} + \dfrac{\partial^2 E_z}{\partial z^2} + k^2 E_z = 0 \\ \dfrac{\partial^2 H_z}{\partial r^2} + \dfrac{1}{r}\dfrac{\partial H_z}{\partial r} + \dfrac{1}{r^2}\dfrac{\partial^2 H_z}{\partial \varphi^2} + \dfrac{\partial^2 H_z}{\partial z^2} + k^2 H_z = 0 \end{cases}. \tag{3.58}$$

Supposite that the intensity of the electromagnetic field in the direction of the axis z exponential law, i.e. $A = A_0 e^{-\gamma z}$, where A – any component of vectors $\vec{E}$ or $\vec{H}$; $\gamma = \alpha + j\beta$ – distribution constant. Then the first and second derivatives are defined as $\dfrac{\partial A}{\partial z} = -\gamma A_0 e^{-\gamma z} = -\gamma A$; i $\dfrac{\partial^2 A}{\partial z^2} = \gamma^2 A$.

For z- components of the electric field E_z we have $\dfrac{\partial^2 E_z}{\partial z^2} = \gamma^2 E_z$. Similarly for magnetic field $\dfrac{\partial^2 H_z}{\partial z^2} = \gamma^2 H_z$

Subseating the obtained values to the system (3.58), we obtain

$$\begin{cases} \dfrac{\partial^2 E_z}{\partial r^2} + \dfrac{1}{r}\dfrac{\partial E_z}{\partial r} + \dfrac{1}{r^2}\dfrac{\partial^2 E_z}{\partial \varphi^2} + \gamma^2 E_z + k^2 E_z = 0 \\ \dfrac{\partial^2 H_z}{\partial r^2} + \dfrac{1}{r}\dfrac{\partial H_z}{\partial r} + \dfrac{1}{r^2}\dfrac{\partial^2 H_z}{\partial \varphi^2} + \gamma^2 H_z + k^2 H_z = 0 \end{cases}. \tag{3.59}$$

Enter the designation $g^2 = \gamma^2 + k^2$ – transverse wave number of light. Then for the nucleus of the light plant we have

$$\begin{cases} \dfrac{\partial^2 E_z}{\partial r^2} + \dfrac{1}{r}\dfrac{\partial E_z}{\partial r} + \dfrac{1}{r^2}\dfrac{\partial^2 E_z}{\partial \varphi^2} + g_w^2 E_z = 0 \\ \dfrac{\partial^2 H_z}{\partial r^2} + \dfrac{1}{r}\dfrac{\partial H_z}{\partial r} + \dfrac{1}{r^2}\dfrac{\partial^2 H_z}{\partial \varphi^2} + g_w^2 H_z = 0 \end{cases}. \tag{3.60}$$

where $g_w = \sqrt{k_w^2 - \beta^2}$ (excluding attention) – transverse wave number of the nucleus; $k_w = k n_w$ – wave number of the core with the terrification indicator n_w.

The solution of equations (3.60) for the nucleus must be expressed through cylindrical functions of the first kind – the Bessel functions, which have fin values when $r=0$. Therefore, you can write

$$\begin{cases} E_{zw} = A_n J_n(g_w r) e^{jn\varphi} e^{-\gamma z} \\ H_{zw} = B_n J_n(g_w r) e^{jn\varphi} e^{-\gamma z}, \end{cases} \tag{3.61}$$

where A_n and B_n – constant integration.

Using the equation (3.53), consider the relationship between the transverse and longitudinal components of the field. In particular, for the E_r we have

$$j\omega\varepsilon_w E_r = \dfrac{1}{r}\dfrac{\partial H_z}{\partial \varphi} - \dfrac{\partial H_\varphi}{\partial z}$$

$$-j\omega\mu_w H_\varphi = \dfrac{1}{r}\dfrac{\partial E_r}{\partial r} - \dfrac{\partial E_z}{\partial r}. \tag{3.62}$$

Let's take the derivative of the second expression by ∂z

$$-j\omega\mu_w \dfrac{\partial H_\varphi}{\partial z} = \dfrac{\partial^2 E_r}{\partial z^2} - \dfrac{\partial^2 E_z}{\partial z \partial r}. \tag{3.63}$$

Given that $\dfrac{\partial^2 E_r}{\partial z^2} = \gamma^2 E_r$, a $\dfrac{\partial E_z}{\partial z} = -\gamma E_z$, то $\dfrac{\partial^2 E_z}{\partial z \partial r} = -\gamma \dfrac{\partial E_z}{\partial r}$.

Than

$$-j\omega\mu_w \dfrac{\partial H_\varphi}{\partial z} = \gamma^2 E_r + \gamma \dfrac{\partial E_z}{\partial r} \text{ або } \dfrac{\partial H_\varphi}{\partial z} = -\dfrac{1}{j\omega\mu_w}\left(\gamma^2 E_r + \gamma \dfrac{\partial E_z}{\partial r}\right). \tag{3.64}$$

We base this expression in the equation for E_r. We get

$$j\omega\varepsilon_w E_r = \frac{1}{j\omega\mu_w}(\gamma^2 E_r + \gamma\frac{\partial E_z}{\partial r} + \frac{j\omega\mu_w}{r}\frac{\partial H_z}{\partial \varphi})\ \text{або}$$

$$-k^2 E_r - \gamma^2 E_r = \gamma\frac{\partial E_z}{\partial r} + \frac{j\omega\mu_w}{r}\frac{\partial H_z}{\partial \varphi}. \tag{3.65}$$

In the end we get

$$E_r = -\frac{1}{g_w^2}(\gamma\frac{\partial E_z}{\partial r} + \frac{j\omega\mu_w}{r}\frac{\partial H_z}{\partial \varphi}). \tag{3.66}$$

Аналогічно можна встановити зв'язок між повздовжніми і іншими поперечними компонентами поля

$$\begin{cases} E_\varphi = \frac{1}{g_w^2}(-\frac{\gamma}{r}\frac{\partial E_z}{\partial \varphi} + j\omega\mu_w\frac{\partial H_z}{\partial r}) \\ H_r = \frac{1}{g_w^2}(\frac{j\omega\varepsilon_w}{r}\frac{\partial E_z}{\partial \varphi} - \gamma\frac{\partial H_z}{\partial r}) \\ H_\varphi = -\frac{1}{g_w^2}(j\omega\varepsilon_w\frac{\partial E_z}{\partial \varphi} + \frac{\gamma}{r}\frac{\partial H_z}{\partial r}) \end{cases}. \tag{3.67}$$

Using the equation (3.59) let's take the corresponding derivatives.

Then the expressions for the transverse components of the electrical and magnetic fields in the core, fixing that $\gamma = \beta$, look like (multiplier do not write):

$$\begin{cases} E_{rw} = -\frac{1}{g_w^2}[A_n\beta g_w J_n'(g_w r) - B_n\frac{\omega\mu_w n_w}{r}J_n(g_w r)] \\ H_{rw} = -\frac{1}{g_w^2}[A_n\frac{\omega\varepsilon_w n_w}{r}J_n(g_w r) - B_n\beta g_w J_n'(g_w r)] \\ E_{\varphi w} = \frac{j}{g_w^2}[-A_n\frac{\beta n_w}{r}J_n(g_w r) - B_n\omega\mu_w g_w J_n'(g_w r)] \\ H_{\varphi w} = -\frac{1}{g_w^2}[A_n\omega\varepsilon_w g_w J_n'(g_w r) + B_n\frac{\beta n_w}{r}J_n(g_w r)] \end{cases}. \tag{3.68}$$

For the shell we have a similar system of equations:

$$\begin{cases} \frac{\partial^2 E_z}{\partial r^2} + \frac{1}{r}\frac{\partial E_z}{\partial r} + \frac{1}{r^2}\frac{\partial^2 E_z}{\partial \varphi^2} + g_p^2 E_z = 0 \\ \frac{\partial^2 H_z}{\partial r^2} + \frac{1}{r}\frac{\partial H_z}{\partial r} + \frac{1}{r^2}\frac{\partial^2 H_z}{\partial \varphi^2} + g_p^2 H_z = 0 \end{cases}. \tag{3.69}$$

where $g_p = \sqrt{\beta^2 - k_p^2}$ (without taking into account the attention) – transverse wave number of the light-water shell; $k_p = \omega\sqrt{\varepsilon_p\mu_p} = kn_p = \frac{2\pi}{\lambda}n_p$ – shell wave number with terlament n_p.

To solve these equations, based on the condition that when $r_p \to \infty$ field should go to zero, it is necessary to use cylindrical functions of the third kind – Hankel functions:

$$\begin{cases} E_{zp} = C_n H_n^{(1)}(g_p r)e^{jn\varphi}e^{-\gamma z} \\ H_{zp} = D_n H_n^{(1)}(g_p r)e^{jn\varphi}e^{-\gamma z} \end{cases}, \tag{3.70}$$

where C_n, D_n – constant integration.

Then for the transverse components of the field in the shell, you can write the following ratios:

$$\begin{cases} E_{rp} = -\dfrac{1}{g_w^2}\left[jC_n\beta g_p H_n^{(1)'}(jg_p r) + D_n \dfrac{\omega\mu_p n_p}{r} H_n^{(1)}(jg_p r)\right] \\[2mm] H_{rp} = \dfrac{1}{g_p^2}\left[C_n \dfrac{\omega\varepsilon_p n_p}{r} H_n^{(1)}(jg_p r) - jD_n\beta g_p H_n^{(1)'}(jg_p r)\right] \\[2mm] E_{\varphi p} = \dfrac{1}{g_p^2}\left[jC_n \dfrac{\beta n_w}{r} H_n^{(1)'}(jg_p r) - D_n\omega\mu_p g_p H_n^{(1)}(jg_p r)\right] \\[2mm] H_{\varphi p} = \dfrac{1}{g_p^2}\left[C_n\omega\varepsilon_p g_p H_n^{(1)'}(jg_p r) + B_n \dfrac{\beta n_p}{r} H_n^{(1)}(jg_p r)\right] \end{cases} \qquad (3.71)$$

Constant integration A_n, B_n, C_n, D_n can be defined if you use boundary conditions. We will use the conditions of equality of tangential components of stresses of electrical and magnetic fields on the surface of the core-shell section (when $r=r_w$):

$$\begin{aligned} E_{zw}(r_w) &= E_{zp}(r_w) \\ H_{zw}(r_w) &= H_{zp}(r_w) \\ H_{\varphi w}(r_w) &= H_{\varphi p}(r_w) \end{aligned} \qquad (3.72)$$

After we find constant integration of them into equations, and after the corresponding transformations we obtain such a transcendental equation:

$$\left[\frac{\mu_w}{g_w}\frac{J_n'(g_w r_w)}{J_n(g_w r_w)} - \frac{j\mu_p}{g_p}\frac{H_n^{(1)'}(jg_p r_w)}{H_n^{(1)}(jg_p r_w)}\right]\left[\frac{\omega^2\varepsilon_w}{g_w}\frac{J_n'(g_w r_w)}{J_n(g_w r_w)} + \frac{j\omega^2\varepsilon_p}{g_p}\frac{H_n^{(1)'}(jg_p r_w)}{H_n^{(1)}(jg_p r_w)}\right] = n_w^2\beta^2\left[\frac{1}{g_w^2 r_w} + \frac{1}{g_p^2 r_w}\right] \quad (3.73)$$

The obtained equations make it possible to identify unknown permanent ones and find the structure of the field in the nucleus and shell of the fiber light. In general, the equations have a series of solutions, each of which corresponds to a specific field structure, which is called a light-output mode.

3.6.2. Типи хвиль у світловодах

There can be two types of waves in light water: symmetrical E_{0m}, H_{0m} asymmetric dipole EH_{nm}, HE_{nm}. In the index n – number of field changes by diameter; m – Number of field changes around the perimeter. Symmetrical electric waves E_{0m} and magnetic H_{0m} have circular symmetry ($n=0$).

Asymmetric wavelengths cannot be separated by light. In the light water they exist only together, that is, there are longitudinal components E and H. These waves are called mixed, dipole and are marked through HE_{nm}, if a field in the cross section resembles a field H, or EH_{nm}, if the field in the transverse intersection is closer to the waves E.

From all the nomenclature of mixed waves in optical cables, the greatest use was received by a wave type HE_{11} (or EH_{10}). On this wave work single-mode lighters, which have the highest throughput.

You can match the specified classification of electromagnetic waves with the radiation classification.

As noted in [31-33], fibres can transmit two types of rays: meridional and oblique. Meridional rays are located in a plane that pass through the axen of the fiber light. Oblique rays do not cross the adm of the light water (see paragraph 3.6.3 for more detail)

Meridional bees correspond to symmetrical electrical E_{0m} i magnetic H_{0m} waves, obliquely – asymmetric hybrid EH_{nm} and HE_{nm} waves.

If the point radiation source is located along the axis of the light, then only meridional rays occur and symmetric waves, respectively, E_{0m}, H_{0m}. If the point source is located outside the axis of the light output or we have a complex source, then both meridional and oblique rays and their corresponding symmetrical rays appear at the same time E_{0m}, H_{0m} and asymmetric hybrid (EH_{nm} and HE_{nm}) waves.

Asymmetric wave type EH_{nm} and HE_{nm} in fiber floodlights can not exist. These waves are excited only in metal waves.

The main equation of transmission via fiber light for the case $\frac{n_w - n_p}{n_w} \ll 1$ can be greatly simplified for different types of waves.

For symmetric waves, the right part of the equation (3.73) is zero, than we have two different equations for electrical E_{0m} and magnetic H_{0m} waves:

for E_{0m}

$$\frac{\varepsilon_w}{\varepsilon_p} \frac{g_w}{g_p} \frac{J_1(g_w r_w)}{J_0(g_w r_w)} + j \frac{H_1^{(1)}(jg_p r_w)}{H_0^{(1)}(jg_p r_w)} = 0. \tag{3.74a}$$

for H_{0m}

$$\frac{g_p}{g_w} \frac{J_1(g_w r_w)}{J_0(g_w r_w)} + \frac{H_1^{(1)}(jg_p r_w)}{H_0^{(1)}(jg_p r_w)} = 0. \tag{3.74б}$$

For mixed dipole waves, the following approximate equations can be obtained:
for HE_{nm}

$$\frac{J_{n-1}(g_w r_w)}{g_w r_w J_n(g_w r_w)} = \frac{H_{n-1}^{(1)}(jg_w r_w)}{jg_p r_w H_0^{(1)}(jg_p r_w)}, \tag{3.75a}$$

for EH_{nm}

$$\frac{J_{n+1}(g_w r_w)}{g_w r_w J_n(g_w r_w)} = \frac{H_{n+1}^{(1)}(jg_w r_w)}{jg_p r_w H_0^{(1)}(jg_p r_w)}, \tag{3.75б}$$

For an area that is far from the critical frequency frequently, you can use simpler ratios:
for HE_{nm}

$$g_p r_w J_{n-1}(g_p r_w) = g_w r_w J_n(g_w r_w). \tag{3.76}$$

This expression allows you to determine the field structure, wave parameters and characteristics of the fiber light for different types of waves and frequencies.

Each type of wave (fashion) has its own critical frequency and wavelength. The presence of a critical frequency in fibre lighters is explained by the fact that at very high frequencies almost all energy is concentrated inside the nucleus of the light drive, and with a decrease in frequency, the field is redistributed and the energy passes to the surrounding space. At a certain frequency f_0 – critical, or clipping frequency, the field no longer spreads along the light drive and all energy dissipates in the surrounding space.

Previously, the following ratios were given:

$$\begin{aligned} g_w &= \sqrt{k_w^2 - \beta^2} \text{ при } r \leq r_w \\ g_p &= \sqrt{\beta^2 - k_p^2} \text{ при } r > r_w \end{aligned}, \tag{3.77}$$

where β – phase coefficient in light water; k_w i k_p – wave numbers, respectively, of the core and shell of the light; g_w и g_p – Transverse wave numbers, respectively, for nucleus and shell; r_w – fiber kernel radius.

Given that $k_w = \dfrac{\omega}{c} n_w = \dfrac{2\pi f}{c} n_w = k n_w$, $k_p = \dfrac{\omega}{c} n_p = \dfrac{2\pi f}{c} n_p = k n_p$

we get

$$g_w = \sqrt{k^2 n_w^2 - \beta^2}\ \text{при } r \le r_w$$
$$g_p = \sqrt{\beta^2 - k^2 n_p^2}\ \text{при } r > r_w \tag{3.78}$$

thinking that r=a, can be recorded

$$g_w^2 + g_p^2 = k^2(n_w^2 - n_p^2). \tag{3.79}$$

To determine the critical frequency f_0 must be accepted $g_p = 0$. At all values $g_p > 0$ field is concentrated in the nucleus of the light drive, and when $g_p = 0$ it exits the nucleus and the process of spreading the wave through the light drive stops. By law geometric optics condition $g_p = 0$ corresponds to the condition of complete internal reflection, in which there is no fractured wave, but there is only falling and reflected waves. Then, when $g_p = 0$ we have

$$g_w^2 = k^2(n_w^2 - n_p^2), \tag{3.80}$$

or given that $k = \dfrac{2\pi}{\lambda} = \dfrac{2\pi f}{c}$ can be recorded $k^2 = \dfrac{g_w^2}{(n_w^2 - n_p^2)} = \left(\dfrac{2\pi f_0}{c}\right)^2$.

Where is the critical frequency

$$f_0 = \frac{g_w c}{2\pi \sqrt{n_w^2 - n_p^2}}. \tag{3.81}$$

Multiplying the numerator and denominator by the parameter r_w (kernel radius), we get the value of the critical frequency

$$f_0 = \frac{g_w c r_w}{2\pi r_w \sqrt{n_w^2 - n_p^2}} = \frac{g_w r_w}{2\pi r_w \sqrt{(n_w^2 - n_p^2)\mu_0 \varepsilon_0}} = \frac{g_w r_w}{2\pi r_w \sqrt{\mu_w \varepsilon_w - \mu_p \varepsilon_p}}. \tag{3.81}$$

and critical wavelength

$$\lambda_0 = \frac{2\pi r_w v_w}{g_w r_w} \sqrt{\mu_w \varepsilon_w - \mu_p \varepsilon_p}. \tag{3.82}$$

where $g_w r_w$ – roots of besselev functions, v_w – the speed of light propagation in the environment.

Since lighters are made of non-magnetic materials $(\mu_w, \mu_p = 1)$, than

$$f_0 = \frac{g_w r_w}{2\pi r_w \sqrt{(\varepsilon_w - \varepsilon_p)\mu_0 \varepsilon_0}}, \quad \lambda_0 = \frac{2\pi r_w v_w}{g_w r_w} \sqrt{(\varepsilon_w - \varepsilon_p)\mu_0 \varepsilon_0}. \tag{3.83}$$

A fundamentally similar result can be obtained by the radiation method directly from the laws of geometric optics by considering the processes that occur when a wave falls on the boundary of the partition - the nucleus-shell of the light water.

Analyzing the resulting ratios, we can say that the chim thickness of the core of the light and chim are more different $\mu_w \varepsilon_w$ i $\mu_p \varepsilon_p$, especially the critical wavelength and, accordingly, the critical frequency of the fiber light. From the formulas it can also be seen that with the equality of optical characteristics, first of all, the dielectric

insight of the nucleus and shell, that is, when $\varepsilon_w = \varepsilon_p$, critical wavelength $\lambda_0 = 0$, and the critical frequency $f_0 = \infty$ and transmission of the signal through such a light drive is not possible. This fact has its own logical justification as already mentioned, the fiber light output works on the principle of multiple wave reflection from the boundary between the nucleus and the shell, and this boundary is the guide medium for the proliferation of electromagnetic energy. At $\varepsilon_w = \varepsilon_p$ light output stops working as a transmission system.

Table 3.1

n	Root value $(g_w r_w)$ at m, equal			Type of wave
0	2,405	5,520	8,654	E, H
1	0,000	3,832	7,016	HE
1	3,832	7,016	10,173	EH
2	2,445	5,538	8,665	HE
2	5,136	8,417	11,620	EH

To determine the critical frequencies of different types of waves, consider the roots of the previously obtained ratio of bessel functions $J_{0m}(g_w r_w)$ for symmetrical and asymmetric waves $J_{nm}(g_w r_w)$. These equalities give an infinite number of roots, the values of which are given in Table. 3.1.

Consider the physical content given in Table. 3.1 roots of besselev functions $g_w r_w$. Because when clipping $g_p=0$, that is $\beta = k n_p$, then from the expression $g_w = \sqrt{k_w^2 - \beta^2}$ we have

$$g_w r_w = r_w \sqrt{k_w^2 - \beta^2} = r_w \sqrt{k^2 n_w^2 - k^2 n_p^2} = r_w k \sqrt{n_w^2 - n_p^2} = r_w \frac{2\pi}{\lambda} \sqrt{n_w^2 - n_p^2}. \quad (3.84)$$

The last ratio is inversely proportional to λ_0, i.e. directly proportional to the critical frequency f_0. In addition, it contains the initial fiber parameters: r_w, n_w, n_p. This expression is called the normalized frequency and in this form (see paragraph 7.1.4) is often used in light-water technology.

With this interpretation, Table. 3.1 contains normalized frequencies V waves, the type of waves specified in the right column of the table, and the nm consists of the numbers of the left column and the top row of the corresponding cell, in which this value is located V_0. Each V_0 corresponds to the critical frequency f_0.

At $V<V_0$ we have $f<f_0$, that is, the frequency is less critical and the wave through the fiber core does not spread, in another language does not exist. Wave habitat with a normalized clipping frequency $V>V_0$ is $f>f_0$.

From Table. 3.1 shows that for asymmetric wave HE_{11} meaning $V_0=0$; therefore, this wave has no critical frequency and can propaed at any frequency and diameter of the nucleus. All other waves do not extend at frequencies below critical. Table. 3.1 can be converted and converted to this form (Table 3.2)

Table 3.2

Frequency range	Additive mods	Number of mods
0,000–2,405	HE_{11}	2
2,405–3,832	H_{01}, E_{01}, HE_{21}	6
3,832–5,316	HE_{12}, EH_{11}, HE_{31}	12
5,316–5,520	EH_{21}, HE_{41}	16
5,520–6,380	H_{02}, E_{02}, HE_{22}	20
6,380–7,016	EH_{31}, HE_{51}	24
7,016–7,588	HE_{13}, EH_{12}, HE_{32}	30
7,588–8,417	EH_{41}, HE_{61}	34
8,417–11,620	EH_{22}, E_{03}, H_{03}, EH_{13}, HE_{23}, EH_{23}	40

From Table. 3.2 It follows that with increasing frequency, new types of waves appear. Yes, starting with V=2,405 waves appear H_{01}, E_{01}, HE_{21}, at V=3,832 there are additional fashions HE_{12}, EH_{11}, HE_{31} etc.

Thus, the interval of $V=g_w r_w$, in which only one type of wavelength is propagated in the light HE_{11}, is within the limits of $0< V <2,405$, therefore, when choosing the transmission frequency or thickness of the nucleus of a single-mode light output, the following conditions are obtained:

$$f_0 > \frac{2.405c}{2\pi r_w \sqrt{n_w^2 - n_p^2}}. \tag{3.85}$$

The singlemode mode is practically achieved when using very thin fibers equal in diameter to the wavelength $d = \lambda$. In addition, it is necessary to try to reduce the difference between the terrification of the kernel and shell.

Діаметр ядра волоконного світловоду для одномодового передавання може бути визначений з такого співвідношення:

$$d \leq \frac{2.405\lambda_0}{\pi \sqrt{1 - (\frac{n_w}{n_p})^2}}. \tag{3.86}$$

Example: for a fiberglass light drive with a kernel terlament rate of 1.48 and a 1.447 shell relapation rate in fashion E_{01} with a wavelength of 1.55 microns for singlemode transmission we get $d = \frac{2.405 \cdot 1.55}{3.14 \sqrt{1 - (\frac{1.447}{1.48})^2}} = 5.65$ microns.

3.6.3. Features of wave propagation in cylindrical wave thugs in terms of radiation approach

Consider the features of wave propagation in cylindrical wavelets in terms of radiation approach. Imagine that a parallel beam falls on the end of such a wavelet at any angle. In this case, only a small part of the exchanges will enter the wavelep through the plane in which the wave ale lies. This plane (meridional plane) is indicated in Figure 3.20a in gray. Such rays are called meridional. They are marked in the figure with the letter (1). All other rays are called oblique. Oblique rays are indicated by the letter (2). It can be shown that the spread of meridional rays is similar to the spread of waves in flat wavelengths. These rays spread along the meridional plane. Accordingly, all physics, ratios, patterns established for flat wavers are fair for cylindrical fibers.
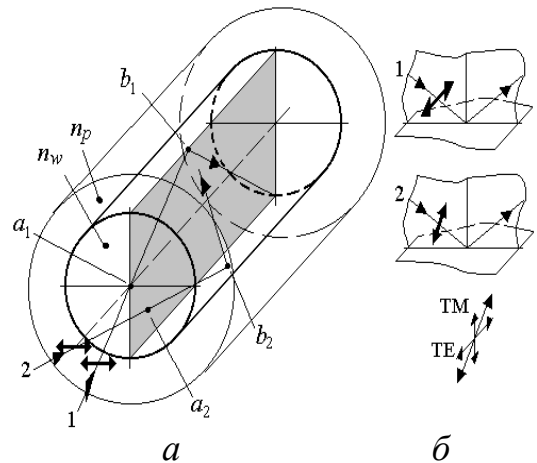
Fig. 3.20

As for oblique rays, the process of their distribution is much more complicated. Therefore, we focus only on some facts.
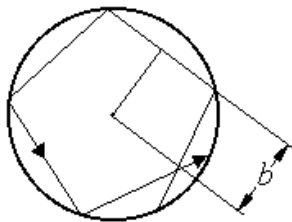
1. Unlike meridional rays, the trajectory of oblique rays does not lie in the plane, but forms some loman spiral. In this case, the projection of this spiral to the plane perpendicular to the fiber axis (Fig. 3.21) forms a certain system of chords located at one distance from the center of fiber b.

Fig. 3.21

2. Note that for "TE-, TM-lighting" fiber, the state of polarization for meridional rays does not change and corresponds to the polarization of falling radiation, since the meridional plane is perpendicular to the fiber surface (see Figure 3.20 b, situation (1)). At the same time, the plane of the fall of oblique rays is a certain angle with a plane tanty to the fiber at the point of encounter of a beam with fiber (Fig. 3.20 b, situation (2)). Then the process of spreading the wave in fiber should be considered as the proliferation of TE- and TM-fashion, on the decomposing wave at the point of the meeting. It is known that TE- and TM-mods acquire different phase delays when the wave interacts with the surface of the fiber.

So in general, the field at the output of fiber (in any case multimode) is polarized heterogeneously and elliptically. For the situation of single-mode fiber, everything is somewhat more complicated (or simpler) and in a certain case the lighting (inlet

Fig. 3.23

Heat field (intensity distribution) at the output of multimode fiber.

beam perpendicular to the end of the fiber) the state of polarization can be preserved.

3. In the vast majority of cases, the field at the output of multimode fiber can be described as a heat field (Fig. 3.23), the intensity of which is a set of randomly placed spots, of different sizes and brightness. The polarization of such a field is characterized by spatial heterogeneity and varies from linear to circular, regardless of the state of polarization of the inlet beam. However, after a certain signal distribution distance, the time delays associated with different mods become much longer than the source coherence with which they are created. In this case, the resulting intensity becomes the superposition of non-coherent signals. As a result, in the end, the intensity distribution at the output of the fiber is regulation and becomes almost gaussic.

4. BASIC ELEMENTS OF INTEGRAL OPTICS. PASSIVE ELEMENTS
[16-18]

Passive elements of integral optics are awakened elements of I/O and planar optical elements of integral optical circuits, light dividers, fork extenders.

4.1. I/O elements (integral-optical elements of communication)

Naturally, in order for the wave to spread along the wave, it is necessary to somehow generate electromagnetic radiation in its middle or in one way or another to introduce radiation into the wave. The devices carrying out such an operation were called integral-optical communication elements, or I/O elements. The easiest way to enter a wave into the wave is to create a suitable irradiation of the end of the wave. But such a seemingly simple way did not find widespread implementation, since it has significant drawbacks:

1. Complex spatial, angular coordination of geometrical parameters, directional angles of the iciring beam with wavelevel parameters is required.

2. Low efficiency of radiation injection into the wavelet, and as a result, significant energy losses.

3. Great criticality of such systems to any changes in the lighting conditions of the end of the wave.

The exception is the case when the radiation source (semiconductor laser) is formed directly in the waveguode or directly joins the end of the waveguod and forms a non-detachable connection with it.

In the course we will consider only two types of the most effective and most common elements of I/O:
   - the prism element of I/O;
   - lattite element of input/output.

4.1.1. Prissy element of I/O

The prism element of I/O is widely used in laboratory practice.

At the heart of the work of the prissy element of input and output is the fact that in the phenomenon of complete internal reflection, the reflected wave plunges into the intercom environment. Diagram of the item is shown in Figure 4.1.

We will place the prism near the surface of the wavelet at a short distance h_{pr}. We will direct a laser beam to the prism at some angle. Moreover, the angle between the beam and the normal to the surface of the prism is such that the full internal reflection of the beam from the lower surface of the prism is realized. At the same time, a standing wave (prism fashion) with a distribution constant is formed in the gap between the prism and the wavelead β_{pr}. If h_{pr} – a fairly small gap (about a few tenths of the wavelength), it can be argued that if a certain fashion was spreading in
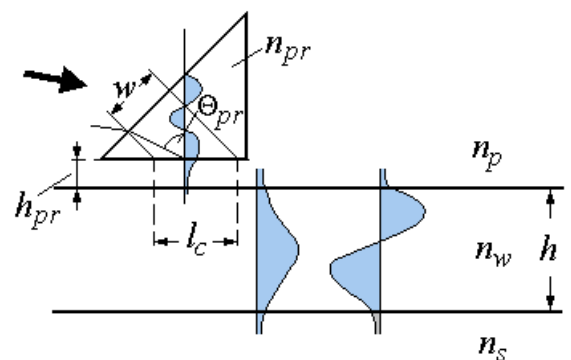
the wavelength β_m, its "tail" would also be in the gap h_{pr} and overlapped with the tail of fashion β_{pr}. In this case, the condition of synchronization between these mods should be met (phase vesity matching):

$$kn_{pr} \sin \Theta_{pr} = \beta_m. \qquad (4.1)$$

Then the tail of the wave formed in the prism begins to "pump" into the wave. Figuratively speaking, the waves are the same where to return to the prism, or in the wave.

Naturally, the coefficient of radiation input efficiency depends on the value of the gap. The more h_{pr}, the less effectiveness of entering.

l_{zv} – communication length, limited by prism size. l_{zv}, which is necessary for the complete pumping of energy is determined by the ratio of:

$$l_{zv} = \frac{w}{\cos \Theta_{pr}} = \frac{\pi}{2\sigma}, \qquad (4.2)$$

where σ –the so-called coefficient of communication of modes, which depends on the indicators of thyrization of the prism, wavelep, material and the value of the gap. To achieve an effective connection (100 percent input of radiation into the wavelet) the value of l_{zv} should be selected in such a way as to prevent the re-exchange of the fashion waver again to the prism. If the length of contact between the prism and the wave water is greater than l_{zv}, which is determined by the expression (4.2), the reverse process of pumping energy from the wave to the prism will begin.

The disadvantages of the prism element of I/O include the fact that the material from which the prism is made should, as a rule, have a relapation indicator n_{pr}, greater than the thyrization rate of the wave layer. This follows. In practice, very often the entrying indicator of the substvo n_s close to the wave layer indicator n_w (e.g. diffusion wave waves). In this case, wave mods spread almost along the surface of the wave $(\Theta_m \rightarrow 90^\circ)$ и $\beta_m \approx kn_w$. Then with (4.1) it follows that since $\sin \Theta_{pr} < 1$ то $n_{pr} > n_w$.

For the most part, the whole prism is made of rubyl $(n \approx 2.87)$ or gallium phosphide monocrysal $(n \approx 3.3)$.

4.1.2. Lattite i/o element

Let's turn to Figure 4.2. The diagram of feeding the wave in the wavelength differs from the similar scheme, which is shown in Fig. 2. 4.1, only by that, unlike Fig. 4. 4.1 the modulating lattice has the final dimensions. Such a grid can be used to inject radiation into the wave. The question arises – what length should this lattice be in order to ensure optimal energy injection into the wavelet?
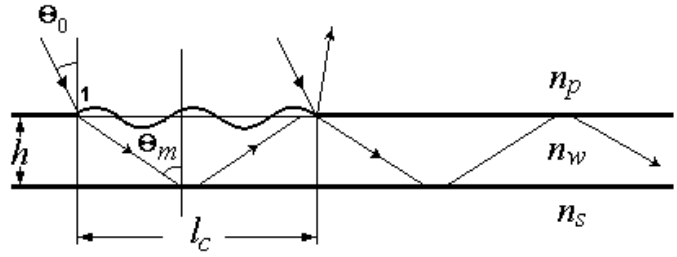
Fig. 4.2

Let the "beginning" of the beam that we try to introduce into the wave falls on the grid at its beginning (point 1). The multiple interaction of such a beam with the grid leads to the fact that when distributed with each such act, it loses part of the energy due to diffraction in the cover layer. In the end, its amplitude decreases so much that its contribution to the common field, which is formed in the lattice zone, can be neglected. We will assume that at the same time the wave spreads along the wave to the distance l_{zv}. Obviously, if you continue to increase the size of the grid, it will not lead to an increase in energy in the wavelead, since a certain energy balance is established (how much energy is injected, the same amount is excreted). Recall that the maximum intensity of the wave, which spreads in the waveguid, is achieved when the angle of irradiation of the lattice is such that the wave diffraged on it spreads in the direction of wave mod (expression 3.42). Otherwise, this expression can be rewritten as:

$$\beta_m = k(n_p \sin \Theta_0 + \frac{i\lambda}{T}), \qquad (4.3)$$

where i – diffraction order number, m – fashion number.

Let's make an estimate of the length l_{zv}. We will assume that the wavelength is absolutely transparent and when spreading the wave from point 1 to the distance l_{zv} Wave formed N zigzags, that is, N times we spent with a grid. Thus, compared to the point (1), its amplitude has changed by the multiplier R_0^N ($|R_0| < 1$ –amplitude diffraction efficiency of the lattice during diffraction in zero order for reflection). As before, we will assume that the energy of the wave can be neglected when its amplitude has decreased in $1/e$ times. Accordingly, to this criterion we have:

$$e^{-1} = R_0^N \text{ або } N = -1/\ln(R_0). \qquad (4.4)$$

Given the length of the zigzag (expression 3.27) we have a ratio for l_{zv}:

$$l_{zv} = -\frac{n_f}{\ln R_0 \left(n_w^2 - n_f^2\right)^{\frac{1}{2}}} 2\{h + \frac{1}{k}\left[\left(n_w^2 - n_p^2\right)^{-\frac{1}{2}} + \left(n_w^2 - n_s^2\right)^{-\frac{1}{2}}\right]\} \qquad (4.5)$$

Note that for small depths of lattice modulation (wavelength particles), it can be argued that the greater the depth of modulation of the lattice, the less R_0 and, accordingly, the less l_{zv}.

4.2. Planar optical elements
4.2.1. Change the direction of wave propagation. Integral optical LEDs

As is known in conventional optics, the change in the direction of distribution of the wave is carried out with the help of mirrors, prisms of various types. In the planar version, the direction can be changed if strip wave gauge is used, which have not only the final thickness, but also are limited in width in the transverse direction (see Figure 4.3).
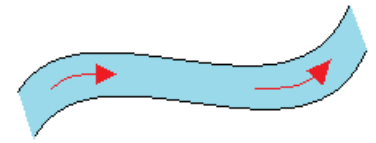
Fig. 4.3

You can divide the bundle into two or more beams with the help of the so-called U-branchers (see Figure 4.4). Thanks to the use of microelectronics technologies that allow to reproduce trace elements of integral clutches with almost one hundred percent accuracy, the ratio of intensity directed to different channels at the outlet of the splitter can be almost single.
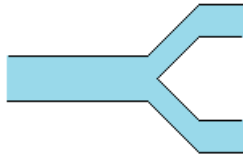
Fig. 4.4

The next problem with controlling the structure of waves in a plane is the change in the curvature of wave fronts, for example, their focus. In conventional optics, such an operation is carried out using lenses and lenses. A similar operation in integral optics is carried out using planar lenses of various types.

4.2.2. Leverberg lenses

The most common design of Lhuneberg lenses is a composition of several layers of different thicknesses $h_1, \ldots h_N$ with different relature indicator $n_1, \ldots n_N$ (Fig. 4.5a). The shape of the layers is spherical (Fig. 4.5b).

a   *б*
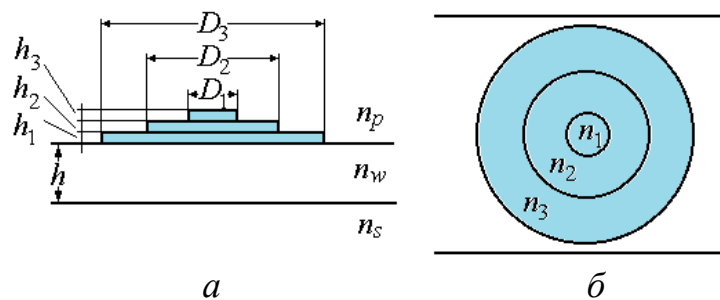
Fig. 4.5. Diagram of the formation of the Lhuneberg lens:
a – side view, *b* – top view.

Thanks to this structure, an effective fracture rate in the lens area has a certain gradient. The gradient distribution has spherical symmetry. The phase latency received by the beam distributed in the wavelevel in the lens area is similar to the phase delays observed in the normal lens. Consequently, the Lhuneberg lens has focusing properties. The calculation and technology of such a lens is very complex. However, in the case of paraxial approximation (narrow bunches), one layer is often enough.

4.2.3. Geodetic lens

Geodetic lens (Fig. 4.6) is a submersible of spherical or aspherical form. The depth ale of the submersible symmetry is perpendicular to the plane of the wavelet. The depth edge forms a circular path. Recess is done before applying a wave water layer. After applying the waveguard, the area with such a lens acquires focusing properties. The length of optical pathways for rays passing through different areas of the geodesic lens is different, and similar to the delays of a conventional lens.
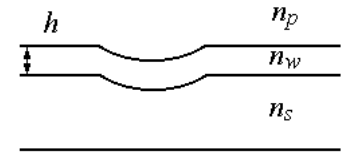
Fig. 4.6

4.2.4. Diffraction lenses

Consider some diffraction structure shown in Figure 4.7. Let the period of the diffraction grid change in the direction of x. A parallel beam ipherizes this structure perpendicular to the axis x. Imagine that all the rays that have passed through the structure will gather at one point at a distance f. The question arises, what should be the pattern of changing the lattice period?
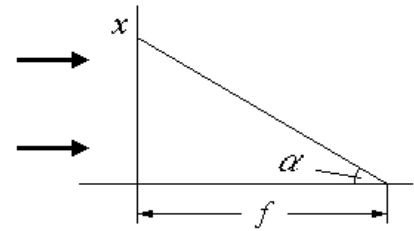
Fig. 4.7

Tangent of the corner α in this case equals:

$$\tan \alpha = x/f. \tag{4.6}$$

According to the lattice formula, the diffraction angle of the first diffraction order is determined by the expression:

$$n_w T \sin \alpha = \lambda. \tag{4.7}$$

With (4.6) and (4.7) we have:

$$T(x) = \frac{\lambda \sqrt{x^2 + f^2}}{n_w x}. \tag{4.8}$$

If the inlet of the lens is much smaller than f then $\sqrt{x^2 + f^2} \approx f + \frac{x^2}{2f}$ and (4.8) is converted to:

$$T(x) = \frac{\lambda(x^2 + 2f^2)}{2n_w x f}, \tag{4.9}$$

or, if there is an even more brutal approximation of $\tan \alpha \approx \sin \alpha \approx \alpha$, то

$$T(x) = \frac{\lambda f}{n_w x}, \tag{4.10}$$

So, if you make a grid with a variable period, which changes in accordance with (4.9), then such a diffraction structure will work as a lens. As you know, such structures are called the Fresnel lens, or diffraction lens. In integral optics, such lenses can be obtained if an additional layer with a different relamination coefficient is applied to the wave by the pattern (4.9). In these places, radiation will be taken out of the wavelets. So, what will be distributed in the layer will be the corresponding diffraction field, which will be gathered at a point at a distance f. To increase the
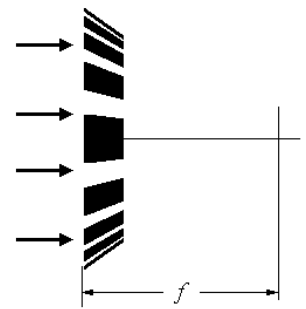
Рис. 4.8

efficiency of such a lens, sometimes the shape of the strokes is performed in the form shown in Fig. 2. 4.8 (analogue of a thick hologram). The effectiveness of such a lens can reach 100%.

5. ACTIVE ELEMENTS OF INTEGRAL OPTICS [18]

The active elements of integral optics include various kinds of modulators, deflectors, switches. Their principle of operation is almost the same. The difference is determined by the modes of operation, design features, their purpose.

5.1. Electro-electronic devices

Electro-optic devices are sold on a wide class of materials, which include semiconductor materials $A^{II}B^{VI}$ і $A^{III}B^{V}$ (for example,, *GaAs*), and active dielectrics – lithium, tantalum, potassium niobates, etc. The greatest curiosity is caused by switch modulators. These include switch modulators based on the effect of tunnel light pumping (or switch modulators on connected wavelets, interference type switch modulators).

At the heart of the work of electro-modulator-switches is the electro-optic effect of Pokkels. Its essence lies in the fact that in some optical materials the relature indicator changes in proportion to the applied intensity of the electric field.

The value of the linear electro-optic effect, determined by the change in the circuit Δn, field intensity-related expression:

$$\Delta n = -\frac{n^3}{2} r_{ij} E, \qquad (5.1)$$

where n – material relature indicator in the absence of an electric field, r_{ij} – electrooptic coefficient (tenor value). As a result, the light that will pass in such a material path l acquires a phase delay in the amount of:

$$\Delta \Phi = -\frac{\pi n^3}{\lambda} r_{ij} E l. \qquad (5.2)$$

So, there is a corresponding modulation of the wave by phase. Unlike volumetric optical devices, where additional devices (e.g. polarizers) are widely used to analyze this type of modulation, in integral optics, the transformation of phase modulation into amplitude is carried out using various interference schemes. If there is a phase difference between the interfering beams, then in the resulting field it manifests itself as a modulation of intensity.

The main characteristics of modulators include modulation depth (modulation coefficient) M and width of modulating frequency band Δf, which, in turn, determines the amount of information processed by the.

The generalized indicator of quality is the value of specific power $\Delta P / \Delta f$ or quality factor, which is defined as excitation power up to a unit band of frequencies equivalent to 84% intensity modulation.

As a rule, the basis of the wave modulator is a dielectric wave, for example, lithium niobate $LiNbO_3$ or tantalum $LiTaO_3$. Further, diffusion technology or epitaxial growth form a structure with specified properties.
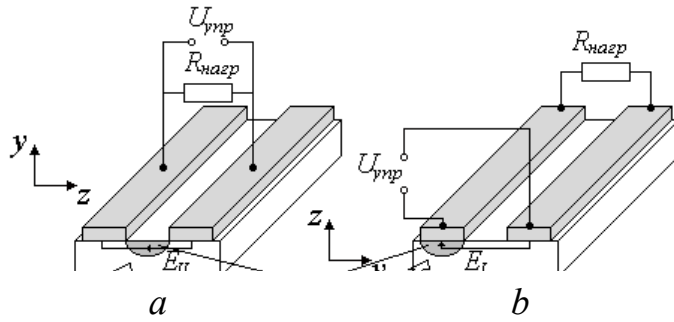
Fig. 5.1

The principle scheme of action of such modulators is shown in Fig. 2. 5.1. The values of electrooptic coefficients that determine the value of change in the circuit coefficient depend on the crystallographic orientation of the material (on the mutual location of the crystal and the direction of the electromagnetic wave), used to create the active element. In the case of anisotropic crystals such as lithium niobate, the optimal orientations for the wave structure are y- and z-slices, as shown in the figure. It is generally accepted that in order to bind to the coordinates of x,y,z crystalline directions, the z axis must be directed along the optical axis of the crystal. Therefore, if we are talking about y- or z-slice, it means that the corresponding axis is perpendicular to the large plane of the crystal.

To obtain maximum electrooptic coefficients, the control electric field must be directed along the axis z. In the case of using y-slice (Fig. 5.1 a), electrodes are located symmetrically on both sides of the wavelet. As a result, the control component of the electric field is its parallel component E_{II}. In the active elements on the z-slice (Fig. 5.1 b) for storing the direction of the modating field along the axis z one of the electrodes is applied on top to the wave layer (1) and the working component is the vertical component of the electric field $E_\perp$. We focus on the fact that the material of the control electrode is metal. As a result, the wave-like fashion, which spreads along the wave drive with a metal boundary, is suffocated. In order to avoid this, a thin insulating layer with a low (relatively wavering) relature indicator is applied between the electrode and the wavelead. This is a generally accepted technological technique and further, when we will say that a layer is applied to the surface of the waveleg, which is a conductor (except for special cases when it is necessary to create the removal of radiation from the wave ovary), we will bear in mind that it is separated from the wave insulator. Mostly aluminum sedi canons are used as a buffer layer ($n \approx 1.6$) or silicon ($n \approx 1.5$) about 20 microns thick.

The scheme shown in Figure 5.1 also illustrates the main scheme configurations of wave-like active elements with concentrated parameters (Fig. 5.1 a) and the type of running wave (Fig. 5.1 b). For circuits with concentrated electrodes parameters, a concentrated capacity of the switch modulator is created. Its band of frequencies is limited to the product of the capacity of electrodes on the value of load resistance $R_{\mathrm{нагр}}$ and the time of distribution of the luminous flux through the switch-modulator.

In the circuit, the type of running wave light and the modulating wave of ultra-high frequency (about gigahertz) spread in one direction. If the phase speeds of the control electric field and optical radiation are equal, the value of the electrode capacity and the time of light propagation through the modulator do not affect the frequency band. The frequency band is limited to the degree of resolution of the speeds of optical and ultra-high frequency waves. If such a situation is small, then the characteristics of the modulator deteriorate little. It should be added that

modulators-switches of the type of running wave are also characterized by higher efficiency compared to structures with concentrated parameters. For modulators with parallel plates, the ratio of quality factors is:

$$\frac{(\frac{\Delta P}{\Delta f})_{tr\,wave}}{(\frac{\Delta P}{\Delta f})_{lamp\,par}} = 1/3. \tag{5.3}$$

5.1.1. Switch modulators based on the effect of tunnel light pumping, or switch modulators on connected waveguides

The basis of electro-optic switch modulators on the basis of connected wave motors is two (or more) near the parallel controlled wave conductors. In Figure 5.2, a modulator-switch X-type is presented. When one of them excites in the process of radiation propagation, energy is redistributed between the wavelets, which depends on the voltage applied to the control electrodes. The essence of the phenomenon of energy redistribution is as follows. If the waveleggers are located at a short distance h_c, then the tails of wave-like fashions, which extend beyond the wavelets, overlap. Consequently, there is a distributed relationship between wavewater fields. This distributed relationship has a number of

Fig. 5.2

unique properties. First of all, it is that its occurrence does not require other structural elements. It is only necessary to shift the waves to a fairly short distance. This type of relationship is continuous. For example, if we change the distance between the waves along the structure, we get at each place our own communication coefficient. This allows forming complex integral-optical devices, for example, on one wave-line to form modulating devices with different functional purposes.
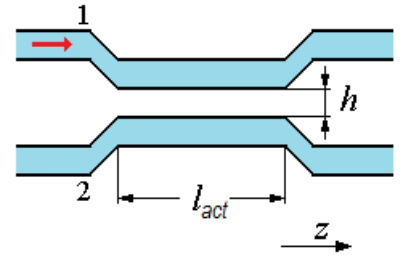
Complex amplitudes of electric field change in wavelets according to regularity:

$$\begin{cases} U_1 = A_0 e^{j\beta z} \cos \sigma z \\ U_2 = -jA_0 e^{j\beta z} \sin \sigma z \end{cases} \tag{5.4}$$

where σ – communication coefficient. First, the energy from the wavelet (1) is pumped into the wavelet (2), and then the inverse process begins.

So, in a system of two wavers there is something similar to the oscion process.

If the length of the active area l_{act} *equals the so-called length of the relationship* $l_{zv} = \frac{\pi}{2\sigma}$ there is a complete pumping of energy from the wave drive (1) to the wave (2). If at length l_{act} there is a complete pumping of energy, then this state of the system is called crossed. If, the pumping of energy does not occur and the light comes from the same wavelet into which it entered, then this state of the system is called parallel.

Note that as follows from (5.4) radiation phases in wavelets shifted to $\pi/2$.

It should be added that the 100% pumping efficiency occurs only when the simulated mode distribution constants in both wavewaters are absolutely consistent. Accordingly, the thicknesses and coefficients of rinsing of wavelets should be carefully monitored.

The main disadvantage of such elements is the impossibility in practice of implementing 100% efficiency. For example, it is impossible to make wave wavess with a length that is exactly equal to l_{zv}. However, the scheme can be made two-way and at the same time change asymmetric parameters in two wavelets. In addition, the voltage can be submitted to such a scheme on different lines with different polarity. Then in one wave drive the relapation rate will increase, and in the second – decrease.

$$\begin{cases} n_1 = n_0 + \Delta n \\ n_2 = n_0 - \Delta n \end{cases} \tag{5.5}$$

So, we have a relative change in the distribution constant $\Delta\beta$ twice as much as in a system with one electrode.

Figure 5.3 shows a Y-splitter, which works on a similar principle, but the pumping of wave energy occurs simultaneously in two channels.

5.1.2. Interference type switch modulators

The basis of integral-optical modulators-switches of interference type are planar interferometers Maha-Tsander. It is created by two parallel wavers, which are connected at the entrance and outlet by splitners (Fig. 5.4). The input signal with the help of the first splitter is divided into two hours of astines. Both parts of the signal, each of which passes through the interferometer's shoulder, are summed up at the output of the second -forklift, taking into account the phase changes that occur during the spread. Control electrodes are applied to the waves in the shoulders of the interferometer. The electric field through the control circuit induces a phase shift of such a magnitude, at which waves come to a common point either in the phase or in the antiphase. So, at the output of the U-splitter, either we have or do not have a signal.

Рис. 5.4. Схема модулятора перемикача інтерфернційного типу:
1 – керуючі електроди; 2 – хвилевід;
3 – підкладенка

Naturally, the depth of modulation at the output of the interferometer is determined by the ratio of intensity in the shoulders of the interferometer. 100 percent modulation is achieved only in cases where these intensity are exactly the same. Note that there are active means of intensity correction in the shoulders, but they require additional power sources (>30 v) and significantly complicate the modulator circuitry. However, the modern technique of photolitography allows you to perform U-branchers with high accuracy (it depends on the ratio of intensity) and achieve almost 100 percent modulation.

Today for z-slice-based modulators $LiNbO_3$, the following characteristics are achieved: control voltage ~ 3.5 v; frequency band ~ 17 GHz; quality factor ~ 7 mcV/MHz.

5.1.3. Electric-electronic modulators on the basis of the Brega effect

A typical modulator based on the Breg effect is provided in Fig. 2. 5.5 s consists of a pair of electrodes "intertwined" with each other like two combs. When the voltage is pressed on the electrodes, the thyroid thyme ratio under them changes. As a result, a "thick" phase grid is formed in the wave drive with a period equal to double the distance between the pins.
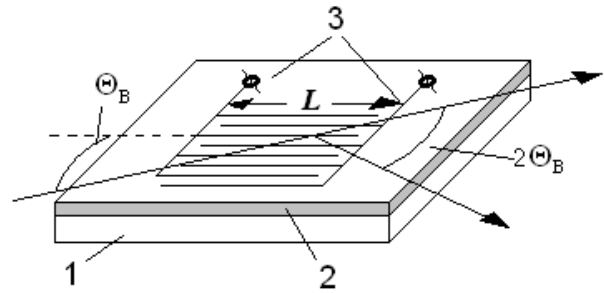
Fig. 5.5. Bregg modulator
1 – sub, 2 – wavelevid, 3 – positive and negative electrodes

In this case, the condition is fulfilled, which characterizes the grid as a thick:

$$2\pi\lambda L \gg T^2, \qquad (5.6)$$

where L – length of modulator pins

The light that spreads in the waveguode diffraets on such a lattice. At the same time, as a result of the fact that the lattice is a thick result of diffraction depends on the angle at which it is illuminated Θ_B. As a result of the so-called Breg effect, diffraction is effective only if the diffraction angle is twice as high as Θ_B. It can be shown that the lighting angle of the grid is set by the ratio of:

$$\sin\Theta_B = \frac{\lambda}{2Tn_w}. \qquad (5.7)$$

When changing the lighting angle of the lattice, the intensity of the diffraged wave decreases. Range of changes in lighting angles (angles Θ_B small and $\sin\Theta_B \approx \Theta_B$), at which the intensity drops to 50% of the maximum is the value of the

$$\Delta\Theta_B = 2T/L. \qquad (5.8)$$

Naturally, the intensity of the diffraged wave depends on the voltage U supplied to the modulator:

$$\frac{I}{I_0} = \sin^2 Ub, \qquad (5.9)$$

where b is the coefficient that characterizes the efficiency of the modulator and depends on the thyrization coefficient of the wave drive medium and other parameters of the structure.

5.1.4. Electroabsorption modulators
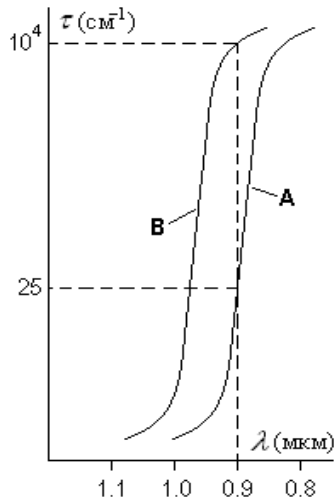
Fig. 5.6

Curve A corresponds to the case when there is no voltage, B – voltage is applied to the structure.

This type of modulators can also be considered electro-optic, since to change the optical characteristics of the modulator use the influence of an electric field. However, the effect that is not used is not the Pokélos effect. Instead, the Franz-Keldish effect is used in electroabsorption modulators. When presenting a strong electric field, the boundary of the absorption strip in semiconductors shifts towards long wavelengths. So in Fig. 2. 5.6 an illustration of this phenomenon is provided for the GaAs compound when presenting voltage 1.3×10^5В/см. As you can see in the absence of voltage (curve A) the absorption rate at the wavelength λ=0.9 microns is a value 25 cm^{-1}. When voltage is applied, the absorption curve shifts to the long-wave region and the absorption rate for this dozhin wave increases by almost three orders of order.

Today, electroabsorption modulators have been created, the supply voltage of which does not exceed tens of volts when changing the absorption coefficient within 20 dB and the working bandwidth ~ 1 GHz.

Recently, this type of modulators are becoming increasingly widespread not only in integral optics, but also in modern fiber optic telecommunication systems.

5.2. Accetopathic modulators

One of the effective methods of wave control in wave-wave devices is to use to modulate the wave of results of interaction of sound oscillations with elements of integral-optical structure.

Acoustic wave is a process of transfer of mechanical deformations – volumetric and shear. When sound waves spread in the environment due to the photo-spring effect, there is a regular change in the indicator of entrification of the environment, which is determined by the characteristics of the acoustic wave. Such characteristics are: wave intensity, period of sound oscillations, etc. The interaction of light with this given structure is similar to the diffraction of light on diffraction grids. The photo-spring effect is a linear effect – the magnitude of the change in the relapse indicator is proportional to deformation δS:

$$\Delta n = \frac{1}{2} P n^3 \delta S, \tag{5.10}$$

where P – characterizes the elastic properties of the material. In the transparency area, this coefficient practically does not depend on the wavelength of light, but depends on the direction of distribution and polarization of light and sound.

Acoustopathic active elements can be constructed using both volumetric and surface (PA) acoustic waves. The energy that is carried by the paX is concentrated in the near-top layer with a thickness approximately equal to the wavelength. So, if such a wave spreads in the area of the optical wave, then taking into account the thickness of the optical wave, which is also in the same order, it can be argued that the overlap of sound and optical waves is almost complete. As a result, there is a sufficiently effective modulation of radiation, which is distributed in the wave water. It should be added that the practical implementation of PAH modulation is relatively simple. That is why this type of modulation is widely used in integral optics.

Groin excitation is carried out with the help of so-called counter-pin converters (Fig. 5.7), which are formed from electrodes similar to electrodes of the electro-electronic Bregiv modulator.
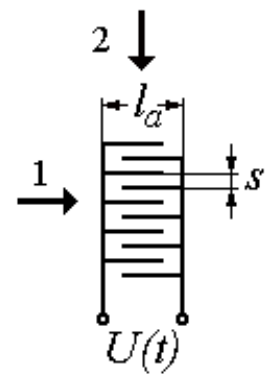
Fig. 5.7. Pin-chick scheme of counter-pin converter:
1 – Collinear wave modulation 2 – non-collinear wave modulation

On a pre-applied dielectric layer with good piezoelectric properties, metal electrodes are created, which are made in the form of combs nested in each other. Control voltage is applied to their ends.

Note that such a relatively simple converter ensures the efficient conversion of electrical signal modulation into the modulation of the optical signal in a strip about a hundred megahertz wide. The most efficiently converted acoustic waves with a length equal to the double distance between adjacent electrodes s. Methods of expanding the frequency band that are converted will be considered a little later.

Існують дві схеми модуляції хвилі, яка розповсюджується у хвилеводі:

a   *b*

==треба переклад==

Fig. 5.8. Wave diffraction schemes on PAX-modulators: a – diffraction is similar to diffraction on a thin grid; b – diffraction similar to diffraction on a

1. Colinar (situation 1) – the wave spreads in the direction parallel to the direction of the acoustic wave, that is, a dynamic lattire element of I/O is created. The parameters of radiation excreted from the wavelet (primarily the intensity and angle at which it spreads in the cover layer) are uniquely related to the characteristics of the lattice, and therefore related to the characteristics of the control voltage.

2. Non-colored (situation 2) – the wave spreads in the direction perpendicular to the direction of distribution of the acoustic wave. In this case, diffraction phenomena occur, which are by nature similar to the phenomena considered in the description

of planar diffraction optical elements.

The second method of modulation is more common and promising. Therefore, we will consider it in more detail. For non-collineary converters, two circuits of wave diffraction are possible, which is distributed in the wavelength (Fig. 5.8).

1. The first scheme (Fig. 5.8 a) is similar to the scheme of diffraction on a thin grid. The condition of such a process:

$$l_a \ll \frac{\lambda_a^2}{\lambda}. \tag{5.11}$$

We have a set of diffraction orders. The efficiency of the diffraction grid depends on the l_a. However, this value cannot be relatively large, as acts of re-diffraction are possible.

2. The second (Fig. 5.8 b) is a similar diffraction on a thick grid (as in the case of Bregiv electro-modulator). The condition of such a process:

$$l_a \gg \frac{\lambda_a^2}{\lambda}. \tag{5.12}$$

In this case, if the light falls on the grid at an angle (Braga angle), which is determined by the ratio of

$$\sin \Theta_{br} = \frac{\lambda}{2\lambda_a}, \tag{5.13}$$

interference resonance occurs and after diffraction on the grid in the ideal case we have only one beam, which has the direction of the first order of diffraction.

So, even if the optimal conditions of light diffraction on the Bregovsky modulator are not met, its effectiveness is much higher than the efficiency of the previous modulator. In addition, the selectivity of the Breg angle modulator gives additional opportunities when creating integral-optical devices, for example, selectors (filters) of a certain frequency of electric signal or spectroanalyzators, if you use optical beams with a wide angular spectrum (beams that converge or diverge).

5.3. Magnetic optical modulators

The work of integral-optical active elements with magnetic control is based on the transformation of wave-like modes due to magnetimation of waveguid film. In many materials used in integral optics, non-diagonal components do not equal zero insematic permeability in the dielectric penetration theorem. Therefore, systems of equations (for each component), similar to the material equations we consider for electrical and magnetic fields, are not independent. So TE and TM fashion are also addicted. At the same time, there is a pumping of energy from TE- to TM-fashion. As for modulators, on connected wavers, you can enter the interaction distance and communication coefficient. At the same time, for the complete (effective) pumping of energy from one fashion to another, it is necessary to agree on the constants of distribution of TE- and TM-mod. Changing the difference between these constants (in order to obtain $\Delta\beta=0$) can, for example, be carried out by changing the orientation of the magnetic moment of the wave film.

5.4. Light generation in integrated optics systems

The most important requirement for coherent light sources in the integral-optic device (in addition to the fact that it is necessary to satisfy the fundamental technical requirements for coherence, wavelength power, etc.) is the easy integration of the radiation source into the integral circuit. The first way is the formation of a non-negative connection of a standard emiator with an integrated circuit. The second is the formation of a laser in the scheme itself. Injectable semiconductor lasers with distributed inverse communication and distributed Bregiv reflectors are most suitable for these purposes. We will talk more carefully about the problem of the source in wave optics when studying light-water systems.

6. INTEGRAL OPTICS IN DEVICES AND DEVICES

By analogy with the devices of microelectronics of the integrated optics system is very often called optical integral circuits (OIS). From the preliminary consideration it follows that such devices must have unique properties and characteristics. Let's list the main ones:

1. Means of integral optics allow to achieve the minimum size of optical circuits and implement (at least in one-dimensional version) most algorithms of traditional optics.

2. Technological capabilities of integrated optics (in most cases, OIS technology - advanced electronic industry technology) allow to obtain large batches of OIS with relatively small costs.

3. The physical features of the distribution of optical signal, inherent only in integral optics allow to build a number of fundamentally new optical devices.

These features include, first of all, the selective properties of integral-optical systems, which are manifested in the modal nature of radiation propagation.

6.1. Sensors of physical quantities and devices based on lattite I/O elements [34,35]

Recall that in real waveguode spreads a continuous spectrum of radiation. The ratio of intensity (amplitude modules) of these waves is determined by the following characteristics of wavelets: the coefficient of passing of the wavelength environment; wavelength length; scattering of the waveleft medium, the state of the boundary between the wave water and the intersex environments.

Accordingly, if you enter light into such a system, for example, with the help of an I/O lattile element, then not only a wave agreed with wavelength modes will be introduced into the OIS, but also waves that spread in close directions. So, in the real OIS there is some area of angles within which a flat wave can be introduced into the wave. This corner area is called the input area.

The width of this area $\Delta\Theta_m$, is determined by the angles within which the intensity of radiation injected into the wavelet falls to the level of 0.1 from the maximum intensity. Naturally, for different mods, this value is different. Note

Fig. 6.1

that $\Delta\Theta\_m$ is defined both by the characteristics of the wavelength (its length, losses) and the characteristics of the I/O element, such as the length of the bond, which in turn is determined by the depth of modulation of the lattice. Figure 6.1 shows intensity dependences, within which oscillations can spread in the wave zone with a
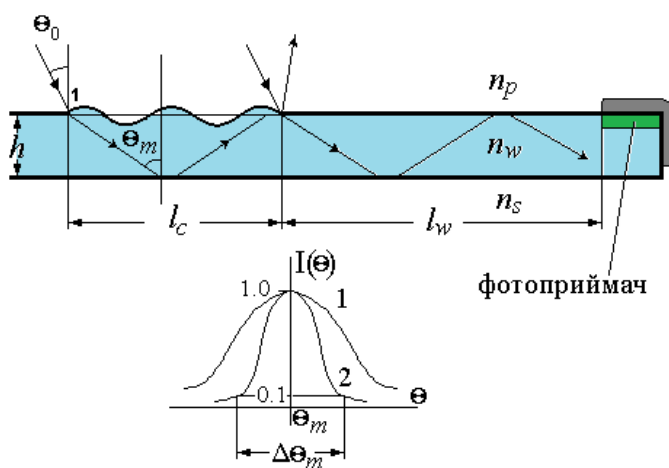
grid (curve 1) and in the area of the waveleshed directly (curve 2). Ultimate $\Delta\Theta_m$ is defined by a narrower curve. In our case, the curve 2, that is, the characteristics directly waver. It should be added that this situation arises almost always with the exception of special cases that we will not consider.

6.1.1. Angle measuring sensors

As a characteristic example of devices that use the angular selective properties of OIS, consider the work of the angle sensor, which is schematically shown in Figure 6.2.
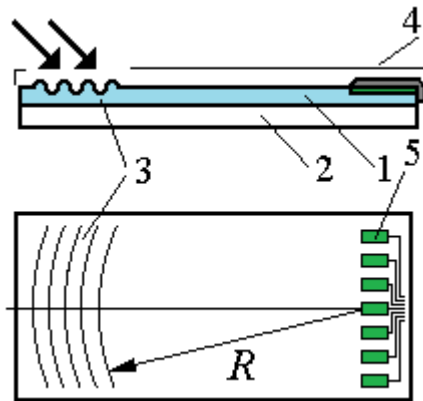
Fig. 6.2. Diagram of the angular sensor with a lattite input element:

1 – waveguid, 2 – substantive, 3 – focusing lattile element of input/output, 4 – protective casing, 5 – matrix of planar receivers

As an element of I/OIS, the focusing lattite element of I/O is used. Such an element is made using holographic technology and is a number of concentric circles, the center of which is located on the receiving plane of the central photo receiver of the matrix of planar photo receivers. Thanks to this design, the input/output element, the radiation introduced into the IOI, focuses in the plane of the matrix of photo receivers. At the same time, the characteristics that affect the process of entering a wave in the OIS remain the same as that of a regular lattice with the same period, modulation depth and communication length. The width of the input area of such a sensor is from 10 angular seconds to half a degree, depending on the parameters of the wavelet. OIS is designed to measure the angles at which parallel beams of radiation spread with a certain wavelength. It is for this wavelength that the sensor is calculated (characteristics of the wavelength and I/O element). OIS is able to measure angles in two planes. In one plane, changing the direction of the beam leads to a change in the signal on any receiver and is due to the degree of consistency of the direction of the icing beam with the directions of wave-like modes. In the second plane, changes in the irradiation angle lead to the drift of the light spot along the matrix of receivers, which also allows you to measure this angle.

The second type of angle sensor is shown in Figure 6.3. The OIS input/output element is made in the form of a two-dimensional grid. The period of such a grid is designed so that for the working wavelength of the wavelength, the introduction into the
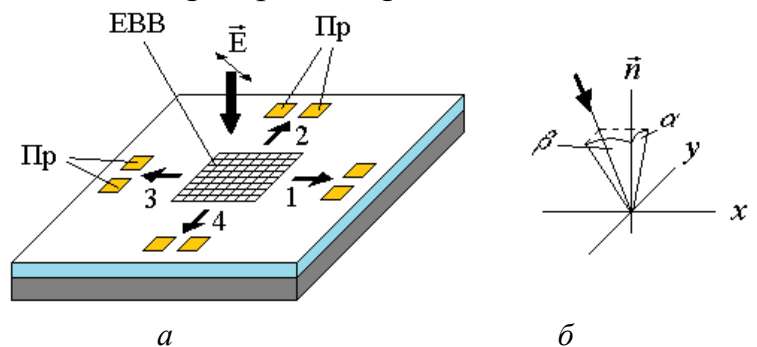
Fig. 6.3. Angular sensor with two-dimensional I/O element: a – sensor circuit, b – orientation of the beam of light relative to normal to the surface of the sensor

Треба переклад

wavelength occurs at an angle close to 00 (see Figure 6.4, dashed curve), that is, the maximum intensity of the introduced wave is observed at the angle of irradiation $\Delta\Theta_{max}$. Note that the parameters of the I/O element and the waveleader were calculated to polarize the beam, in which the direction of oscillation of the electric vector was 45^0 with strokes of the grid, or for a circular-polarized beam. This limitation is due to the fact that the conditions for the introduction and spread of waves in the wavelength are different for TE0- and TM-mod. Then, when the beam falls normally on the grid, light is injected into four opposite-directional wave-like channels. Accordingly, the intensity of radiation in all four channels is equal. As a result, the signal on all four receivers (Pr, see Figure 6.4 a) by module is the same.
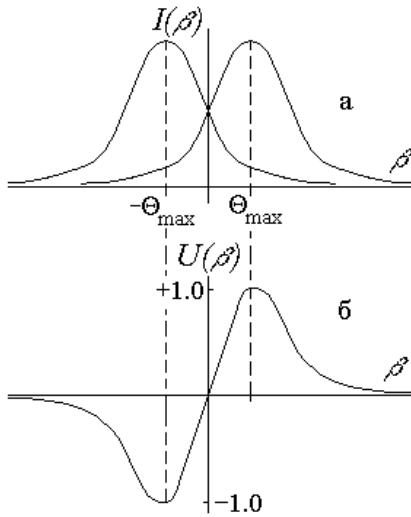
The direction of the beam falls is characterized by two angles α and β(Fig. 6.3 b) relative to normal $\vec{n}$ to the detector surface.

We will assume that the angle $\alpha = 0$ and the beam is tilted only in the plane $\vec{n},x$. Figure 6.4 shows the change in intensity in channels 1.3, depending on the angle β (Fig. 6.4a). Included priymachy 1, 3 and priymachy 2, 4 for the differential scheme. In the second vipadku, yakshcho intensivnosti hvil at the channels however, the sumarny signal priymachiv dorivnyuje zero. The signal on the sensor in the area of the system β shown in Fig. 6.4 b. The maximum signal in the module corresponds to the angle of orientation of the beam, which lies near the angle Θ_{max}. After that, the angle of the output signal of the detector begins to fall. Accordingly, the angle area in which angular measurements can be carried out is equal to:

Рис. 6.4

$$\Delta\beta \approx \Delta\Theta + 2\Theta_{max}. \qquad (6.1)$$

In this case, the sensitivity of the detector is doubled compared to a single channel sensor with the same angular selectivity.

It should be added that the detector operation is practically independent in the planes $\vec{n},x$ and $\vec{n},y$ wide range of angles. At a fixed angle β angle α can vary widely, which significantly exceeds the value of the $\Delta\beta$. Yes, change corners α can reach degrees. All of the above also applies to the measurements of angles in the plane $\vec{n},y$.

6.1.2. Wave-like filters based on abnormal reflection phenomena [16,36]

Let us turn to Figure 6.5, which depicts a wavelet with one boundary promodulated diffraction grid. Let the lattice period be such that behind the boundary of the environments, the cover layer-wavelead can exist only one diffraculation order. Accordingly, only one (zero) order can exist in the cover layer.

Then after the interaction of the initial wave U_0 with the grid we have the following processes:
1. Diffraction 0_t pass order (field U_3).
2. Diffraction $+1_t$ order in waves.
3. Diffraction 0_r reflective order (field U_1).
4. Wave wave reflection from the lower boundary.
5. Wave wave diffraction in $+1_r$ order of reflection. This order applies in the same direction as 0_t order and forms a field U_4.
6. Wave wave diffraction in -1_t order in the covering environment. This order extends in the same direction as 0_r order and forms a field U_2.

Рис. 6.5

It should be added that in accordance with paragraph 4.1.2, some stationary field is installed in the wave drive.

It can be shown that for the ideal wave drive and the direction of irradiation, which coincides with the direction of excitation of wave-like mods, the field U_3 and U_4 are the same in amplitude, but differ in phase on the π. At the same time, the fields U_1 and U_2, which are also distributed in the same direction, are the same in phase.

So, as a result of interference summation, the field in the subduction has zero amplitude, and in the cover layer, on the contrary, it is strengthened. This phenomenon was called abnormal reflection-passing. If, change the wavelength, then this phenomenon occurs at a different angle of lighting structure.

Typical dependencies of reflection and bandwidth coefficients for such a structure are shown in Figure 6.6. Curve 2 is a curve of dependence of radiation intensity, which is skipped by the structure. Curve 1 – the dependence of the intensity of reflected radiation from the structure. One hundred percent reflection (absorption) is observed for the angle Θ_{36}.

Fig. 6.6
Abnormal reflection-passing by a wave-like structure.
1 – dependence of the intensity of the reflected radiation, 2 – dependence of the intensity of radiation, which is missed by the structure

Треба переклад

The half-wide area in which the phenomenon of abnormal reflection is observed, the passing depends on the depth of modulation of the lattice. The lower the modulation depth, the smoother the curve. If the structure is illuminated by

polychromatic radiation, then the half-wide spectral line, which can be distinguished by such a filter can be very narrow and coincide in order with a similar characteristic for interference filters, that is, do not exceed $20A^{\circ}$.

A similar phenomenon is observed for the non-ide wavelead and lattice, which forms more than one diffraculation order, but the queasing and amplification do not occur in full.

6.2. Integrated optical information signal processing devices. Principles of optical wave-wave signal processing. OIS construction methods for information technology [17,18]

Consideration of the general principles of optical wave-wave signal processing and OIS construction methods for information technology is closely related to the classification of OIS, the choice of basic wave-based elements and materials for them.

6.2.1. Types and main classes of OIS for information processing

Classification OIS can be carried out in many ways. For example, according to the design, technological and physical principles of construction, for the purpose of the type of materials used, etc. From a practical point of view, the most significant difference between OIS is related to the possibility and /or necessity of their docking with fiber optic systems. Depending on the type of connection, there are three main types of OIS:

1. OIS, which require docking with fiber light water both at the entrance and at the outlet;
2. OIS, which require docking with fiber light water only at the outlet;
3. OIS that do not require docking with fiber light water.

OIS of the second third class are docked at the entrance, as a rule, with an emiper or with another OIS, and the IOIS of the third type is docked at the exit with a photo receiver or other OIS. From the point of view of functional purpose, there are three main classes of OIS for information processing:

1. Analog OIS for signal processing;
2. Digital and logical OIS for computer technology;
3. Switching OIS.

Examples of OIS of the 1st class are IO spectroanalyzators, correlators, analog-digital and digital-analog converters (ADC and CAA), etc. The second class includes arithmetic and logical OIS multi-type OIS, etc. Third-class OIS are different robes and switches.

6.2.2. OIS for signal processing
6.2.2.1. Integral optical spectroanalysis of high-frequency signals

Figure 6.7 illustrates the scheme of the integral-optical spectrum analyzer. Lining – silicon/silicon edicles (*Si/SiO₂*)

We will evaluate the transformation of spatial parameters of the information signal with the help of AI-modulator:

Рис. 6.7. Схема інтегрально-оптичного спектроаналізатора:
1 – напівпровідниковий лазер, 2 – градієнтні лінзи Френеля, 3 – ПАХ – перетворювач, 4 – матриця приймачів, 5 – хвилевід, 6 – підкладенка (Si/SiO₂), 7 – шар оксиду цинку.
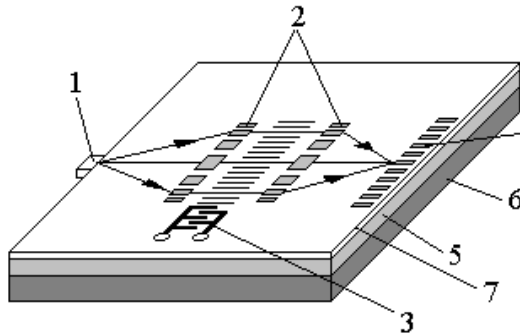
- Electric signal modulation frequency $\sim 10^6 \div 10^7$ Гц;
- Beep modulation rate (same) $\sim 10^6 \div 10^7$ Гц;
- Electrical signal propagation rate $\sim 10^5$ м/с;
- Beep propagation rate $\sim 5 \times 10^2$ м/с.

From the known ratio $\lambda = \frac{c}{f}$ it follows that $\lambda_{electr} \sim 10^{-2} \div 10^{-1}$, and the length of the acoustic wave and, accordingly, the period of the given lattice $\lambda_{ac} \sim 1\text{mcm} \div 0.1\text{mm}$. Naturally, such periods of the lattice are easily placed within the resolution limits of most materials. Consequently, the transformation of the signal from the radio to the sound range leads to a significant simplification of its analysis. Add that the limit frequencies that can be analyzed with this type of analyzers reach a value of 500 MHz.

A significant drawback of such a spectroanalysis is that the pin converter is able to effectively excite a surface acoustic wave of only a certain relatively small band of frequencies (no more than 100 MHz).

This disadvantage can be greatly overcome if you use not one, but a number of pin converters, which are designed for different frequencies (Fig. 6.8). Such modulators are turn on in parallel. Different distance of PAX-modulators to fourier-converting lens leads to a phase shift in the plane of receivers. However, since the intensity of signals is fixed,

Fig. 6.8
Треба переклад

as shown above in paragraph 2.7.2, this phase multiplier disappears. So, in the plane of receivers, the spectrum of power of the electrically sound signal is fixed. The operating frequency band in these converters can reach 1000 MHz.

We will conduct an evaluation calculation of the resolution of the spectroanalyzator by the frequency of the electric signal.

Recall that the lens creates in the focal plane Fourier-image of the field, which is formed in front of the lens:

$$U(\xi) \sim \Im(\xi) = \int_{-\infty}^{\infty} U_0(x) \exp\left(-j \frac{k n_w}{f} x \xi\right) dx, \tag{6.2}$$
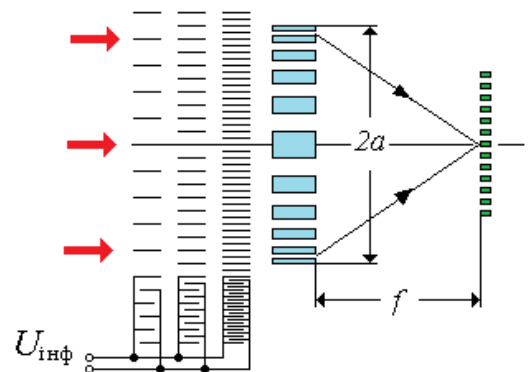
where ξ – Spatial coordinate in focal plane, $f = \dfrac{R}{(\frac{n_f}{n_w}-1)}$ – focal length of the lens, n_f – lens relapation indicator. However, the start field U_0 – specified in the area $2a$ (see Figure 6.8), which is limited to the modulator's working area (if it is smaller than the lens input) or the lens input slot (if the modulator's working area is larger than this hole). In this case, (6.2) is transformed to:

$$U(\xi)\sim \int_{-\infty}^{\infty} P_a(x)U_0(x)\exp(-j\frac{kn_w}{f}x\,\xi)dx \qquad (6.3)$$

According to (6.3)

$$U(\xi)\sim\Im\{P_a(x)\}\otimes\Im(\xi) \qquad (6.4)$$

Consequently, any flat wave is focused by the lens into a spot whose dimensions are customary defined as the dimensions of the area occupying the zero diffraculation maximum function $\Im\{P_a(x)\} = 2a\,\dfrac{\sin(\frac{kn_w}{f}\xi a)}{\frac{kn_w}{f}\xi a}$. Accordingly, the dimensions of this order (and the minimum possible diffraction spot) are determined by the ratio of:

$$d_{min} = \frac{\lambda f}{n_w a} \qquad (6.5)$$

From this ratio follows a number of conclusions:

1. It makes no sense to make the size of the receiving planes of the photo receiver less than this value

2. Spectroanalysis resolution determined by diffraction angle difference

$$\Delta\varphi > d_{min}/f, \qquad (6.6)$$

which corresponds to the periods of running waves formed by close in frequency signals. The period of running "acoustic" lattice is equal to the length of the acoustic wave:

$$T = \lambda_a = \frac{v_a}{F}, \qquad (6.7)$$

where v_a – sound speed in wave water layer, F – frequency of electrical signal. Then, based on the grid formula $Tn_w\sin\varphi = m\lambda$ (on the condition that the $\sin\varphi\approx\varphi$ and use the first diffraculation order) we have

$$\Delta F > \frac{d_{min}n_w v_a}{f\lambda}, \text{ або } \Delta F > \frac{v_a}{a}. \qquad (6.8)$$

At v_a=1000 m/s, and a=10 mm, $\Delta F = 100$ Khz

6.2.2.2. Integral optical correlations

Integrative optical correlators (IOC) can be used to implement convolution type operations in image recognition tasks for decision-making purposes.

IOC can be divided into two types:

1. Corelators with prostorovim integruvannyam.

2. Correlates with time integration.

The diagram of the correlator with spatial integration is shown in Figure 6.9. With the help of two PAX modulators that form acoustic waves spreading towards the second, two running grids are formed, thereby ensuring the shift of two modulating functions in time. The integration is done with a 7 lens. In the plane of the photo receiver, a certain signal is formed, which is a convolution of signals: reference $S_1(t)$ and comparison signal $S_2(t)$.
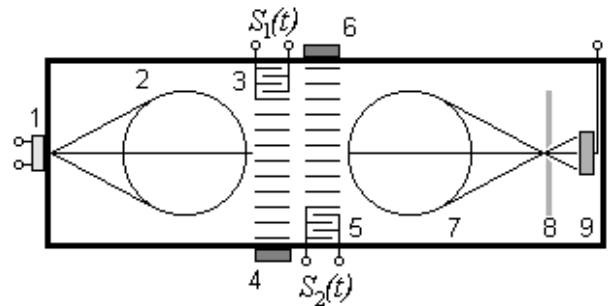
Fig. 6.9

1 – semiconductor laser, 2,7 – planar lenses, 3,4 and 5,6 – PA-modulators of reference (reference) signal $S_1(t)$ and comparison signal $S_2(t)$, 8 – frequency filter, 9 – receiver
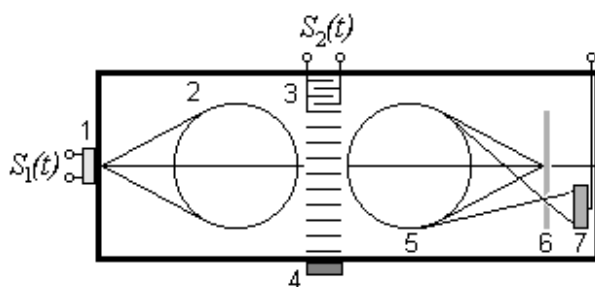
Fig. 6.10

1 – semiconductor laser – reference signal generator $S_1(t)$, 2.5 – planar lenses, 3.4 – PAX modulator – comparison signal modulator $S_2(t)$, 6 – frequency filter, 7 – receiver

The diagram of the correlator with time integration is shown in the figure 6.10. Reference signal $S_1(t)$ is set by modulation of the current pumping source of the radiation source. Comparison signal $S_2(t)$ signal that modudes a certain high-frequency signal (intermediate frequency signal). Then the frequency of the running grid remains sustainable. So the diffraculation order always has one direction. Lattice modulation depth is determined by modulating signal $S_2(t)$, which moves along the modulator with the speed of acoustic wave propagation. Spatial signal shift τ the speed of acoustic wave propagation. The field behind the modulator 3.4 can be considered as the product of two functions $S_1(t)$ and $S_2(t+\tau)$, diffraets on the grille. Integration is done with lens 6. In the plane of the photo receiver, a certain signal is formed, which is a convolution of signals: reference $S_1(t)$ and comparison signal $S_2(t)$.

Figure 6.11 shows a schematic diagram of the integrated optical correlator of digital signals. Reference signal, comparison signal, ("filter function") $U_{етал}$ is fed to the electrooptic spatial modulator 10. With the resolution excitation of individual segments of the modulator, reference functions of various types can be formed in a wide range with high resolution. In other words, when supplying voltage to the sections of the modulator due to an electrooptic change in the circuit of the wave layer, a stationary (stationary) diffraction grid is formed, which makes it possible to modulate a homogeneous beam 4 in parallel with several information channels (their number is equal to the number of sections of the modulator). PAH modulator 6 forms a running surface acoustic wave $U_{інф}$, which in turn forms a dynamic grid.

Input signals are converted into paah pulses, the length of which is consistent with the length of the
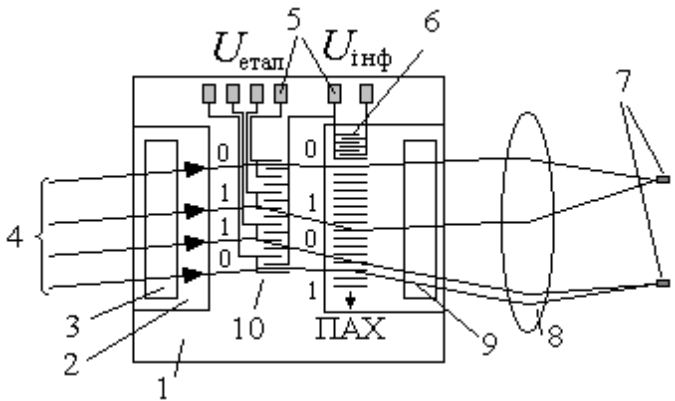
Треба переклад

Fig. 6.11. Schematic diagram of the integrated optical correlator of digital signals:

1 – wavelet made of lithium niobate, 2 – contact plane for prism, 3,9 – prismen of communication elements, 4 – entrance beam, 5 – terminals for supplying information signals, 6 – pax transducer, 7 – photo receivers, 8 – lens,

modulator elements. Unit is encoded by high-frequency PAX, zero – low-frequency.

The multiplication operation is performed by double diffraction on two grids (movable and stationary). Integration is done with a 8 lens. The geometry of the device is as follows (periods of diffraction grids) that the light beam, which corresponds to the convergence discharges of the input parcel (1-1, 0-0), falls on one receiver, and if it corresponds to incomparable discharges (1-0, 0-1), – to another receiver.

Shown in Figure 6.11 integral-optical correlator, designed to process 32-bit codes at a performance of 32 MBit/s.~ 10^9 operations per second.

6.3. Analog-to-digital converters. Four-bit ADC

The basis of integral-optical ADC is a matrix of modulators of interference type (Fig. 6.12 a).

Laser radiation with sampling rate $f_Д$ submitted for OIS entrance. Analog signal U is fed to the control electrodes (A) of the matrix of interferometers. Note that each subsequent interferometer has a length of two times less. Consequently, the same voltage leads to half the change in the relature rate. As a result, the phase difference changes by half. Modulation of intensity on interferometers, depending on the voltage, is shown in Figure 5.3.2.

00	0000
01	0001
02	0010
03	0011
04	0100
05	0101
06	0110
07	0111
08	1000
09	1001
10	1010
11	1011
12	1100
13	1101
14	1110
15	1111

a   *b*

Fig. 6.12

Зміна напруги після нелінійного елемента

Fig. 6.13

Треба переклад

At the output of interferometers are receivers and nonlinear elements, which are triggered at some threshold level, which is indicated in Figure 6.13 dotted. The flux level is set by the reference signal, which is formed by a light flux that has not passed through interferometers. Then at the output of such a scheme we will have a sequence of pulses frequency f_D and the amount determined by the U According to Figure 6.13 (thick lines).

The initial phase difference in all interferometers is set equal to the value $\pi/2$. *To do this, the design of the ADC provides for the initial regulation of interferometers by voltage U_{zm},* electrodes (V). A compass is installed at the system output. So, the source elements of OIS form the code in accordance with the table shown in Fig. 2. 6.12 b.

6.4. OIs for computing

At this point we will consider bishabic and multistabil integrated optical devices. It is known that it is on the basis of bistabil and multi-capital elements that logical cells of modern electronic computing machines are built.

Fig. 6.14

Optical bistabil element is called a device, dependence of the power of the optical signal $P_{вих}$ which is from the power at the in entrance of the element $P_{вх}$ has the form of a hysteresis loop (Fig. 6.14).
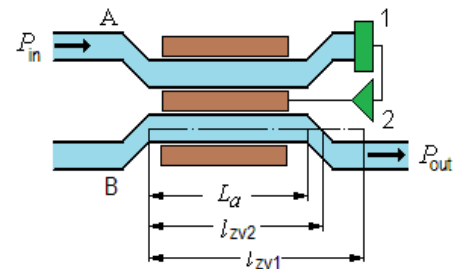
One of the first devices in which the phenomenon of optical bistebility was observed is a certain resonator filled with a nonlinean environment (Fig. 6.15). At low intensity of input signal of a certain wavelength λ the condition of the standing wave in it is not met:

$$L_r n(I) = (2m + 1)\frac{\lambda}{2} \qquad (6.9)$$

where L_r – resonator length, $n(I)$ – nonlinean environment relaining indicator that fills it, $m=1,2,…$ – Integer. In such a situation, the resonator acts as a certain absorbing filter. Consequently, the intensity of radiation at its output is significantly less than at the inlet.

With an increase in intensity, the terlacation indicator of the environment and the "frequency" of the resonator settings increasingly coincide with the frequency of wave oscillations, that is, the left and right parts of the ratio (6.9) are increasingly

Fig. 6.15

1,1 – resonator, 2 – nonlinean electro-optical environment, 3 – light divider, 4 – photodeteur, 5 – voltage amplifier, 6 – control electrodes

different. As a result, the intensity of radiation in the resonator itself and at its output begins to increase, which in turn leads to an additional increase in $n(I)$. In fact, a link of positive inverse bond is formed, so the process will continue until the ratio (6.9) of the power gain curve at the output of such an element has a jumping-like character similar to the curve shown in Fig. 2. 6.14. With a decrease in the input intensity, the presence of nonlineanity of the medium and the fulfillment of the condition (6.9) will "maintain" at a certain level the output power of radiation until the system "breaks". In this case, the input intensity level is precisely insufficient to ensure that equality (6.9) and the left and right parts of it differ in magnitude close to $\lambda/4$. Thus, a hysteresis loop similar to the curve shown in Fig. 2 is implemented. 6.14.

However, the implementation of such devices with "clean" optical bistebrity is problematic, since significant changes in the relapse rate require significant laser source capacities (close to 1 MW/cm2). Hybrid technology allows you to get out of this situation and create bisabile elements that work at relatively low
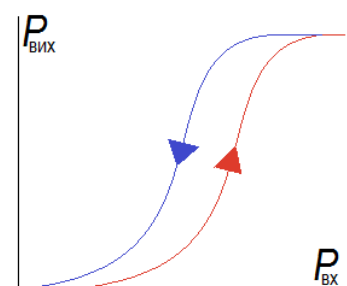
Рис. 6.16

capacities. To do this, electro-optical material is used as a nonlinean medium. Part of the radiation at the output of the element is given to the photo receiver 4 (see Figure 6.15). After that, the electrical signal is amplated and fed to the control electrodes. Due to this, the relapation rate of environment 2 changes further.

Note that modern technology allows you to create such devices in a planar version in the form of OIS.

Figure 6.16 depicts a bistable element made on the basis of connected wave overs. At low intensity, the length of the active area of the X-branching is less than the length of the bond. Consequently, the light wave spreads, both in channel B and in channel A. The signal from the output of channel B enters the photo receiver 1 and through the amplifier 2 is fed to the control electrodes. With an increase in intensity as a result of the action of light, a decrease in the length of communication occurs. Accordingly, an increasing part of the luminous flux is pumped into channel B. However, the system parameters are selected in such a way that for a long time the intensity in channel A increases in absolute units of measurement. Such a process will occur until the ratio between the length of the active area and the length of the communication is close to the unit and due to a decrease in the fate of the intensity that remains in channel A, the signal on the photo receiver will not cease to grow. At the same time, the increase in intensity in channel B occurs much faster than the growth of this value at the entrance of the OIS, the attenuation of intensity in this channel occurs with a certain delay.
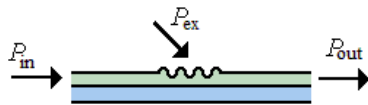
Рис. 6.17

The following device is made on the basis of a nonlinean wave drive and a lattile communication element (Fig. 6.17). At low intensity P_{in} beam P_{ex} wave waves are not introduced, since the diffraction angle in the wave-drive environment does not correspond to the direction of wave mods. With increasing input intensity P_{in} *3D* irraction indicator begins to change, which in turn leads to a change in the angle of diffraction of the beam P_{ex}.

In the rest, the angle of diffraction becomes close to the angle at which the fashion and intensity in the middle of the wave water spreads (and at the OIS output too) begins to grow rapidly. With a decrease in input intensity, the initial behaves in the same way as in the previous two cases. Naturally, to ensure the operation of such an element at low intensity in the construction of such a bistabil device, hybrid technology can also be used with the organization of an electronic link of positive inverse communication.

6.5. Examples of building logical elements

On the basis of bistabil elements, all logical cells can be built on the basis of which electronic computing machines are built. Figure 6.18 and the diagram of the integral-optical element of type "I", which is built on the basis of the bistebil element depicted in Fig. 2. 6.17. For convenience in Figure 6.18 b a table of input and output signals for such an element is given.

Note that in the absence of a signal P_{in1} signal P_{in2} not injected into the waveguide, because the angles at which diffraction orders are propagated are inconsistent with the distribution constants of waveguide mods β_{m0}.

Let in the first stage the structure depicted in the figure immines only the signal P_{in1}. At the same time, the indicator of thyrization of the wavelep environment changes and the wave changes P_{in1} spreads along the wave drive with the distribution constant β_1. This constant is close to the constant β_2, which has a wave P_{in2} diffraction on the grid. After distribution in a certain area of the wave, this fashion is displayed in the cover layer using the second element of I/O. The direction of distribution of diffraction orders 1 is determined by the lattice equation and the constant β_1. While

а   б

Рис. 6.18

imenting the structure with both signals as a result of changes in the fracture indicator, the signal P_{in2} partially introduced into the wavelen, which in turn leads to an additional change in the n_w In the end, a stationary field is installed in the wave drive, which corresponds to a wave-like fashion with a distribution constant β_{1+2}. Then, when withdrawing it from the wavelet in the cover layer, it will spread in the direction 2, which does not coincide with the direction 1. This allows you to distinguish them, for example, by using a set aperture. So we have such a table of directions of wave propagation in the cover layer, depending on what signals are fed to the inputs of the OIS:
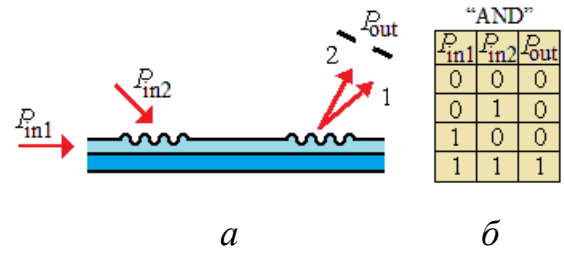
P_{in1}	P_{in2}	Direction of distribution in the cover layer
n/a	n/a	n/a
n/a	is	n/a
is	n/a	1
is	is	2

So, the table is fully implemented, which is shown in Figure 6.18 b.

In Figure 6.19, the OIS is depicted, which works as an element "NO"-"AND". The basis of the element is a planar modulator of the interferometric type, in its initial state it is configured for zero phase difference between signals that spread over its various branches. Accordingly, in the absence of signals $P_{вх1}$ and $P_{вх2}$ at the output of the modulator, the maximum intensity of the.
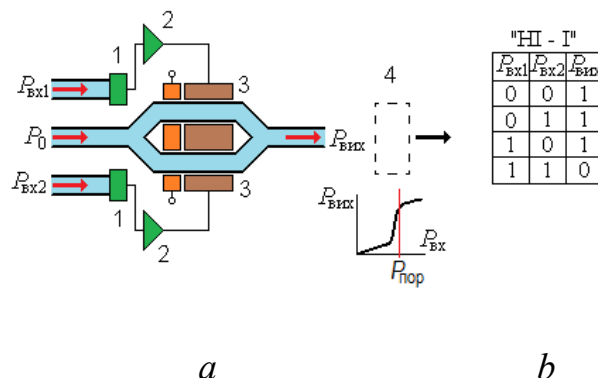
In the presence of both signals, the branches of the inverse are triggered in such a way that the final phase difference is set equal to π. If there is a signal $P_{вх1}$ or $P_{вх2}$ The phase difference has a value close to $\pi/2$. So the initial intensity becomes close to half the intensity from the maximum. If a nonlinear element with a threshold sensitivity curve is set at the output of the interferometer, then the

а   b

Fig. 6.19

Треба переклад

signal levels in the second and third cases become equal, that is, the presence or absence of signals at the output of the device fully corresponds to the table shown in Figure 6.19 b.

7. ELEMENTS OF FIBER OPTIC TRANSMISSION SYSTEMS
7.1. Physical characteristics of optical fiber [21-27]
7.1.1. The main elements of optical fiber
The main structural elements of optical fiber (OV) are shown in Figure 7.1.
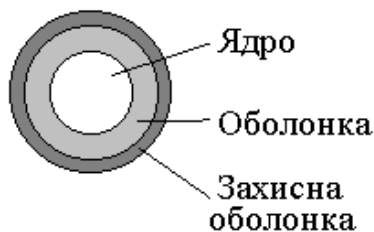
Fig. 7.1. Optical fiber structure

Треба переклад

Each fiber consists of a nucleus (core) and a shell. This is a waveguide system.

Core – made of glass or plastic. The number of mods transmitted by wavelegum depends on the diameter of the core.

The protective shell provides fiber strength, absorbs impacts, creates additional fiber protection against environmental impact. Such buffer shells are usually multilayer, are made of plastic and have a thickness of 250 to 900 microns.

The dimensions of the fiber are generally determined by the outer diameters of its nucleus, shell and protective shell. Usually these dimensions are recorded through a tilted dash. For example, 50/125/250 means that the diameters of the nucleus, shell, and protective shell are 50.125.250 microns, respectively. The protective shell is always removed when the fibers are connected.

7.1.2. Types and characteristics of optical fiber
The fiber type is identified by the modal composition of oscillations that can be distributed in fiber. Fibers are divided into two main types – multi mode fiber and single mode fiber. These fibers differ in the diameter of the core and shell and the profile of the core relapation rate.

Multimode fibers can be stepped or gradient. Singlemode fibers are divided into stepped, or standard fibers (SF), shifted dispersion fibers (DSF), and nonzero displaced fibres (NZDSF), which differ in the relature indicator profile..

7.1.2.1. Profiles of relature indicator
Профілі показників заломлення наведені на рисунку 7.2

Multimode fiber with stepped profile (Fig. 7.2 a). Currently, fibers of two types are mainly produced: 100/140 and 200/240. Multimode fiber with gradient profile (Fig. 7.2 b) is more common. Unlike fiber with a stepped profile, the fiber core with a gradient profile consists of numerical layers of glass, in which the latture rate decreases from the center to the edges of the fiber. Due to the fact that the distribution of the entrization indicator has a nonlinean profile, it turns out that the distribution constant for modes with a higher number and mods of low orders is approximately equal.

Thus, to some extent, modal dispersion is eliminated, which is known to significantly limit the range of the transmitting area and leads to distortion and destruction of the information signal.

a $\qquad$ b $\qquad$ c $\qquad$ d
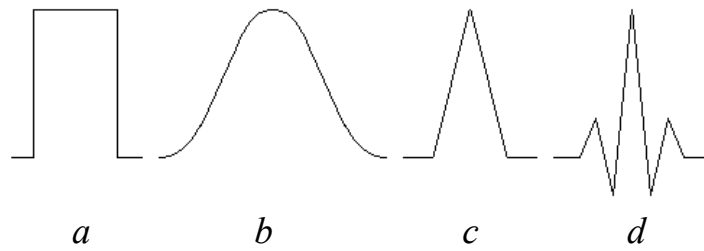
Fig. 7.2. Types of profiles of optical fiber latification indicator
(a) stepped monomode and multimode fiber; (b) multimode fiber with gradient profile; (c) single-morse fiber with shifted dispersion; (d) singlemode fiber with offset nonzero dispersion

Fibers with gradient relature indicator are presented on the market in sizes: 50/125, 62.5/125, 85/125.

Single-mode fiber, presented on the market, can be mainly of three types: single-mode fiber with a stepped profile (Fig. 7.2 a); monomode fibers with displaced dispersion (Fig. 7.2 v); single-mode fibers with displaced nonzero dispersion (Fig. 7.2 g).

Single-model fibers are characterized by dimensions: 8-10/125.

7.1.3. Properties of optical fibers as a passing medium
7.1.3.1. Absorption in optical fibers

Recall that the state of the quantum system in energy terms is characterized by energy levels and is described by the expression [1]:

$$(\omega_{12})B_{12}N_1 = A_{21}N_2 + U(\omega_{21})B_{21}N_2 \qquad (7.1)$$

where $U(\omega_{12}), U(\omega_{21})$ − energy density of radiation at frequency ω in a single frequency interval, B_{12} − probability of quantum transition from state 1 to state 2 (1→2), N_1 − number of electrons at level 1, A_{21} − coefficient or probability of spontaneous radiation (accidental transition) of electrons from level 2 to level 1 (2→1), B_{21}− coefficient of stimulated or forced radiation, N_2 − number (population) of electrons at the level of 2.

The left side of the expression characterizes the absorption of the system and the transition of electrons to the highest level 2. Rights − radiation (transition of electrons from level 2 to level 1).

Analysis of the expression (1) shows that the system can be in three states (Fig. 7.3)

State (a) number of electrons at the lower level N_1 (in an un aroused state) is greater than at the level N_2. In this case, the $U(\omega_{21})B_{21}N_2 = 0$. The system is in stable condition and is absorbent. It can only absorb photons. At the same time, photons are most

Fig. 7.3. Scheme of quantum states of matter.

a) – absorbent medium, b) – equilibrium or neutral environment c) – emitting medium.

intensively absorbed, the frequency of which coincides with the frequency of transition ω_{12}. Second state (b) – state at which N_2 approximately equal to N_1. $U(\omega_{21})B_{21}N_2$ is also zero, and the probabilities of moving from level 1 to level 2 and vice versa are approximately the same. The system in this state is neutral in relation to the falling radiation (naturally to a certain limit), that is, transparent. For many substances, in particular for pure quartz, such a system is stable. This explains the high transparency of optical fibers.

Most fiber optics devices use illuminators that run at wavelengths of 0.85, 1.31, 1.55 microns. It is at these lengths that "windows of transparency" of glass are observed.

Accordingly, optical fibers are optimized for absorption for these wavelengths.

Common losses are known to consist not only of absorption, but precisely they make up the bulk of the losses in optical fibers.

In modern fibers, quite high parameters for absorption are achieved. For example, for a multimode fiber of 50/125 at a wavelength of 0.85 microns, losses of approximately 3 dB/km are observed. For the same fibers at wavelength 1.31 microns loss does not exceed 1 dB/km.

In a single-mode standard fiber (SF) (with a step-by-step distribution of the entrization indicator). The standard aternation curve for such fiber is shown in Figure 7.4. For standard fiber, the singlemode mode is implemented for wavelengths of 1.31 and 1.55 microns and the following parameters are achieved:

    1.31 micron – 0.3-0.4 dB/km;
    1.55 micron – 0.2-0.25 dB/km.

However, despite the fact that the

Fig. 7.4
Треба переклад

second wavelength of absorption is less, the first wavelength is more often used, since it is in the neighborhood of this wave that there is no chromatic dispersion.

Singlemode fiber with displaced variance (DSF)

In order to optimize single-mora filament for absorption by selecting the profile of the thyrization indicator, shift the zero dispersion point to the wavelength area of 1.55 microns. With the help of such fibers, signal transmission areas without relay devices up to 100 km long can be implemented.
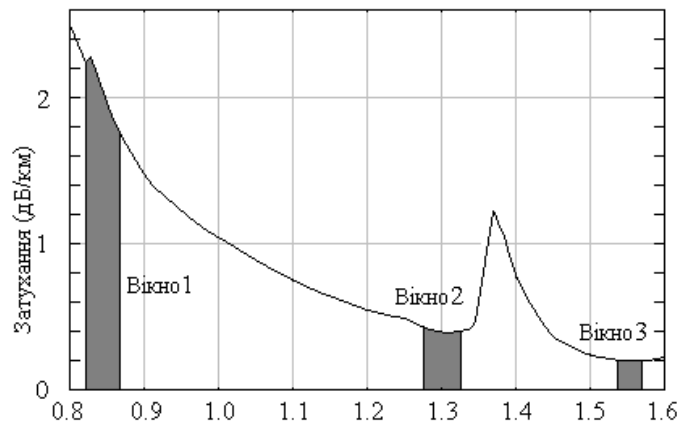
Singlemode fiber with displaced nonzero dispersion (NZSDF)

Unlike DSF fiber it is fiber optimized for multiple wavelengths.

Such fibers are made by creating a depressive ring in the optical shell. These fibers are also called monomode fibers with smoothed (leveled) dispersion. The dispersion of such fibers is approximately the same as that of a standard fiber with a stepped profile for a wavelength of 1.31 microns. However, with the increase in wavelengths, the tails of the waves penetrate into the depressive ring with a greater relapse rate. Accordingly, the total speed of wave propagation along the wavelength increases. At the same time, it is known that for a longer wavelength, the entrification rate of the medium is less than for waves with a lower length. This phenomenon is known to be called common variance or "material" variance. Thus, the "wave" dispersion (penetration of the wave into the layer of light with a higher entrification rate) compensates for the "material" dispersion. As a result, the distribution constants of all oscillations with different wavelengths remain approximately the same, that is, the ability to transmit signals with several wavelengths (multiplex wave signal) is created.

7.1.3.2. Wavewater dispersion

Once again, let's return to the phenomenon of dispersion and summarize the known facts (see p. 3.4). Variance is divided into intermodal (modal) and chromatic. Chromatic dispersion, in turn, can be divided into material (ordinary) dispersion and wave, which takes place gradient fibers. In our consideration, another type of variance is released – the so-called polarization dispersion. This type of dispersion can occur, for example, in fibers in which deviations in the shape of the fiber cross section from the circle are observed. The optical wave is known to have a vector character [1.2], that is, the process of wave propagation in fiber can be represented as the proliferation of TE- and TM oscillations. If the fiber structure is homogeneous, the cross section of the correct shape, then TE- and TM waves have the same distribution constants. However, in the process of manufacturing or laying fiber, the circle can turn into an ellipse. In addition, due to bends, other mechanical perturbations, local anisotropy may occur. In this case, TE and TM mods have different distribution constants. Consequently, the process of information signal propagation is accompanied by the destruction of the signal due to different speeds inherent in orthogonal-polarized modes. Note that polarization variance in order is much less than intermodal and chromatic. Consequently, such dispersion can be neglected (especially for multimode fibers). However, in the case when modal and chromatic dispersions are practically compensated and on boundary-length sections of lines

2 –волокно з зміщеною дисперсією;
3 – волокно з складним профілем показника заломлення

(especially for monomode fibers), the effect of polarization dispersion becomes quite noticeable.

Modal variance τ_m (for more information, see <a0/&gt p. 3.4) is mostly measured in ps/km (delay time per unit length). Chromatic dispersion τ_h is characterized by a coefficient of dispersion measured in ps/ (nm km). The behavior of the coefficient of chromatic dispersion is shown in Figure 7.5.

Full variance in fiber is determined by expression:

$$\tau = \sqrt{\tau_m^2 + \tau_h^2} = \sqrt{(L^E D_m)^2 + (L\Delta\lambda D_h)^2}, \qquad (7.2)$$

where D_m – intermodal dispersion coefficient, D_h – chromatic dispersion coefficient, $\Delta\lambda$ – width of spectral characteristics of the emiator, L – fiber length, E – mod bond coefficient, which is an empirical value with a value 0.6-0.7. The expression (7.2) is fair if you ignore polarization dispersion. The coefficient E occurs due to the fact that the process of distribution of mods is not always independent. Under appropriate conditions, the energy of one oscillation can be pumped into another fashion, etc..

As can be seen from the figure for fibers with a complex profile of the fracture indicator, several points of zero variance can be observed.

7.1.4. Geometric parameters of fiber

Note that a certain physical substantiation of the introduction of these parameters for the characterization of optical fiber is given in paragraph 3.6.2.

7.1.4.1. Відносна різниця показників заломлення ядра та оболонки

One of the most important parameters that characterizes fiber in particular is the, *there is a relative difference between kernel and shell fracture rates* Δ:

$$\Delta = \frac{n_w^2 - n_p^2}{2n_w^2}. \qquad (7.3)$$

For gradient fibers instead of n_w some effective relapation rate is taken n_{ef}. For example, for gradient fiber with a parabolic profile of the entrization indicator:

$$n_{ef} = \sqrt{\frac{n_w^2(0) + n_p^2}{2}}, \qquad (7.4)$$

where $n_w(0)$ – maximum relamination rate on the fiber axis.

7.1.4.2. Числова апертура волокна

Minimum angle Θ_{cr} (see Figure 7.6), under which a wave in fiber can still spread, is known to be determined by the condition of complete internal reflection:

$$\Theta_{cr} = \sin^{-1}\frac{n_p}{n_w}. \tag{7.5}$$
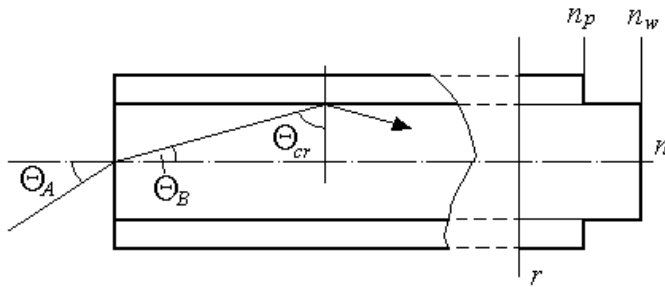
Рис. 7.6

Maximum angle Θ_A, under which the end of the light flue is irreversibly irredient and the possibility of a wave-like process is called aperture. This angle is associated with the numerical aperture of fiber:

$$NA = \sin\Theta_A \tag{7.6}$$

From Figure 7.6 it follows that,

$$\sin\Theta_B = \cos\Theta_{cr}. \tag{7.7}$$

Then, according to Sneeliuss's invariant, it is possible to record

$$NA = \sin\Theta_A = n_w\cos\Theta_{cr} = \sqrt{n_w^2 - n_p^2} = n_w\sqrt{2\frac{n_w^2 - n_p^2}{2n_w^2}} = n_w\sqrt{2\Delta}. \tag{7.8}$$

For gradient fiber with a parabolic profile of the entrization indicator:

$$NA_{ef} = \sqrt{\frac{n_w^2(0) - n_p^2}{2}}. \tag{7.9}$$

Numerical aperture is indicated in the passport of fibers, which are made by industry.

7.1.4.3. Нормована частота

Rationed frequency is the value determined by an expression:

$$V = \frac{\pi d NA}{\lambda}. \tag{7.10}$$

This value is related to the number of M mods that can be distributed in fiber. For stepped fiber:

$$M = \frac{V^2}{2}. \tag{7.11}$$

For gradient fiber:

$$M \approx \frac{V^2}{4}, \tag{7.12}$$

that is, in gradient fiber, the number of mods M distributed is twice less than in the stepped.

7.1.4.4. Cutoff wave

Cutoff wave – This is the minimum wavelength at which fiber supports only one spatial fashion. In fact, it is this parameter that determines the nature of the fiber – one- or multimode mode is implemented.

7.1.4.5. Approximate estimate of intermodal variance of multimode fiber

Recall that the speed of distribution along the wave drive is determined by the ratio [1,2]:

$$v_m = \frac{c}{n_{fm}} \tag{7.13}$$

where $n_{fm} = n_w \sin \Theta_m$ –effective relature indicator for m-th fashion. The maximum time delay when transferring a signal in different modes is determined by the delay between the time of the main fashion (*m=0*) and the time of passing the fashion with the maximum number (*m=m*$_{max}$). Accordingly, the length of the wavelengthy L така затримка має величину:

$$\Delta \tau = \frac{Ln_w}{c}(\sin \Theta_0 - \sin \Theta_{max}) \tag{7.14}$$

At the same time, the main fashion in the wavewater spreads almost along the surface, that is, $\sin \Theta_0 \approx 1$. Mode distribution angle m_{max} close to Θ_{kr}, that is, $\Theta_{kr} \approx \frac{n_p}{n_w}$. Then

$$\Delta \tau \approx \frac{Ln_w}{c}\frac{(n_w-n_p)}{n_w} = \frac{Ln_w}{c}\left[\frac{n_w^2-n_p^2}{n_w(n_w+n_p)}\right] \tag{7.15}$$

Given that in fiber the lag in the core and shell are very close to the delay in fiber with a stepped profile of the latture indicator (7.15) can be rewritten in the form of:

$$\Delta \tau \approx \frac{Ln_w}{c}\frac{(n_w^2-n_p^2)}{2n_w^2} = \frac{Ln_w}{c}\Delta \tag{7.16}$$

It can be shown that a similar ratio for fiber with a parabolic profile is described by the ratio of:

$$\Delta \tau \approx \frac{Ln_{ef}}{c}\frac{\Delta^2}{2} \tag{7.17}$$

where n_{ef} determined according to (7.9). However, expressions (7.16, 7.17) take place when the fiber length does not exceed the length of the bond between Lz fiber modes, which is determined by the coefficient E. This length of communication for stepped multimode fiber is close, as a rule, to 5 km, for a fiber with a parabolic profile up to 10 km. Definitively expressions 7.16, 7.17) can be written as:

$$\Delta \tau = \begin{cases} \frac{Ln_w}{c}\Delta, & L<L_z \\ \sqrt{LL_z}\frac{n_w}{c}\Delta, L>L_z \end{cases} - \text{ stepped fiber} \\ \begin{cases} \frac{Ln_{ef}\Delta^2}{c}\frac{}{2}, & L<L_z \\ \frac{\sqrt{LL_z}n_{ef}\Delta^2}{c}\frac{}{2}, L>L_z \end{cases} - \text{ gradient fiber} \tag{7.18}$$

7.1.5. Optical fiber specifications according to ITU-T recommendations [36-40]

The characteristics of optical fibers intended for use in communication networks must comply with the characteristics of the international advisory committee on telephony and telegraphy (ICCT). The English abbreviation for this organization is ITU-T (old abbreviation ITU-E).

Characteristics of optical multimode gradient fiber optic cables 50/125 microns are given in the recommendations G.651.1 (Old Recommendation G.651 excluded August 16, 2008).

Table 7.1.

ITU-T G.651.1 Recommendations – Characteristics of multimode gradient fiber optic cables 50/125 microns

Fiber-fiber characteristics		
Sign	Details	Magnitude
Shell diameter	Nominal	125 microns
	Admission	±2 microns
Core diameter	Nominal	50 microns
	Admission	±3 microns
Core eccentricity	Максимум	6% (3 microns)
Shell flattening	Максимум	2%
Numerical aperture	Nominal	0.20
	Admission	±0.015
Losses on macrobending *	Raduis	15 mm
	Number of revolutions	2
	Maximum 850 nm	1 dB
	Maximum per 1300 nm	1 dB
Checking tension	Minimum	0.69 GPa
Zero variance wavelength	Minimum 850 nm	500 MHz·km
	Мінімум на 1300 нм	500 МГц·км
Chromatic dispersion coefficient	λ_{0min}	1295 nm
	λ_{0max}	1340 nm
	S_{0max} for $1295 \le \lambda_0 \le 1310$ nm	≤ 0.105 ps/nm^2&×km
	S_{0max} for $1310 \le \lambda_0 \le 1340$ nm	$\le 375 \times (1590 - \lambda0) \times 10^{-6}$ ps/nm^2×km
Cable characteristics		
Sigh	Details	Magnitude
Atering coefficient	Maximum 850 nm	3.5 dB/km
	Maximum per 1300 nm	1.0 dB/km

* – When using multimode fiber outside the area of this recommendation, losses on the macro are determined in [IEC 60793-2-10].
* – To check the macro losses, use [IEC 61280-4-1].
** – Worst atering coefficient at 850 nm ($S_0 = 0.09375$ ps/nm^2×km at $\lambda_0 = 1340$ nm $S_0 = 0.10125$ ps/nm^2×km at $\lambda_0 = 1320$ nm) –104 ps/nm×km

Characteristics of optical singlemode fiber optic cables are given in the G.652 – G.657 Recommendations [36-40].

Specifications for standard fiber (ITU-T G.652 recommendations) are given in Table 7.2

Table 7.2

ITU-T G.652 Recommendations – Standard SingleModal Fiber.

Characteristic	G.652.A	G.652.B	G.652.C	G.652.D
Wavelength, nm	1310	1310	1310	1310
Mod spot diameter, microns	8,6–9,5±0,6	8,6–9,5±0,6	8,6–9,5±0,6	8,6–9,5±0,6
Shell diameter, microns	125,0±1	125,0±1	125,0±1	125,0±1
Diameter of protective coating, microns	250,0±15	250,0±15	250,0±15	250,0±15
Core eccentricity, microns	0,6 maximum	0,6 maximum	0,6 maximum	0,6 maximum
Shell flattening	1,0% maximum	1,0% maximum	1,0% maximum	1,0% maximum
Cable cutoff wavelength, nm	1260 maximum	1260 maximum	1260 maximum	1260 maximum
Losses on macrobending, dB	0.1 maximum per 1550 nm	0.1 maximum per 1550 nm	0.1 maximum per 1550 nm	0.1 maximum per 1550 nm
Checking tension, GPa	0,69 minimum	0,69 minimum	0,69 minimum	0,69 minimum
Wavelength of zero variance, nm	from 1300 to 1324	from 1300 to 1324	from 1300 to 1324	from 1300 to 1324
Chromatic dispersion coefficient, ps/nm*km, not more than in wavelengths: 1285-1330 1525-1575	3,5 18	3,5 18	3,5 18	3,5 18
Variance Sign	+	+	+	+
Coefficient of aternation, dB/km; wavelength, nm	0,5 | 1310	0,4 | 1310	0,4 | all*	0,4 | all*
	- | -	0,35 | 1550	0,35 | 1383	0,35 | 1383
	0,4 | 1550	0,4 | 1625	0,3 | 1550	0,3 | 1550
PMD coefficient, ps/√ km	0,5	0,2	0,5	0,2

The first version of recommendation G.652 was approved in autumn 1984. This statement is taken from the seventh version, adopted in the summer of 2005.

Characteristics for fiber with displaced variance (ITU-T G.653 recommendations) are given in Table 7.3

ITU-T G.653 recommendations – Single-moron fiber with zero shifted dispersion (DSF-dispersion-shiftedfibre). Note: for high-speed communication lines with a large length of regeneration area without the use of optical sealing technologies.

Characteristic	G.653.A	G.653.B
Wavelength, nm	1550	1550
Mod spot diameter, microns	7,8–8,5±0,8	7,8–8,5±0,6
Shell diameter, microns	125,0±1	125,0±1
Diameter of protective coating, microns	250,0±15	250,0±15
Core eccentricity, microns	0,8 maximum	0,6 maximum
Shell flattening	2,0% maximum	1,0% maximum
Cable cutoff wavelength, nm	1270 maximum	1270 maximum
Losses on macro, dB	0.5 maximum per 1550 nm	0.1 maximum per 1550 nm
Checking tension, GPa	0,69 minimum	0,69 minimum
Wavelength of zero variance, nm	from 1500 to 1600	from 1300 to 1324
Chromatic dispersion coefficient, ps/nm*km, not more than in wavelengths: 1525-1575	3,5	3,5
Coefficient of aternation, dB/km; wavelength, nm	0,35 | 1550	0,35 | 1550
PMD coefficient, ps/√ km	0,5 ps/ √km	0.20 ps/√km

2006 Edition Statement.

7.2. **Neliniyni optical appearances in single-mod** fibers [23,24]

Attempts to increase the length of passive areas of FOCLs (i.e. without regenerators and optical amplifiers) caused the need to introduce large optical power into the fiber. However, it was shown that at radiation power of several mW and above, nonlinean optical phenomena begin to arise and affect the quality of communication. For example, for fiber with a core section of 10 microns at radiation power of about 10 mW, the radiation density is 1.27×10^4 W/cm2. This is already sufficient power for the intensity of radiation to affect the relature indicator and the absorption rate in fiber. Dependence of the relature coefficient on intensity leads to several effects.

7.2.1. Phase self-modulation (FSM) and cross phase modulation (FCM)

One of the first nonlinean effects, which begins to manifest itself at the power of an optical signal of about 8-10 mW, is self-modulation, or automodulation of the optical bearing phase – FSM (SPM). This phenomenon is observed when the relapation rate changes. Note that the energy in the signal is transmitted in portions (pulses). Thus, different components of the pulse spread with different distribution constants. This causes the impulse to expand. Obviously, at the same time the signal spectrum is expanded. Phase self-modulation is significantly manifested in the duration of the impulses τ_i<100 ps. With a duration of pulses of about 10-20 psyches, the expansion can reach two or three or more times. In addition, oscillations may occur on impulse fronts (see Figure 7.7).
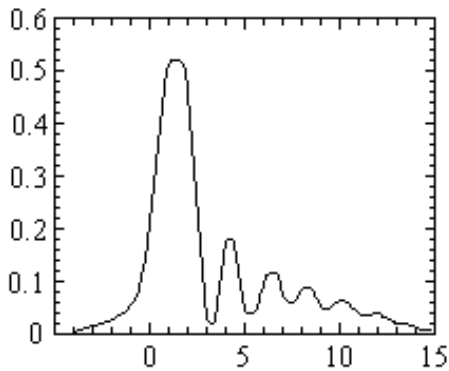
Fig. 7.7

If two optical waves are distributed in fiber and each of them has a capacity of about 10 mW or more, then the nonlineanity of the environment causes their interaction. At the same time, the power of one of the waves causes the modulation of not only its own signal, but also the neighboring one. Naturally, this influence is mutual in nature and is called cross-phase modulation or cross-modulation of FCM (CPM).

Let's return to the phenomenon of self-modulation phase of one light wave. The occurrence of oscillation on the fronts of impulse is caused by the so-called wave insatiability. As noted, the FSM expands the spectrum of optical impulse. At the same time, the longer-wave components of the spectrum are promoted at a higher speed compared to the shortwave ones. These components of the spectrum interfere with what oscillations are caused by. Since the environment is not linear in this case, the frequency shift causes new frequencies to $2\overline{\omega}_1 - \overline{\omega}_2$ i $2\overline{\omega}_2 - \overline{\omega}_1$. So, in addition to the two components in the spectrum, two more appear. With their further distribution of these components of the spectrum, their interaction occurs, which leads to complication of the process and enrichment of the spectrum with new components.

Similar phenomena occur in the case when two optical signals are introduced into the fiber at different wavelengths. The phenomenon of two additional optical frequencies is the so-called four-wave mixing phenomenon (FWM), which manifests itself as cross-interference in multiwave seal systems (WDM).

As already noted, cross-phase modulation leads to cross-interference in systems with multi-wave sealing. These interference increases with a decrease in the frequency interval in the frequency grid for systems with spectral sealing. The phenomena in question are especially manifested in the complete coordination of the constants of wave propagation, which are introduced into the wavelength, that is, in fibers with zero dispersion. This is explained by the fact that in optical fiber with zero dispersion there are optimal conditions for optical components with a lower frequency to have a higher distribution speed than high-frequency components. Due to this, the former can meet with the second, create beatings and oscillations on the

fronts of impulses, while expanding the spectrum of the signal. Thus, taking into account nonlinear phenomena for systems with multi-wave sealing, it is advisable to use monomode fibers with nonzero dispersion with a slight inclination of dispersion characteristics.

7.2.2. Forced combination (Raman) scattering of AKR (SRS) and scattering of Mandelstam-Brillyuen VRMB (SBS)

Forced combination scattering of AKD, which is otherwise called the scattering of Raman-Mandelstam, occurs in fiber when the power reaches a certain relatively high threshold. The approximate value of the threshold power is determined by the ratio of:

$$P_{sh} \approx 10^{12} S\alpha/L, \qquad (7.19)$$

where S – cross-sectional area in cm^2, α - loss ratio in cm^{-1}.

Calculation according to this formula for single-mortise fiber $\alpha = 0.2$ dB/km and a diameter of 10 microns gives a threshold power of 1.4 W (with a fiber length of 5 km). With an increase in fiber length, this threshold is rapidly reduced. For the length of the same fiber 20 km threshold power is reduced to 0.6 W. From the point of view of physics, VKR occurs when photons pass through the environment with molecules and atoms of this environment. At the same time, situations may arise when molecules absorb part of the energy of passing radiation. As a result, if the photon had a frequency of v0, then after colliding with the molecule and transferring part of the energy to it, the energy of the photon decreases by a certain value $\Delta E = h\Delta v$. So, after the interaction of radiation will have two frequencies v_0 and v_0–Δv. The second component will be noticeable when the energy of the initial radiation reaches a level higher than the threshold. One of the important properties of OCD is the large frequency range of radiation interaction passing through the environment with molecules and substance atoms. For quartz, it reaches dozens of teraghertz. In the analysis of OCD, the coefficient of combination reinslation was introduced g_R, depending on the composition of the substance and may vary due to the elements by which the substance is alloyed. For quartz fiber, it is maximum at offset frequency $\Delta v \approx 13$ ТГц. Frequency v_0–Δv is called stock components. With an increase in the power or length of interaction, the second, third, etc. stock components arise (v_0–$2\Delta v$, v_0–$3\Delta v$ etc.).). In addition, when a certain power threshold is exceeded, high-frequency components appear v_0+Δv, v_0+$2\Delta v$, v_0+$3\Delta v$ etc. and the spectrum shifts towards shorter wavelengths (antistox components).

Forced scattering of Mandelstam-Brillyuen VRMB (SBS)

The change in the energy quantum states of molecules and atoms at a sufficiently high level of power is manifested in the fact that there are fluctic movements of molecules that lead to fluctuations in the density of matter, the so-called acoustic phonons. On these phonons there is a nonlinean scattering of light (photons give some energy to acoustic phonons). As a result, new components appear in the radiation spectrum, which, by analogy with OCD, are called stokes. Unlike VKR, VRMB occurs at much lower capacities and is directed to the side opposite to the distribution of information signal. At the same values S and α, as for OCD, the threshold capacity of the VRMB is three orders of order lower and for fiber with a length of 5 km is 1.44 mW. In the case of short pulses, this power is up to 10 mW. It should be added that the frequency shift of the optical carrier at the VRMB is 10-15 GHz at the width of the spectrum ~ 20Mhz. However, if there is heterogeneity in the form of bends, compression, stretching in the light drive, then the VRMB spectrum can reach 100-500 MHz. This fact is used in diagnostic equipment to detect mechanical effects on the optical cable.

In VOLZ systems, VRMB is manifested in an increase in the atertion of the optical signal, the occurrence of relatively low-frequency modulation. The main impact of the WRSF is that the radiation diffused in the direction of the source affects the laser, creates parasitic modulation of radiation, which manifests itself, first of all, in the form of noise.

7.3. Single-mode fibers of new types produced by LUCENT TECHNOLOGIES CORNIGS [23,42]

In this paragraph we present the characteristics of single-model fibers, which are produced by recognized world leaders in the development and manufacture of the most advanced (both monomode and multimode) optical fibers.

LUCENT TECHNOLOGIES has developed several newest types of monomode fibers. Among the first to be called fiber "True Wave". This is fiber with nonzero dispersion.
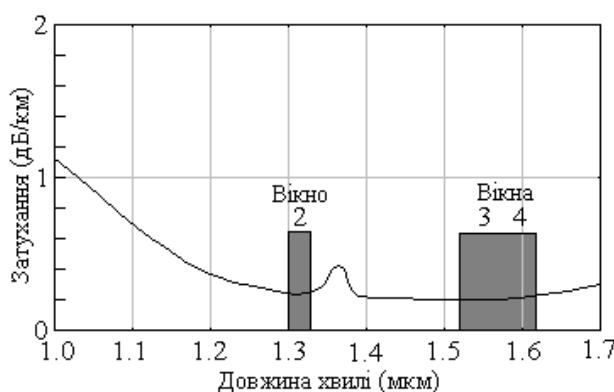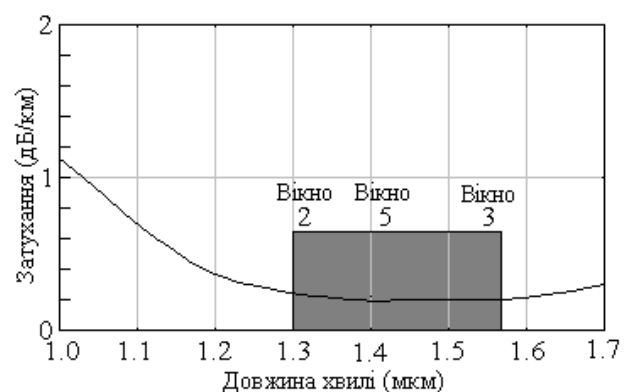
Fig.7.8   Fig.7.9

Треба переклад

«True Wave»

Aternation The maximum atm rate (loss) can be specified in the range from 0.22 to 0.25 dB/km. In this case, this value is maintained in the range from 1550-1600 nm
Dependence of aternation on wavelength Maximum atcut in the range from 1525 to 1620 nm does not exceed aterm for wavelength 1550 nm more than 0.05 dB/km
At the point of maximum water absorption The atering coefficient at the point of maximum absorption on (1383 3 nm) does not exceed 1.0 dB/km

Atening at macrobends

The maximum atgrowth caused by bends does not exceed the specified values under such bending conditions.

Bending conditions	Wavelength	Attenuation
One cot diameter 32 mm	1550 nm	≤ 0.5 dB
	1600 nm	0.6 dB
100 cot with a diameter of 75 mm	1550 nm	≤ 0.05 dB
	1600 nm	≤ 0.05 dB

Local heterogeneity There are no local heterogeneity of atering exceeding 0.1 dB at 1500 and 1600 nm

Chromatic dispersion

3rd window 1530-1565 nm	from 2.6 to 6.0 ps/(nm km)
4th window 1565-1620 nm	from 4.0 to 8.6 ps/(nm km)
Slope of variance curve	0.05 ps/(nm2 km)

Mod spot diameter

At 1550 nm	8.4 0.6 microns
At 1600 nm	8.4 0.6 microns

Cutoff wavelength The length of the cutoff wave in the cable is   1260 nm

«All Wave»

Atering	
The maximum aternation coefficient (loss) can be specified within:	
Wavelength	**Maximum atcenance**
of 1310 nm	0.35 dB/km
1385 nm	0.31 dB/km
1585 nm	from 0.21 to 0.25 dB/km.

Dependence of aternation on wavelength

Maximum attainment in the range from 1285 to 1330 nm does not exceed aterm for wavelength 1310 nm more than 0.1 d B/km

Maximum attainment in the range from 1525 to 1575 nm does not exceed the atcening for a wavelength of 1550 nm more than 0.05 dB/km

At the point of maximum water absorption

The atcening coefficient at the point of maximum absorption on (1383 3 nm) does not exceed 0.31 dB/km

Atening at macrobending

The maximum attainment caused by bends does not exceed the specified values under such bending conditions.

Bending conditions	**Wavelength**	**Attenuation**
One cot with a diameter of 32 mm	1550 nm	$\leq$ 0.5 dB
100 cot with a diameter of 75 mm	310 nm	$\leq$ 0.05 dB
	1550 nm	$\leq$ 0.1 dB

Local heterogeneity

There are no local heterogeneity of aternation exceeding 0.1 dB at 1310 and 1550 nm

Chromatic dispersion	
Wavelength corresponding to zero variance λ_0	1300-1322 nm
Maximum slope of the dispersion curve at a point λ_0	0.092 ps/(nm^2 km)

Mod spot diameter	
At 1550 nm	9.3 ± 0.5 microns
At 1600 nm	10.5 ± 1.0 micronss

Clipping wavelength	
The wavelength of the cutoff in the cable	≤ 1260 nm

Fiber is able to work in the 3rd and 4th transparency windows (see Figure 7.8) and has a gentle variance dependence curve on the wavelength in these windows, low bend sensitivity, low polarization dispersion (PMD).
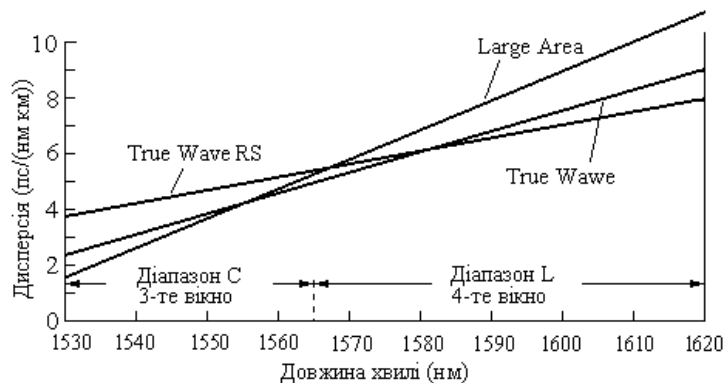
In Fig. 2. 7.8 is given the curve of dependence of the aternation coefficient on the wavelength for true wave fiber. All Wave fiber (Fig. 7.9) differs from the rest in that it managed to eliminate the peak of aterm in the region of 1.3-1.4 microns, which is due to the presence of a hydroxyl group OH.

Fig. 7.10 Треба переклад

Due to this, except 2OP (1.28-1.325 microns) 3OP (1.53-1.565 microns) and 4ОП (1.58-1.625 microns), All Wave fiber can also work in the fifth 5OP transparency window (1.35-1.45 microns).

Figure 7.10 shows the behavior of dispersion, depending on the wavelength for these types of fibers. As you can see, True Wave fiber has a relatively smooth gentle characteristic.

8. Optical cables [23-27]

Compared to metal coaxial and symmetric cables consisting of copper conductors, optical kabuls (OK) have a number of features. Optical fibers (OV) are made of ultra-pure quartz with the necessary additives or – less often – from polymers. These materials are good dielectrics. Consequently, optical fibers, and as a result optical cables, are not sensitive to electromagnetic interference. In addition, they are much more resistant to various kinds of aggressive chemical media. Small diameter of the OV (together with a protective shell of no more than 250 microns) and a small mass allow producing an OK of significantly smaller diameter and drive weight than metal cables corresponding in characteristics. Moreover, for some systems of information transmission to optical cables there is no alternative at all. Structurally, when equal with metal cables, the diameters of the OK have a greater number of information-leading cores. Due to low attenuation and slight distortion of the shape and duration of the optical impulse, optical cables have a much longer "construction" length – up to 6 km (for underwater systems up to 50 km).

However, since the base is OK – quartz (less often polymer) light water, there are certain difficulties in their tying. Despite these features, optical cables must meet a number of requirements for the characteristics of metal communication cables. They should ensure that:

- the possibility of gaskets in the same conditions in which metal cables are laid;
- maximum use of methods and equipment of traditional cable-laying technology; the possibility of germination and installation in the field with sufficient ease and for a short time;
- resistance to external influences in accordance with the operating conditions of the communication network;
- reliability in operation in accordance with the specified indicators of reliability, durability and suitability for repair.

8.1. Features of the design of optical cables

Conventionally, the design of the OK can be divided into four types:

a) multi-story, or cables with a structural structure;
b) cables with a bunch structure;
c) cables with a profile bearing core;
d) tape cables.

This list should also include single-fiber cables, including for connecting in the middle of the ceilings. These are 3 m long patchcord cables with ends, which are equipped with optical connectors. This list will also include underwater gasket cables, suspension cables on high-voltage lines or along the contact network of railway roads.

Figure 8.1 shows sketches of cross-sectional optical cables of various types: cables of type "a" and "b" belong to the cables of the classic type; types "in", "d" are typical for most optical cables.

OC type "a" is made in the form of leds from optical modules that are twisted around the central strengthening element. This design is effective with a number of

optical modules no more than 20. A typical led OC has an outer diameter of 12 mm and 6 to 8 optical modules. The optical module is a polymer tube with freely enclosed fiber in it.

OC type B consists of bunches of optical modules that are cited around the central strengthening core. The beam is a polymer tube, in the middle of which are the cores with longitudinal grooves. In these grooves freely enclosed OF. Cable of this type can consist of 50-100 fibers. Outer diameter 15-25 mm.
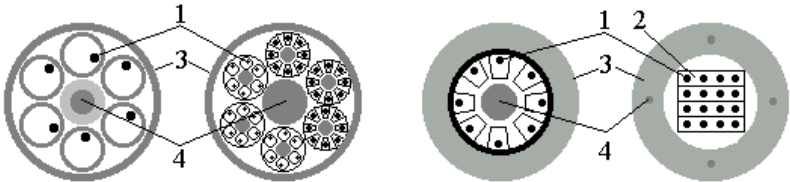
Fig. 8.1. Types of optical cable designs:
a) a healer twist; b) bunch twist; b) with a profile core; d) tape; 1 – fiber; 2 – tape; 3 – polymer protective cable shell; 4 - strengthening core

Optical cable type "c" consists of a core, which is a plastic element with screw grooves, in which light drives with a primary protective shell or optical modules are freely enclosed. The core of the OV or OM is wrapped with an isostrix and covered with a shell. In some designs, the strengthening core has a round section, around which gaskets with freely nested optical modules alternately curl. In cables type "in" there are 8-10 floodlights. External cable diameter up to 20 mm.

The core of the cable type "d" is assembled from flat tapes with parallelly nested at a distance of several tenths of a thousand particles of light water. Twisted tapes form the core of the cable. The strengthening elements in this OK are located in the shell. Due to the tight fit, a cable of this type can be of very small diameter. Thus, a cable with 144 optical fibers has an external diameter of 12 mm.

The cable can also include armor made of steel wire. The cable may also contain copper veins or several fuel cores and other technical needs.

Cables can also be classified for functional purposes:
- mainline;
- zone;
- urban;
- village.

Cables can be freely or rigidly placed optical fibers.

The table shows the disadvantages and advantages that are inherent in these types of styling.

Table 8.1

Cable characteristics	Cable design	
	with free placement of fibers	with hard placement of fibers
Bend radius	big	small
Sprain force	high	low

Impact resistance	low	high
Pressure resistance	low	high
Influence of temperature	low	high

There are a lot of types of optical cable designs, as many and types of their labeling. Only in Russia more than 10 factories for the production of OC.

In addition, during the construction of main and zone systems of SSROs, the domestic industry is not able to fully provide. In communication systems of this level, equipment of well-known foreign companies is currently being introduced: SIMENS, ALCATEL, NEC, etc. These are SDH and PDH systems for speeds of 2.4 Gbps, 622 Mbps, 155 Mbps.

Foreign cable companies: MOHAWK/CDT (USA), FUJIKURA (Japan), SEL (Germany) and Dr..

Most cables currently available are 90% made up of single-mode optical fibers. This is due to the fact that fiber optic transmission systems are in most cases high-speed systems of considerable length – from tens to thousands

Fig. 8.2. Construction of mounting cables for local connections:
a) cable optical object two-strand company MOHAWK/CDT; b) Bveakout cable object of the same company;
1 – optical fiber; 2 – buffer coating 900 microns; 3 – rein strengthening threads; 4 - Outer PVC shell

of kilometers. Moreover, the concept of a broadband access network (Gigabits to home) is currently being actively developed. Consequently, the requirements for a sharp increase in the band of frequencies transmitted on the subscriber area are increasing.

At the same time, in local, object and on-board automatics systems, cables made of multimode fibers are widely used (Fig. 8.2).

Currently, the world leader in OC production is the transnational company ALCATEL, which produces a complete range of OC, from transocial to mounting.

8.2. Installation of optical cables
8.2.1. Analysis of losses that occur during the installation of optical communication cables [1-3]

OC connections cause loss of optical signal energy. Compared to traditional cables, losses in the connection of optical fibers can be quite large, reach and even exceed the level of signal atering in areas of length of several kilometers.

The causes that cause such losses can be divided into "internal" and "external".

The first group includes losses arising from the inconsistency of the optic-geometrical parameters of the connected OR. These are the following parameters: difference in the diameters of the cores, the difference in numerical apertures, the discrepancy in the profiles of relapse indicators and the latture indicators themselves, the ellipticality and non-concentricity of the OV that are connected.

Fig. 8.3 <mark>переклад</mark>

The second group of losses is due to the design of the connector used. These are losses as a result of: transverse and longitudinal shear axes, vaporality (angular displacement) of axes, impperpendicularity of the ends of the OV with their axes, reflection when moving from one medium to another (Frenel loss).

Frenel losses occur on the boundary of the section of two environments (Figure 8.3)

When connecting fibers using inconsistent mechanical connectors or optical connectors, when there are two partition boundaries (glass-air-glass), losses can be calculated by the formula:

$$A = -10\lg B, \tag{8.1}$$

where B – transmission ratio, which is determined by the ratio of the:

$$B = \frac{4n_w n_v}{(n_w+n_v)^2} = \frac{4K^2}{(1+K)^2}, \tag{8.2}$$

where $K = \frac{n_w}{n_v}$, n_v –environmental relapion indicator (mostly air). The transmission coefficient is the ratio of the radiation power that passed through the boundary to the power of the wave that fell on the boundary of the section.

If n_w =1.46, n_v =1, то B =0.96 і V =0.16 dB, which is a theoretical minimum of losses in such connections. To reduce such losses in mechanical compounds, imersium substances are used, which have a relamination indicator similar to the terlament of the core. In this case, the losses are less than 0.1 dB.

It should be added that the inverse wave can interact with the active environment of the laser emiator and eventually lead to false additional light signals.

It is also possible to significantly reduce the gap if the ends of the connected fibers are made spherical. This allows you to make the so-called physical contact of the ends (physical contact PC).

Inverse scattering can be further reduced by angular (tilt) physical contact (angled PC, APC), when the ends of the OV are processed at a certain angle (8-12°) to the plane, perpendicular to the fiber axis. Reflected wave will not enter the light water if the angle of spread of the reflected wave is greater than the aperture angle.

In the presence of transverse shear of optical fibers, the power of the wave that passed through the boundary between the media depends on the profile of the lerture indicator, the amount of shear and the diameter of the core.
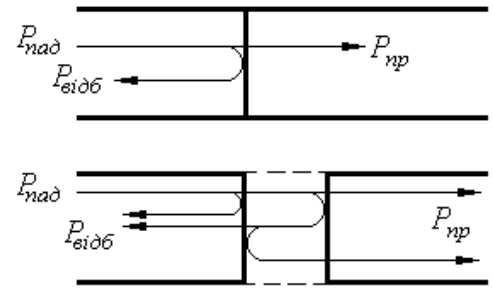
For stepped and gradient multimode optical fibers, transmission coefficients are determined accordingly by expressions:

$$B = \frac{1}{\pi} \frac{4K^2}{(1+K)^2} \left\{ 2\cos^{-1}\frac{x}{d} - \sqrt{\frac{2x}{d}\left[1 - \left(\frac{x}{d}\right)^2\right]} \right\}; \qquad (8.3)$$

$$B = \frac{1}{\pi} \frac{4K^2}{(1+K)^2} \left\{ 2\cos^{-1}\frac{x}{d} - \frac{2x}{d}\sqrt{4 - \frac{x}{d}} \left[1 - \frac{1}{d}\left(2 + \frac{4x^2}{d^2}\right)\right] \right\}, \qquad (8.4)$$

where x – Offset amount, d – optical fiber core diameter, $K = \frac{n_w}{n_v}$, n_w – core relature rate (stepped fiber) or $n_w = n(0)$ ($n(0)$ – maximum relamination rate on the gradient fiber axis).

For monomode fibers, in which the field amplitude module is described by the Gauss distribution, the connection transfer coefficient has the form:

$$B_{om} = \frac{4K^2}{(1+K)^2} \exp\left(-\frac{x^2}{w^2}\right), \qquad (8.5)$$

where w – diameter of the fashion spot. For gauss beam w can be approximated by the formula:

$$w = d(0.65 + 1.62V^{-1.5} + 2.88V^{-6}), \qquad (8.6)$$

where $V = \frac{\pi d NA}{\lambda}$ – rationed frequency, $NA = \sqrt{n_w^2 - n_p^2}$ – numerical aperture of OF.

Fig. 8.4 переклад
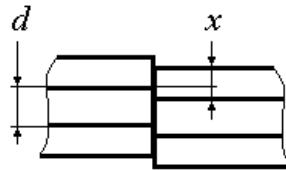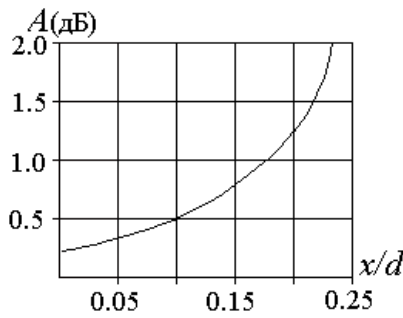
The typical dependence of the amount of losses on the amount of transverse shear is shown in Figure 8.4.

If the value of the transmission coefficient is known, then the losses in the compounds are determined by the formula (8.1). In the case of radial displacement (provided that the transmission coefficient in the absence of a shift is 1) is approximated $\tilde{B}$ can be calculated by the ratio of:

$$\tilde{B} \approx 1 - \frac{x}{d}. \qquad (8.7)$$

A more accurate value can be obtained if you take into account frenetic losses when passing radiation through the boundary.

Another type of optical fiber bias is angular displacement. In this case, for multimode fibers, the power of the light wave that passed through the boundary between the media depends on the throning of the core, shell (in other words, on the relative relature indicator) and angular displacement. For monomode fibers, it also depends on the diameter of the fashion spot.

The transmission coefficient for multimode fibers with a stepped profile and gradient of the thyrization indicator, as well as in the case of single-mode fiber, are determined accordingly by the ratios:

$$B_{st} = \frac{4K^2}{(1+K)^2}\left[1 - \frac{\alpha}{\pi K (2\Delta)^{\frac{1}{2}}}\right]; \qquad (8.8)$$

$$B_{gr} = \frac{4K^2}{(1+K)^2}\left[1 - \frac{\alpha}{3\pi K(2\Delta)^{\frac{1}{2}}}\right]; \tag{8.9}$$

$$B_{om} = \frac{4K^2}{(1+K)^2}\exp\left[-\left(\frac{\pi n_w w\alpha}{\lambda}\right)^2\right], \tag{8.10}$$

where $\widetilde{\Delta} = \frac{n_w - n_p}{n_p}$, α – angular offset.

Without taking into account the frennel losses, the transmission coefficient can be approximated by the formula:

$$\tilde{B} \approx 1 - \frac{\alpha}{\Theta_A}, \tag{8.11}$$

where Θ_A - aperture angle.

The last type of OF displacements is longitudinal fiber shifts. In this case, for multimode fibers

$$B_{st} = \frac{4K^2}{(1+K)^2}\left[1 - \frac{SK(2\Delta)^{\frac{1}{2}}}{2d}\right], \tag{8.12}$$

for monomode fiber

$$B_{om} = \frac{1}{1+(\lambda S)^2}(2\pi n_w w^2)^2, \tag{8.13}$$

where S – distance between ends.

Without taking into account the frennel losses, the transmission coefficient can be approximated by the formula:

$$\tilde{B} \approx 1 - \frac{S\tan\Theta_A}{d}. \tag{8.14}$$

The typical dependence of the amount of losses on the amount of longitudinal offset is shown in the figure 8.5
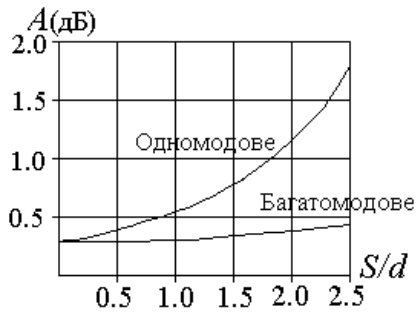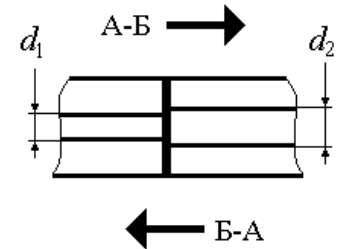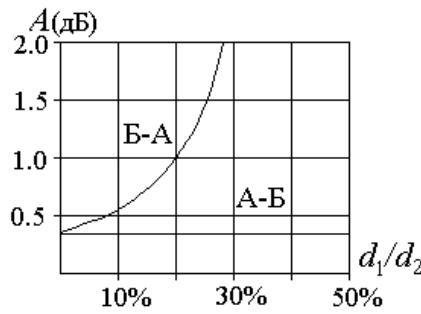
Fig. 8.5   переклад   Fig. 8.6

Among the factors of the first group, which cause losses in the compounds of OV, the most significant are the difference in the diameters of the cores (Fig. 8.6) and numerical apertures.

As you can see from the figure, the magnitude of losses depends on the direction of distribution of the light wave. For the direction of distribution from fiber with a smaller diameter in fiber with a larger diameter, the loss value is determined almost only by frennel losses.

The total losses in the connection are determined by the ratio of:

$$A = \sqrt{A_1^2 + \cdots + A_n^2}, \tag{8.15}$$

where A_n – losses of different nature.

8.2.2. Methods of connection of optical fibers

EIA connections are divided into separate and non-subdivisible. There are the following types of optical fiber connections (see Figure 8.7).

Welding OV is the most common method of connecting fibers. The advantage of this method of connection is the receipt as a result of welding a solid area of fiber. With the correct operation, power losses do not exceed 0.1 dB.

High temperatures at the point of contact of the ends are obtained with the help of:

- electric discharge;
- gas burner flame;
- powerful laser radiation.

Each of these methods has its advantages and disadvantages. The advantage of welding with a laser should be considered the possibility of obtaining "clean" connections, due to the absence of foreign materials in them and, accordingly, rather small power losses of <0.1 dB when radiation passing through such a connection. As a high power source (up to 5 W), lasers are used on the CO_2. Equipment for such welding is manufactured by Cabloptic (Switzerland), Hewlett-Packard (USA).

Fig. 8.7 переклад

Welding in the flame of the gas burner is used mostly when connecting multimode fibers. The advantages of this method include the possibility of obtaining compounds of increased strength. As an active reagent in such a device use a mixture: propane and oxygen or oxygen, chlorine and hydrogen. Losses in the compounds are also small – up to 0.1 dB. Equipment for such welding is manufactured by Cabloptic (Switzerland), AT&T (USA). However, the most common application was the method of welding OV in the field of electric discharge.

Welding in the field of electrical discharge is carried out in the following sequence:

1. Preparation of the end surfaces of the OV.
2. OV Justice It is carried out with the help of special guide devices and consists of the following operations:
    - primary justice – fiber ends are installed and exposed in accordance with special markers;
    - find light that spreads through the core, or find the cores of the connected fibers;
    - justin limbs of fibers on geometric grounds or on a minimal loss;
    - establish a regulated gap between the ends of the.
1. Preliminary melting of the ends of fibers. This operation is performed to partially eliminate micro-nervousness.
2. Direct welding of fibers.
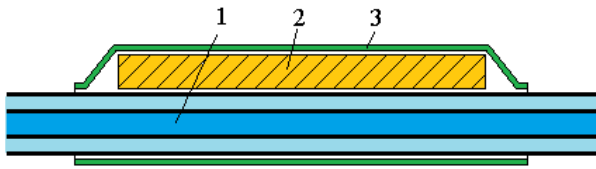
Fig. 8.8. Kit SMOUV

1 – case; 2 – metal rod, shrink tube

Modern welding machines for welding OV automatically carry out optimal fiber justice, choose the optimal welding mode and control losses at the junction. The welding process can be controlled visually in two coordinates (for example, on an LCD display). An example of such a device can be a FUJIKURA device.

Connection locations are protected with the help of special devices of optical couplings. For example, the junction is protected by thermal deposition of a set of parts to protect the welding site. Such kits are available both abroad (Raychem kit SMOUV – Fiber optic splice protection and support sleeve (Fig. 8.8)) and in Ukraine (KDZ kit).

Fig. 8.9. Types of adhesive compounds

1 – OV; 2 – glass capillary; 3 – glue; 4 – rectangular tube; 5 – body with V-groove; 6 – cover; 7 – guide rods; 8 - Coupling

8.2.3. Adhesive connections

Another way to obtain OV compounds is to glue them together. The advantages of this method include efficiency, the absence of deformation of the cores of fibers. This helps to reduce losses, lack of tension in the joint area, ensuring good strength, etc. However, such connections have limited service life and loss time instability.

To obtain the adhesive compound, use (see Figure 8.9): combining and fixing the OV in the capillary, in a rectangular tube, with the help of V-shaped grooves, with the help of rods.

8.2.4. Mechanical connectors

Recently, the connection of OV with the help of mechanical connectors has become widely used. Advantages of such connectors:

- relatively low cost;
- efficiency (the time of connection is not more than 3 minutes);
- high repair capacity;
- to obtain a connection does not require highly skilled workers.

Scope – transmission lines with relatively low requirements for the amount of losses (short inter-station lines, local networks, etc.)
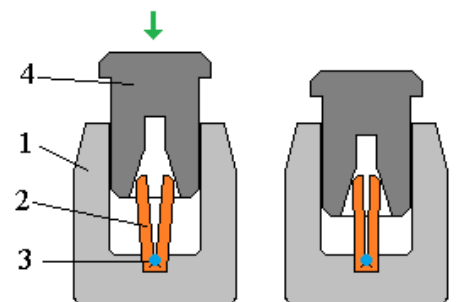
Fig. 8.10. Fiberlock type mechanical connector:

1 – plastic-aluminum base; 2 – metal element made of soft aluminum alloy; 3 – OV; 4 – plastic cover
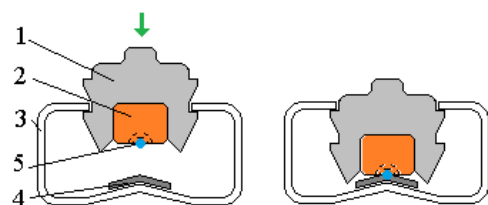
Fig. 8.11. Lucent Technologies
CLS Light Splice Connector:
1 – transparent plastic case; 2 – glass
capillary tube; 3 - metal spring; 4 –
thin layer of elastic material; 5 -
Optical fiber

To reconcile the junction of fibers in mechanical connectors, various liquids, gels, lubricants and adhesives can be used, with gels most often, and liquids only occasionally.

Figure 8.10 shows the design of one of the most successful mechanical connectors such as Fiberlock (manufacturer 3M).

The design of another rather successful mechanical connector – Lucent Technologies CLS Light Splice connector – is shown in Figure 8.11. It is designed to connect fibers with a diameter of 250 to 900 microns. Connection loss not more than 0.2 dB. Works in a wide range of temperatures.

8.2.5. Connecting [23,24,30]

The need for connecting connections arises when the OV is repeatedly connected to sources (receivers) and the docking of fibers with each other.

The most used were plug-ins. Their main elements are two fins plugs, in which the OV and coupling are fixed, which serves to connect the plugs. Sources of losses in such a connection are transverse and angular shifts of optical fibers. To reduce frennel losses, physical contact and angular physical contact of the ends are used.

They also use sockets with the possibility of justization (correction of the position) of the ends of fibers. The fibers at both ends of the part are mounted in bushings, which can revolve around the axis of the rose. In this case, the ends of the fibers are shifted relative to the axis of the jack by a small value of about 1 micron. Rotating the bushings at both ends of the open and monitoring the signal level, you can achieve almost complete coincidence of the fiber axes. Losses in such disassembly can be minimized to the values <1 dB.

8.2.6. Types of optical roses [22]

The design of any optical layout is based on the following general principles:

The part has a tip, the so-called ferrule, into which fiber is inserted. Fiber (Fig. 8.12) is centered in ferrouli and filled with epoxy resin. Part of fiber protrudes from ferrulus.

Fig. 8.12. translation
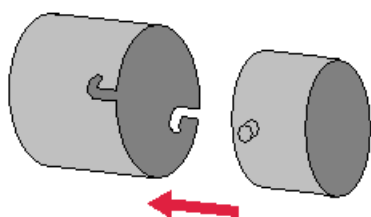
The use of epoxy resin minimizes the effect of temperature changes, the difference between fiber expansion coefficients and metal ferrul. Allows you to calmly polish the end of the fiber. The limbs of the fiber can be rounded in order to achieve a simpler optical contact between different fibers.

Fig. 8.13.

Optical connection type ST.

This type of connection is formed on the basis of a bayonet connection (Fig. 8.13).

The main use of multimode fibers. Loss 0.5 dB.

SC connector. The body and shank of the connector are made of plastic of different colors: for multimode applications – beige (or green), for monomode fibers – from blue (see Figure 8.14). The ceramic tip of the connector, interchanging with the connector housing and cable shell, which ensures the stability of the connection in the socket to vibrations and shocks. In the manufacture of duplex cords, it is possible to connect connectors with a clip (Fig. 8.15). Loss 0.4 dB or less.

Fig. 8.14
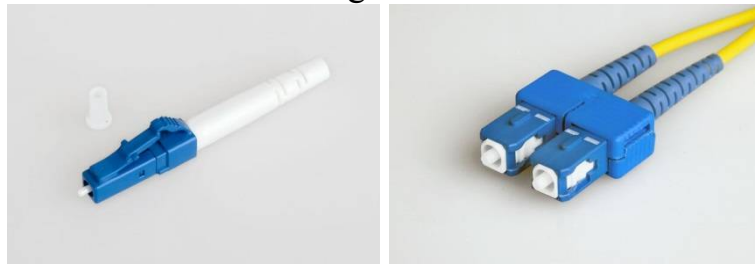
Fig. 8.15

FC connector. The connector body is made of nickel brass. For fixation on the socket connector, equipped with a cap nut with thread M8 x 0.75. The spring-spring ceramic tip of the connector is fully interchanged with the connector housing and cable shell, which ensures high mechanical reliability of the connection. The polymer shank of the connector serves to identify it: single-mode connectors are equipped with yellow tails, multimode - black. Connectors for optical fiber in the buffer coating have smaller dimensions and weight, which greatly simplifies their installation in large-capacity switching and distribution devices. Loss not more than 0.4 dB.

FC connector has a configuration device that makes it possible to further reduce losses (up to 0.1 dB) due to additional justice at a minimum loss in connecting cables (see p. 8.2.5).

Fig. 8.16

LC connector. Miniature jack with 1.25 mm ceramic tip diameter and RJ-45 type fixation mechanism (Fig. 8.16). The connector body is made of plastic of different colors: for multimode use – beige, for single-mode use – from blue. Ceramic connector tip, fully interchanging with connector housing and cable shell, which ensures high mechanical reliability of the connection. In the manufacture of duplex cords, it is possible to connect connectors with a clip.

9. PASSIVE OPTICAL ELEMENTS OF VOLZ [21-25,27]

Passive optical elements of VOLTS include: branchers, splitters, switches, optical insulators, circulators, polarizers, multiplexers and demultiplexers.

9.1. Fiber optic branches and splitter
9.1.1. Welded branchers

To control the parameters of THE NODs, the organization of two-way communication of one fiber is used by directional X-branchers. Figure 9.1 shows the scheme of such a brancher.

The branch is made of two segments of optical fibers. At some length L, each fiber is scraped (or removed by digestion) part of the working shell. After that, both fibers are welded using a welding machine. As a result of such an operation, the cores of the fibers are located parallel to the length of L. So, after such an operation, we have a fiber analogue of two bound wavelets. As you know [15], such a system is characterized by a communication coefficient, which depends on the value of H, and the length of the bond l_{zv}, on which there is a complete pumping of energy from one fiber to another. Naturally, choosing the length of L, you can adjust the part of the energy pumped into the second wavelength. Yes, for example, if $L = \frac{L_{zv}}{2}$, such an outseller will divide the energy that was put into one of the channels, equally.

рис. 9.1
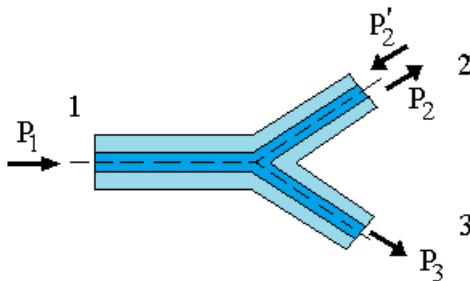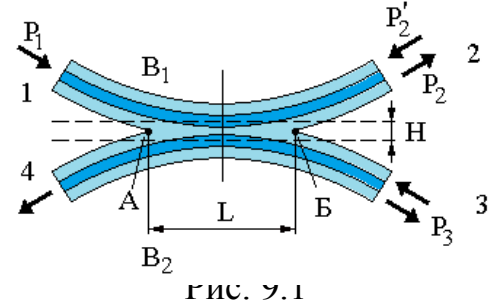
No less widespread found another type of brancher - *Y-brancher* (Fig. 9.2). The number of channels at the output of such a brancher can reach 32. This number is achieved by sequentially dividing each output channel of the two channel of the two-channel brancher with the help of the next brancher.

Fig. 9.2

This brancher is mostly used as a two-part power divider, so it is often called a forklift. This type of splitter is basic for the manufacture of various kinds of multi-channel matrix spliters and (as in the planar version) various kinds of interferometers.

Both types of branches are characterized by the following parameters: transmission coefficient

$$k_{12} = \frac{P_2}{P_1}, \text{ або } k_{12} = -\lg\frac{P_2}{P_1} \text{ (дБ); } k_{12} \cong k_{21}$$
$$k_{13} = \frac{P_3}{P_1}, \text{ або } k_{13} = -\lg\frac{P_3}{P_1} \text{ (дБ); } k_{13} \cong k_{31}$$

(9.1)

solution coefficient (isolation), or transient aterm $k_{23} \cong k_{32}$.

This option determines the part of energy that penetrates, for example, into the arm 3 when radiation is injected into the arm 2.

The third parameter is the loss factor k_v:

$$k_v = \frac{P_2 + P_3}{P_1}, \text{або } k_v = -\lg\frac{P_2 + P_3}{P_1} \text{ (дБ)} \qquad (9.2)$$

In addition to welded spliters, other structures are also used.

9.1.2. Branches with gradient cylindrical lens

A cylindrical gradient lens is a segment of gradient fiber with a parabolic profile of the entrization indicator. However, unlike OV, it has a larger diameter (about 1-2 mm) and does not have a shell. The distribution of the cylindrical gradient lens reramining indicator in the radial direction axis is set by the g parameter, which is called the degree of focus and is determined by the expression:

$$n(r) = n(0)[1 - 0.5(gr)^2], \qquad (9.3)$$

where $n(0)$ – Axis fracture indicator.

The stroke of rays that spread in such axial and non-axial light is shown in Figure 9.3.

The "sinusoidal" trajectory of ray propagation has a period of $F = \frac{2\pi}{g}$, called a pitch, or focal length of the lens. The flat ends of the lens allow to build on its basis a variety of mechanically durable and compact devices,

Fig. 9.3. Branches with gradient cylindrical lens: a – non-aisal lighting; b – axial lighting; JV – light separator

for example, matching combines for the transmission of radiation from a laser dio in fiber, splitter, etc..

9.1.3. Spectral-selective spliters (multiplexers/demultiplexers)

Spectral-selective splitters (multiplexers/demultiplek-soras) are used in FOP systems with multi-wave sealS WDM, DWDM and CWDM, in fiber optic amplifiers, in local networks with wave routing, etc. Such elements are built mainly on the basis of interference filters and diffraction grids.

9.1.3.1. Spectral-selective spliters based on interference filters

In spectral-selective spliters on the basis of interference filters (Fig. 9.4) sequential branching (merging) of channels is carried out. Therefore, an increase in the number of channels causes a proportional increase (filters, lenses) and, accordingly, radiation losses. Consequently, the use of such spliters makes sense when the number of channels is small.

a   *б*
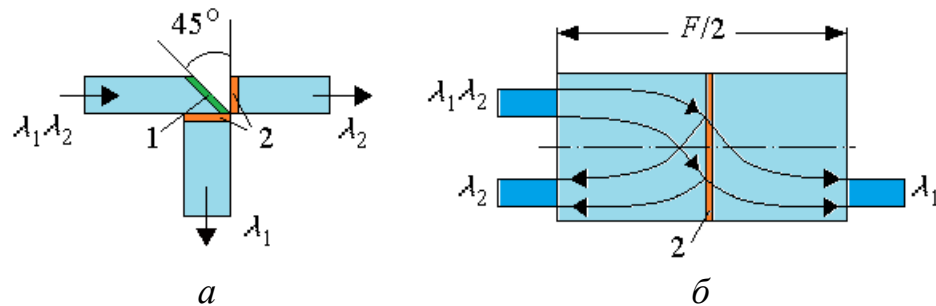
Fig. 9.4. Spectral-selective rozgaluzhuvači:
a – a design of three pieces of fiber; b – design with gradient lenses; 1 – interference light divider; 2 – interference filters

In the design of three pieces of fiber to fix their position on the floor made V-shaped grooves. The working planes of the segments of the OV have multilayer interference coatings, which are layers SiO_2 та TiO_2, alternating. The interference filter on the beveled end of the input fiber allows you to divide the radiation of two wavelengths by directions. Filters at the ends of the output channels are filters of lower and high frequencies. These filters slightly increase overall power losses (by~ 0.1 дБ), проте істотно знижають рівень переходних завад (to – 40 dB and below when split λ_1= 0.85 microns and λ_2= 1.3 microns).
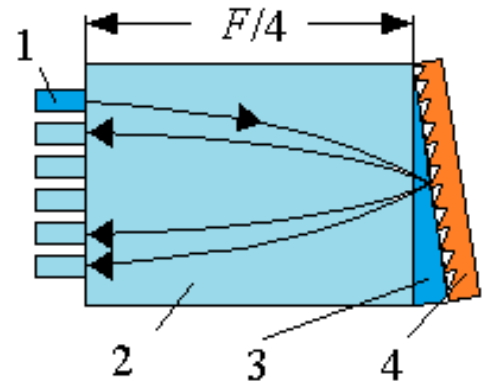
Fig. 9.5. Splitter based on diffraction grid:
1 – optical fibers; 2 – cylindrical gradient lens; 3 – the prism of insertion; 4 - diffraction lattice

9.1.3.2. Selection of wavelengths with a diffraction grid [3]

Figure 9.5 shows a splitter based on the diffraction grid. A diffraction grid is glued to the cylindrical lens on one side through the prism of the insertion, which divides the total flow of the input channel into several channels in accordance with the diffraction order.

9.1.3.3. Selection with Bragg lattice and fiber optic grid Bragg
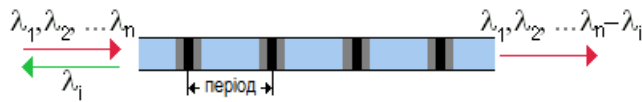
Fig. 9.6. Selection along the wavelength with the help of a fiber optic brag lattice

Figure 9.6 shows a scheme of selection along wavelengths using the fiber-optic bragg grid. Fiber is made in the form of a structure with periodically variable properties (local changes in the entractive index). In such fiber, radiation spreading from heterogeneity to heterogeneity, when met with heterogeneity, is reflected in the opposite direction. As a result, streams with different wavelengths spread in the opposite direction. In this case, their interference assembly occurs. As a result, only a stream can spread in this direction, in which the wavelength and the lattice period are coordinated in such a way that the summation of the paired waves occurs synphatically. Thus, after some distance in the opposite direction, only one wave with a certain λ_i. This stream can be withdrawn from the fiber using a brancher.

9.1.3.4. Selection with the fiber-optic echelon of Maixelson

Figure 9.7 shows a diagram of a demultiplexer built on the basis of an interferometer – the echelon of Maikelson, elements of which are made of fiber segments of different lengths. At the entrance of such an interferometer, the flow with the help of a fork is divided into particient streams, each of which is transmitted by a separate segment of fiber. The lengths of the segments are selected in such a way that in the output plane only for one λ_i the parathal streams remain synphasic. As a result, it is radiation with

Fig. 9.7

this wavelength that becomes the maximum intensity. The remaining streams are weakened in accordance with the phase ratios. Next, the partial flows are combined into a group with the help of a fiber unit (multiplexer).
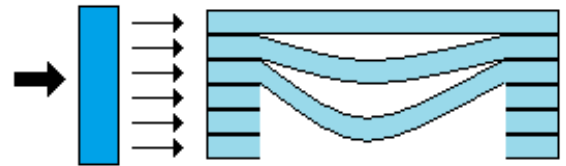
9.1.3.5. Selection with the help of The Fabry-Perot interferometer
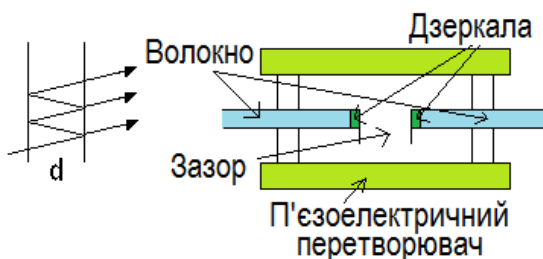
Рис. 9.8

Figure 9.8 shows the scheme demultiplexer, built on the basis of the classic interferometer Fabry-Perot. As you know, such an interferometer transmits radiation only with a wavelength that satisfies the next ratio:

$$L = \frac{m\lambda_i}{2},$$

(9.4)

where L – gap value between mirrors.

Note that this value can be adjusted using a piezoelectric converter, thereby changing the wavelength to which the interferometer is configured.

The spectral band allowed by such a filter depends on the ratio of mirror reflectance coefficients.

9.1.3.6. Selection with the help of the Mach-Zander interferometer
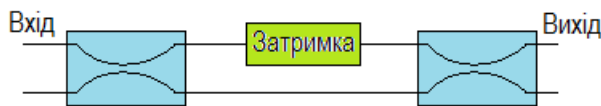
Переклад Fig. 9.9

As in previous cases, selective radiation amplification with a certain wavelength is used for selection with this type of interferometer. For this purpose, one of the channels interferometer (Fig. 9.9) additional delay is introduced, which ensures the coordination of the interferometer with a certain λ_i.

A chain of such interferometers can be used as a wavelength filter.

At the end of this paragraph, we note that wave selectors of any type (including interference filters) can be used as equalizers to correct the characteristics of linear amplifiers in SFOs (usually fier amplifiers, legitimized erbius ions) and chromatic dispersion compensators.

Typical characteristics of multichannel multiplexers from different manufacturers are presented in tables 9.1 and 9.2.

Table 9.1

Specifications of the company's 32-channel multiplexer NEL

Setting	Magnitude	Note
Wavelength range	1500-1600 nm	Accuracy < 0.05 nm
Interchannel Spacing	0.4, 0.8, 1.6 nm (50, 100, 200 Ghz)	In accordance with the recommendations of the ITU - T
Number of channels	8, 16, 32, 40, 48	
Loss	From 6 to 9 dB	At the level of 3 dB on the spectral line
Cross losses	< -30 dB	
Polarization-dependent losses	<0.5 dB	At the level of 3 dB
Temperature changes	0.011 nm / deg	

ECI Telecom Ltd Propriaty

Multiplexer	WDM		STAR			
	8 chan	16 chan	8 chan	16 chan	32 chan	40 chan
Losses per channel, dB	4.5	7.55	9.5	12.5	16	17
Total losses per multiplexer (demultiplexer), dB, not more than	7	14	14	20	29	30
Loss on reflection, dB, not more than	-45	-45	-40	-40	-35	-35
Cross losses	-55	-55	-60	-60	-35	-35

9.1.4 . Optical blocks with more than one input and output number

Figure 9.10 shows the scheme of fiber optic unit (VOB), which is used to combine devices in local communication networks. The basis of the unit consists of 6 *Y-branchers*, which combine 3 inputs (A,E,C) and 3 outputs (B,F,D). The arrows show the directions of light propagation in optical fibers.
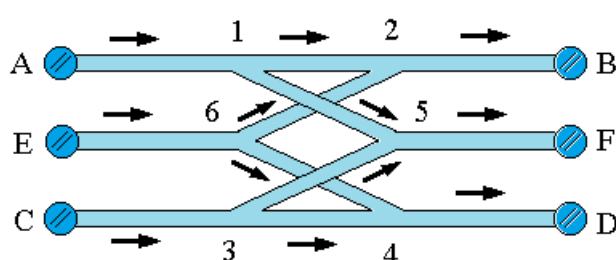
Fig. 9.10
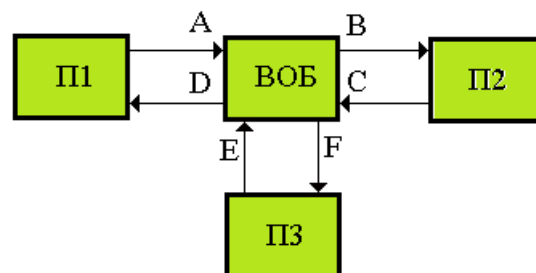
Fig. 9.11 переклад

Figure 9.11 shows the scheme of inclusion of the block in the local network.

At the end of this point we give the optical scheme of the circulator. Circulaters, like the previous unit, can have several (more than 3) input and output ports. An example of such a circulator is shown in Figure 9.12

The signal from port 1 is sent to port 2. The signal from port 2 is sent to port 3. And the signal from entrance 3 is sent to exit 4. Such a circulator can be created on the basis of Y-branchers.
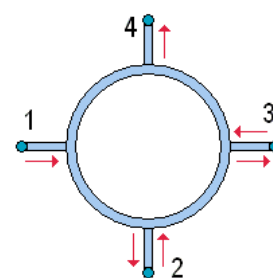
Рис. 9.12

9.2. Fiber optic switches

Replacement of fiber optic network architecture, operational routing in access networks and local SSOs are impossible without fast and efficient switching of optical flows. This switching is carried out using fiber optic switches. There are a

large number of types of fiber optic switches: electromechanical, thermooptic, acoustic, electro-optic and switches with optical signal control.

9.2.1. Electromechanical switches

The principle of operation of electromechanical switches is similar to the action of a traditional relay. The ends of the OV different ways are located opposite each other. When the relay is triggered, the ends of the OV enter into direct contact.

Losses in such switches are small. transmission coefficient ~ 0.3-1.5 dB. The power consumption is also small ~ 2-20 mW.

Disadvantages: low performance, sensitivity to external influences (especially vibrations), relatively large sizes and impossibility of their use in integral optical circuits.

9.2.2. Thermoplastic switches
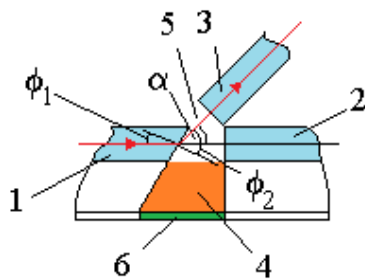
Fig. 9.13

Figure 9.13 shows one of the designs of this type of switches. Light drive 1 is a common input channel. The butt of OV 1 is treated at a certain angle to the axis of light distribution. OV 2 is placed conexistently to fiber 1. The angle of the "cut" of the end is such that the radiation entangleed on it extends further at an angle α to the axis of optical fibers 1 and 2. In this case, the direction of spread of the beam coincides with the fiber axis 3.

Thus, the wave that came out of the light water 1 passes into fiber 3. Power losses are only losses on Frenlewian reflection. The gap between the light 1 and 3 is filled with liquid 4. The fluid level is such that it does not reach the cores of fibers 1 and 2. The remaining space 5 between the floodwaters is filled with air under pressure of 1.1-1.2 atm. Below the fibers is a heater 6. When it is heated, the fluid level rises and it covers the cores of the fibers 1 and 2. The indicator of fluid relature is close to the ilving of the core of OF 1. Thus, when the liquid is heated, an optically homogeneous system occurs and the wave spreads along the initial direction in fiber 2. After lowering the temperature, compressed air displaces the liquid from the gap between the ends of OF 1, OF 2 and the wave again spreads in the direction of fiber 3.

Switch characteristics: thermal impulse energy, which is necessary for heating the liquid ~ 10 mcJ; heating time not more than 100 ns.

For another type of switch, see Figure 3.2.2. Light water with a terrification rate of the core n3 is made under a cone and with the help of glue is rigidly connected with light water n1 and n2. At the same time, under normal conditions (the temperature is about 20º) real ratios:

$$\begin{cases} n_3 = n_1 \\ n_3 > n_2 \end{cases}. \tag{9.4}$$
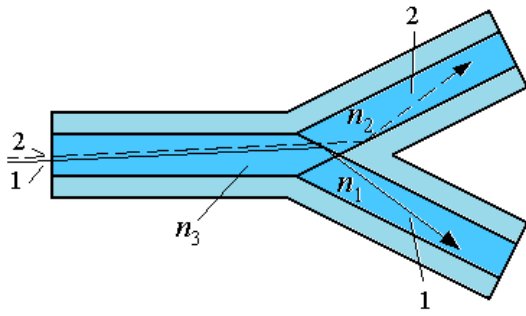
Рис. 9.14

and on and on the verge of floodwaters 3-2 conditions of complete internal reflection are fulfilled. At the same time, the boundary between the lighters 3-1 due to the uniformity of thyrization indicators in the optical sense is absent. Accordingly, the wave from the light 3 enters the light 1. When heated, the situation with the entrization indicator changes. Due to the nonlinean dependence of the values of relaining indicators, the ratio between them acquires the form:

$$\begin{cases} n_3 = n_2 \\ n_3 > n_1 \end{cases} \qquad (9.5)$$

Thus, the boundary between the floodwaters 3-2 becomes transparent, and the complete internal reflection occurs at the limit of 3-1. Accordingly, light from drive 3 enters the light drive 2.

Japanese company NEL is produced serial thermal switch for 8x8 directions with the following technical characteristics:

- operating range of wavelengths – 1.53-1.57 microns;
- losses are made (for 8 directions) – <8 dB;
- performance – <3 ms;
- supply voltage – 5 V;
- dimensions - 145x100x20 mm.

9.2.3. Electro-electronic switches

Electro-optic switches are switches that, together with acoustopathic switches, have found the most widely used in modern SSROs, local networks, etc. [15] Which are known to exhibit anisotropic properties under the influence of an electric field. The scheme of electro-esthetic switch is shown in Figure 9.15.
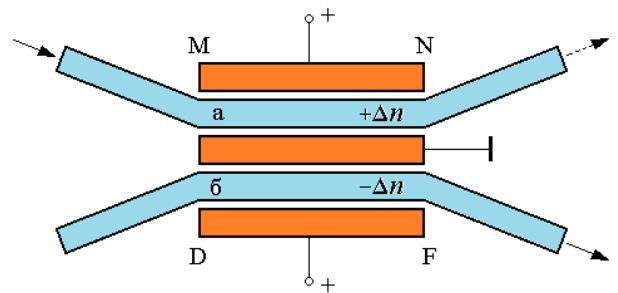
Worlds (a) and (b) on the site with electrodes are made of electro-optic

Fig. 9.15

material. The principles of operation of such a modulator do not differ from the principles of operation of such a modulator in integral-optical design [15]. Moreover, the integral-optical version of such a switch can be easily combined with THE VOLZ. This is the advantage of this type of modulators (acousto-ing ones also) over thermal and electromechanical.

Electro-optic switches have high performance – the order of units of nanoseconds. The supply voltage of such modulators is small and this can also be attributed to the advantages of electro-electronic switches.

It should be added that all types of electro-optic modulators (including interference) can be implemented in THE SSE, the construction of which is possible in the IC variant.

9.2.4. Optical isolators
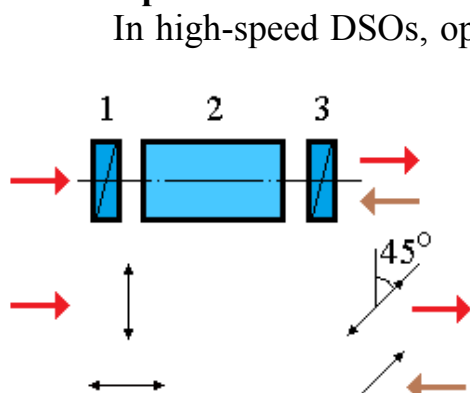
In high-speed DSOs, optical insulators are used to protect laser diodes from parasitic reflections. Optical insulators provide radiation in one direction almost without loss, and in the other (reverse) direction, the intensity of radiation passed through the insulator is almost zero.

Рис. 9.16

Figure 9.16 explains the work of one of the possible designs of such a device. Laser diot radiation passes through polarizer 1. After the polarizer, a linear-polarized wave enters the entrance of Faradeus's cell. When passing the cell, the polarization azimuth returns to the 45º. Through the output polarizer, radiation enters the input of the device to enter the fiber. Reflected parasitic beams spreading in the opposite direction have a polarization close to the linear with the same azimuth that came out of the radiation insulator. After polarizer 3, the reflected beam becomes linearly polarized with azimuth, which coincides with the initial azimuth. Faradeja's cell action is such that the result of the action does not depend on the direction of light propagation. Thus, after the cell, the polarization azimuth returns to 45º. Accordingly, compared to the initial orientation of the field vector, the final 90º.

With this mutual orientation, the axis of the polarizer and the wave vector behind the polarizer 1 light intensity, formed by reflected parasitic beams, is practically zero.

In communication lines built on the basis of single-mode fibers, in which the state of polarization of the signal transmitted practically does not change, another type of optical insulators can be applied. The design of such an insulator is shown in Figure 9.17.

Laser radiation passes through the polarizer 1 and a quarter-wave plate 2. The adle

Fig. 9.17

of the plate forms an angle 45ºpolarizer axis. In this case, linear-polarized radiation will turn into circular-polarized radiation. If the light water does not change polarization, then all the light streams reflected on the track remain circular-polarized. However, the direction of rotation of the field vector when reflecting changes to the opposite. For example, at the output of the system, the signal was right-polarized. Then the reflected signals (radiation returning towards the source) are left-polarized.
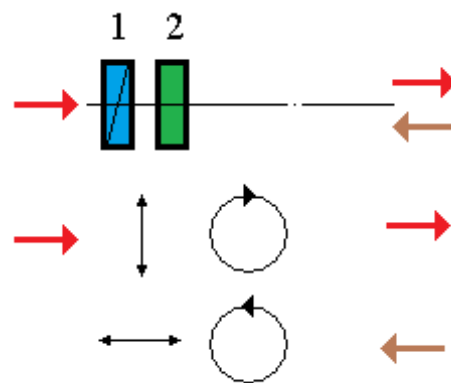
When passing through the plate $\lambda/4$ in the opposite direction, such radiation will again turn into linearly polarized, but it will be orthogonal in relation to the original. As a result, after the polarizer 1 the intensity of radiation returned from the optical track is almost zero.

10. FOLC ACTIVE ELEMENTS [21-24]

10.1. Radiation sources

The radiation source for THE FOLC must meet the following requirements:

- The radiation of the source must have a wavelength lying in one of the transparency windows (0.85-1.6 microns).

- The radiation source must withstand the required modulation frequency.

- The directional diagram of the source should be narrow enough to ensure the effective introduction of radiation into the fiber.

- The radiation source should have sufficient power, so that the signal passes as long as possible sections of the communication line, but nonlinean interactions with the fiber material do not occur.

- Temperature fluctuations should minimally affect the operating mode of the radiation source.

- The cost of the source should not be high in order to maintain the competitiveness of the FOLC.

Today, such requirements are met by two types of sources. These are LED and semiconductor laser diods (LD).
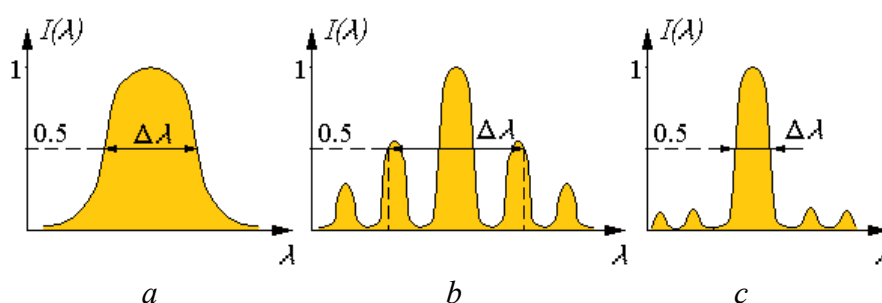
Fig. 10.1. Spectral characteristics of different types of sources:
a – led – $\Delta\lambda$=30-50 nm; b-multimode laser $\Delta\lambda$=1-3 nm;
c – single-mode laser $\Delta\lambda$=0.1-0.4 nm

The main difference between these devices is the width of the radiation spectrum (see Figure 10.1).

10.1.1. LEDs

Due to its simplicity and low cost, MDs are much more common than LD. The basic materials for the creation of modern semiconductor emitters and photodelets are gallium arsenide (GaAs) and indium phosphide (InP), as well as compounds based on them. LD and MD are built mainly on the basis of double heterostructure, the schematic image of which in simplified form is presented in Fig.10.2
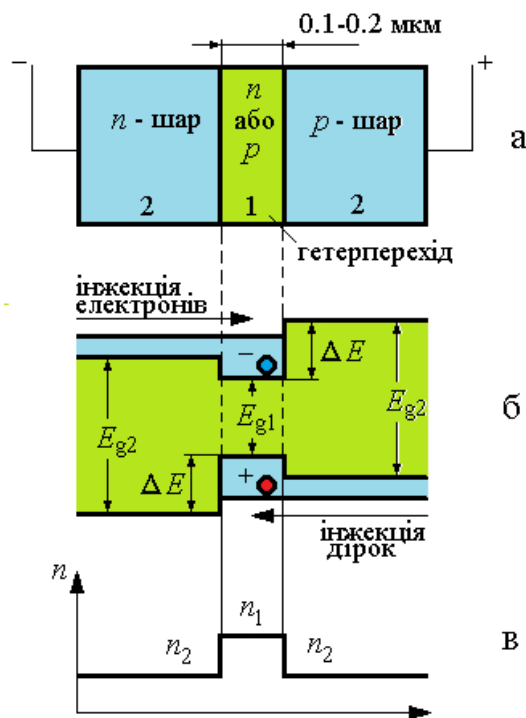
Fig. 10.2 переклад

The principle of operation of the LED is based on the radiating recombination of charge carriers in the active layer 1, placed between the limiting (passive) layers 2, which were formed from a semiconductor with a large width of the prohibited zone. The boundary of the partition between two layers of semiconductor materials with different Eg is called hetero-transdation. The peculiarity inherent in hetero-transitions is one-way engineering, due to the potential barrier ΔE. This potential barrier arises on the edge of the partition as a result of the leap of potential. Therefore, if you apply a direct displacement to the heterostructure, that is, to pass current through it, electrons and holes penetrate into the active layer (heterotranslation) from the bordering passive layers (*n*- and *p*- layers). After that, the electrons and holes spontaneously recombinate, accompanied by radiation.

The wavelength of radiation is associated with the width of the prohibited zone of the active layer Eg_1 (in eV) energy conservation law $\lambda = 1.24/E_{g1}$.

Active layer relature score n_1 greater than the relautation rate of layers limiting the active layer, the resulting wavewater effect. As a result, radiation spreads along the active layer, repeatedly reflecting, which leads to a significant increase in the efficiency of the source.

For work in the range of 0.8-0.9 microns, heterostructures are used on the basis of a three-component compound of the type $Ga_{1-x}Al_xAs$. For semiconductor sources operating in the range of 1.1-1.7 microns, a four-component compound is used $Ga_{1-x}Al_xAs_yP_{1-y}$.

Note that the radiation of LEDs occurs as spontaneous radiation. Therefore, such radiation is incoherent, relatively broadband and poorly directed. The width of the LED direction diagram is usually the order value 120º.

It is especially necessary to allocate superhuminiscent LEDs. In these diodes, in addition to radiation due to spontaneous recombination, radiation that occurs during induced recombination is used; accordingly, the output radiation can be considered as enhanced in an active environment. Superhuminiscent LEDs are end LEDs that work at such current density of injection that inversion populism of energy levels begins to be observed in the material of the active layer.

To increase the effectiveness of the introduction of radiation into the light water, microlenses are used both those that are formed directly on the surface of the device, and external ones.

The most common are two main modifications of MD: surface and end.

In surface MDs radiation is output in the direction perpendicular to the plane of the active layer, in the end MD - in the plane, parallel plane of the active layer. Radiation output in surface type MD on gallium arsenide is carried out through a round hole in the LED subfolder. Optical fiber is inserted into this hole and attached with epoxy resin. This design of the MD is called the Diode of Barras. There are also known designs of surface MDs with radiation output directly through the floor. Such designs are used in MD on a four-component GaInAsP. In this case, a transparent window – a substentry with InP.

10.1.2. Laser diots (LD)

The fundamental difference between a laser LED and a simple LED is the presence of a built-in resonator, which allows, when exceeding a certain amount of current (threshold current), to obtain an induced radiation mode, characterized by a high degree of coherence.

Thus, LD works at high pumping currents than MD at the same time has a much smaller width of the radiation spectrum.

The dependence of radiation power on the pumping current is described by the watt-amper characteristic of LD. With low pumping currents, the laser is characterized by small spontaneous radiation (see Figure 10.3). When some pumping threshold is exceeded I_{nop} the radiation power begins to increase sharply, and it becomes coherent. Therefore, to ensure the normal operation of the LD in dynamic mode, an initial displacement of the working point by direct current is required, which is approximately equal to I_{nop}, to the point slightly to the right of this value. Otherwise, the radiation power and LD performance are significantly reduced, and the width of the radiation spectrum is significantly expanded.

Slope of wat-amper characteristic by point I_{nop} characterizes *differential quantum efficacy* $\eta_d = \dfrac{dP}{dI_{\text{нак}}}$. Typical values of this value are 0.1-0.2 mW/mA, and the limit current lies within 10-100 mA.
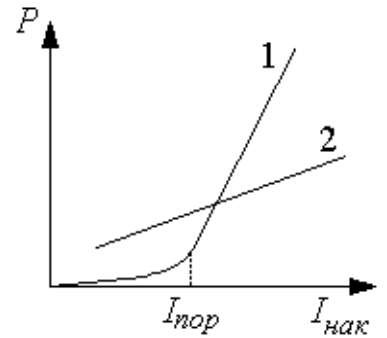
Fig.10.3. <mark>переклад</mark> Dependence of the power of MD and LD on the current of the swap:
1 – laser diode;
2 – LED

LD is characterized by dependence I_{nop} and η_d temperature. As the temperature rises, the threshold current increases, but η_d falls. Temperature change also leads to a change in the wavelength of radiation.

To reduce the dependence of LD characteristics on temperature, special measures are used to stabilize the temperature of the LD, for example, with the help of elements (micronutrients) Peltier.

To characterize the radiation power LD $P_{вих}$ use not only traditional (mW, μW) but also specific units (decibel-milliwatt (dBm)):

$$\alpha_{out} \text{ [dBm]} = 10\lg P_{\text{out}} \text{ [mW]}. \tag{10.1}$$

This unit characterizes the power level compared to 1 mW. For example, 1mW corresponds to 0 dBm; 50 μW corresponds to −13 dBm. The use of such a unit is

caused by the fact that its use simplifies the energy calculations of the budget of the lines.

The radiation power given in the characteristics of optical transmitters can vary in a certain range. In such cases, indicate the range of radiation power. For example, a record of 19/–4 dBm indicates, that $\alpha_{out\ min}$ −19 dBm, a $\alpha_{out\ max}$ −4 dBm.

The fiber bandwidth is inversely proportional to the width of the radiation spectrum passing through the OV. Naturally, this value is associated with the width of the radiation spectrum of the source. Yes, for example, if $\Delta\lambda$=4 nm bandwidth per 100 km is 63 MHz, and at $\Delta\lambda$ = 0.2 nm 1260 Mhz..

The following types of LD have become the most common:
- LD with Fabry-Pero resonators (Fabry-Pen Laser);
- Distributed feedback LD (RZ-laser);
- Distributed Bragg reflective LD (RBV laser);
- LD with external resonator.

10.1.3. Fabry-Perot Laser

The Fabry-Pen Laser is a crystal in the form of a parallelepiped, the end faces of which are created by the Fabry-Perot resonator. Resonator dimensions L=100-500 microns and width 100 microns. The width of the active area is 10 microns, the thickness is 1 micron. The diagram of the direction of optical radiation in the cross section is an elongated ellipse with a difference in smaller diameter 2-10°, 30-60° for more. The Resonator Fabry-Perot is created by two opposite faces of the parallelepiped, perpendicular to its longitudinal axis. The resonator mirrors are the limits themselves, since, given the halium arsenide relature coefficient (n_{AT}=3.6), reflection coefficient for normally falling rays is quite large (R=0.3).

The wavelength of the wavelength entering the generation must satisfy the standard condition $L = m\frac{\lambda}{2}$ (L- resonator length).

Modern LD is produced in a metal case, in which on one floor there is actually a LD, a photodiode and a thermistor. In turn, the entire substlet is placed on the micronutrient (Peltier element). The photodiode is placed behind the rear edge. In this case, the receiving platform of the photodiod bends against the optical axis of the system in order to avoid parasitic reflections. The purpose of the photodiode is to create negative feedback in the electronic circuit of laser pumping. Such a connection allows you to stabilize the power of the laser by adjusting the pumping current. Thermal stabilization (stabilization of the wavelength of radiation) ensures the use of the thermistor and micronutrients.

The body of the laser module may also include a single-module optical fiber included in a single fiber optical cable, as well as a justifiable device. All this is also placed on the same floor on which the laser is formed.

Table 10.1 shows the main characteristics of some LD produced in Russia.

Table 10.1

Characteristics	Laser module type			
	POM - 03543	POM- 03545	LPN- 602m - 602м	POM-514 "TELAZ"
Wavelength of radiation, microns	1.28-1.33	1.5-1.55	1.5-1.55 1.3-1.33	1.25-1.35
Radiation power, mW	1.5	25	0.5 - 2.0	1.0
Pumping current, mA	20	25	30	40
Operating current pumping at $P_{вих}$ = 1.0 mW, mA	31	41	50	70
The current of the built-in FD at $P_{вих}$ =1.0 mW, µA	380	348	200	200
Resistance photoresistor, kOm	19	19	10	10
Maximum current of micronutrifiers, A	0.5	0.5	1.0	1.0
Maximum transfer speed , Mbps	155	155	622	155
Stabilization temperature, C°	18	18	18	20

Laser diots of this type are used mainly in relatively low-speed DSP systems. They can be both multimode and monomode, that is, radiate in one longitudinal fashion. However, the width of the spectral line in such lasers is not less than 1 nm.

Рис. 10.4

Note that such lasers when the current of pumping changes not only the power, but also the wavelength of radiation (Fig. 10.4). Thus, if these lasers apply a direct modulation mode (power modulation by changing the value of the pumping current), this leads to an expansion of the spectrum (by a value of 20-40 nm), per information signal.
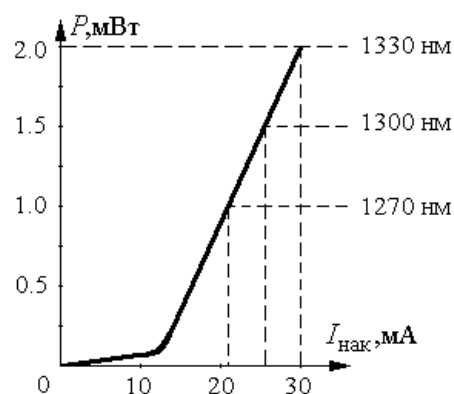
Naturally, this type of modulation can only be used on shorter lines, since for longer transmission lines, spectrum expansion can lead to a significant increase in chromatic fiber dispersion. In addition, as a rule, such systems use a one-wave mode of operation.

In multiwave transmission systems with frequency intervals (about 100 GHz), the use of direct modulation becomes impossible. In such transmission systems, external modulation is used. With this method, the working point of the laser on the watt-amperes is maintained in a constant position (in most cases in the middle of the linear area). Stabilization of the working point is carried out using an electronic diagram with a loop of negative feedback, which contains a photodiode built into the body of the laser. Acoustic, electro-modtic and other light modulators are used as an external modulator.

Recently, electroabsorption modulators have been widely used. This is due to the fact that such modulators are characterized by low power voltages (at 100 percent

modulation). In addition, such modulators are easily integrated with elements such as optical isolator.

Significantly higher characteristics have three other, more advanced, types of lasers.

10.1.4. Distributed feedback lasers (RZ-lasers) and distributed bragg reflectors (RBV lasers)

In RZP lasers (Fig. 10.5 a), positive feedback is created by reverse bragging reflection from the periodic structure (diffractor of wavelengths released into generation). The temperature stability of such a laser is determined by temperature changes in the relature indicator and is the value of the order 0.1-0.6 nm/K. In some types of RZ-lasers optical insulators can be built-in, which is especially important when using them in analog lines (cable TV) and for transmission systems with speeds of ≥622 Mbps. In lasers with distributed Bragg reflection (Fig. 10.5 b) periodic structure is carried beyond the active area. The advantages of ROS and RBV lasers over Fabry-Perot lasers are:
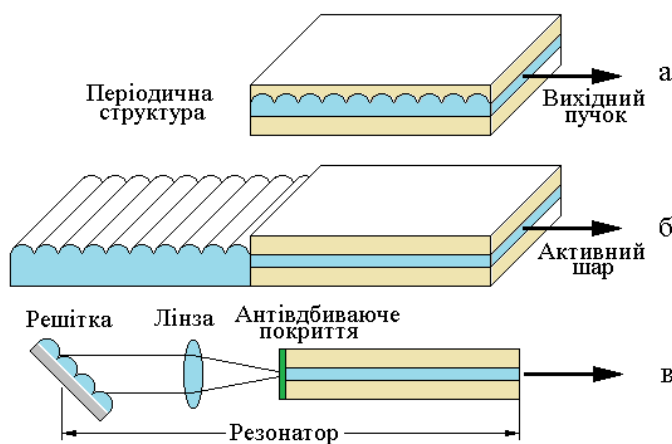
Переклад Fig. 10.5. Fundamental schemes of RZP and RBV lasers:

a – Distributed feedback LD (RZ-laser); b – LD with distributed Bragg reflection (RBV laser); in – LD with external resonator

- reducing the dependence of the wavelength of the laser on the current of injection and temperature;
- high stability of keeping one fashion;
- almost 100% modulation depth;
- lower temperature coefficient $\Delta\lambda/\Delta T$: For Fabry-Pen Laser, this coefficient is 0.5-0.1 nm/K, for ROS laser - 0.07-0.09 nm/K;
- allows the implementation of combining laser sources with integral-optical circuits on one sub-tab.

The main drawback is the complex technology of manufacturing such lasers and, as a result, the high cost of.

10.1.5. Laser diots with external resonator

In laser diodes with an external resonator, one or both ends are covered with a special layer that reduces reflection. Additionally, one or two mirrors are installed outside the active zone and an external resonator is formed. Figure 10.5 provides an example of such a laser, in which the functions of the mirror are combined with bragging grates. Anti-reflective coating reduces reflection by four orders of order. The reflector coefficient of another end of the active layer remains quite high (about

30%). To improve the feedback parameters between the mirror and the active body, a lens is placed.

It should be noted that the use of the lattice instead of a mirror gives an additional opportunity to control the spectral composition of the radiation of such a laser:

1. The Bregg lattice, as in previous cases, plays the role of a spectral selector.

2. Changing the slope of the grid leads to the fact that the generation is a different wavelength, for which the lighting conditions of the grid are optimal. Thus, by turning the grille, you can change the working wavelength of the laser.

It should be noted that the range in which the wavelength can vary can reach 30 nm. Therefore, such LD are indispensable in the development of wave sealing equipment and measuring equipment for FOCS.

According to its other characteristics, LD with an external resonator is close to RSZ and RBV lasers.

10.1.6. The most important characteristics of radiation sources for FOLC

The most important characteristics of radiation sources for FTA are:

- average radiation power when working in continuous mode;
- wavelength of radiation;
- width of radiation spectrum;
- the time of increase and decrease of the pulse of radiation at pulse excitation of pumping current;
- voltage drop on the diody;
- developments for refusal.

In addition, for LD and end MD, with a narrow directional diagram, differences are essential, determined by the level of half power. As a rule, these angles are determined by the directions of radiation in parallel and perpendicular to the active layer of planes (see Figure 10.6).
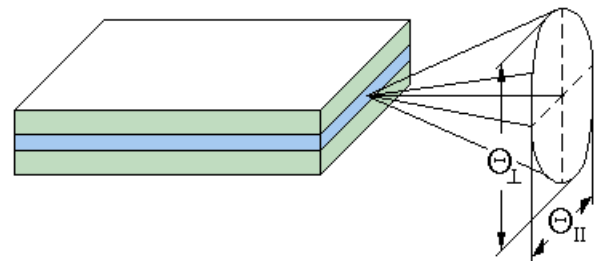
Рис. 10.6. Схематичне зображення діаграми спрямованості лазера

Типові значення кутів у вертикальній і горизонтальній площмнах – Θ_{II}=10º – 30º; $\Theta_\perp$=30º – 60º.

For high-speed FPZs, dynamic features of LD are important, which are manifested depending on the spectral characteristics of LD on the transmission speed in direct modulation (changes in pumping current).

For RSV and RVC lasers, when modulating in the 0.25-2 GHz range, there is only a slight shift λ_0(about 0.2 nm) with a high degree of extinguishing side modes. Therefore, such diots are often called dynamically monomode.

The speed of radiation sources is estimated by the time of increase τ_H and at times of decline τ_c radiation power during modulation by pulses of pumping current rectangular shape of sufficient duration ($t \gg \tau_H$). To evaluate them, as a rule, use levels 0.1 and 0.9 of the usual power. Often the speed of radiation sources is characterized by the maximum frequency of modulation. For MD, this frequency can reach 200 MHz, for LD (multiple GHz).

By the time the pulse builds up and descends, you can determine the frequency band for which optical fiber must be selected. If we consider these intervals to be approximately the same (but this situation is not always true), then the bandwidth can be determined by the estimated formula:

$$\Delta f = 0.35/\tau_{\text{н}}. \qquad (10.2)$$

Degradation and reliability of radiation sources is characterized by the time of development of the source for failure. The time of development on the "failure" of modern MD and LD, is the value of about 50 000 hours (5-8 years).

10.2. Constituent elements of the transmission optoelectronic module

In order to organize the transmission of optical signal via FPZ, in addition to the source of the emient, it is necessary to have a number of optical and electronic components, which together constitute a transmitting optoelectronic module (POM). As a rule, all POM elements are mounted on a special holders of the POM housing.
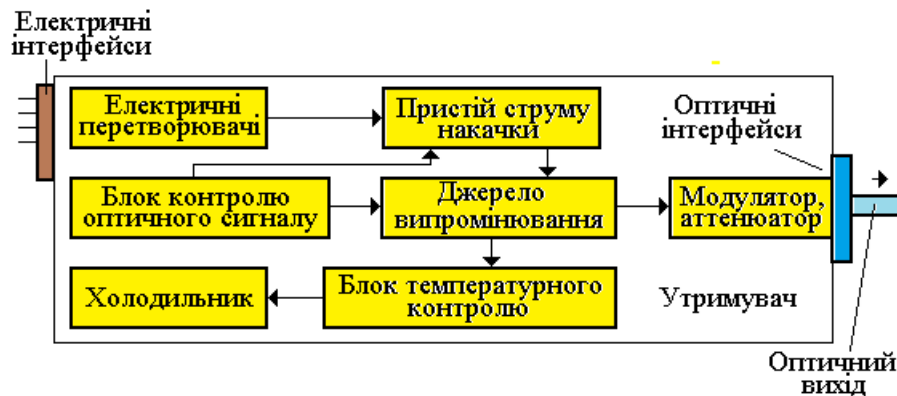
Fig. 10.7 переклад

PoM usually includes the following elements::
- radiation source;
- electric interface unit;
- block of connection with fiber;
- pumping current circuit;
- temperature control system;
- optical signal output control unit.

The general functional scheme of the optical transmitter is shown in Figure 10.7.

11. RECEIVING OPTOELECTRONIC MODULES. REPEATERS, AMPLIFIERS [21-24]

11.1. Receiving optoelectronic modules (ROM)

Receiving optoelectronic modules (ROM) are important elements of fiber optic systems. Their function is preliminary optimization of the optical signal obtained from the fiber into the electric one, which is processed by electronic devices.

11.1.1. Functional composition of ROM

The main elements of UM are:

1. *Photo receiver*, converting the received signal into an electric one.

2. Cascade of electric amplifiers that send a signal and turn it into the type necessary for processing.

3. *Demodulator* (regeneration unit), which restores the initial signal shape.

In Fig. 2. 11.1 elements of digital reception of optoelectronic module are given.
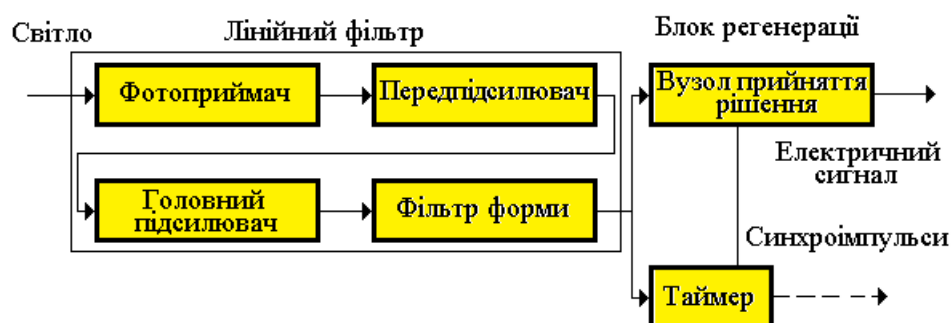
Fig. 11.1 переклад

As you know [1], when receiving digital signals, it is enough that the receiver is able to distinguish the constituent signals of type 0 and 1, accurate reproduction of the signal shape is not required at all. Thus, a digital reception, like a regeneration unit, must have a decision-making node, or discriminator, which distinguishes signals of type 0 and 1 at some threshold level.

There are synchronous and asynchronous modes of signal reception and transmission. In synchronous mode, the bit rate flow between the transmitter and the receiver is continuous. In asynchronous mode, data is transmitted in the form of organized bit sequences – packets. Between packages, the line is silent.

During synchronous reception mode, the timer, the receiver, distinguishes from the sequence of bits that special signals receive – synchroimpuls. By analyzing these pulses, the receiver regularly configures (or adjusts) its own timer to correctly identify all bits.

In asynchronous reception mode – reception has its own independent timer. By accepting the initial bits of the packets (preamble), the receiver timer configures the receiver's decision-making node so that the incoming bit identification is in its middle. The electric signal that gives the decision node works at the timer frequency.

During this, due to the existing timer error, as the packet bits arrive, the incoming bit is smoothly placed on one side or the other relative to the middle of the bit. Thus, for the correct identification of all bits of the package, it is important that the offset

during the reception of the package remains less than 0.5 bit lengths. Naturally, the lower the receiver timer error, the longer the package length can be used to transmit.

11.1.2. P-I-N PhotoDiodes

The personality of the P-I-N-photodiode (Fig. 11.2) is the presence of an i-layer (weakly alloyed n-type semiconductor) between the layers p^+- and n^+-type (sign + means strong alloying).
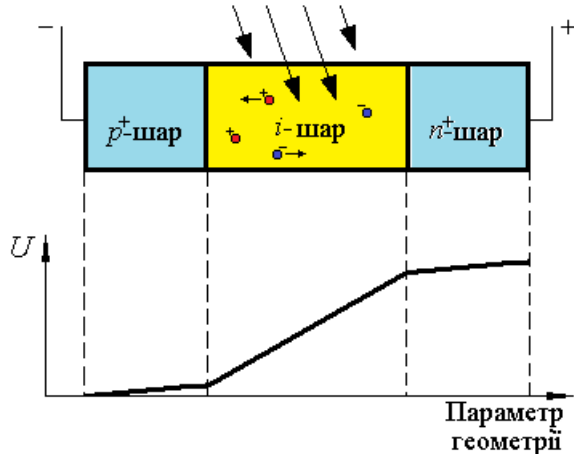
Рис. 11.2

This i-layer is called an impoverished layer because it does not have free media. The P-I-N-structure is powered by reverse displacement voltage U_{oc}. Strong doping of the extreme layers makes them conductive. Thus, all voltage falls on the i-layer and it creates the maximum value of the electric field. As long as the i-layer has no free media and, accordingly, does not leak electric current.

When light falls on the P-I-N-structure, free media appear in the i-layer – electron-hole vapors, which, under the influence of an electric field, separate and move in opposite directions. Thus, current occurs in the structure. This pod proceeds as long as the light shines. Effective is the interaction only with the i-layer, so it is made more extended compared to the extreme layers.

Photodiodes are made of various materials that determine the wavelength of radiation interacting effectively with the receiver (see Table 11.1).

Table 11.1

Material	Working range of wavelengths, nm
Silicon	400-1000
Germanium	600-1600
GaAs	800-1000
InGaAs	1000-1700
InGaAsP	1100-1600

The quantum efficiency of the impoverished area in the working range reaches 80-100%. However, part of the falling radiation undergoes Fresnel's reflection due to a jump in the circuit indicator on the boundary between the surface of the photodelete and the environment. To reduce the reflection, the receiving surface is covered with an enlightening layer, a thickness of λ/4 and a relapation indicator $\sqrt{n_1 n_2}$, where n_1 and n_2- air relapation indicators and i-layer environment, respectively.

11.1.3. Avalanche photodiodes

If the structure of layers of a regular photodiod p$^+$-i-n$^+$, then in the avalanche photodiod (LFD) add a layer p^+-i-p-n^+ (fig. 11.3). In this case, the profile of the distribution of alloy impurities is chosen so that the greatest resistance, and therefore the greatest tension of the electric field, has a p-layer.
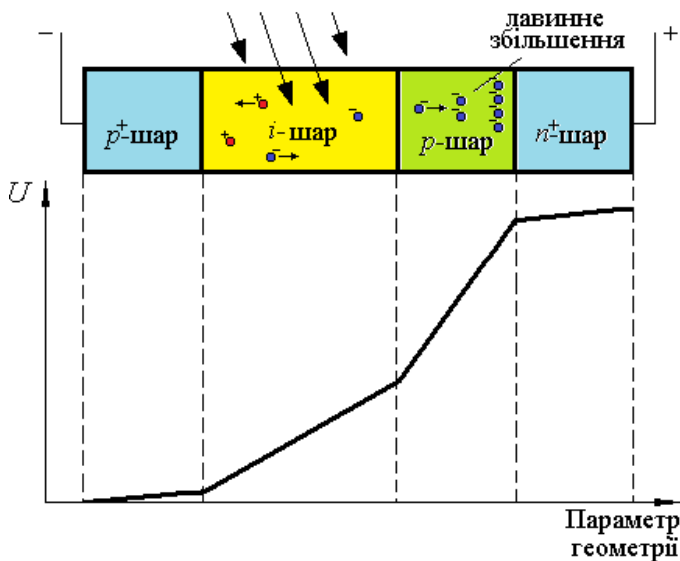
When light interacts with the i-layer, electron-hole vapors arise, which, thanks to a small field, drift in the direction of the corresponding poles. When electrons come from the i-layer to the p-layer, their acceleration increases due to the high intensity of the electric field in the p-layer. Accordingly, they receive considerable energy in order to knock out additional electrons from the valence zone into the conduction zone. This process is

Fig. 11.3 переклад

called avalanche boosting the photostage. The coefficient of increasing the number of media is usually several dozen and therefore the current sensitivity of the LFD is much higher than that of conventional P-I-N photodiodes.

The increase coefficient M is determined by the empirical formula:

$$M = \frac{1}{1-(\frac{U}{U_{о6}})^m},$$ (11.1)

where U - external reverse shear voltage; $U_{о6}$ - reverse shear voltage at which the photodiode breaks through (usually ~ 100 V); m – number between 3 and 6.

LFDs have high speed, but the random nature of the avalanche current creates significant noise. Unlike a useful signal that increases proportionally to M, noise increases faster ($\sim M^{2.1}$). As a result, the optimal M value in most cases lies between 30 and 100.

When choosing a photo receiver for fOX, it is necessary to be guided by such considerations. With the minimum radiation power that a photo receiver can take, the error rate should not exceed the required value. LFDs in this sense have some advantages over P-I-N diodes. However, they also have certain drawbacks.

The main disadvantage of LFD is a higher value of the operating voltage of the power supply compared to P-I-N diodes. In addition, for the LFD there is a fairly strong dependence of the coefficient M on temperature. This requires the use of special electrical power circuits and thermal stabilization circuits.

11.1.4. Technical characteristics of photo receivers

a) Current sensitivity (monochromatic) $S_{тч}$ (A/W):

$$S_{тч} = \frac{I_ф}{P(\lambda)},$$ (11.2)

where $I_ф$ – photocurrent; $P(\lambda)$ – full radiation power at wavelength λ.

The default current sensitivity setting for P-I-N-diodes in operating ranges is 0.5-0.8 A/W, and for LFDs it is 20-60 A/W.

Current sensitivity characterizes the photo receiver at low modulation frequencies.

b) Quantum efficiency η (dimensionless value) is determined by the ratio of:

$$\eta = \frac{N_e}{N_\phi}, \qquad (11.3)$$

where N_ϕ – number of photons falling per unit of time per photo receiver; N_e - number of electrons born during this time (or electron-dir pairs).

Quantum efficacy for P-I-N-diodes may not be greater 1 (100%).

c) Dark current $I_m(A)$ – current flowing through the load of the photodiod shifted back, in the absence of a photodiod of light flux falling on the photodiod. Dark current is otherwise called leakage current. The amount of dark current depends on the material of the photo receiver, ambient temperature and the design of the photo receiver. Typical characteristics of photo receivers are given in Table 11.2.

Table 11.2

Photo receiver	Current sensitivity, A/W	Dark current, nA	Growth time, ns
p-i-n - photodiod (InGaAs)	0.8	0.1-3	0.01-5
p-i-n - photodiod (Si)	0.5	10	0.1-5
LFD (InGaAs)	10-60	30	0.3
LFD (Ge)	20-60	400	0.3-1

From this table we can see that LFDs made from Germanium have the greatest value of dark current, which is the value from parts to hundreds of units of milliamphimeter.

d) Growth time $\tau_{нар}$ (descending $\tau_{сп}$) –characterizes the work of photo receivers in pulse mode and is its important dynamic characteristic. The increase time is determined by the signal growth time from level 0.1 to level 0.9 (signal drop from level 0.9 to level 0.1) from the level of the maximum value, provided that strictly rectangular pulses of long duration are fed to the input. These times depend on the geometry of the photodiod, material, the tension of the electric field in the poorly alloyed area, temperature. Maximum value from $\tau_{нар}$, $\tau_{сп}$ – is taken as a characteristic of the response time of the photo receiver.

As the modulation frequency of input optical pulses increases, the maximum photost frame value decreases. The limit frequency at which the photodeaent can still work is defined as the modulation frequency at which the current sensitivity is 0.707 from the current sensitivity value at low modulation frequencies. As the table suggests, the P-I-N-photodiode is a higher-frequency radiation receiver compared to LFD.

e) Recurrence rate of errors. In digital systems, when information is transmitted by bits, the degree of quality of the received signal is the probability of incorrect reception of 0 or 1, called the frequency of errors (BER) . It is defined as the ratio of the number of incorrectly taken bits to the total number of bits transferred. In

telecommunication systems, this value should not exceed 10-9. In computing networks, the requirements for this value are much higher, and the frequency of error recurrence should not exceed the value of 10-12 BER depends on the transmission speed. The lower the transfer speed, the lower the BER.

f) The sensitivity of digital UM is the minimum input signal strength, at which BER does not go beyond the maximum allowable value set for this application package. For the normal operation of the application package, the input signal strength must be not less than the sensitivity of UM. UM sensitivity is usually measured in dBm.

g) ROM saturation. The saturation of the digital ROM is the maximum input power, above which BER begins to exceed the maximum allowable value for this package of applications.

The range of power values from sensitivity to saturation is called ROM dynamic range.

h) Maximum allowable reverse voltage U_{max} − is a voltage excess of which can lead to a breakdown of the photo receiver and its destruction.

i) Operating temperature range (ºC). Eats two characteristics of the photo receiver, which are strongly influenced by temperature changes.

First, it is quantum efficacy, which can behave quite difficult depending on the change in temperature.

Secondly, an increase in temperature leads to an exponential increase in thermally excited electron-hole pairs, and as a result, dark current increases exponentially. This value usually becomes twice as large when the temperature rises by8-10ºC.

j) Developments for refusal (thousand hours). When operating photo receivers in accordance with the technical specifications, the resource of photo receivers is higher than the resource of emitters.

11.2. Electronic elements of ROM
ROM, as a rule, include the following nodes:

11.2.1. Electronic pre-amplifiers and amplifiers
Typical optical signal power at the input of the photo receiver is about 1-10 µW or less. If P-I-N-N-photodiode with current sensitivity of 0.6-0.8 A/W is used in the ROM as a photodepend, then its output current is several microampers. For normal operation of the following ROM units, pre-emitting low noise and power amplifiers are used.

11.2.2. Alignment Node
The alignment node is used to restore the correct ratio in low-frequency and high-frequency areas of the spectrum, since these frequencies are enhanced differently. An alignment node is an additional signal alignment circuit.

11.2.3. Filter Node

The filtration unit allows you to increase the ratio of signal-noise due to the suppression of noise in a certain range of frequencies of the signal spectrum.

11.2.4. Knot of discrimination

The discrimination unit is designed to distinguish and distinguish between 0 and 1 of the total sequence of the accepted digital signal. The need for its use is caused by the presence of distortion of the signal shape due to the dispersion of THE VOLZ. To restore the rectangular shape of the signal, a discriminator is designed, which is characterized by a certain threshold of actuation.

If the signal amplitude is less than a certain value, the output of the discriminator is obtained (0), if more (1). The main disadvantage of such processing is the possibility of breaking the duration of impulses.

In order to maintain the correct time ratio in the information signal, the discriminator must receive information about the frequency with which pulses follow.

11.2.5. Timer

The main function of the timer is to suppress signal resynchronization. This function in UM is necessary, because during the transmission and relay of the signal, time errors can accumulate and reach the level of duration of the pulse itself. As a result, the receiver may mistakenly interpret the accepted bit or "lose" it. Such random time errors are called "jitter" and their appearance is characteristic of the asynchronous transmission mode. You can reduce the jitter by increasing the requirements to the pulse generator frequency standard. However, with prolonged reception, such errors may still appear.

Further reduction of errors due to jitter is achieved, for example, in the technology of SDH main optical networks, in which, in synchronous transmission in a bit stream, along with useful information, there are special synchroimpuls, according to which the receiver timer is adjusted (smoothly adjusted to the frequency of the transmitter). In a complex SDH network, there is one independent wired timer through which other network devices are configured.

12. REPEATERS AND OPTICAL AMPLIFIERS [21-24]

When the optical signal spreads through the fiber, its weakening occurs, as well as the expansion (destruction of the form) of impulses as a result of dispersion. Any of these factors may be the reason for limiting the maximum length of the VOLZ section, which does not require the relay of the information signal. If the maximum length of the FOI section is exceeded, then one or more points in which the repeaters should be placed must be provided on the track. In general, the repeater performs the function of amplification of the optical signal and additionally (with digital transmission) can restore the shape of pulses, reduce noise and eliminate errors arising during transmission. Such a repeater was called a signal regenerator.

12.1. Types of repeaters

According to the method of optical signal amplification, repeaters are divided into repeaters and optical amplifiers. Repeaters are much wider common in local fiber optic networks. Amplifiers play an exceptional role in the formation of main optical communication lines.

12.1.1. Repeaters

The repeater (electro-optical repeater) first converts the optical signal into an electric one, amplifies it, corrects it and converts it back to optical (Fig. 12.1).

Переклад Fig. 12.1

Repeater is sequentially connected receiving and transmitter modules. Typically, the regeneration unit contains a discriminatory node and a timer.

The regeneration unit restores the form of pulses, eliminates noise, resynchronizes transmission so that the output pulses fall into the corresponding time slots. The repeater may not have a timer and restore the rectangular shape of the pulses at a certain threshold, regardless of the speed at which the transmission takes place. Such "environment dependent" repeaters are used in local networks where the asynchronous mode of information transmission is.

Repeaters are common in local networks that convert signals from multimode fiber (MMF) to singlemode (SMF). Such repeaters were called converters. Widespread FDDI-(100 Mbps), ATM- (155 Mbps), ATM- (622 Mbps) MM/SM converters.

12.1.2. Optical amplifiers

Optical amplifier (OP) unlike repeater does not perform optoelectronic transformation, but immediately performs amplification of the optical signal (Fig. 12.2).

Note that the OP amplifies both the signal itself and the noise. In addition, the OP makes additional noises to the signal. Comparative characteristics of repeaters and amplifiers are given in Table 12.1.
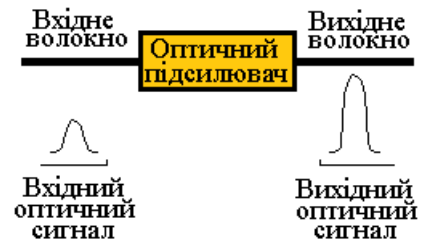
Переклад Fig. 12.2

Table 12.1

Characteristic	Repeater	Optical amplifier
Design	Complex	Simple
Cost	Low	High but changing in the direction of decrease
Reliability	High	Very high
Signal	Allowed	Excluded
Binding to signal transmission speed	Needed	Not required
Possible single-chan transmission of several signals	Excluded	Allowed
Working wavelength	0.85, 1.31, 1.55 microns	Area 1.53-1.56 microns
Signal-to-noise ratio	High	Low
Scope	Local networks, regional networks, interregional networks	Regional networks, interregional networks

12.1.3. Fabry Perot amplifiers

Amplifiers are equipped with a flat resonator with mirror translucent walls. They provide a high gain factor (up to 25 dB) in a very narrow (1.5 GHz) strip, but can be rebuilt in a very wide spectral range (800 GHz). In addition, such amplifiers are insensitive to the polarization of the optical signal and are characterized by a strong suppression of the lateral components (weakening by ~ 20 dB outside the 5 GHz interval due to the optical properties of the resonator interferometer).

Optical amplifiers, similar to lasers, use the principle of induced radiation. There are five types of optical amplifiers listed in Table 12.2.

Table 12.2

№ з/п	Amplifier type	Scope
1	Amplifiers with Fabry-Perot cavity	One channel boost (one wavelength)
2	Amplifiers on fiber that use Blueluen scattering	Amplification of one channel
3	Amplifiers on fiber that use Raman dissipation	Amplification of multiple channels at the same time
4	Semiconductor laser amplifiers	Amplification of a large number of channels in a wide area of wavelengths at the same time
5	Amplifiers on impurity fiber	Amplification of a large number of channels in a wide area of wavelengths at the same time

Due to its characteristics, Fabry-Perot amplifiers are ideal for working as demultiplexers in a multichannel WDM system (a system with a multi-wave seal), as they can be rebuilt to amplification of only one specific wavelength (single channel).

12.1.4. Amplifiers on fiber using Blueluen scattering

Stimulated blur scattering is a nonlinear effect that occurs in silicon fiber when energy from radiation at the optical frequency f1 passes into radiation energy with a displaced frequency f2. If powerful optical pumping in silicon fiber occurs at f1 frequency, the stimulated Bluluen scattering can amplifies the signal at frequency f2. The output signal is concentrated in a narrow range, which makes it possible to choose a channel with an error not higher than 1.5 GHz.

12.1.5. Amplifiers on fibers using Raman dissipation

Such amplifiers are also built on the principle of using the nonlinean effect of the occurrence of stimulated Ramanian scattering. Unlike the previous type of amplifiers, the frequency shift between the swap wave and the signal wave is greater, and the output spectral amplification range is much wider. Therefore, such amplifiers on the one hand allow for amplification of several wavelengths, but, on the other hand, are characterized by large transitional obstacles.

12.1.6. Semiconductor laser amplifiers

Semiconductor laser amplifiers (NPLP) have the same active environment as semiconductor lasers, but there is no mirror resonator (Fig. 12.3). Thus, such devices work in quantum amplifier mode (no feedback branch). To reduce Frenelian reflection on both sides of the active layer, a

Рис. 12.3

special coating with a thickness is applied $\lambda/4$ with an agreed relature indicator.
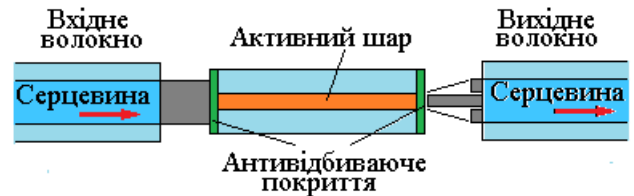
Semiconductor amplifiers have the following two significant drawbacks:
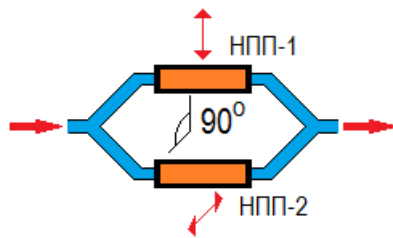
Fig. 12.4

The active layer has a transverse size (in one direction) of the order of one micrometer, at the same time as the smallest diameter of the core of the input fiber has a value of about 8-10 microns (single-mode fiber). As a result, most of the luminous flux does not fall into the zone of the active layer, which significantly reduces the K.K.D. amplifier. You can increase the K.K.D. by applying a focusing lens at the entrance of the amplifier. However, this leads to a complication of the design of the amplifier.

The second drawback is a thinner nature. The gain factor of the amplifier depends on the azimuth of polarization of the input signal and may differ by 4-8 dB for two orthogoric polarizations. This is a very negative characteristic of the amplifier, since the polarization of the optical signal spreading in the fiber is not controlled (for a monomode fiber, the azimuth of water polarization is almost random if we have linear-polarized radiation at the input). The solution of the problem in such a situation may be as follows (see Figure 12.4). With the help of a brancher, the signal is divided into two channels. Signals in each channel arrive at the entrance of a separate amplifier, in which the placement (thickness and width) of the active layer is mutuallyperpendicular. However, such a technical solution will again lead to a complication of the design and an increase in the cost of the device.
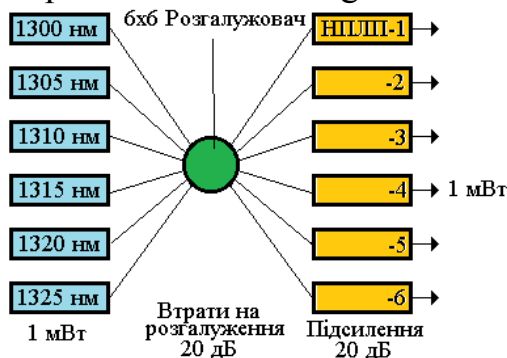
Переклад Fig. 12.5

However, there are situations when the use of NPLP is very useful: devices are created on the basis of such devices, if the characteristics of optical signals are known and controlled in advance, for example, in devices used at the beginning of the optical track. Figure 12.5 shows the implementation of a broadband multiplexer forklift.

Several narrow-striped semiconductor lasers at different wavelengths generate light signals that multiplex and multiply using an optical forklift. The NPLP is installed in each channel at the outlet of such a device in order to compensate for losses arising from the branching of the signal.

12.2. Amplifiers on impurity fiber. Fiber optic amplifiers

Fiber optic amplifiers (OPPs) are the most common type of amplifier in SSRIs and are a key element in the technologies of fully optical networks, as it allows to ampln the light signal in a wide spectral range.
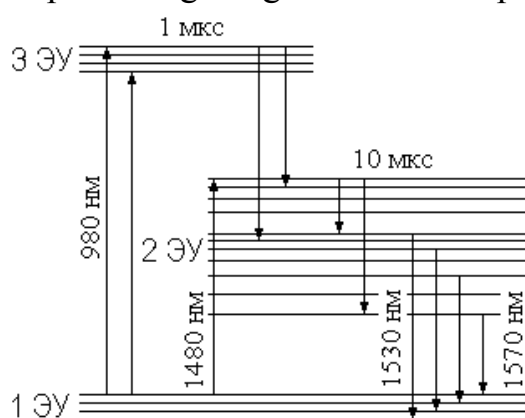
Fig. 12.6

The active environment of the amplifier is a monomode fiber, the core of which is alloyed by a rare earth element. Figure 12.6 shows a diagram of the energy levels of the dosed Er^{3+}.

This scheme is the standard diagram of a three-level quantum amplifier. Metastabilic level 2 ER width is wider than level 3 ER width. Level 2 ER expansion is due to the so-called Starka effect. This effect is that there is a splitting of energy levels under the action of a strong electric field [12].

It is known that there is a strong magnetic field in the kernel zone. Since the tension of the electric field quickly decreases when the distance to the nucleus increases, it is the metastable level that breaks down most, disintegrating into several subleans. This expansion ultimately leads to an increase in the area of the radiation spectrum in which forced radiation may occur.

The lifespan of electrons on metastalled levels decreases with an increase in the distance to the nucleus. Thus, the sub-levels with the highest energy have the least time of life. Average lifespan at 2 ER approximately 10 ics.

If such a system is excited by the radiation of the pumping laser from the $\lambda=980$nm (wavelength is necessary to achieve the optimal gain), then electrons pass from the level of 1 ER to the level of 3 ER. After that, the electrons relax to the metastable level of 2 ER. This process is accompanied by radiation in the long-wave region of the spectrum or without radiation with the birth of acoustic phonons. The lifespan of electrons at the level of 2 ER is much longer than at the level of 3 ER. Thus, at the level of 2 ER, inverse settlement of electrons is created.

Naturally, in the absence of an information optical signal with a wavelength lying in the range of 1530 - 1565 nm, spontaneous radiation occurs in this spectrum interval. Like any spontaneous radiation, this radiation is random in nature (different wavelengths, different directions of photons distribution, etc.). If you send a directed stream of photons corresponding to the information signal to such an environment, then the process of forced radiation (twin photons), which in turn cause regular acts of forced radiation, begins. In other words, we have an avalanche-like signal boost.
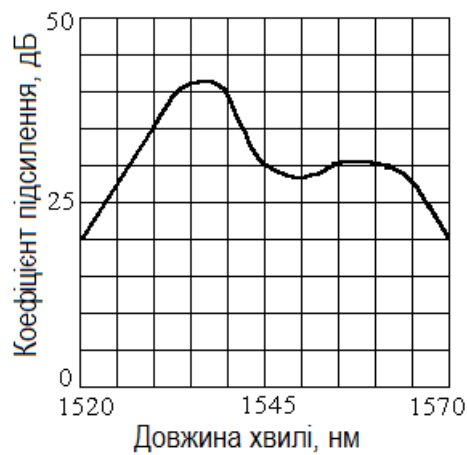
Fig. 12.7

Add that the system can also be excited by radiation with a wavelength of 1480 nm (two-level system), but this type of pumping is characterized by a high level of noise spontaneous radiation.

As a three-level system, pumping can also be carried out with wavelengths of 665,807 nm. However, pumping radiation with a wavelength of 980 nm is the most effective (the lowest level of spontaneous noise).

Such amplifiers are called erbie amplifiers (EDFA).

Due to the dependence of the probability of transition from the metastabilic level to the distance of the metasablic level from the stable one, this probability increases with an increase in this distance. The gain factor will be different for different wavelengths. The characteristic dependence of the gain factor on the wavelength is shown in Figure 12.7.

Amplification in another transparency window can be obtained by alloying the OV with the help of impurities with prazeodim. However, such amplifiers have not been widely used.

It can be shown that in order to increase the efficiency of the active pumped fiber, it must have an increased numerical aperture (NA) (more energy of the pumping laser enters the fiber). Accordingly, for this purpose, the OV nucleus is additionally legalized with Germanium oxidation GeO_2 and aluminum Al_2O_3. According to these impurities, two types of fibers are produced for EDFA. Table 12.3 shows the characteristics of EDFA with fibers of both types.

Fiber type	Numerical aperture	Pump wavelength, nm	Pumping power, $P_\text{н}$, Mw	Coeff. Gain G_A, дБ	$G_A/P_\text{н}$ dB/mW
SiO_2/GeO_2	0.16	532	25	34	1.35
SiO_2/GeO_2	0.16	980	10.5	24	2.2
SiO_2/Al_2O_3	0.18	514	100	22	0.22
SiO_2/Al_2O_3	0.14	514	100	16	0.16
SiO_2/Al_2O_3	0.14	528	100	31	0.31
SiO_2/GeO_2	0.2	665	100	26	0.26
SiO_2/GeO_2	0.3	807	20	8	0.4
SiO_2/Al_2O_3	0.12	1480-1490	14	2	0.14

According to these data, the largest gain factor per 1 mW is fiber of the 1st type when pumping a wavelength of 980 nm. The minimum threshold power is inherent in fibers of the 2nd type when pumping a wavelength of 1480 nm. Although the table implies that the minimum power required for the excitation of fiber of the 1st type corresponds to the wavelength of 980 nm, nevertheless in the first case the power of 14 mW is introduced at a lower numerical aperture.

12.3. Other characteristics of erbie fiber amplifiers

In the process of strengthening the optical signal, the population of the metasablic level is impoverished. Since the number of electrons at this level is distributed evenly along the entire active area of fiber, impoverishment increases as the optical signal progresses along the fiber (avalanche increase in twin photons). In other words, the environment tries to move to a state of saturation, in which the degree of settlement of the main and metastabilic levels are the same. The speed and degree of impoverishment depends on the power entering the fiber, that is, on the number of photons carried by the optical signal.
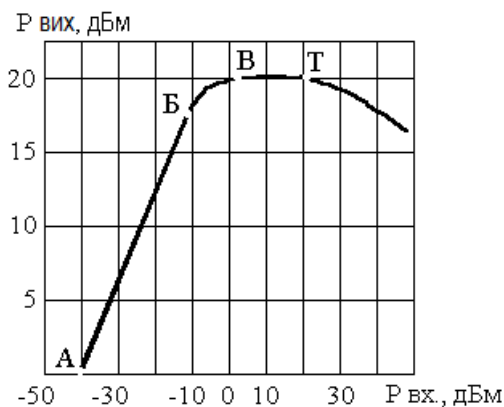
If the number of such photons is small compared to the number of electrons at the metastabilic level, then this has little effect on the degree of settlement, since the number of electrons that go to the main level during forced radiation is quickly compensated by pumping radiation. At the same time, the GA gain is maximum. With an increase in signal photons, the compensation of electrons at metastabil levels gradually decreases and at a certain radiation power saturation occurs. At such a capacity G_A strives for a unit, and with a further increase in capacity, it becomes even less than a unit.

Переклад Fig. 12.8

Figure 12.8 shows the dependence of the initial power of EDFA on the input signal power.

As you can see from the graph, the output power increases linearly at input capacities from -30 to - 10 dBm. On the site - 10.0 dBm output power increases nonlinea. And finally, on the B-T site, it practically remains unchanged (saturation

zone). When the output power becomes the same order as the input power, the curve goes down. Such dependence of the output power on the input leads to the fact that at high input signal capacities there is a distortion of its shape (the effect of electronic amplifiers is known).

This dependency is obtained at zero modulation frequency. Naturally, with an increase in frequency (the time of active influence of impulse on the active environment decreases), the situation begins to improve. At the same time, at ultra-high frequencies, it no longer matters in what mode the amplifier works.

Another important parameter of the IOP is the noise factor. This value is determined mainly by spontaneous radiation:

$$NF = \frac{2P_{сп}}{h\nu_s \Delta\nu(G_A - 1)},$$ (12.1)

where P_{cn} – spontaneous radiation power, ν_s – operating frequency (light), $\varDelta\nu$ – width (frequency) of optical radiation spectrum.

To the noise level of spontaneous radiation, it is also necessary to add residual pumping radiation and parasitic radiation, due to the reflection from the ends of the amplifier.

- Thus, the main characteristics of the FOP are:
- wavelength range amplated, ($\varDelta\nu$ або λ_1, λ_2);
- gain at linear area (dB);
- the level of input power at which saturation occurs (dBm);
- noise coefficient (dBm);
- level of final pumping radiation power (dBm);
- reflected power level at the in and out of the IOP.

12.4. Schemes of pumping erbius fiber (FOP)

Figure 12.9 shows the most common FOP pumping schemes.

Figure 12.9 a demonstrates the option when pumping radiation from source 3 is injected into the incoming end of the erbius fiber 7 through multiplexer 2. An input optical signal is supplied to the other input of the multiplexer. If limited only to these devices, then due to the reflection of radiation from the ends of the EV, additional feedback is created and the amplifier can start working as a generator. In order to exclude such a situation,

Рис. 12.9

elements 1.4 – optical insulators are introduced into the amplifier circuit. The disadvantage of such a scheme is that the radiation of the pumping source passes to the output of the amplifier. Such a scheme is widespread when used at the transmitter end of the system to amplification of the signal when entered into linear OV. If the wavelength of pumping is 980 nm, then such radiation quickly fades when spread over linear optical fiber. However, if this is not enough, then optical filters that do
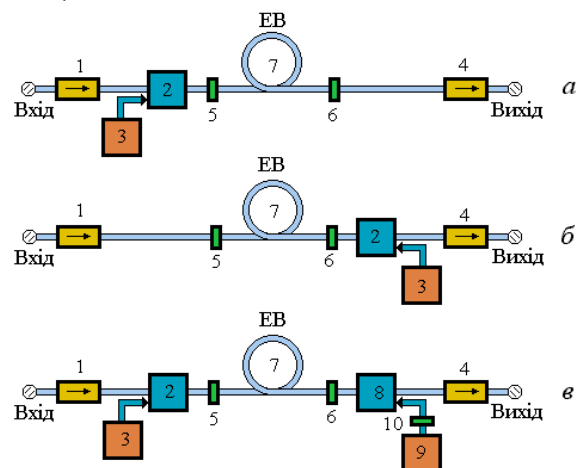
not transmit radiation with this wavelength are sometimes placed at the output of the amplifier.

In Figure 12.9 b radiation pumping source 3 is injected through the output end of EB with the help of multiplexer 2. This scheme is used in most cases at the receiving end of the line.

To increase the pumping power, this radiation can be injected at both ends of the EV from two different sources of pumping 3 and 9 (Fig. 12.9 c).

To further increase the radiation power use polarizing multiplexers 10. As you know, the radiation of the semiconductor laser is characterized by a pronounced ellipse. Thus, using elements of the type of plate $\lambda/4$, you can convert it to linearly polarized, i.e. optimally use both orthogonal oscillations.

According to the schemes under review, the IOP is divided into three types:
- power amplifiers (BOOSTER) of the optical signal at the inline;
- previous, included on the receiving side in front of the receiver;
- intermediate or linear amplifiers included on a specific area of the line.

Today, linear amplifiers are often combined with a dispersion compensator. Linear amplifier consists of a power amplifier and amplifier. A variance compensator is placed between them.

For high-speed SSOs, in which the transmission goes at the same wavelength, the unevenness of the gain characteristic in the working range of wavelengths matters. At the same time, for systems with multi-wave seal (WDM), the unevenness of frequency characteristics should not exceed ± 1 dB. To equalize the frequency characteristics, CHP equalizers are added to the VZU scheme.

There are several types of equalizers. The most common of them:
- a Bragg lattice is built into the fiber, the period of which is selected for the appropriate wavelength;
- Mach-Tsander interferometer (interferometer of two Y-branchers), included sequentially with erbiic fiber. The use of both types of equalizers will reduce the unevenness of HX to 0.5 dB.

Modern EDFA operating in the range of 1550-1565 nm have the following characteristics.

Power amplifiers. Output power up to 10 W. Amplifiers with iteration – up to 50 W. However, for communication systems such power is not required. The maximum power that is currently injected into the FOZ is 1 W (+30 dBm). Booster noise factor is in the range of 6-7 dB.

Pre-amplifiers are characterized by a large gain factor and a small noise factor. The record value of the gain factor - 51 dB - was obtained in an erbius amplifier with a length of EB 22 m..

Linear amplifiers. In recent years, there has been a noticeable tendency to use remote radiation supply pumping into linear IOP. In this case, pumping is carried out at wavelengths $\lambda = 1480$ nm. It turns out that with such pumping, the power threshold at which inversion settlement is achieved is quite low – less than 10 mW. This creates favorable conditions for remote pumping of EDFA, since radiation at a wavelength of 1480 nm is characterized by not much greater absorption than at the

working wavelength (about 1550 nm). Pumping is carried out as follows. Wavelength radiation $\lambda = 1480$ nm is fed in the opposite direction from the reception station. Linear optical amplifier with such feeding can be placed at a distance of up to 100 km from the receiving station.

The development of SSRS systems with a multi-wave seal in the direction of increasing the number of channels through which information is transmitted requires a significant expansion of the IOP bandwidth. There are developments in which instead of one IOP use parallel included two IOP, built on the basis of fibre alloying with different admixturation. For example, one of the samples you created has a bandwidth of 54 nm. This amplifier operates in two sub-bands 1530-1560 and 1580-1610 nm. One of the fibers of alloyed, as always, only erbius ions Er^{3+}, and the rest – also tulya ions Tm^{3+} (additionally). The first fiber provides amplification in the first range, the other – in the second. A well-known amplifier that amplifiers in two ranges and has a bandwidth of 113 nm. The first fiber enhances in the range of 1450-1480 nm. It is fiber alloyed by ions Tm^{3+}. The second strengthens in the range of 1530-1608 nm and is doped with ions Er^{3+} and telur ions.

Pumping of these amplifiers is carried out:

- first – at wavelength λ=1047 nm (400 mW);
- the second – at wavelength λ=1480 nm (160 mW forward and 100 mW back).

13. SIGNAL AND TRANSMISSION SYSTEMS [21-24]

13.1. Digital signal transmission systems

13.1.1. Basic concepts and terminology

Information is a collection of information or data about certain events, phenomena or objects, that is, a set of knowledge about the world around us. Unlike material and energy resources, the information resource is not reduced by use, but, on the contrary, accumulates over time and with the help of technical means can be processed, stored and transmitted over considerable distances. The transfer and preservation of information is carried out using signs (symbols) that allow you to depict it in some form.

Message is a collection of characters that display one or another information. The transfer of messages (and, accordingly, information) to a certain distance is carried out using a certain media.

Modulation is the process of changing the parameters of the media.

Signal is a physical process that displays (transfers) the transmitted message.

Discrete or discrete signal in a level (amplitude) is a signal that receives only certain discrete values by magnitude (amplitude).

Continuous or analog signal is a signal that can receive any levels of values in a certain magnitude interval.

Time-time discrete signal is a signal set only at certain points in time.

Time-continuous signal is a signal set over the entire time axis.

Digital signal is a discrete signal in both level and time.

Next, basically, we will consider only communication systems designed to transmit digital messages. The information contained in such a message is transmitted by means of digital signals from the message source (DP) to the recipient of messages (OP) through the digital message transmission channel (CCC).

Since the object that transmits messages to such channels is a digital signal, the technique of such communication, in fact, is the technique of transporting (transmitting) digital signals through communication channels.

Basic signal parameters:

Signal duration T_c - determines the amount of time a signal exists.

Dynamic Range D_c – is the ratio of the highest instantaneous power to the minimum power, which must be distinguished from zero at a given transmission quality.

Signal spectrum width F_c –this is the frequency range within which its main energy is concentrated. It determines the rate at which the signal changes in the middle of its existence interval. In communication technique, the spectrum of signal transmitted is often deliberately reduced to save losses on communication line equipment. The value of the signal spectrum interval at which it can be shortened is determined based on the maximum signal distortion allowed during transmission. For example, when calling, it is necessary that the conversation is so legible that subscribers can recognize each other by voice. To do this, it is enough to transmit the voice signal in the frequency band 300-3400 Hz. The modulated signal spectrum is usually wider than the spectrum of the message sent and depends on the type of modulation.

Signal strength V_c:

$$V_c = T_c \times F_c \times D_c. \tag{13.1}$$

The volume of the signal gives a generalized idea of the possibility of this set of signals as message carriers. The larger the signal volume, the more information can be "invested" in the given signal volume and the harder it is to transmit such a signal with the required quality.

13.2. Structure of communication systems

Figure 13.1 shows the structural diagram of a single-channel communication system.
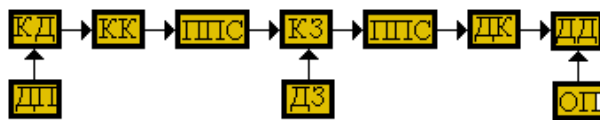
Переклад Fig. 13.1. Structural diagram of a single-channel communication system

GP – the source of the message; KD – source coder; QC – channel coder; PPS – signal conversion device; DK – channel decoder; DD – source decoder; OP – recipient of the message; DZ – source of interference

Message source and recipient – people or all sorts of devices (automaton, computer, etc.).

The source'scode performs the task of reducing redundancy when transmitting a message to a communication channel, and the source decoder is the restoration of a message accepted through the communication channel.

The presence of these devices in the communication system is explained by the fact that redundancy is peculiar to the message received from the GP. For example, this may be due to the fact that the characters $a_i \in A$ (where A – transmitted message) can be statistically related (for example, unions, punctuation, etc.). Such a character association allows part of the message not to be transmitted, to restore it at the receiving end of the line according to a known statistical connection.

Elimination of redundancy causes more messages to be transmitted over specified intervals, and, as a result, a communication channel is more efficiently used.

The channel encoder performs redundant message encoding in order to increase the reliability of the transmission of correct information. At the receiving end, the channel decoder performs a reverse conversion (decoding), as a result of which we get a combination of source code. Often, the coder and decoder are called an error protection device (PPPs).

Signal conversion devices – devices contained at both ends of the communication channel and used to reconcile the encoder and channel decoder with the communication channel environment. In some cases, for this purpose, a modulator and demodulator may be used.

When a signal passs through a real communication channel, the signal is distorted and therefore may be restored at the receiving end of the message with some error. The cause of such errors can be both distortions caused by the communication channel itself and interference affecting the signal from the external environment.

Interference refers to any random (sometimes deterministic) effect on the signal, which impairs the correctness of the recovery of transmitted messages.

Obstacles can be quite diverse both in origin and in their physical properties. Atmospheric interference is due to electrical processes in the atmosphere and, above all, thunderstorm discharges.

The energy of this type of interference is mainly concentrated in the area of long and medium waves.

Industrial obstacles arise due to sudden changes in current in various kinds of industrial equipment.

Interference caused by third-party communication channels and radio stations is also common.

In modern communication systems, the main type of interference is *impulse interference and communication termination*. The appearance of pulse interference is often associated with automatic switching and cross-reference. Termination of communication is a phenomenon in which the signal in the line abruptly fades or disappears.

Almost in any frequency range there are internal noises of equipment.

In the range of ultra-short waves, *cosmic obstacles* associated with electromagnetic processes occurring in the sun, star, etc. are important.

In the optical frequency range, quantum noise caused by the *discrete nature of light* is essential.

In the real channel, as a rule, there are *additive n(t)* (added to the signal) and *multiplicative k(t)* (those multiplied by the signal) obstacles. Therefore, the signal *Z(t)* in the presence of obstacles can be recorded in the form of:

$$Z(t) = k(t)s(t) + n(t). \tag{13.1}$$

Among additive obstacles of different origin, there are concentrated on the spectrum (narrow-zone) obstacles concentrated in time (pulsed) obstacles and so-called *flucation* obstacles that are not concentrated either on the spectrum or in time.

In the technique of communication there are *synchronous* and *asynchronous* digital channels.

In *synchronous digital* channels, each single element that is transmitted is entered into the channel at strictly certain points in time. These channels are only intended for transmitting isochronous signals, so they are called *code-dependent* or *opaque*.

In *asynchronous channels*, the transmitted signal can be entered into the channel at any time, that is, such a channel can transmit any signals - isochronous and anisochronous. Therefore, such channels were called *transparent* or *code-independent*.

A discrete channel together with a channel encoder and decoder is called an *extended channel*.

The digital channel is characterized by the following parameters:

1.   **Transfer rate of information** measured in bits per second (bit/s).

2.   **The speed of B telegraphing**, which is measured in bods. This is the number of single characters passed per second. In the technique of data transmission, instead of the speed of telegraphing, the term modulation speed is used.

3.   **The effective speed of information transmission**, which is determined taking into account the fact that not all elements transmitted to the channel, carry information; not all combinations that came to the entrance of the channel are given to the recipient (some combinations may be rejected).

4.   ***The error rate on the elements***, which reveals the correctness of the passage of single elements through the channel and the determined relationship of erroneously accepted elements $n_{ош}$ to the total number of transferred $n_{пер}$ per time interval:

$$K_{ош} = \frac{n_{ош}}{N_{пер}}. \tag{13.2}$$

5.   ***The coefficient of errors by code combination***, which characterizes the correctness of the message through the communication channel and is determined by the ratio of the number of mistakenly accepted code combinations to the number of time transferred in a given time interval.

6.   ***Sometimes*** T_k, during which the channel is possible to transmit information.

7.   ***Dynamic channel range*** D_k, which is determined by the ratio of the permissible power of the transmit signal to the power of obstacles that are inevitably inherent in the signal. D_k expressed in decibels.

8.   ***Generalized characteristic of the channel***, which is its capacity (volume) and is determined by the expression:

$$V_k = T_k \times F_k \times D_k. \tag{13.3}$$

At the same time, a prerequisite for transmitting unproductive information through the channel with the volume of signal V_c obviously there must be a condition:

$$V_c < V_k. \tag{13.4}$$

The transformation of the primary signal into a high-frequency signal, as a rule, aims to coordinate the signal with the characteristics of the channel. In the simplest case, the signal must be coordinated with the channel in all three parameters:

$$\begin{cases} T_c < T_k \\ F_c < F_k \\ D_c < D_k \end{cases}. \tag{13.5}$$

In this case, the volume of the signal completely "fits" into the volume of the channel. However, inequality (13.4) can also be performed when one or two of the inequalities (13.5) are not met. This means that in the process of transmission it is possible to "exchange" their duration to the width of the spectrum or to the value of the dynamic range, etc. than the speed at which it was recorded. At the same time, all frequencies of the initial signal decrease by 10 times and the time of its transmission increases by the same number of times. Similarly, the signal can be transmit faster if the channel is wider than the width of the signal spectrum.

In the communication system shown in Figure 13.1, the message is transferred only in the direction from the source to the recipient. This mode of communication is called *simplex*. The communication mode, which provides the ability to

simultaneously transmit messages in both directions, is called *duplex*. *Half-duplex* mode is also possible, when messaging takes turns in both directions.

13.3. Methods of signal transmission

In digital communication systems (CCDs), digital signals can be transmitted in a variety of ways. Let us consider them in more detail.

13.3.1. Sequential and parallel signal transmission

When transmitting a digital signal *sequentially*, single elements of the digital signal follow in the channel one at a time. In *parallel* transmission, single elements of the digital signal are combined into groups transmitted simultaneously (usually on different bands of frequencies) by separate channels. At a given transmission rate, serial (single-frequency) systems have several advantages over parallel (multi-frequency) systems. Such systems better use the power of the transmitter, less critical to the nonlineability of the channel, easier to implement, etc..

13.3.2. Synchronous and asynchronous signal transmission

In *synchronous** transmission of a digital signal, its instantaneous value (MZ) is in a constant phase ratio (required ratio) with the MZ of any signal transmitted. In case of *asynchronous* transmission of the digital signal, its MZ can be in any phase ratios with the MZ of another signal.

---

* *Synchronization* is the process of establishing and maintaining specific time relationships between two or more processes.

13.3.3. Поелементна передача сигналів

When element-by-element transmission on the receiving side, the type of element ("0" or "1") is first determined, and then code combinations are formed from the elements, the decoding of which will allow you to determine the characters of the transmitted message. The type of item transmitted is usually determined by comparing it with the reference. For binary signals, it is enough to have one or two references. At the reception, in order to correctly restore the elements of code combinations, it is necessary to correctly separate one element from another. To do this, various methods of element synchronization can be used.

13.3.4. Signal transmission by code combinations

During code transfer, the correct separation of one code combination from another is carried out by group synchronization methods, which allows establishing and maintaining the necessary phase ratios between the Ministry of Health of the beginning of groups and groups of accepted elements. You can separate one code combination from another at the reception, for example, if you enter special starting and stop elements at the beginning and end of the group. Such a sequence of transferred elements is called startstup. The method of transfer in question is asynchronous, since the transfer by any code combination can be started at any time.

13.4. Features of communication channels

Both analog and digital communication channels can be used to transmit voice messages and data. Consider their features on the example of telephone communication.

13.4.1. Features of analog communication channels

One of the main problems with the transmission of messages is the problem of their correct transmission, which consists in determining whether messages are transmitted through the communication channel without distortion, and in case of distortion, whether they can be correctly restored by the recipient. The analog signal directly transmitted through the communication channel can be distorted by amplitude, phase, frequency or time scale. These distortions are the result of natural or artificial limitations of the communication channel, such as the dynamic range and/or bandwidth, as well as the impact of external interference.

** Element-by-element synchronization is the synchronization of transmitted and accepted digital signals, in which the necessary time ratios between the instantaneous values of the transmitted and accepted elements of these signals are set and maintained.

When transmitting messages over long distances, it is energetically advantageous to use a high-frequency carrier as signals, the parameters of which are moduled by the transmitted message. To transmit voice messages through the communication channel, as a rule, two methods of modulation of the carrier are used: amplitude (AM) and frequency (CHM). Let f_0– carrying frequency, and Δf – the main band of frequencies occupied by the signal. Also note that modulation is a nonlinear process, as a result of which additional harmonics appear (left and right lateral frequencies) $f_0 \pm \Delta f$ (where m depends on the modulation index). Then the band of frequencies occupied by the modulated signal (or its spectrum), which determine the width of the frequency band required for the communication channel is equal to AM-$2\Delta f$, and for ЧС-$14\Delta f$. Based on this, we see that the World Cup requires a much larger width of the band frequencies of the communication channel. However, the World Cup can significantly reduce the distortion of the transferred signal. For example, today the most developed system of communication is the telephone system, which recently, due to the spread of personal computers, began to be used for data transmission. For economic reasons, telephone systems used different methods of channel compaction and were built as multichannel systems that provide the ability to simultaneously transmit a large number of telephone conversations on one cable. The main band of frequencies of the transmitted voice spectrum was optimized according to the articulation index 0.7, which corresponds to the level of word recognition of 85-90%. When using this criterion, the width of the strip is 3100 Hz. This band was located in the range of 300-3400 Hz. Due to the fact that the signal with such a band of frequencies is filtered by a real analog band filter, which has the final steepness of the frequency characteristic decline (has some bandwidth outside this band), as the estimated width of the **main band of the standard telephone channel** is taken frequency band of *4 kHz (protective band* Δf_z between the two adjacent channels at the same time is 900 Hz).

13.4.2. Features of digital communication channels

Currently, in communication systems simultaneously with analog modulation, more progressive impulse modulation methods are used, in particular *amplitude-pulse modulation* (APM). Pulse modulation methods allow to improve the energy characteristics of the process as a whole, because the duration of the pulse emitted may be small compared to the bearing period. To transmit an analog signal through communication channels by pulse modulation methods, *sampling* and *quantization* processes are used.

Resampling of the transmitting analog signal is the formation of a sequence of sampling (selective values) of the analog signal, taken with the *sampling rate* f_d. This frequency is selected on the basis of the condition that it is possible to restore the analog signal without distortion of the analog signal using the lower frequencies filter. For signals with a limited spectrum, which in principle can be attributed to the signal of a standard telephone channel, which has a cut frequency f_{cp}=4 кГц, The kotelnikov-Shenon theorem, or Kotelnikov-Naikvist, or Shenon, according to which f_d.=$2f_{cp}$. Then, for a standard telephone channel, the sampling rate is 8 kHz. Thus,

sampling (selective values) of the analog signal are formed with a period of sampling T_d = 125 мкс).

Impulse sample amplitude quanting is the process of determining for each sample its equivalent numerical (digital) value.

These two operations (sampling and quantization) determine the processes carried out during pulse code modulation (IMM) and ensure the transition from analog representation of the voice signal to digital.

IKM, known since 1938, but was first implemented only in 1962, allows you to create digital telephony systems that have the following advantages over analog telephony:

- eliminates significant signal attenuation and its change both during the session and from session to session;
- practically eliminated extraneous noise;
- improves voice legifulness and increases dynamic transmission range.

13.5. Digital communication system settings

Digital communication systems are described by a set of parameters divided into external and internal.

External parameters are set by a set of parameters *{y1, y2, …, yn}*, describing the digital communication system from the point of view of the customer or consumer.

Internal parameters are set by a set of parameters *{x1, x2, …, xn}* and describe the digital communication system from the developer's point of view. When designing digital communication systems, certain types of parameters are subject to certain restrictions that are formed based on the requirements of the technical specification or from the area of permissible values. Mathematically, these constraints can be set as:

$$y_i=a, \ y_k \leq b, \ y_s \geq c, d \leq y_p \leq e,...$$
$$x=g, \ x \leq h, \ x \geq k, l \leq x_p \leq m,...$$

$$(13.6)$$

The set of external parameters is divided into three main subsets of parameters: *information, technical and operational, technical and economic*.

Information parameters characterize the process of digital data transmission through the communication system. These parameters include correctness, speed, time and time of information transfer. The named parameters are determined by comparing the input parameters (c_{inp}) and output (c_{out}) signals (symbols). For example, the correctness of signal transmission is determined by the probability of the complete match of the adopted character with the transmitted, that is, $y_1=p(c_{вх}=c_{вых})$.

To account for the time delay in receiving information, enter the parameter $t_{зam}$, what is called the delay time. The delay in reception is determined by the interval of time between moments t_1 ($c_{вх}$) message by the source and moment of the t_2 ($c_{вы}$) registration of this message by the recipient. Then

$$y_2= t_{зад}= t_2(c_{вых})- t_1(c_{вх})..$$

$$(13.7)$$

Technical-operational parameters characterize the physical process of operation of the communication system. These include parameters such as average uptime, temperature range of operation, mechanical characteristics, etc..

Technical-economical parameters characterize the communication system in terms of both the full cost and the specific cost of communication and equipment. These parameters include cost, overall dimensions, weight. To estimate the cost of the system, as a rule, use the cost of transmitting 1 bit of information, which is fully determined by the cost per year for the communication system and consists of capital costs for the manufacture of equipment and its operation.

The internal parameters of the communication system include, for example, the characteristics of the element base, the characteristics of interference and the complexity of the system. Distinguish *algorithmic and structural complexity of the system*.

The *algorithmic complexity* of the system can be estimated by the number of logical and arithmetic operations and the amount of memory needed to ensure transformations.

The *structural complexity* of the system is determined by the number of basic components necessary to build a reliably functioning system. The complexity of the base node is considered equal to one. Basic can be considered nodes, the production of which was mastered by industry (for example, various kinds of integrated circuits).

External and *internal characteristics* of digital communication systems are associated with certain dependencies. In general, each of the external parameters of the system can be presented as a function of its internal parameters:

$$y_1 = f_i(x_1, x_2, \ldots, x_n), \quad i = 1, 2, \ldots \ . \tag{13.8}$$

This system of equations is called the equations of communication and sets the mathematical model of the projected digital communication system.

When evaluating the operation of the digital communication system, it is necessary, first of all, to take into account the accuracy of the transmission of messages, which determines the quality of transmission, the system provides at this speed of information transmission.

The most general indicator of digital communication is the information efficiency of η, which is defined as the ratio of the speed of information transmission to the bandwidth of the:

$$\eta = \frac{R}{C}, \tag{13.9}$$

where the bandwidth of the channel is understood as the maximum possible (limit) transmission speed. Informational effectiveness characterizes the degree of use of the channel. Note that indicators such as the cost of transmitting 1 bit of information and information efficiency are closely related.

14. FIBER OPTIC COMMUNICATION SYSTEMS [21-24]

14.1. Fiber optic communication line structure

Figure 14.1 shows the generalized structural diagram of the FOLC.

In fact, FOLC contains functional nodes inherent in any electrical communication systems. Moreover, when forming signals, in principle, it is possible to use various methods of coding and types of modulation used in the radio range. However, a number of features of the optical range and features of the element base, used under FOLC, imposes certain restrictions on the possibility of implementing fiber optic transmission systems and leads to technical solutions that differ from traditional communication technologies.
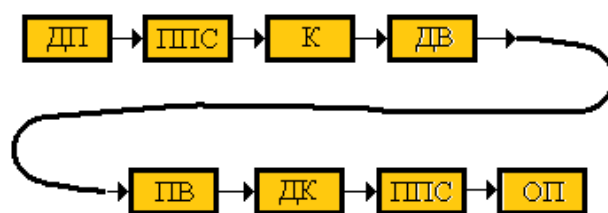
Переклад Fig. 14.1

GP – the source of the message; PPS – signal conversion device; KD – source coder; MP – transmission module; MT – receiving module; DC – channel decoder. OP - Message Recipient

14.2. Advantages of using optical fibers in communication systems

1. Wide bandwidth – due to the high frequency of carrying 1014 Hz, which provides a potential possibility of transmitting one optical fiber flow of information to several terabits per second. Large bandwidth is one of the most important advantages of optical fiber over copper or any other information transfer medium.

2. Low light attenuation in fiber. As you know, modern fibers have fading at the level of 0.2-0.3 dB per kilometer at a wavelength of 1.55 microns. Low attenuation and low variance allow you to mount sections of lines without relaying more than 100 km long.

3. Low noise in fiber optic cable allows you to increase bandwidth by using various modulation methods with a slight excess of information signal encoding.

4. High noise immunity. Since fiber is made of dielectric material, it is not sensitive to electromagnetic interference that may occur from nearby electrical cables and equipment. Multi-fiber optic cables also do not have cross-impact problems inherent in stranded copper cables.

5. Light weight and volume. Fiber optic cables have less weight and volume compared to copper cables designed for the same throughput. For example, a 900-pair telephone cable with a diameter of 75 mm on a metal base can be replaced by a single-fiber optical cable with a diameter (along with metal "armor"), less than 15 mm. Another example: 300 m single fiber cable weighs 2.5 kg, and the same length is similar to a coaxial cable – 32 kg.

6. High protection against unauthorized access. Since there is practically no field outside the optical cable and, as a result, the signal transmitted through the cable can only be "removed" by violating the integrity of the fiber. At the same time, monitoring systems (continuous control) of the optical communication line integrity (due to the high sensitivity of fiber to external influences) can instantly disable such a communication channel and send an alarm.

7. *Гальванічна розв'язка*. Ця перевага оптичного волокна випливає з його діелектричних властивостей. Волокно дозволяє уникнути так званих «земельних» петель, що виникають, коли два мережевих пристрої неізольованої обчислювальної мережі, пов'язані мідним кабелем, мають заземлення в різних точках будови, наприклад на різних поверхах. В електричній мережі це може привести до виникнення великої різниці потенціалів, яка, в свою чергу, може пошкодити мережеве обладнання та бути небезпечним для персоналу. При використанні волоконно-оптичного кабелю таких проблем просто не існує.

8. *Explosion and fire safety*. Due to the absence of spark formation, optical fiber increases the safety of communication networks in the maintenance of systems (structures) in which technological processes with an increased risk are used.

9. *Economy*. Fiber is made of quartz, the basis of which is silicon dioxide, is widespread in nature and which is, unlike copper, a relatively inexpensive material. Today, the cost of optical fiber and copper steam correlate as 2:5. At the same time, fiber optic cable compared to a copper cable allows you to transmit signals without relaying over much longer distances, which allows you to sharply reduce the number of repeaters on long communication lines.

10. *Long service life*. Over time, fiber degrades. This means that the damping in the laid cable increases. However, today the life of the OC is approximately 25 years. During this time, several generations of standards of receiving and transmitter systems may change.

11. *Possibility of power supply*. Fiber itself is not intended for electric current. However, you can use mixed cables, where several copper conductors are laid on a row with optical fibers.

Naturally, fiber optic systems also have disadvantages, which mainly include the high cost of precision mounting equipment, laser radiation sources and the requirements for special protection of optical fiber.

15. DESIGN (PLANNING) OF FIBER OPTIC COMMUNICATION LINE [21]

The content of the work on the design (planning) of the communication line is to determine the means of communication, the most profitable in cost and efficiency in building a line of communication and transmitting messages from the source of messages to their recipient. The designer should take into account the advantages and limitations of the functioning of various components of communication lines and design the physical configuration of the system taking into account the specific conditions for the transmission of messages.

When solving the first of these tasks regarding the quality of the digital signal, first of all, factors such as the width of the system bandwidth and the level of bitmap errors (BER) should be taken into account.

The next step is to determine the minimum optical power of the optical signal, necessary for a confident reception of the signal on the side of the receiver. This information can be obtained from the technical documentation provided by the manufacturers of each component.

15.1. ANALYSIS of VOLZ bandwidth

The productivity of THE FAA primarily depends on the bandwidth and attenuation of the line.

Lans usually require bands from 20 to 600 MHz/km, so multimode fibers can be used at such frequencies. Long-distance signal transmission systems require a fiber strip of about 100,000 MHz/km, which can only be provided by single-mode fibers.

Reducing the optical signal in the working band of frequencies by 3 dB means the loss of half of the initial power.

Conversion in the communication system of the "electric" *strip ΔF_e* into optical ΔF_o or the implementation of such a transformation between any components of it, such as fiber, receiver or transmitter is determined by the formula:

$$\Delta F_o = 1.41 \Delta F_e. \tag{15.1}$$

Quite often, the company producing receivers or transmitters, brings in the passport to these devices the value of the time of increase of the working impulse. Electric strip ΔF_i (Mhz) for such a VOLC component is mapped over time t (ns) the increase in momentum from 0.1 to 0.9 from its peak value as

$$\Delta F_i = 350/t. \tag{15.2}$$

(ns) the increase in momentum from 0.1 to 0.9 from its peak value as:

$$\frac{1}{\Delta F^2} = \frac{1}{\Delta F_R^2} + \frac{1}{\Delta F_C^2} + \frac{1}{\Delta F_T^2}, , \tag{15.3}$$

where ΔF_R, ΔF_C, ΔF_T − electrical strips of the receiver, cable and transmitter, respectively.

For digital communication systems, bandwidth sizes will depend on the R data rate (bit/s) and the encoding format according to the formula:

$$\Delta F = R/K, \tag{15.4}$$

where $K = 1.4$ for a format without returning to zero (NRZ) i $K = 1.0$ for return-to-zero format (RZ).

The width of the system strip is limited by the frequency band components with the narrowest band of frequencies in the line. For example, when using fiber with a fairly wide bandwidth, the operating bandwidth of the system may be limited to terminal equipment. Therefore, when choosing terminal equipment, special attention should be paid to the choice of receiver – it must be chosen with a strip of this level or one that exceeds the width of the system strip. The transmitter and fiber should have a strip 1.5-2 times wider than the width of the receiver strip.

Communication systems tend to be more economical at high speeds of data transmission. Therefore, the margin along the width of the strip makes it possible to improve the throughput of the system. When connecting cables sequentially with a total length greater than 1 km, it is necessary to accurately evaluate the optical strip (MHz/km) of optical fibers, since approximately the ratio between the full width of the cable strip ΔF_C and the width of the strip of fiber length of 1 km ΔF_f this:

$$\Delta F_f = \Delta F_C L^x, \tag{15.5}$$

where L – cable length in kilometers, x=1.0 for segments 1 km long or less, x = 0.75 for segments longer than 1 km.

15.2. Losses and constraints in communication lines

As noted above, the design (planning) of communication lines involves solving the following two tasks:

- Calculation of optical power losses occurring between the light source and the photodector;

Determination of limitations associated with bandwidth transmitter, fiber, receiver and affect the ability of the system to transmit signal. Optical power losses are determined, as is known, in dB/km:

$$\partial Б = 10\lg\left(\frac{P_0}{P_1}\right). \tag{15.6}$$

Losses of 3 dB correspond to the loss of half the power, 10 dB – only 0.1 power reaches the receiver. As a rule, FSOs are able to function at reception of 0.001 power from the source located at the other end of the line (that is, power losses are about 30 dB).

Power loss during transmission:

- when introducing light into the fiber (loss of injection);
- attenuation in optical fiber;
- at connection points by connectors;
- on non-negative joints: at welded joints, in couplings. The line usually consists of several parts, the length is equal to the building length (~ 6 km).

The amount of losses in each individual component between the transmitter and the receiver is the budget of the power of the optical line (Fig. 15.1, Table 15.1).
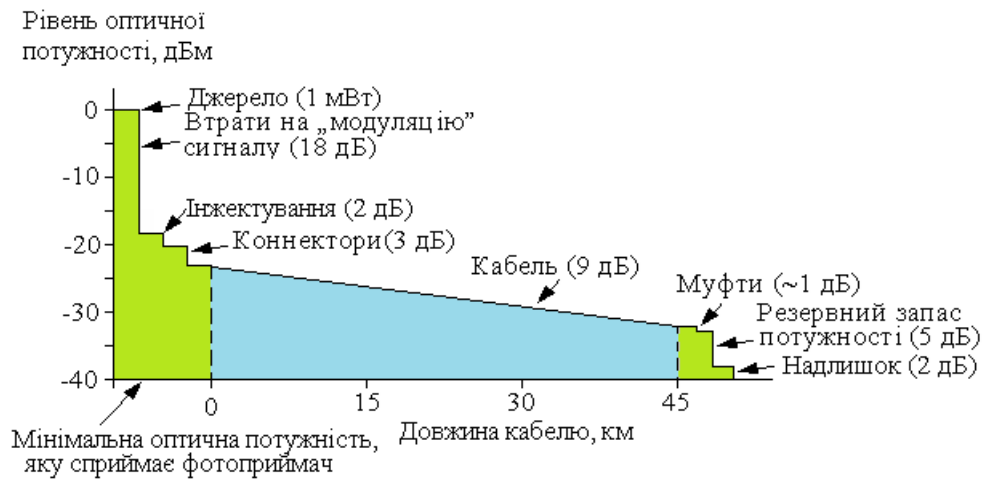
Fig. 15.1

Note that part of the power should be reserved for the creation of appropriate signal/noise vinning (loss per modulation) ~ 18 dB.

Table 15.1

Power characteristics	Real power	Optical power level
Minimum optical power required for photo receiver operation	0.1 μW	-40 dBm
Optical power at source output	1 Mw	0 dBm
Full working budget		40 dB
The ratio of signature/voltage noise required for FP -36 dB robot. Equivalent optical power ratio		18 dB
Residual optical power of the line		22 dB
Power loss in line: Cable 9 dB Connectors 3 dB Non-detaable connections 1 dB Engineering 2 dB		15 dB
Power reserve		5 dB
Budget Balance		2 dB

As a rule, for THE COMPONENTS, you can specify the exact loss values, so manufacturers usually lead the ranges of their values or the values of the largest losses. In addition, it is necessary to take into account the dependence of the corresponding parameters of the COMPONENTS component on the temperature. It is also necessary to take into account a certain power reserve for future repairs, the installation of couplings in the system, as well as a reserve for the time degradation of the radiation source. For example, repair and aging of the emitter is given in most cases from 3 to 6 dB.

Losses in the introduction of radiation in fiber. The level of optical power injected into fiber depends on the physical parameters of the source and fiber. Obviously, the larger the diameter of the fiber, the greater the fiber's ability to receive light. However, it should be remembered that fibers with a large core diameter have some limitations on bandwidth. Another characteristic responsible for the effectiveness of radiation input is known to be the numerical aperture of NA.

To take into account the influence of NA and the diameter of the core, a characteristic called optical absorption coefficient is introduced, which can be considered as a measure of the efficiency of fiber input and transmission of optical power.

Table 15.2 shows the typical optical absorption coefficient values for different NA and nucleus diameters.

Table 15.2

Core diameter	Numerical aperture	Optical absorption coefficient	
		Relative[*]	Ratio in dB
200	0.27	3.5	+5.4
100	0.29	1.0	+0.0
62.5	0.275	0.35	-4.54
50	0.2	0.12	-9.25
[*]Value normalized relative to short fiber segment with 100 μm core			

16. SYSTEMS OF INFORMATION TRANSMISSION [21-24]

In modern networks and communication lines among various types of services, the main type is telephone services. As you know, the telephone channel occupies a strip of about 4 kHz. However, in analog form, it is transmitted only from the subscriber to the PBX and back. Along the lines connecting PBX urban, zone, main channels messages (ideally) transmitted digitally. After conversion thanks to IMM, the analog signal will turn into a stream of bits at a transmission speed of 64 kbps..

Formation of group digital signals intended for transmission over the communication line is carried out by linear coding. To do this, use a number of binary codes, the main of which are: 1b2b, ADI, AMI, B3Z9, B6Z9, B6ZS, B8ZS, CMI, HDB2, HDB3, mBnB, NRZ, RZ, Miller code.

Today the most commonly used codes in electrical communication systems: HDB3 and AMI.

In accordance with the norms of ITU-T and GOST, 30 (main) DS0 channels are transmitted on such communication lines in European countries and Latin American countries. In addition, two additional signaling and control channels are additionally transmitted in the group linear flow. Thus, the number of channels transmitted is 32. The product of the number of channels (32) at the DS0 channel speed (64 kbps) gives a group digital stream transfer rate equal to 2048 kbps (2.048 Mbps). In the USA and Canada, a similar channel has a speed of +1544 kbps (24 DS0 channels). If the initial digital channel (64 kbps) is named (OCC), then the group channel at 2048 (1544) kbps is called the primary digital channel (PCC or DS1).

Obviously, the number of telephone channels, which is 30 (24), especially when transferring zoned, and even more so the main lines of communication is not enough. Therefore, international agreements have found that the transmission speed of the PCC and each channel of this order can be increased by multiplexing at a multiple of 4. If we use, for example, the method of time multiplexing with a new higher (4m times) clock speed, we get a number of speeds of information transmission: 2048, 8448, 139264, 564992 kbit/s. This is because additional bits are introduced to identify groups, channels (or blocks, packages) that violate the above multiplicity. However, by the number of major digital channels, the multiplicity remains clear: 30, 120, 480, 1920, 7680. Listed speeds create a hierarchical series or digital hierarchy. For European and Latin American countries, each digital hierarchy has its own designation:

- primary digital hierarchy - PDH (2048 kbps) - E1;
- secondary digital hierarchy – SDH (8448 кбіт/с) - E2;
- third digital hierarchy – TDH (34368 кбіт/с) - E3;
- fourth digital hierarchy – FDH (139264 кбіт/с) - E4;
- fifth digital hierarchy – FDH (564992 кбіт/с) - E5.

Note that in the listed transmission speed hierarchies, the clock frequencies of neighboring levels, and even more distant ones, do not have to be synchronized. In addition, the frequencies of multiplexed channels may not match. However, they are very close in value and can be included in the sync channel capture bar, that is, they are "almost" synchronous. Such systems are called plesiochronous (almost) digital

transmission systems, and the corresponding digital hierarchy is a plesiochronous digital hierarchy (PDH).

The above-mentioned TIC systems were originally developed for communication lines in which either an electric (metal) coaxial cable or radio relay lines were the distribution environment of group signals. For such transmission lines, appropriate equipment for E1-E4 hierarchies was developed. For such lines due to a small bandwidth and a large attenuation in cables, the length of the regeneration area for E1-E2 did not exceed 5 km, and for E4 – 1.5-2 km. Such lines were very expensive and did not become widespread, let alone E5 communication lines, where the length of the regeneration site is less than 1.5 km. It should be added that this is not the only reason why the lines of the E4-E5 hierarchy have not become widespread. Another equally important reason is associated with the features of the plesiohronous transmission system. The lack of rigid synchronization of clock speeds of different levels E1-E5, as well as the addition or selection of inserts (staffing) in the form of additional bits in the appropriate code for leveling code combinations leads to the impossibility of selecting channel DS0 or DS1 from the stream at any intermediate point of the zone, or the main line , higher level (for example, level E3 or E4) without the complete demultiplexation of the group flow. If for level E2 this task is simple and the cost of performing this task with equipment increases insignificantly, then for the level of E3 the cost of similar devices increases significantly, for E4-E5 levels due to the need for a sharp increase in the speed of electronic devices, this cost increases to exorbitant values.

Thus, the use of optical fiber as a media, and light as the basis of the information signal made it possible to significantly increase the length of regeneration areas. For E1-E2, this length is up to 200 km, for E3-E4 – about 100 km. Due to this, the cost of plesiochronous transmission systems has decreased significantly.

Naturally, when designing (planning) systems with FOCIs, it is necessary to take into account the peculiarities arising from the specificity of physical processes occurring in fiber. One of these features is related to the choice of linear binary code.

Note that the code, as a rule, HDB3 entering the input of electric equipment of the FOLC, is.

Figure 16.1 shows a generalized structural diagram of a single-race (i.e. without intermediate points) FOLC with one-way signal transmission.
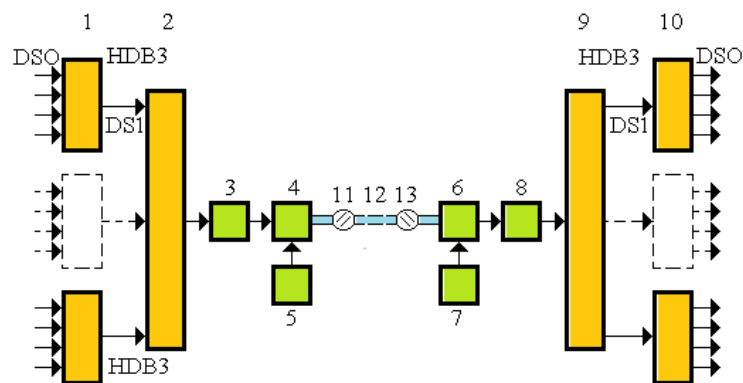
Fig. 16.1. Generalized structural diagram of single-run FOLC

1 – electronic multiplexers of the main DS0 level information flows into the DS1 level information flow in the HDB3 code; 2 – electronic multiplexer and HDB3 code converter into linear code; 3 – unit of coordination (pumping) of the emiment 4 with the output of the code conversion device 2; 4 – emiator; 5 – stabilization unit of optical power and radiator temperature; 6 – FP; 7 – source of electrical shear voltage for FP; 8 – broadband electric signal amplifier; 9 – linear code converter into DS1 level codes and demultiplexer; 10 – demultiplexers of signals in the DS1 level code in DS0 level signals; 11,13 – optical parts; 12 – optical cable

The most common line codes (рис. 16.2) [22]

I. **NRZ** code (Non Return to Zero, Fig. 16.2 a)

Code creation is very simple "1" is encoded as "1", "0" is encoded as "0". The NRZ code can be used in SSRS, but is practically not used in electrical communication lines.

Features and disadvantages:

• Permanent component, due to the probability of the appearance of "1". Due to this, in addition to the transmission of signals, the supply voltage is supplied. At the output of the chain is divided with a transformer.

Fig. 16.2

• Possible synchronization failure for "0" with a large number of such continuously "0" (the line is silent). Similarly, synchronization failure at level "1" is possible.

II. **mBnB** code with redundancy.

Type code 1V2B (RZ - Return to Zero, Fig. 16.2 b). "1" is encoded by the sequence "10", "0" is encoded using the sequence "00". The code can be used in SSOs at relatively low transmission speeds (up to 140 Mbps).

Features and disadvantages:

1. A synchronization failure at the level "1" is removed.

2. Twice the transfer speed requirements.

III. **Code** HDB3 (High Density Bipolar of order 3, Fig. 16.2 c).

The HDB3 code is one of the most used in leading communication lines with a transmission speed of up to 34 Mbps. Units of binary sequence are transmitted by impulses, the polarity of which changes to the opposite when each subsequent unit (or zero) is transferred, that is, units are transmitted by alternating "+1", "-1". Zero is passed to zero. However, when passing a sequence from "0", the number of which more than 3 is transmitted a single pulse of the same polarity as the previous unit. As a result:

1. A synchronization failure at both level "0" and level "1" is removed.

2. This code does not contain a permanent ingredient. Thus, the average signal strength is close to zero. that meets the requirements put forward when selecting a code for an electric transmission line.

3. However, unlike an electrical cable through which it is possible to transmit current pulses of both positive and negative polarity, optical impulses that have no negative values can be transmitted through optical fiber. Therefore, such a code is butt code for WSPS electrical equipment and cannot be directly used in SSRS, due to its bipolarity.

IV. when transmitting bipolar code HDB3 through optical fiber with the help of pulses of optical radiation at one wavelength, these codes are converted into unipolar with a constant component. The sequence of pulses of the HDB3 code type can be realized when raising the zero signal to a certain level (Fig. 16.2 d).

The use of such converted code in THE NOP lines is impractical for the following reasons:

1. The power of neighboring pulses of type "11" is twice less than the maximum power emitted by an optical source. This is equivalent to two times the loss of power (3 dB);

2. The presence of a permanent component requires stabilization of the working point on the watt-amperes of the laser, which complicates the design of the transmitter optical module;

3. Value dependency P_0 from statistics of code modulations leads to the emergence of a parasitic variable component, which as a result also reduces the energy potential of the line;

4. The presence of a constant component is equivalent to some background light. As a result, additional noise appears in the photo receiver when receiving such a signal. Thus, the signal/noise ratio is reduced; different levels of adjacent pulses lead to different signal-noise ratios in adjacent time slots.

V. One solution to this problem is the use for coding radiation of two wavelengths (Fig. 16.2 e). Positive pulses are encoded as pulses with wavelengths λ_1, negative – like pulses with wavelengths λ_2. This method of transmitting pulses of opposite polarity can be called wave coding.

VI. In modern VOLZ, designed to transmit information for TIC E1-E3, use the conversion of HDB3 code to another, more profitable for use in optical systems. The most commonly used are linear SMEs (Coded Mark Inversion) (Fig. 16.2 f), or AMI (Alternate Mark Inversion) (Fig. 16.2 g), optimized for the optical tract.

The disadvantage is the same as in the previous ones – the use of such codes requires a double increase in the clock speed and frequency band.

In higher speed systems of type TSI E4 use codes 5V6V, 10B1P1R, etc.

VII. In local and on-board computing systems, the so-called Manchester codes - bi-impulsive BI-L and biphaz bi-M - are quite common. In the biphal code (Fig. 16.2 and) when transmitting "1", the sequence of alternation of pulses "0" and "1" is preserved, while during the transmission "0" the order of their alternation changes to reverse.

16.1. Communication systems of the plesiochronous digital hierarchy [21-24]
16.1.1. Communication systems for communication lines of primary digital hierarchy E1

Data transmission systems of the digital hierarchy E1 are, as a rule, systems of local, object communication, allocation from zonal or main systems to small settlements or objects located in the line area at a considerable distance (100-150 km).

"Domestic" equipment – equipment developed in the former Soviet Union, which are currently manufactured in Russia and Ukraine (partially or completely).

One of the representatives of such equipment is the linear optical terminal LOT-1C1, the structural diagram of which is shown in Figure 16.3.
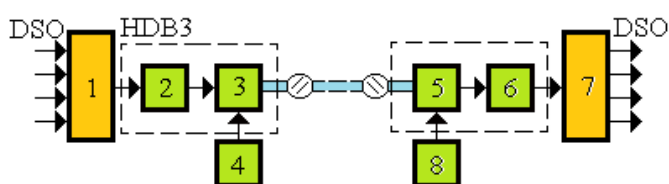
Fig. 16.3. Structural diagram of the linear optical terminal LOT-1C1:

1,7 – equipment of group channel formation "CEDAR"; 2 – block of digital stream conversion of DS1 – HDB3 format into an electrical signal in biphaceous code or CM1; 3 – optical transmission module; 4 – control unit of parameters of the transmitted and receiving modules; 5 – receiving optical module; 6 – block of line code conversion to HDB3 code

A special feature of this equipment is the presence of a control unit 4, which allows you to control the:

- optical output power at the output of the optical jack (µW);
- input optical power coming to the photo receiver (NWT);
- laser pumping current (mA);
- supply voltage of the entire terminal (60 V).

The control is carried out visually with the help of a digital board placed on the front of unit 4.

LOT-1C1 has the characteristics shown in Table 16.1.

Table 16.1

Characteristic	Magnitude
Working wavelength	1.3 або 1.55 мкм
Optical power level at the output of the optical module	0 ± 1 дБм
Minimum level of optical signal at the input of the optic receiving module at the error coefficient $K_{пом} \leq 10^{-9}$	$-5\,6$ дБм
Transfer rate	2048 кбіт/с
Line code	CM1
Code at electrical joints	HDB3 (або AMI)
Supply voltage	-60 ± 12 В

The LOT-2C optical terminal is also manufactured, designed to transmit two digital streams at speeds of 2048 kbps at one optical fiber at two wavelengths of 1.3 and 1.55 microns. Optical cable in LOT-1C1 and LOT-2C is connected by optical cords of "packard" type using FC optical connectors.

JSC NPP Rotek (Russia) manufactures equipment T-31, designed to transmit streams of type DS1 at a speed of 2048 kbps..

Table 16.2

Characteristic	Magnitude
Working wavelength	1.3 microns
Carriers	Monomode fiber
Minimum level of optical signal at the input of the optologic receiving module at the error coefficient $K_{пом} \leq 10^{-9}$	−42 dBm
Transfer rate	2048 kbps
Optical connection type	FC
Code at electrical joints	Satisfied with the recom. ITU-T G. 703
Supply voltage The first option (constant voltage) Second cooker (variable voltage)	-43 – −72 В, or −21 – −27 В 220В $\pm$ 10 %, 50 $\pm$ 5 %

Equipment of LOT and T-31 type is assembled on a modern element base using modern electronic and quantum optical elements.

16.1.2. Communication systems for communication lines of the secondary digital hierarchy E2

In the Soviet Union, equipment sonata-2 was developed and manufactured, designed for use in urban networks as lines connecting communication nodes. This equipment allows one pair of optical fibers (multimode) to transmit round-trip 120 telephone channels in digital format at a speed of 8448 kbps.

Figure 16.4 presents a generalized structural diagram of the communication system "Sonata-2"».

The unit of analog-digital equipment 1 consists of 4 cells, each of which takes four primary DS0 digital streams (64 kbit/s, 30 telephone channels) and forms one information flow in binary DS1-HDB3 level code. Then four such streams enter the input of multiplexer 2, which forms the DS2 level stream in the same HDB3 code. Then this stream enters solst-0-2. In Unit 3 (SOLST-0-2), it enters the PC cell, the task of which is to convert the DS2 binary digital stream with the CODE HDB3 to linear code SM1. From the PC's output, an electrical signal in the CM1 code is fed to the input of the transmitter optical module (POM), which converts it into an optical digital stream in the same CM1 code. The optical flux is injected into the optical cable using the optical connection. The solst-0-2 unit, in addition to these cells, also includes devices that perform the following functions: control of linear rack equipment, control of linear tract, service communication.

It should be added that for connecting lines of city telephone networks, in addition to Sonata-2 equipment, similar equipment of IKM-120-5 was produced, which provides transmission of 120 channels at a speed of 8448 kbit/s via optical cable. The equipment was produced in two variants of KT-26 with a working wavelength of 0.85 microns and CTT-24 with a working wavelength of 1.3 microns.

Currently, these systems are outdated, although they are still in use.

Today, modern transmission systems for single-mode fiber signals of the secondary plesiochronic hierarchy E2 are manufactured in Russia: OLP-025 (Morion, Perm) and T-41 (JSC NPP Rotek).
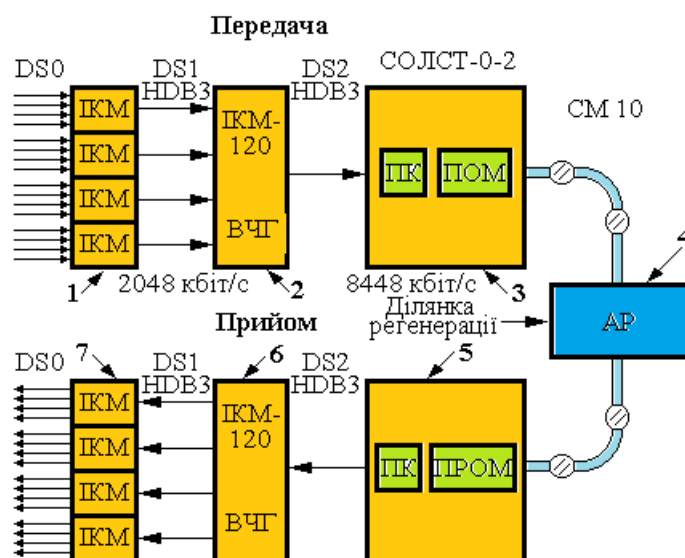
Переклад Fig. 16.4. Structural diagram of the communication system "Sonata-2"»: 1,7 – blocks of analog-digital equipment IKM-30; 2 – multiplexer, or block of secondary time grouping (UGS); 6 – demultiplexer; 3,5 – final equipment SOLST-0-2; 4 – stable intermediate linear light-water tract

16.1.3. Communication systems for communication lines of the third digital hierarchy E3

The company JSC NPP Rotek (Moscow) produces equipment T-51 and T-316. The T-51 is designed to transmit over a multimode or single-mode cable digital stream E3. The T-316 model allows the same cable to transmit from 1 to 16 DS1 streams (2.048 Mbps).

On the river 16.5 the structural scheme of the T-316 communication system is presented. The equipment of the T-316 model contains the following blocks: 4 PPS multiplexer, each of which of the four input streams DS1 (E1) forms one stream E2 per transmission and performs reverse conversion at reception. Then 4 streams of E2 enter the entrances of OLO units.
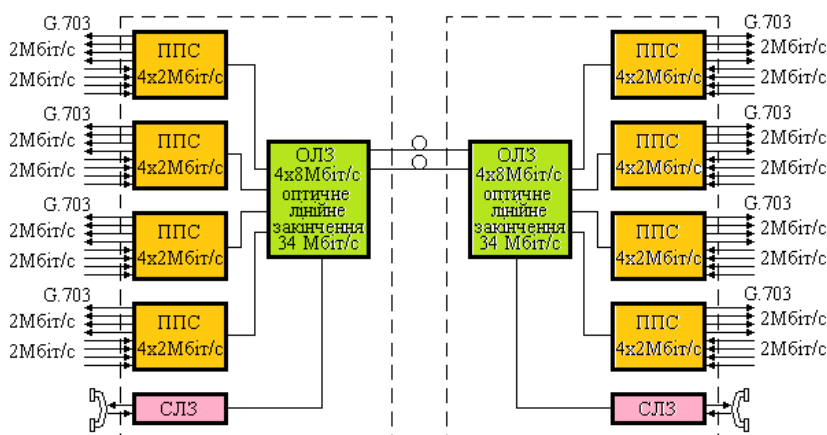
Fig. 16.5. Structural diagram
Communication systems T-316:

MB – multiplexer board 4x2 Mbps; OLO – multiplexer board 4x8 Mbps and optical linear ending 34 Mbps; SLS – service communication fee

This unit consists of a multiplexer that forms from four streams E2 one digital stream of 34 Mbps and an optical linear ending device that performs on transmission, the conversion of the electrical signal of the digital stream E3 in the HDB3 code into linear code. After that, the electrical signal will turn into an optical signal. At the reception, the corresponding blocks perform reverse operations. SLS unit is designed for organization of service communication.

JSC NPP Rotek, in addition to the model T-316, produces version T-316 (21E1). This equipment is designed to transmit digital binary flow through FOCPs at a speed of 51.84 Mbps. Systems with a transmission speed of 51.84 Mbps are designated STM0. The equipment includes a line status monitoring system, two telephone communication channels and an RS-232 channel for monitoring and managing remote equipment (it is possible to control the VOS through the ETHERNET interface).

In addition to the listed equipment, OJSC "Morion" produces tertiary grouping with optical interfaces and service channels OTLS-31. This equipment has the same purpose as the equipment of JSC NPP Rotek, namely: for the creation of inter-station communication, as well as for intra-zone and inter-district communication over optical cable. The equipment allows you to combine 16 digital
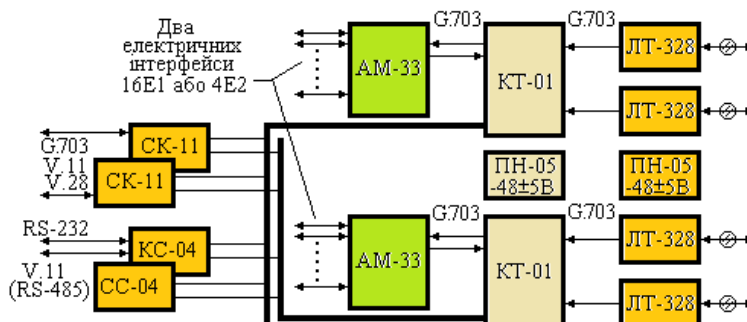
streams E1 or 4 stream E2 into one digital stream E3.

The structural diagram of OLTS-31 is shown in Figure 16.6. On each side of the communication line, the equipment in the linear optical tract has two boards of the optical interface LT (transmission and reception) with an electrical interface in accordance with G.703

ITU-T and optical interface (FC connector) with linear NRZ code with scrambling, due to which the transmission speed over the line increases to 35.84 Mbps. Electric inputs (interfaces) of CT boards through a CT board (reservation device) are connected to the grouping board AM, which is a multiplexer during transmission and demultiplexer when receiving 16E1 or 4E2.

The CT board (reservation device) is designed to insert (staff) or allocate additional channels into the linear signal (or linear signal) by increasing the standard tertiary speed of 34.368 Mbps to 35.84 Mbps.

IC, COP and SS boards interact with the CT device through two 2M tires using the above additional channels.

The COP unit is equipped with RS-232 and RS-485 interfaces, the first of which is designed to connect a personal computer to monitor the condition of the unit and the corresponding remote units. In addition, additional channels are used to organize business communication (CZ block).

In recent years, foreign equipment of the plesiochronous digital hierarchy, especially for levels E2, E3 and E4, has been widely used in communication networks. Compact multiplex and linear optical equipment PLE2-140 of PHILIPS is being introduced quite quickly. This equipment has a user-oriented configuration of the structural diagram with a small number of blocks. In addition to the main modules of multiplexing, the transformation of butt codes into linear and linear optical modules, the equipment includes devices that perform the functions of network control and management without interruption of communication, service communication devices and several service channels with different transmission speeds. The equipment allows transmission over the optical cable of information flows at a speed of 2.048 Mbps, 34.368 Mbps and 140 Mbps. The equipment also provides linear optical endings with low-power or powerful semiconductor lasers in transmitting modules, highly efficient photodiodes in receiving modules connected by FC/PC optical connectors. PHILIPS also manufactures LS34s/CXOF equipment, which is a modular system for transmission speeds of 34.368 Mbps for symmetrical and optical cables. This equipment is designed to transmit signals of the tertiary digital hierarchy E3 and can be used for local and mainline networks. The equipment includes devices for localization and analysis of damage using a personal computer, as well as a service communication unit.

Table 16.3

	Type of equipment					
	T-316	T-316 21E1	ОТЛІС-31	PLE2-140	LS34S/140	STARMUX34F
Pomy-lok coefficient at the output of the maximal length tract	10^{-8}	10^{-8}	10^{-10}	10^{-10}	10^{-10}	10^{-10}

Similar in purpose and technical characteristics of the equipment is manufactured by LGIC (South Korea) – the final device OFRZ STARMUX-34F. This equipment allows transmitting optical information flows via optical cable at a speed of 8.448 Mbps or 34.368 Mbps..

The characteristics of the systems in question are very similar, but there are significant differences, for example, by the error coefficient at the output of the tract of the maximum length.

16.1.4. Communication systems of the digital plesiochronous hierarchy E4

To transmit the information flow of the digital plesiochronous hierarchy E4 in the USSR, equipment "Sopka-4" was produced. More modern STM-1 equipment is produced by OAO "Morion" for transmission of the same number of channels (1920) over optical fiber at a speed of 155.52 Mbps.

Among the foreign companies should be called PHILIPS, which was mentioned in the description of the equipment level E3. This is a variant of the same equipment PLE2-140, designed to transmit information at a speed of 140 Mbps on a single-mode fiber.

16.2. Systems and equipment of synchronous digital hierarchy [21-24] 16.2.1. Synchronous digital hierarchy and networks

The disadvantages of plesiochronous transmission systems and progress in fiber optic systems technologies, which have in comparison with electric cable systems almost unlimited bandwidth and other advantages of SSRIs, stimulated the development and implementation of new digital information transmission systems. This was also facilitated by the urgency of the problem of creating a global integrated information network. These problems could not be solved on the basis of the transmission systems of the plesiochronous hierarchy (PTS or PDH). Therefore, in February 1988, at a meeting of the ICCT Commission (now ITU-T) in South Korea (Seoul), an agreement was signed to adopt a new standard of the Synchronous Digital Hierarchy (SDH) and a single global optical network. This standard, agreed and adopted in Melbourne (Australia) in November 1988 on the basis of SDH in different countries were developed transmission systems. In the USA and Canada, this is the SONET system (Synchronous Optical Network), in Europe – SDH (Synchronous Digital Hierarchy). When adopting a new digital communication standard – SDH – one of the requirements for the new system was to ensure compatibility with PDH systems. This was primarily related to the digital stream of the E4 PDH level (140 Mbps). To solve this problem, redundancy in the form of

additional bits was introduced into the digital stream E4. As a result, the transfer rate of the new level increased to 155.52 Mbps. Taking into account the compatibility requirements of PDH SDH systems, in the UNITED States and Canada it was decided to convert the American PDH standard for a speed of 44.736 Mbps at a speed of 51.84 Mbps (this is the first SDH level for the United States). Due to this, by multiplexing such a stream with odds of 3, compatibility with the European transport module STM-1 (51.84x3=155.52) is achieved. The new American synchronous system was called SONET/SDH. As a result of international agreements, transmission speeds were established in the form of synchronous digital hierarchy (SDH), regulated by the recommendations of ITU-T (MCCT) – G.707, signal structure in the interface of the network node – G.708, the structure of synchronous grouping – G.709. Thus, such gradation of esths for the hierarchy of synchronous signals was adopted:

- STM-1 – 155.52 Mbps;
- STM-4 – 622.08 Mbps;
- STM-16 – 2488.32 Mbps (2.488 Gbps);
- STM-64 – 9.953 Gbps;
- у перспективі STM-256 – 39813.12 Mbps (39.813 Gbps);

Note that with the exception of STM-1, STM-4, STM-16, etc. speed is only used in fiber optic transmission systems.

Unlike plesiochronous networks in the synchronous digital hierarchy use a central reference generator of synchronous frequency (timer). As a result, in SDH, the average frequency of all local set generators is synchronous with accuracy not worse10^{-9}. Hard synchronization at all levels of SDH allows you to enter identification bits, which allows you to get a number of advantages of synchronous networks. The main advantages of synchronous networks are as follows::

1. The ability to allocate from the general group stream of a high level of the hierarchy of streams of a lower level up to the streams E1 without complete demultiplexation (or, conversely, the introduction of such a stream in the group stream);

2. Simplification of the overall structural diagram of SDH equipment due to the fact that all I/O functions are performed by one multiplexer, including it can output (enter) the digital E1 RYDH stream from the STM-1 stream (frame);

3. The ability to output (or enter) digital streams of any level from a higher-level group stream allows you to quickly switch digital tracts in networks, make them more flexible in terms of their configuration;

4. The signal rate at the junctions of network nodes coincides with SDH systems with linear speeds, so that there is no need to use an additional buttcode converter in linear.

The flexibility of SDH networks, their use in cooperation with fiber optic systems with a very large bandwidth width and high speed of quantum-electronic modules, allows automatic switching of digital streams, as well as a computer remote network from one center. In this case, the process of reconfiuging the network takes about one few seconds.

The above advantages of SDH-based SDH systems allow optimal use of channel capacity, prompt switching of digital streams and backup lines.

16.2.2. Main signals SONET and SDH

Basic transfer rate – STS-1 – 51.84 Mbps – synchronous transport signal level 1. Further levels of STS-N signals are formed as a result of byte-interliving, N STS-1 frames by simple multiplexing form a STS-N signal, without additional headings. As a result, the transmission rate of such a signal is Nx51.84 Mbps.

Similarly, higher-level signals are generated for SDH systems. Basic transfer rate - synchronous transport module STM-1 – 155.52 Mbps. Accordingly, the transfer rate of the STM-N transport module is Nx155.52 Mbps. To date, only STM-1, STM-4, STM-16, STM-64 and STM-256 are defined by ITU-T standards.

In both SONET and SDH, frame transfer speeds are 8000 frames/s, which corresponds to the repetition period of 125 ics frames.

Additional 1. The STS-3 transfer rate corresponds to the STM-1 transmission speed.

Additional 2. The difference between SONET and SDH lies not only in the basic transmission speeds, but also in the nature of using headers.

Additional 3. SONET – synchronous optical network does not mean that only optical channels can be used. For example, radio relay communication channels may be used.

16.2.3. Structure of synchronous signals

SONET and SDH technologies are based on synchronous signal, which consists of 8-bit fields – bytes organized into the frame structure.

The frame can be represented as a matrix of N rows and M columns, where each cell of the matrix contains one byte. The upper-left corner of the corresponding frame matrix contains an identification marker that points to the beginning of the frame.

16.2.3.1. SONET

Since the upper levels of signals are formed as a simple animation of the basic signals STS-1 carefully consider the structure of the frame of this signal (see Figure 16.7).
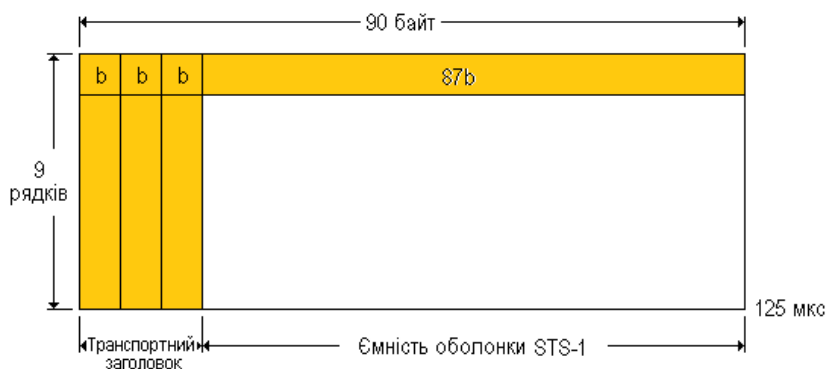
Переклад Fig. 16.7

The STS-1 signal frame is the main module and sonet structural unit. It is transmitted as a sequence of 810 bytes (6480 bits), which contain bytes of different headings and a simultaneous shell capacity that transports the payload. The frame

can be represented as a matrix of dimensions 9x90. If we take into account the frequency of repetition of the 125 cc (8000 fps) frame, we have that the STS-1 transfer rate is 51.84 Mbps. 9 of them – sectional header, 18 – linear header.

Expanding the frame is ordinal.

The STS-1 Synchronous Payload Shell (SPE) occupies the entire STS-1 payload. SPE consists of 783 bytes and can be depicted as a 9x87 matrix. 1 column – route or tract header (POH) contains 9 bytes. In SPE, the 30th and 59th columns are not used for useful loads, but are used for fixed column fillers.

16.2.3.2. Higher-level signal frames
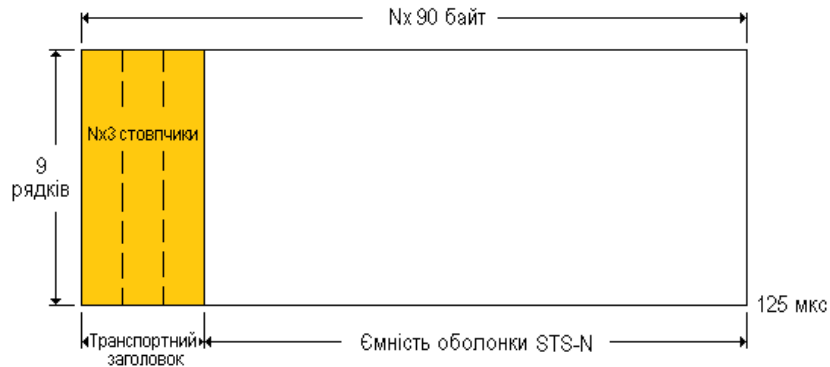
The STC-N frame is formed by byte-interliving modules STS-1 and STS-M (3<=M<=N). Frame structure is shown in Figure 16.8.

Переклад Fig. 16.8

16.2.3.3. SDH frame structure

The STM standard transport module is an information structure used to maintain sectional connections in the SDH network. The module consists of a useful load and

sectional header (SOH), which are organized in the form of a repeating frame every 125 ics. Basic STM - STM-1 (155.52 Mbps). Modules of higher levels N, formed at speeds Nx155.52 Mbps. To date, STM tanks are defined only for N=1,4,16,64 and 256.

Переклад Fig. 16.8

Figure 16.8 shows the structure of the frame module STM-1.
AU - Administrative Module, RSOH, MSOH - Sectional Headers

16.2.4. Equipment STSI (SDH)

In the development of STSI equipment, mandatory compatibility was provided only for speeds, but also joints (interfaces), which are absent in the equipment of the UM. In this regard, the developers of STSI equipment are guided by the relevant ITU-T recommendations, in particular for SDH such recommendations are G.957 and G.691, which regulate optical and electrical interfaces of SDH systems of all levels. In particular, the standard interfaces, which are determined by the recommendations of G.957, include the following parameters: wavelength of optical radiation, wavelength range, width of spectral line of radiation, level of optical power per transmission, atexuality coefficient of receiving device at a given error rate for a given transmission speed. The choice of these parameters is determined by the speed of information transmission and the length of the line. SDH equipment is designed to work with single-mode fibers. Fiber parameters are also regulated (Recommendations: G.652, G.653, G.655).

In cases where the distance between the points to be combined with SDH equipment exceeds the length corresponding to the energy potential of the system (i.e. the necessary amplifier on the track) or at both ends use an optical power amplifier for transmission and pre-amplifier at reception, guided by G.691 Recommendations. In addition, for all levels of SDH equipment standardized optical connectors (optical connectors) of type FC or PC, optical in-device connecting cords (patchcord), type and dimensions of boards, cells, block dimensions and standing, power consumption, supply voltage, etc..

Structurally, SDH equipment consists of such blocks:
- external access equipment (EAE – external access equipment);
- synchronous linear SLR regenerator; synchronous splitters – SLR

- 4D/1 multiplexers, SLR16D/1 multiplexers, which can also be marked ADM (ADD/DROP MULTIPLEXSOR).

SDH systems of any manufacturer are built according to the generalized scheme shown in the figure 16.8.
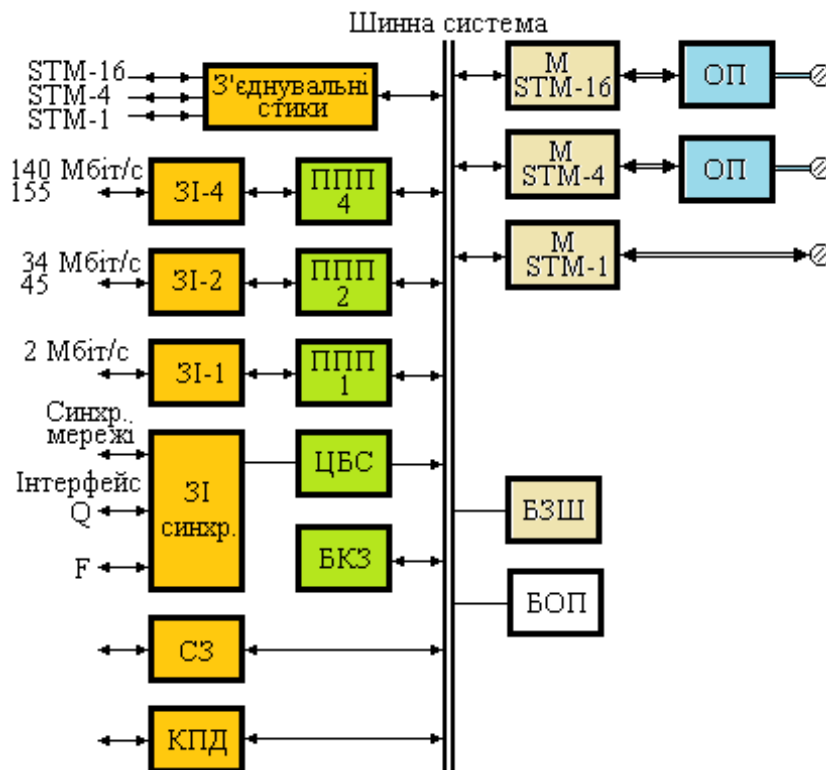
Переклад Fig. 16.8. Generalized structural diagram of the SDH system:

M – multiplexer, OP – optical amplifier, ZS – connecting interface, PPB – primary flow port, CBS – central synchronization unit, BCZ – control and communication unit, SZ – service communication, CPR – data transmission channel, PP – meter processing unit, BZSH – block of connecting tires

In addition to the aforementioned nodes and blocks, SDH equipment includes:

- control system and management;
- emergency and transmitter alarm units;
- power supplies and protection against overloads and external influences, including electromagnetic fields.

The control and control system is a set of sensors of various parameters and circles that combine control points and control points with a personal computer. The computer display displays the values of all necessary parameters , both optical and electric. This system allows you to diagnose the entire communication network area in which this SDH equipment is involved. It is also possible to manage and change the configuration of network sites.

In cases of network damage, for example, a breakdown of the optical cable, in the SDH equipment of all levels to provide the possibility of network recovery and personnel safety, an automatic laser shutdown device is provided in accordance with the ITU-T (G.958) Recommendations. This device periodically turns on the laser at the following time intervals: 70-90 seconds the laser is turned off, 1 to 5 seconds running. When the line is restored, the system automatically restores its functions.

Currently, equipment for SDH systems is produced by most large companies specializing in the development and production of communication equipment.

Main companies:

- Lucent technologies (USA – headquarters, France, Niderlandi),
- Alcatel telecom (Namechchina, USA),
- Siemens (Namechchina),
- NEC (Japan).

16.2.4.1. LUCENT TECHNOLOGIES SDH EQUIPMENT

Consider the functional characteristics and technical parameters (in the aspect of optical interfaces) equipment "WavestarTMADM4/1" synchronous access multiplexer manufactured by Lucent technologies. This equipment of the 4th level of the TIC (SDH) hierarchy – STM-4 is designed to transmit optical fiber of optical digital streams STM-1 or STM-4. Optical fiber must comply with the parameters defined in G.652, G.653, or G.654 Recommendations. At the same time, radiation at a wavelength of 1.27-1.335 microns is used for transmission over short distances (up to 60 km), and over long distances (up to 100 km) in the range of 1.53-1.56 microns.

The equipment can work in the following modes:

1. Multiplexer TM1/1(STM-1) has electrical input joints (interfaces) to connect 16 streams of primary plesiochronic hierarchy (2 Mbps), with flexible layout in a stream of 155.52 Mbps or streams of the 3rd level PDH – E3 (34 Mbps) also with flexible layout. In addition, there is an electrical interface for connecting the PDH stream – E4. The listed streams are called component streams, or by international tributaries terminology. If multiplexer TM1/1 is used as the final equipment, from its source interface, the STM-1 electric stream is fed to the input of the optical module in which it is converted to the corresponding STM-1 optical digital stream. This stream from the original optical interface enters the input of the linear optical cable.

2. On the receiving side, inverse operations are performed, that is, the optical signal from the line cable enters the input interface. After that, in the photo receiving device, it is converted into an electrical digital

Table 16.4

Transfer rate, Mbps	155.52		By Multiplex TM1/1
1	**2**	**3**	**4**
Code used (G.957)	S-1.1	L-1.1	1-1.2/L-1.3
Working range of wavelengths	1270-1360	1285-1330	1530- 1560
Passing block, point S			
Type of radiation source	MLM	MLM	SLM
Spectral characteristics: Maximum band width, nm Maximum at -20 dB, nm Side mode suppression ratio relative to the central frequency, dB	4 - -	3 - -	- 1 30
Average output power injected into fiber: Max, dBm Minimum (including 2 dB aging), dBm Maximum aternation coefficient, dB	-8 -15 8.2	+2 -5 10	+2 -5 10
Receiving unit at point R			
Minimum sensitivity (taking into account 2 dB of aging and 10^{-10} BER), dBm Minimum overload level, dBm Maximum reflected signal factor, measured at point R, dB	-34 -3 25	-34 -3 25	-34 -3 25
Average fiber losses, dBm/km Theoretical maximum length, km	0.4 40	0.4 70	0.25 110

stream, which after amplification to the required amplitude level is fed to the group (aggregate) input demultiplexer. The signal transmitted along the optical line, according to international terminology, is called aggregate signals. Table 6 provides the parameters of optical interfaces for the case when the multiplexer TM1/1 is used as part of the final equipment, that is, as a terminal.

Table 16.5

Transfer rate, Mbps	622.04		Multiplexer TM1/1
1	2	3	4
Code used (G.957)	S-4.1	L-4.1	1-2.2/L-4.3
Working range of wavelengths	1270-1355	1280-1335	1530- 1560
Passing block, point S			
Type of radiation source	MLM	MLM	SLM
Spectral characteristics: Maximum band width, nm Maximum at -20 dB, nm Side mode suppression ratio relative to the central frequency, dB	2.5 - -	- 1 30	- 1 30
Average output power injected into fiber: Maximum, dBm Minimum (beginning of life), dBm Minimum (beginning of life), dBm Maximum attainment rate, dB	-8 -13 -15 8.2	+2 -1.5 -3 10	+2 -2 -3 10
Receiving unit at point R			
Minimum sensitivity (at the beginning of life), dBm Minimum sensitivity (at the end of life), dBm Maximum overload level, dBm Maximum reflected signal coefficient, measured at point R, dB	-29.5 -28 1 25	-29.5 -28 1 25	-29.5 -28 1 25
Average fiber losses, dBm/km Theoretical maximum length, km	0.4 30	0.4 60	0.25 96

3. The equipment also includes an I/O multiplexer – Add&Drop Multiplexer ADM 1/1 for the STM-1 format. With this multiplexer, operations can be performed to cross-communique component flows of low orders of the TMZ hierarchy for input (output), as well as to recommunicate them between two STM-1 aggregate ports.

4. The next component of the equipment "Wavestar^{TM}" is terminal multiplexer STM-4 – TM4/1. For it, the components are four STM-1 level information electric streams, and the aggregate one is the STM-4 electrical flux (622.04 Mbps), which is fed to the input of the optical passing module performing the operation, similar to the case of TM1/1.

Table 16.5 shows the parameters of optical interfaces for terminal multiplexer TM4/1.

Table 16.6

Parametres	Un. of Meas.	Magnitude			
1	2	3	4	5	6
Code used		S-4.1	L-4.1	L-4.2 L-4.3	JE-4.2/JE-4.3
Transfer speed	Mbps	622.08			
Linear code		Binary NRZ, scrambled			
Transmitted device (reference point S (G.957))					
Type of radiation source		Fabry-Perot with reduced power	Fabry-Perot with nominal power	LD distributed inverse connection with rated power	LD with a divided inverse connection with increased power
Spectral characteristics: Max. Shir. bands of radiation,nm Minimum coefficient of suppression of side mods Aterrification coefficient average output power injected into fiber	nm dBdB dBm	<2.5 - >8.2 -15 – - 8	<1.7 - >10 -3 – 0	<0.5 >30 >10 -3 – +2	<0.5 >30 >10 +3 – +6 With opt. Apm. +13 – +16
Receiving device (reference point R (G.957))					
Photo receiver type		Ge-APD in high sensitivity mode	InGaAs-APD in nominal sensitivity mode	InGaAs-APD in high sensitivity mode	InGaAs-APD in nominal sensitivity mode with opt. apm.
The level of nominal power perceived when 10^{-10} BER Overload Level	dBm dBm	-34 -3	-36 -8	-39 -17	-45 -15

In addition to the main functions described above, the equipment includes devices of telecontrol, control, emergency alarm system, power supply, protection, service communication (with address choice).

IT SHOULD BE ADDED THAT LUCENT TECHNOLOGIES ALSO PRODUCES STM-16 STSI EQUIPMENT.

16.2.4.2. SIEMENS equipment

SIEMENS manufactures SL4 equipment, which is a synchronous multiplexer of the 4th level of the digital hierarchy, to transmit the information digital stream of the 4th level of STM-4. It forms a group (aggregate) digital stream at a speed of 622.08 Mbps from four digital streams of CTSI level 1 (STM-1) or 4 digital streams E4 CC at a speed of 139.264 Mbps. The aggregate flow of 622.08 Mbps after conversion from electric to optical is transmitted as a linear optical signal over a single-mode standard fiber (G.652, G.653) in the wavelengths range 1.51-1.56 microns. The equipment can be used in one of two options:

1. Linear terminal multiplexer of the 4th level of the STSI (SLT4);
2. Linear Regenerator (SLR4).

For control and control (in accordance with the ITU-T Recommendation (G.783 and G.784) a special microprocessor with the relevant software is built into the equipment.

The main technical parameters of optical interfaces of SL4 equipment are given in Table 16.6.

SIEMENS also manufactures SL16 equipment, which is a STM-16 multiplexer of the 16th level. This equipment forms an aggregate signal at a speed of 2488.32 from 16 component streams of CTSI level 1 (STM-1) or 16 digital streams E4 TIC at a speed of 139.264 Mbps, as in sl4 equipment. In this case, the aggregate flow after conversion from electric to optical in the passing module according to the standard singlemode fiber (G.652, G.653) in the wavelengths range 1.54-1.56 μm. The equipment can be used in one of two options:

3. Linear end multiplexer of the 16th level of the STSI (SLT16); Linear Regenerator (SLR16).

In both types of equipment SL4 and SL16 optical amplifiers on the transfer and receiving side can be used if necessary.

Similar in purpose, configuration and parameters of equipment 3AL36494AA is produced by ALCATEL (Germany, USA). STSI communication equipment for the transmission of digital streams STM-1, STM-4, STM-16 is also produced by other firms, in particular, NEC (Japan), ERICSSON (Sweden) ect.

17. METHODS OF COMPACTING INFORMATION FLOWS [21,23,24]

There are several ways to increase the bandwidth of information transmission systems. Most of them are reduced to one of the methods of compacting component information flows into one group, which is transmitted by the communication line. To further increase the component information flows, a combination of two or more methods is widely used. The term "compaction" has recently been increasingly replaced by the term "multiplexing".

17.1. Frequency Division Multiplexing (FDM)

With frequency multiplexing (FDM – Frequency Division Multiplexing), the frequency band of the general channel Fk is divided into a certain number of bands (sub-bands or sub-subsales), the frequency band of which corresponds to the main frequency band of the input channel ($\Delta f_{\text{вх}}$). At the same time

$$F_k \geq \Delta f_{\text{вх}}, \tag{17.1}$$

and $n \leq \frac{F_k}{\Delta f_{\text{вх}\,k}}$. These sub-channels (frequency bands) can be used to transmit messages from n sources, organizing for this transfer of the signal spectrum from each source to the allotted frequency range of the general channel, as shown in Fig. 2. 17.1.
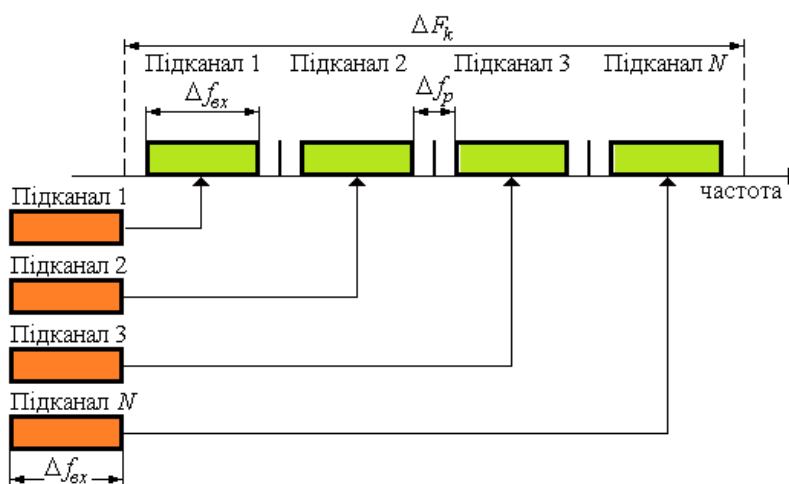
Переклад Fig. 17.1

Such a union of sub-channel spectra into a single spectrum of the general channel is carried out by the transmission signal conversion device (PPS). The structural scheme of message transmission during the frequency compaction of channels is provided in Fig. 2. 17.2.

On the receiving side, the optical carrier enters the photodector, at the exit of which an electric group flow is released. After amplification with a broadband amplifier, the signal enters the inputs of narrow-band filters, the central frequency of which is equal to the upsurface frequencies.

Both digital and analog signals can be component signals. FDM is used in cable multichannel TV systems.
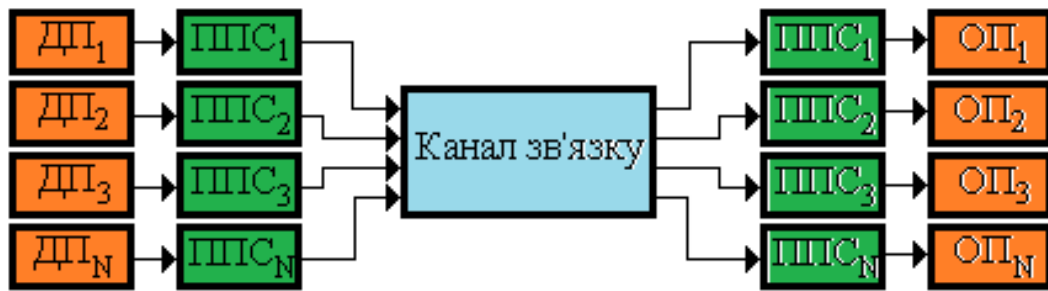
Переклад Fig. 17.2

GP – the source of the message; PPS – signal conversion device; OP - Message Recipient

17.2. Time Division Multiplexing

Currently, the Time Division Multiplexing method is the most common method of time compaction of information flows. It is used when transmiting information digitally. Its essence lies as follows. The transmission process is divided into a series of time cycles, each of which in turn is divided into N subcycles, where N is the number of threads (or channels) that are compacted. Each subcycle is divided into time positions, i.e. time intervals, the freaking of which is transmitted part of the information of one of the compacted streams. In addition, a certain number of positions are given for identification synchroimpuls, inserts and digital flow of service communication. As an example, consider the process of grouping the digital stream E2 (TSI) 8.448 Mbps of four streams of the hierarchy PTSI-E1 (2.048 Mbps). The transfer process is divided into time cycles lasting 125 ics each. These cycles consist of 4 subcycles, the length of each of which is 31.25 ics.

Subcycles are divided into 264 time periods (positions) with a duration of 118.4 ns, of which 8 positions are cited for identification synchroimpuls, insertions and digital flow of service communication. Duration of each time segment τ_i equals the clockwise interval specifying the clock rate (for a group stream of 8.448 Mbps)

$$f = \frac{1}{\tau_u} = \frac{1}{118.4 \cdot 10^{-9} c} = 8.448 \text{ Мгц} \qquad (17.2)$$

The time compaction method is divided into asynchronous or plesiochronous PPIs (PDH), ATM- and synchronous SCI (SDH)-multiplexing. It is clear that pdh and SDH systems described above use time multiplexing methods. The maximum transmission rate of group (aggregate) flow in systems that have found wide implementation in the construction of modern transmission systems is about 2.5 Gbps. However, due to the development of the latest electronic technologies (semiconductor structures based on gallium arsenide, microvacuum elements), laboratory samples of electronic multiplexers for a speed of 40 Gbps (STM-256) have already been created, which are prepared for mass industrial production.

Time multiplexing binary streams

When using digital telephony systems to transmit data at multiplexer inputs, there are already formed streams of binary data, which are represented by pulse signals. Then, in this case, the time multiplexing scheme practically coincides with similar schemes used in computer systems.

We assume that at the inputs of the multiplexer we have incoming binary sequences. Then the multiplex switch consistently selects any logically meaningful sequences of bits and forms a general output sequence from them. This process is called interleaving, or alternation.

There are such types of interliving:

- bit-interliving, or alternating bits – multiplexer output is consecutively dialed one bit from each channel;
- byte-interliving, or alternating bytes – multiplexer output is consecutively switching one byte from each channel;
- symbolic interliving, or alternating of characters – the output of the multiplexer is consecutively communiculated one character from each channel;
- block-interliving, or alternating blocks – multiplexer output is consecutively communiable to one block (which can be several bytes long or be a field that is multiple of another standard format) from each channel.
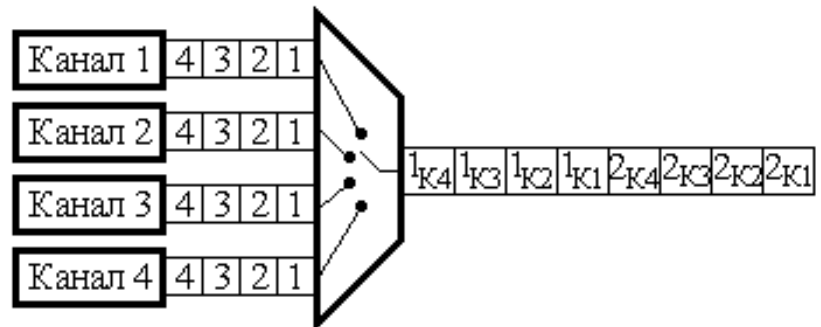
Fig. 17.3

The time multiplexing scheme of the four binary data streams by bit-interliving option is shown in Figure 17.3. Numbers 1-4 correspond to bit numbers, and indices match channel numbers.

17.3. Mod division

In some transmission systems, based on the use of multimode optical fiber, finds the use of modal seal (MDM – Mode Division Multiplexing). The essence of this sealing method is as follows. From geometric optics it is known that the angle at which the beam enters the flat-parallel plate comes out of it at the same angle (Figure 17.4).
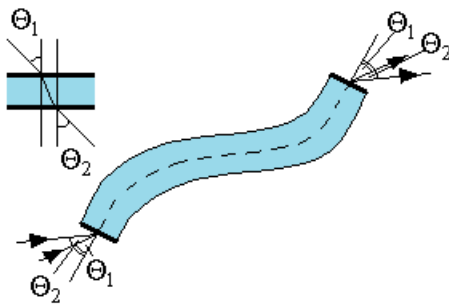
Fig. 17.4

Fiber can be imagined as some flat-steam plate, that is, at what angle from normal to end falls at the entrance of the line beam, at the same angle to normal, it will come out from its other side. So, using angular selectors at the in entrance and output of multimode fiber, it is possible to transfer independent information flows through channels, the role of which is played by fiber fashions. Mod sealing can only be used if the modes are independently distributed, there is no mixing and interchanting. Such conditions are made in the absence of local heterogeneities in the fiber and in the absence of significant bends of it. Such requirements can be met, for example, in automation systems, where signals are transmitted over short distances (about units – tens of meters).

17.4. Polarization Seal

Compaction of information flows with the help of optical bearers, which have linear polarization, is called polarization seal (PDM – Polarization Division Multiplexing). In this case, the polarization plane of each carrier is located at its own angle. Multiplexing is carried out with the help of special optical prisms, for example, the prism of Rochon. Unlike the previous method of multiplexing, single-mode fiber can be used as the medium by which the signal is transmitted. However, the PDM method can only be successfully used if there are no local heterogeneitys in the environment, bends that cause local polarization anisotropy. Consequently, these reasons that affect the multiplexed signal significantly limit this method of signal compaction.

17.5. Multi-wave division optical bearing mods (WDM) [2123,24,31-35]

It can be argued that the further increase in the throughput of TDM-based data transmission is limited not only to technological difficulties in electrical time compaction, but also to restrictions arising from chromatic dispersion in OV (time distortion and impulse destruction). Further increase in the throughput of the optical communication channel can be carried out through the use of another type of multiplexing – multi-wave multi-wave pulpexing of bearings (WDM – Wavelength Division Multiplexing). The idea of this method is that m informational digital streams, each of which is carried on a carrier with its wavelength λ_m and spaced relative to each other using a special device – wave multiplexer are combined into one optical flux $\lambda_1, \lambda_2, ..., \lambda_m$. Over time, this stream is injected into the fiber and transmitted using an optical cable. On the receiving side, an inverse demultiplexing operation is carried out.

Today, WDM plays the same role for optical synchronous systems as ICP frequency-separated multiplexing (FDM) for analog data transmission systems. That is why systems with WDM are often called optical multiplexing systems with frequency separation of OMCP (OFDM). However, in essence, these technologies (FDM and OFDM) differ significantly from each other. Their difference lies not only in the use of optical (OFDM) or electrical (FDM) signal. When FDM, AM modulations with one side strip (OBS) and a corresponding system of subsuring, modulating signal of which are the same in structure, are used, as it is a set of standard TM channels. With OFDM, the modulation mechanism required in FDM for carrier shifting is not used at all, bearing ones are generated by individual emitters (lasers), whose signals are simply combined by the multiplexer into a single multi-frequency signal. Each of its components (bearing) can fundamentally transmit the flow of digital signals, which is formed according to the laws of various synchronous technologies. For example, one carrier can formally transmit ATM traffic, the second SDH, the third PDH, etc..

17.6. WDM INTERACTION MODEL WITH TRANSPORT TECHNOLOGIES

Formally, for WDM systems, it does not matter what methods of encoding and formation of a particular digital signal were used. However, as a rule, the same traffic is transmitted on such systems. This is dictated by the use of appropriate synchronization methods and the monotony of the processing process. Unlike SDH systems, the signal transmitted is not packed in containers and cannot be processed in accordance with the SDH multiplexing structure for the formation of the STM-N transport module, which can only and can be transmitted through the physical level to the communication channel (transmission medium).

If it is simplified to imagine a multilevel model of interaction of basic technologies SDH/SONET, ATM, IP (without taking into account the possibility of transferring IP via ATM), which transport the signal in global digital networks, and WDM, then before the appearance of the latter it looked like, which is given in Fig. 2. 17.5 a. The model consisted of three levels and an optical transmission medium. It showed that in order to transport top-level traffic (ATM and IP) through the optical transmission environment, it must be placed (encapsulated) in the STM-N/OC-n transport modules of SDH/SONET technologies, which are capable of passing through the physical level into the optical transmission environment using the physical interface of these technologies. This was followed by the need to create technologies for encapsulating ATM cells, for example, in SDH virtual containers (ATM over SDH), or IP packets into SONET virtual tubes (IP over SONET). This was done by the relevant subcommittees on standardization in such institutions as ANSI, ISO, ITU-T and ETSI, developing standards for these technologies.

ATM	IP	ATM	IP	ATM	IP
SDH/SONET		WDM		SDH/SONET	
Фізичний рівень		Фізичний рівень			
Оптичне середовище передавання		Оптичне середовище передавання			

a   *b*

переклад Fig. 17.5. Model of interaction of basic transport technologies.
a – implementation of WDM technology,
b – after the introduction of WDM technology.

After the appearance of WDM systems, the model takes the form given in Fig. 2. 17.5 b. Now the model has four levels, not including the optical transmission medium. An intermediate level of WDM has appeared, which, like SDH/SONET, provides a physical interface that allows, through a physical level, to enter the optical transmission environment not only with SDH/SONET technology, but also with ATM and IP technologies. In the latter case, encapsulation of ATM cells or IP packets into the intermediate transport module of SDH/SONET technologies is not required. This not only simplifies the process and transportation of traffic generated by ATM and IP systems, but also significantly reduces the total length of the headers (which are docked along the mayoral passage from the top level to the bottom). Thus, the percentage that the information component of traffic occupies increases, in the total length of the transmitted message, and as a result, the transmission efficiency as a whole increases. Naturally, ATM and IP traffic can also be transmitted through a traditional scheme using SDH/SONET, whose traffic can also be transmitted through WDM systems. This preserves the continuity of old transportation schemes and increases the flexibility of WDM-SDH/SONET composite systems in general.

17.7. FLOWCHART OF WDM SYSTEMS

The main scheme of the system with WDM has the form given in Fig. 2. 17.6. (one direct channel is shown).
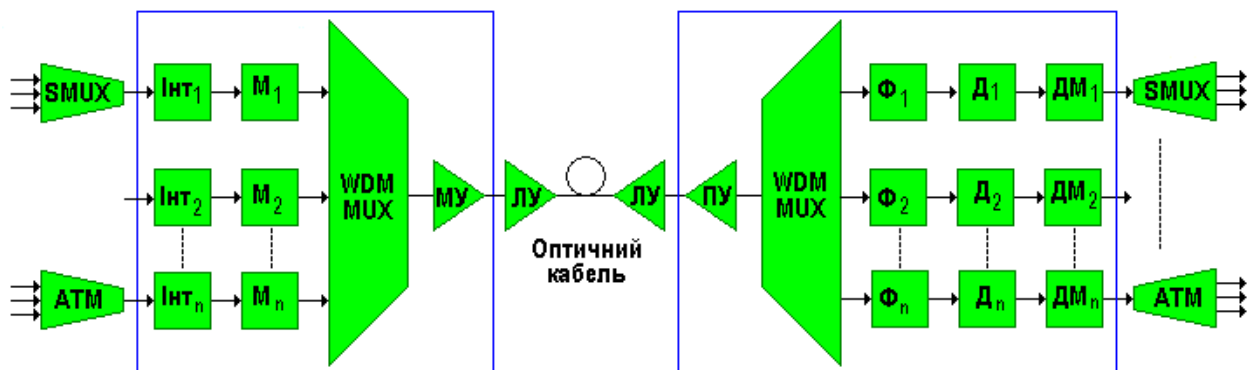
Переклад Fig. 17.6. Flowchart of a system that uses WDM

n input streams of data (encoded digital pulse sequences) are modulated with the help of optical modulators Mi optical bearing with wavelengths λ_i. Modulation load-bearing multiplexesin the WDM MUX multiplexer into an aggregate flow, which, after amplification (with the help of a booster or a powerful amplifier – MU), is fed to the OV. At the receiving end, the flow from the exit of the OV is amplifyed by the previous amplifier – PU, demultiplexed, that is, divided into component streams, modulated load-bearing λ_i, which are thetized with the help of Di detectors (at the entrance of which the Fi strip filters can be used to reduce transient interference and, accordingly, to increase the interference of detectives). At the last stage, the signals are modulated by DMi demodulators, which form the initial digital pulse sequences at the output. Note that in addition to MU and PU, linear amplifiers can also be involved in the system – LA.

17.8. NARROW BAND AND BROADBAND WDM

Wave multiplexing has been practically used for more than 10-20 years in the initially aimed at combining two main bearing 1310 nm and 1550 nm (2nd and 3rd transparency windows) in one fiber. This allowed to double the capacity of the system and was justified by the whole history of VOLZ development. Many standard SDH systems provide this now as one of the configuration options. Some researchers call such systems broadband WDM ("wear" wavelength - 240 nm) as opposed to narrow-band WDM (the spread in which was an order of magnitude lower - 24-12 nm, which made it possible to place in the 3rd window (1550 nm) 4 channels). Such separation of systems does not seem quite correct today, since such "broadband" WDM spectrum did not overlap, but consisted of two isolated lanes. On the other hand, today a class of truly broadband WDM systems is formed, overlapping in the adjacent transparency windows (3rd and 4th) strip close to 84 nm from 1528-1612 nm. This class in the future may overlap the strip of 1280-1620 nm if you focus on the characteristics of the "pioneer" in this area of the WaveStar AllMetro DWDM System of Lucent Technologies, which uses fiber, which eliminates peak absorption in the area of the 5th window (~ 1383 nm).

17.9. ITU-T recommendations regarding wavelengths in WDM systems

Although it is not necessary to rely now on full mutual compatibility of equipment from different WDM system manufacturers, it was necessary to standardize the nominal range of bearings – the so-called ITU-T frequency grid, or the ITU-T frequency plan to give manufacturers a guideline for the future, as well as to position existing WDM systems. This task was solved in the first approximation by the IEA Standardization Sector, which issued the ITU-T Rec. G.692 standard.

17.9.1. STANDARD CHANNEL PLAN AND ITS USE

Initially, the basis of the draft standard was a channel (frequency) plan with a uniform arrangement of carrier frequencies of channels with a minimum spread (step) of channels at 0.1 THz, or 100 GHz. The frequency area selected in the plan covers a standardized range D_{cr}=5,1 THz and practically corresponds to the range of wavelengths (from 1528.77 to 1569.59 nm) amplitude-wave characteristics of ABB

fiber optic amplifiers, the probe is widely used. When choosing a constant step h=0.1 THz (100 GHz) in this range, you can place a maximum of 51 channels with bearings indicated in the top row of table 17.1. For recalculation by wavelengths, the ratio of

$$\overline{\lambda} = 2.99792458 \cdot 10^{17}/f \; [\text{нм/Гц}],$$

in this case, step by step λ different from 0.780 to 0.821 nm, or an average of 0.8 nm).

When using the 0.2 THz step (200 GHz, or an average of 1.6 nm), you can get a 17.2 derivative table.

Similarly, derivative tables can be obtained both when using a larger step of 0.4 THz (400 GHz, or 3.2 nm), 0.6 THz (600 GHz, or 4.8 nm) and 1.0 THz (1000 GHz, or 8.0 nm).

Table 17.1.

Standard channel plan with 100 GHz channel spread

f (THz)	196,1	196,0	195,9	195,8	195,7	...	191,4	191,3	191,2	191,1	191,0
λ (nm)	1528,77	1529,55	1530,33	1531,12	1531,90	...	1566,31	1567,13	1567,95	1569,59	1568,77

Table 17.2

Standard channel plan for 200 GHz channel spread

f (THz)	196,1	195,9	195,7	195,5	195,3	...	191,9	191,7	191,5	191,3	191,1
λ (nm)	1528,77	1530,33	1531,90	1533,47	1535,04	...	1562,23	1563,86	1565,50	1567,13	1568,77

Now, according to the recommendations of G.692. frequency grid has the form (see Table 17.3)

Table 17.3

Frequency grid WDM

Rated central frequencies (THz) for 50 GHz	Rated central frequencies (THz) for 100 GHz	Nominal central wavelengths (nm)
196.10	196.10	1528.77
196.05	–	1529.16
196.00	196.00	1529.55
●	●	●
●	●	●
192.20	192.20	1559.79
192.15	–	1560.20
192.10	192.10	1560.61

Naturally, the presence of such a grid involves the synchronization (calibration) of the corresponding equipment at the reference frequency. Grid reference frequency 193.10

The minimum step between the channels respectively 100 GHz (0.8 nm) and 50 GHz (0.4 nm), was selected based on the characteristics of the optical equipment, first of all, from the minimum reachable width of the spectral characteristics of the emitters.

Strict regulation of optical frequencies for WDM systems makes the question of stability and accuracy of control of optical bearing frequencies quite relevant $(\lambda_1, \lambda_2, \dots, \lambda_m)$. The ITU-T G.692 Guidelines state that this problem is under study and therefore there are no specific numerical values for this parameter in the documents yet. However, based on the established frequencies of spectral channels, it is possible to estimate with sufficient accuracy the permissible width of the laser spectral radiation line $\Delta\lambda$, as well as the permissible amount of optical frequency time instability Δ_l (time shift (flucation) of the laser frequency in time). To do this, turn to the figures. 17.7 showing the position of the central frequencies of the first two wave channels of the DWDM system (50 GHz step).

Consider two adjacent channels, one of which has a central frequency of 192.15 THz and the other 192.2 THz. Today, only one type of modulation is used in optical communication – intensity modulation, which is similar to amplitude signal modulation in an electric channel. We assume that both channels streams are transmitted digital streams of STM-64 level, that is, streams with speeds of 10 Gbps.

Переклад Fig. 17.7

Supposing that the spectrum of the STM-64 digital stream is limited to the first harmonica of the 10 GHz clock frequency (in practice, this is almost always performed). Then the optical spectrum of each channel will consist of 3 components – the central frequency ν_0 and two side $+\Delta\nu_0$ and $-\Delta\nu_0$. Note that the multi-wave (spectral) sealing of optical channels is similar to the frequency sealing of radio channels, or multi-cable systems with analog transmission method. Therefore, for multi-wave optical systems, the same ratios are fair as for the frequency sealing of the mentioned systems, for which the protective interval between the two adjacent channels should not be less than the double upper frequency of the channel modulation. The following picture illustrates when this condition is true. Now supposing that for channel 1 it increased by 10 GHz, and for the 2nd it decreased by the same value. Then the interval between channels will be 10 GHz. In this case, the frequency positions of the 2 harmonic signals of channel 1 and 2 match. Although we neglected their magnitude, under some conditions they can reach a certain significant value (at least in a noise sense). Then the same frequency for 2 harmonics of both signals leads to cross noise in them. Consequently, such a frequency shift (10 GHz) is inadmissable when transmitting signals. 10 GHz frequency interval corresponds to wavelength interval $\Delta\lambda=0.08$ nm.
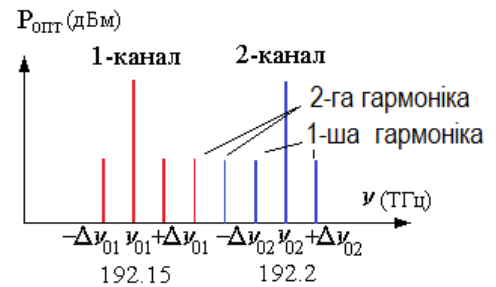
From the above it follows that for the transmission of STM-64 streams by DWDM at spectral intervals of 50 GHz, the width of the spectral interval of the radiation line should not exceed the value of about Δ=0.04 nm, and the instability of the optical frequency should be no worse than the value of approximately $\pm$5 GHz. Naturally, when moving to the transmission of STM-16 digital streams and below, the corresponding values may be increased.

17.9.2. Typical characteristics of WDM systems

Tables 17.4 and 17.5 provide typical characteristics of multiplexers and demultiplexers produced by ADC (USA).

Table 17.4

ADC company WDM Multiplexer Specification

	Number of channels			
	4	8	15	32
Step between channels, GHz	200	100	100	100
Band width at 1 dB (minimum), nm	0.7	0.3	0.3	0.3
Band width at 3 dB (minimum), nm	0.8	0.4	0.4	0.4
Maximum losses made, dB	1.5	2.3	3.3	5.3

Table 17.5

ADC company WDM Demultiplexer Specification

	Number of channels			
	4	8	15	32
Step between channels, GHz	200	100	100	100
Band width at 1 dB (minimum), nm	0.7	0.3	0.3	0.3
Band width at 3 dB (minimum), nm	0.8	0.4	0.4	0.4
Band width at 20 dB (maximum), nm	1.5	0.8	0.8	0.8
Maximum losses made, dB	2.0	2.8	3.8	5.8
Minimum "insulation" wavelengths, dB	30	30	30	30

Recently, there has been a tendency to reduce the frequency interval between spectral channels to 50 and even to 25 GHz. Naturally, the use of such systems significantly increase the capabilities of systems with WDM. This seal was called dense wave seal (DWDM – Dense Wavelength Division Multiplexing).

Note that sometimes in the literature the abbreviation DWDM is also used for systems with a frequency of 100 GHz.

It was mentioned above that optical interfaces of WDM and DWDM equipment must be compatible with SDH hardware – STM-16 and STM-64. However, in accordance with the G.957 Recommendations for SDH systems, the permissible parameter values at the output optical joints (interfaces) have the following values: spectral line width $\Delta\lambda \cong \pm0.5$ nm (for STM-16) and $\Delta\lambda \cong \pm0.1$ nm (for STM-64), and the central optical wavelength can have any value from an interval of 1530 – 1565 nm. Obviously, if you send signals from the source channels of SDH systems to the optical inputs of the WDM system multiplexer (DWDM), then such a system will not work. Thus, there must be a specific device at the input of the WDM (DWDM) system that performs such signal conversion so that they comply with the regulated G.692 Recommendations. Such a device was called a transponder. It has the number of optical inputs and outputs, equal to the number of optical signals compacted.

17.9.3. Other features of WDM systems functioning

It should be noted that, as is known [21-24] with optical sealing by wavelengths in the optical multiplexer there are significant losses. Thus, in DWDM transmission systems 16 spectral channels loss is ~ 7-9 dB (on one side). Taking into account losses on transmission and reception, the total losses are 14-18 dB. Such losses significantly reduce the energy potential of the system, so without optical amplifiers it is possible to transmit only over short distances – about 50 km (for 8 channels). In order to provide transmission over longer distances, fiber-optic power amplifiers (BOOSTER) are used. If such power is not enough, then the optical amplifier is used additionally on the receiving side.

In DWDM systems with more channels, individual amplifiers are often used for each wave channel. In this way, a high power of about 10 mW or more is injected

into the fiber at the OUTPUT of the DWDM system with a rich number of channels. As you know [21], at such capacities, signal distortion due to nonlinean phenomena in the OV is possible. Therefore, taking into account the impact of such phenomena and safety requirements for service personnel, the maximum power injected into the fiber is limited to a value of +17 dBm (50 mW) (Recommendations G.692). However, this value is not final and ultimately in the relevant Recommendation it is increased to 23 dBm.

In addition to the above parameters (optical frequency grid and maximum power), standards are also set on the structure of line connections with WDM. Three variants of structural line construction are offered:

- L (long) – a long line with a passive area up to 80 km and total losses of up to 22 dB. On the basis of such lines, transmission lines up to 640 km long with the number of intermediate optical amplifiers up to 7 pieces are built;
- V (very) – a very long line with a passive area up to 120 km and total losses of up to 33 dB. On the basis of such lines, transmission lines up to 600 km long with the number of intermediate optical amplifiers up to 4 pieces are built;
- U (ultra) – ultra-long line, which consists of one passive area up to 160 km and total losses up to 44 dB.

In the above variants, the connections of losses in the line are compensated by installing optical amplifiers. However, the length of the optical line is determined not only by energy losses, but also by distortion of the signal resulting from chromatic dispersion. This limitation is overcome by means of so-called chromatic dispersion compensators. Compensators are discrete and protracted.

Переклад Fig. 17.8 Structural diagrams of construction of transmission systems:
OMUX – optical multiplexer; BA (Booster Amplifier) – booster optical amplifier; ILA – linear intermediate optical amplifier; ODMUX – optical demultiplexer; PA – preliminary optical receiving amplifier

The basis of discrete compensators are Bragg grids, which work as certain wave filters. The design of such compensators is similar to the spectral demultiplexers discussed above.

Extended compensators, as already mentioned in the study of dispersion, can be built on the basis of fibers with negative dispersion.

As illustrations of the above optical lines from DWDM, Figure 17.8 shows structural diagrams of transmission systems produced by NEC Corporation (Japan))

Similar systems (V – 3x33 dB – 360 km) and (L – 8x22 dB – 640 km) respectively with two and seventh amplifiers are manufactured by LUCENT TECHNOLOGIES.

Note that WDM systems operate in the wavelength range of 1530-1565 nm. Therefore, special attention should be paid to the development (improvement) of optical amplifiers, which should have the same gain factor in this range in the whole range..

In terms of solving this problem, the literature provides data according to which the company PHOTONICS LAB. NTT ELECTRONICS CORPORATION (Japan), developed amplifier with a bandwidth of 80 nm (development ready for implementation) and 113 nm.

This expansion of the range allowed to proceed to the development of WDW systems with a large number of spectral channels. ALCATEL, PIRELLI, LUCENT TECHNOLOGIES announced the practical implementation of systems with 128 channels. Moreover, LUCENT TECHNOLOGIES develops a system with 256 channels.

One of the important points in the development of WDWM systems is the problem of organizing channels for managing and transmitting service messages. In accordance with the requirements for the organization of such channels, another channel is added to the channel grid, regulated by the relevant ITU-T Recommendations. To this end, it is recommended to use one of two wavelengths – 1510 or 1625 nm – that lie outside the passing of the erbius optical amplifier and the corresponding mesh.

Note that for modern WDW systems, the wavelength does not exceed 0.8 nm (100 GHz). However, in some countries (USA, Canada, Europe, Russia) a large number of fiber optic cables based on standard single-mode fiber (G.652) is laid. For such transmission systems, the CWDM (Coarse Wavelength Division Multiplexing) method is proposed. In these systems, the step between spectral channels is 20 nm and they use the 2nd and 3rd transparency windows. Although these systems are characterized by large energy losses, they have reduced requirements for the spectral characteristics of emitters.

17.10. Optical time division multiplexing (OTDM) [21]

The emergence and development of new types of communication services requires the transfer of more and more information in real time. In this case, it is not enough to require only an increase in the bandwidth of the transmission system. It is relevant not only the amount of information that the system can transmit, but also the time during which this transmission occurs. Consequently, real-time transmission of real-time information about processes occuring at high speeds requires the presence of lines and transmission systems in which this operation also occurs at high speed. For example, if you want to digitally transmit a phone message at a speed of 64 kbps, however, if you want to transfer a high-definition TV channel image, you need a speed of 994.3 Mbps (135 Mbps compression).
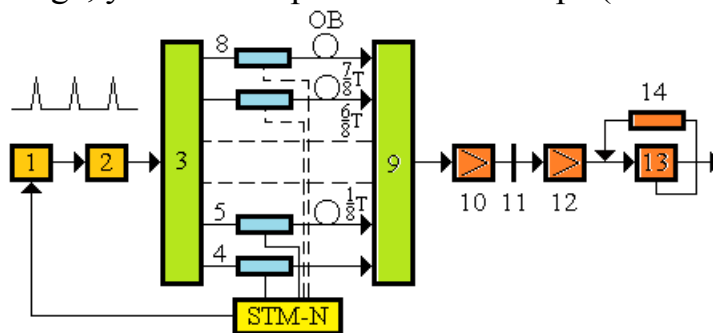
Fig. 17.9

Thus, the need to create systems with a time seal remains relevant. It is known that recent successes in the field of electronic elements creation allowed to create a system with electronic time sealing (ETDM) at a transmission rate of about 40 Gbps. (OTDM – Optical Time Division Multiplexing). Figure 17.9 shows the scheme for the implementation of this type of division.

The 1 mod sync laser is synchronized from the reference timer of multiplexed electronic systems SDH – STM-N. The flow of optical pulses with the duration and period of follow-up through optical amplifier 2 is fed to optical splitter 3, which spatially divides the luminous flux into eight equal parts, each of which enters optical modulators 4 – 8. From the output of each modulator, radiation passes through the corresponding segments of optical fibers, which play the role of optical delay lines. In this case, the delays at the output of the channel with the 1st modulator (position 4) are almost zero. After the release of the 2nd modulator (position 5), optical pulses are delayed by 1/8T, etc., and after the modulator 8, the delay is 7/8T. Then the signals from all outputs go to the input of sumator 9 (the same as splitter 3, but turned on in the opposite direction). From the outlet of the splitter, the combined group flow after amplification in amplifier 10 is fed to the transmission line. To compensate for losses (if necessary) an additional optical amplifier 11 can be included in the line. From the exit of the line, the optical signal amplifier 12 is fed to the optical time demultiplexer 13, which is synchronized using the device 14. Consequently, in the described system by the method of optical time sealing (OTDM) eight digital streams of 10 Gbps are transmitted. The system uses fully optical elements: laser, optical splitter, modulators made on crystals $LiNbO_3$, optical amplifiers and optical delay lines. This fully fits into the promising concept of creating fully optical networks and transmission systems.

17.11. Methods of compaction of canals by polarity [21]

Quite often there are situations when on the existing line of communication, which transmits, for example, 480 telephone channels (level E3), it is necessary to transfer an additional 30 or 60 channels (one or two digital streams E1). This problem can be solved in several ways:

1. Lay a new optical cable (or use pairs of backup fibers in an already built OK) and install new equipment, including the control and receiving modules.
2. Install the equipment at a higher level.
3. Apply equipment that implements the method of modulation bearing polarity for optical signal.

The polarity modulation method has been known for a long time and is used, for example, to transmit a stereo signal by radio. The essence of the method is that positive polarity is modated by one signal, negative – by another. At the same time, as for the usual amplitude modulation, the frequency of modulation $f_{мод}$ and frequency of carrying $f_{нес}$ must be in the ratio of $f_{нес} \geq 10 f_{мод}$.
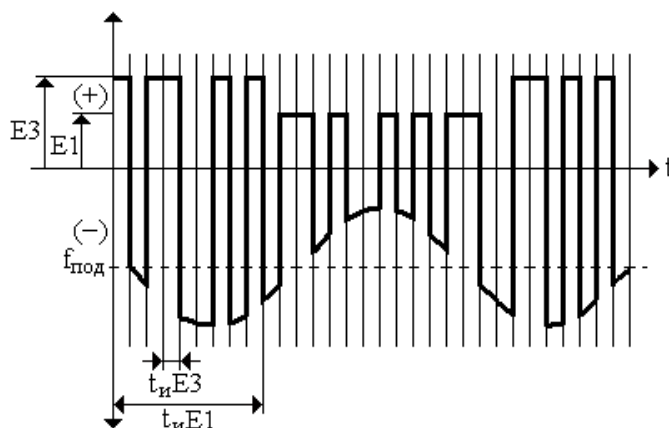
Переклад Fig. 17.10
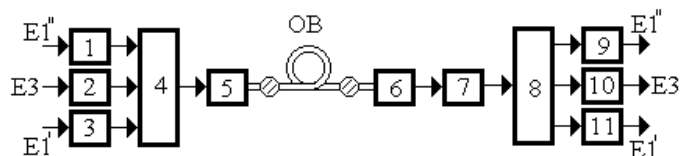
Переклад Fig. 17.11. Structural diagram of the transmission system for compaction of channels by polarity:

1-3 – diagrams of coordination of E1 signals with a modulator by polarity 4; 2 – the scheme of normalization of the bearing for coordination with the modulator 4; 5 – pumping scheme; 6 photodector; 7 – electronic amplifier; 8 – demoduulator

In our case, the sequence of linear signal with which the optical carrier is moduloed can be used as a carrier. As noted above, the linear code in the SME systems (2.048 Mbps, 8.8 Mbps, 34 Mbps and 140 Mbps) apply codes of type SM1 5V6V that do not have a constant component in their spectrum.

Taking into account these circumstances, such a signal in the electric tract can be moduloed with a certain coefficient: positive polarity by one signal, negative – by another. This process is illustrated by Figure 17.10, where a grid is applied along the time axis, one bar of which corresponds to the duration of half the time interval of the digital signal $E3 - t_u E3$. The positive polarity of this stream is modulated by an amplitude of a digital signal corresponding, for example, to the level of the PTS E1 at a tact interval $2t_u E3$, and negative signal – analog signal, the frequency of which is $f_{нес} \geq 10 f_{такт}$. So, using the digital flow signal E3 (E4), you can transmit three independent information flows: E3 (E4) and two streams E1 or E3 (E4), one stream E1 and analog signal, or E3 (E4) and two analog signals. The structural scheme of implementation of the system for compaction of canals by polarity is given in Fig. 2. 17.11.

In this way, with the help of a relatively simple electronic device, one laser and one optical fiber, it is actually possible to transmit three information flows.

18. Waterless optical communication. Principles. Loss
18.1. Conductive optical communication systems. Main abbreviations

WOTS – wireless optical transmission systems, WOCS – wireless optical communication systems. Main abbreviations: AOCL – atmospheric optical communication lines, FSO-systems, FSO-communication lines (Free space optics – systems).

18.2. General characteristics. Principles of construction [36-49]

The most common today are atmospheric data transmission lines with:

- 10 Mbps to 1–2.5 Gbps
- with ranges from 100 m to 4 km.

Topology – unlike waterless radio networks, which allow the connection "point – multipunsk" and allow connecting to the same base station several tens, hundreds, and sometimes thousands of subscribers, AOLZ mainly implement two-point connections: data are transmitted between two optical terminals, each of which has a separate receiver and transmitter, as a rule, with spaced optical tracts to avoid possible interference.

Fig. 18.1.

The required condition for the system is direct visibility. Data are transmitted by directional oncoming beams of modulated light. Light source – light diode or laser.

The mechanisms of light absorption in a transparent atmosphere (not taking into account specific factors such as weather conditions) are in many ways similar to those that occur in fiber. In a "clean" atmosphere, light with wavelengths used in SSOs (850, 1310 and 1550 nm) spreads almost without absorption. This allows you to use a developed element base, which is used in fiber optics and which is produced on an increasing scale.

In addition, this situation leads to the fact that it is also possible to attract most of the technologies already developed (it would take not small means and means to create new ones – lasers, photo and LEDs, microlenses, optical amplifiers, spectral masks, holographic optics, attenuators and methods of spectral sealing of channels).

The general element base and principles of signal processing determine the total range of speeds – the upper limit is determined rather by solvency, since there is no wave-water dispersion in AOCL, which mainly limits the transmission speed in FOLC.

Moreover, atmospheric optical lines use the same modulation as in DSP. That is why FSO systems are "all-inivorable" in relation to data transfer protocols. In other words, the system is the same as transmitting, be it E1, Fast, Gigabit Ethernet or ATM streams.

18.3. Advantages of FSO systems

1. One of the main advantages of FSO systems is the short installation time Another fundamental advantage of atmospheric optical lines is self-sufism.

2. Installation costs are one-time, license deductions and permission to use frequencies is not required anywhere in the world. *The development time of the devices is determined primarily by the life of the laser and can reach 20 years or more – the MTBF of the whole system has similar values*.

3. FSO systems can be installed not only on the roof of the building. The optical terminal can be placed in the middle of the building near the window, without changing the appearance of the building and not attracting the attention of passers-by and other interested observers.

4. Rather narrow beams of light make it possible to neglect the restrictions inherent in radio frequency systems, and compactly place several receiving and transmitter terminals, since when using the FSO system, problems with electromagnetic compatibility disappear.

5. *High protection of the AOCL channel from unauthorized access* is another of the characteristics of FSO. Some sources even believe that the level of data protection in AOLZ exceeds the protection of FOLC.

6. *The use of the general element base with fiber optics systems causes*: a gradual decrease in the cost of construction and an increase in the reliability of electronics without significant investments in development and design work; gradual simplification of procedures for the installation of optical terminals and the use of dynamic guidance systems for maximum ease of installation, reducing the requirements for load-bearing structures; high speed of data transfer and automatic reconnection with improved weather conditions.

18.4. Disadvantages of FSO systems

The disadvantages of FSO systems boil down to:

1. Relatively high cost systems, which still inhibits the use of FSO on short lines

2. Relatively low reliability of communication on long lines, where the impact of weather factors is especially significant.

3. The quality and reliability of atmospheric optical lines is also adversely affected by micro-indicators and vibrations of bearing structures

4. In addition, it should be noted that the convection of warm and cold air flows (atmospheric turbulence) generates heterogeneity of the thramination indicator – microlenses, which cause the optical signal to freeze up to 30 dB.

A little further, each of the shortcomings of FSO systems will be considered separately.

18.5. Application areas

All of the above rigidly defines the areas of use of FSO technology:

1. First of all, it is the *creation of high-speed mobile highways* in the case of obstacles that are difficult to get around in the usual ways - railway tracks and junctions, water obstacles, expensive, etc..

2. The *corporate sector*, in which the situation with offices already connected to the Internet is *quite often widespread, and the organization of a high-speed network* between branches that are in direct sight becomes relevant. In this case, the problems

of communication channel availability come to the fore, since critical traffic can always (or almost always) be allowed through low-speed communication channels.

3. Fast deployment of *high-speed temporary* communication. It should be noted that to solve this problem, there is practically no alternative to FSO systems.

4. Solving the problem of the *last mile* when organizing computer networks. This is especially true for few powerful providers, the number of subscribers of which has units and dozens of customers.

5. The use of FSO *in mobile networks* (including in 3G networks) in places of high crowding of subscribers, base stations are located quite tightly at relatively short distances from each other. The use of FSO in such a scenario significantly reduces the duration of the project and the initial cost of creating a network. In the future, according to its development and reducing the need to use FSO systems, FSO systems can move around the perimeter of the network – if, of course, there is a threat of competition from the operator offering better services.

6. "Exotic" or promising areas of use of optical waterless communication:

- application of optical waterless communication in *space*.

This type of application has wide prospects, since there is no atmosphere that generates the main obstacles in the organization of communication. Accordingly, the length of the optical communication line becomes almost unlimited.

fSona plans to apply optical communication in a unique experiment. The system developed by this company will be used in the next flight to Mars – it will connect a satellite orbiting Mars to earth.

The project was called Mars Laser Communication Demonstration and should implement data transfer speeds from 1 to 30 Mbps (depending on the time of day and the distance between the planets. Note that existing long-distance radio systems provide a transmission speed of no more than 120 Kbps).

On the way to the Earth's surface, a beam of light will have to pass through the atmosphere, so it is planned to use two ground terminals to ensure stable communication in case one of them is closed by clouds.

- the use of optical waterless communication *under water* also has wide prospects, since as is known, the radio channel in sea water cannot be used, since radiation in conductive media quickly dries at distances comparable to wavelength and acoustic methods provide speed only at the level of about 2.4 Kbit/s, which is clearly not enough for military and other practical tasks..

The task of secretive high-speed communication, protected from unauthorized access, remains relevant, especially for communication with submarines, without the ascesing of boats in the overwater position. Today there is data that Ambalux took up this task. Ambalux proposes to use blue-green lasers and reports communication ranges of 10–100 m and transmission speeds of 10–150 Mbps.). Topics are in full swing – there is information about sectoral receiving and the use of spectral sealing methods to ensure full-duplex communication. In the future, the technology can be commercialized (for example, to connect with underwater oil platforms). Note that the number of platforms even today is about 4 thousand. and as ocean stocks develop will only increase.

18.5. Structure of waterless optical communication system [50]

Figure 18.2 shows a generalized structural diagram of the BOSP receiving and transmitter module (duplex version).

In fact, the BOSP contains functional nodes that are inherent in any electrical communication systems. Moreover, when forming signals, in principle, it is possible to use various methods of coding and types of modulation, which are known for traditional transmission systems.

The signal (optical or electrical) enters the interface module. Which transforms the signal into an electric one in the corresponding digital code. This module also provides the transformation of the received signal into a signal in linear code. Next, the signal is appropriately encoded, usually with redundancy (often with great redundancy). This type of transformation is necessary to ensure the increased factory resistance of the communication system. It should be noted that the degree of redundancy can be very significant, and, it is little related (or practically not limited to) the protocol transmission speed. This is due to the fact that when using BOSP systems, such a phenomenon as signal dispersion at propagation speeds is practically absent. And as you know, it is dispersion that limits the transmission speed in THE SSRS. Consequently, signal transmission between the transmitter and the receiver can be carried out at a speed that significantly exceeds the protocol rate of the system transfer. As a result, a large number of additional bits can be transferred, and almost any complexity algorithms can be implemented.
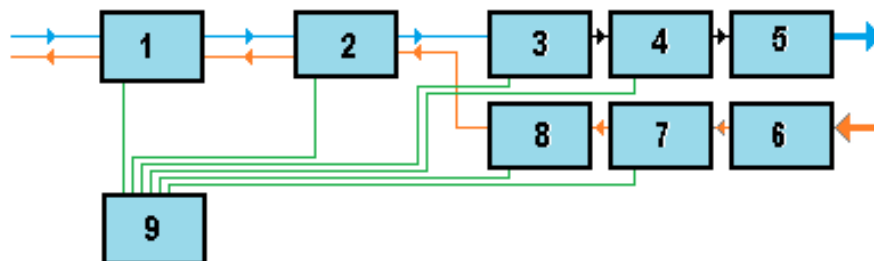
Fig. 18.2

1 – interface unit, 2 – signal encoding-decoding unit, 3 – modulator, 4 – LD, 5 – transmitting optical antenna, 6 – receiving optical antenna, 7 – FP, 8 – amplifier, 9 – module control and power supply.

Next, the signal enters the modulator. Note that in most cases, for those speeds that are implemented in BOSP systems, direct modulation is enough. So the modulator is a block that forms an information signal in the form of an electrical signal transmitted directly to the laser pumping link. The receiving link contains: optical receiving antenna, FP and amplifier.

As a transmitter, LD is used, which works in one of the transparency windows of the SFP. Receiver – PIN, or avalanche photodiode.
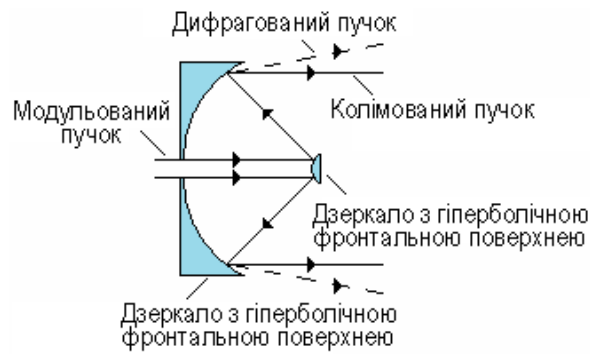
Перекласти Fig. 18.3. Conceptic image of a typical optical antenna

A few words about the transmit or receiving antenna. Such an antenna is nothing more than some optical system "optimized for infinity". In other words, such an antenna is a colliment system of the type of telescope with a large output (input) hole. Such a telescope can be built on the basis of both rebractional and reflective optics. It should be noted that the second option is more attractive, since the antenna elements consist of fewer optical surfaces. This is due to the fact that today the manufacturing technology of reflective surfaces of the aspherical form is well developed. The use of such aspherical mirrors can significantly reduce the number of optical surfaces (not less than twice). An example of such an antenna is shown in Figure 18.3.

We will evaluate the field of view of the receiving unit.
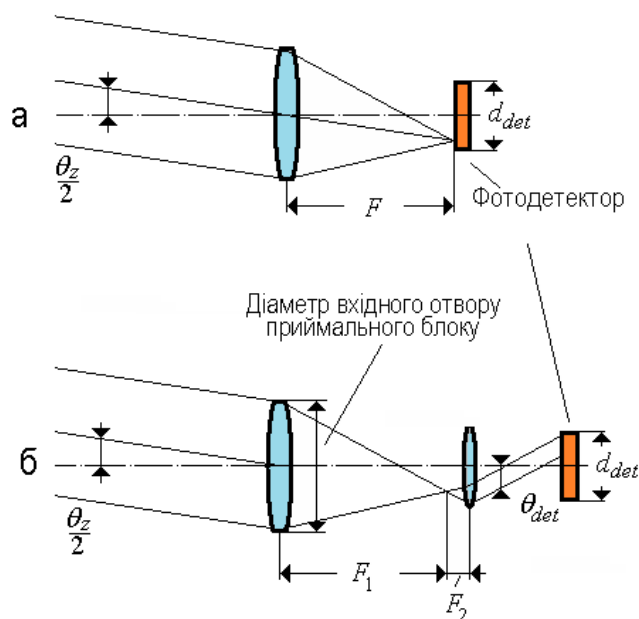
Перекласти Fig. 18.4. Geometric diagrams of receiving optical antennas:
a) focusing antenna; b) colliment antenna.

For simplicity, the assessment will be made for antennas built on the basis of refrxation elements. The results for mirror optics will be exactly the same.

In the focusing antenna type (Fig. 18.4 a), the photodetoctor is installed in the focal plane of the input lens; accordingly, the field of view is determined by the expression

$$\theta_z = \frac{d_{det} - d_{sp}}{F},$$

(18.1)

where F – focal length of the input lens; d_{det} – photodector diameter; d_{sp} – diameter of the focused spot in the lens focus.

If the receiving antenna is designed to work on the diffraction limit, then the dimensions of the focused spot are equal to

$$d_{sp} = 2.44 \frac{F\lambda}{d_{inp}}.$$

(18.2)

where d_{inp} – diameter of the inlet beam

If the size of the diffraction spot is much smaller than the diameter of the sensitive plane of the photodector, then

$$\theta_z = \frac{d_{det}}{F}.$$

(18.3)

The field of view of the receiving unit with a colliment type antenna (Fig. 18.4 b) is determined as follows

$$\theta_z = \frac{F_2}{F_1} \theta_{det},$$

(18.4)

where F_1 and F_2 – focal lengths of colliment lenses.

18.6. Physical model of communication system [50]

Consider communication models using lasers as emitters.

The 3D and spatial coherence of the laser's optical radiation allows you to form a beam with minimal discrepancy, which is practically determined by the diffraction limit:

$$\theta_0 = \frac{1.22\lambda}{d_{\text{inp}}}, \tag{18.5}$$

where λ – wavelength, d_{inp} – diameter of the output pupil of the transmission unit, θ_0 – the angle of radiation discrepancy, or simply the discrepancy.

From 18.5 it follows that the discrepancy in the case of using a laser is a value close to the angular second and less.

However, with fairly long optical tracks, the increase in the cross section of the beam can be relatively large.

The physical model of the laser communication system can be presented in the form of: Modulated laser beam is collied by the optical antenna of the transmitter. The optical signal entering the input antenna of the receiving unit focuses on the inlet end of the receiver, where the optical signal is converted into an electric one. The electrical signal enters the decoder and turns into the output signal of the receiver.

Since there is no infusion of dispersion in the FSO system, the successful operation of the system depends on the balance between the transmitted and accepted energy.

Such a connection between the transmitted and accepted signal energy will be called the equation of the range of the communication system, or simply the equation of the communication system.

18.7. Spatial multiplexing of signals based on edeable bunches

It is known that one of the actual tasks that arise when transmitting signals is the task of effective signal transmission through the communication channel with interference. Signals transmitted along atmospheric (FSO) communication lines are no exception. An additional factor affecting the quality of transmission is atmospheric turbulence. The presence of turbulence leads to distortions of the optical beam, the destruction of its structure, both in phase and intensity.

It should be added that only with direct modulation, which is used when transmitting signals at relatively low speeds (up to 155 Mbps), the transmitted signal can be considered as alternating certain impulses and intervals when the signal strength is zero. During external modulation, as a rule, the average signal strength remains sustainable, regardless of whether the unit "1" or zero "0" of the message is transmitted.

As usual, the recovery of a signal that passes through a channel with interference occurs due to the use of so-called redundant codes, which ensures a fairly reliable transmission of information. But this method has a significant drawback: if the disturbances in the atmosphere are serious enough, then such a signal will be lost, that is, the communication channel will be destroyed.

Therefore, in our opinion, there is a more promising way to solve the problem, (at least for FSO systems) namely, the use of a different type of encoding, which is based on the use of physically stable optical singalar bunches, such as ede.

Such beams are simply implemented by the method of synthesized holograms using spatial-modulators of light.

At the same time, for any communication systems, an increase in the channels along which signals are transmitted remains relevant, which makes it possible to significantly increase the amount of information transmitted by the system.

It should be noted that for optical systems (fiber optic primarily) transmission there are specific sealing methods such as modal or polarization multiplexing. This gives hope that something similar may be offered for FSO systems.

Unlike fiber optic systems, in which the characteristics of optical beams are strictly regulated by physical limitations inherent in wavewater systems, for example, the modal nature of distribution, the corresponding distribution of intensity at the intersection of the beam, etc., such restrictions for FSO systems are absent.

Therefore, in our opinion, the use of singalar bunches in FSO systems is quite promising.

18.7.1. Some information about edrus beams.
Back to expression (1.25):

$$U = x \pm jy, \tag{1.25}$$

The distribution of the phase in the vorch area (phase map) given by the equation (1.25) is illustrated by Figure 18.5 a.
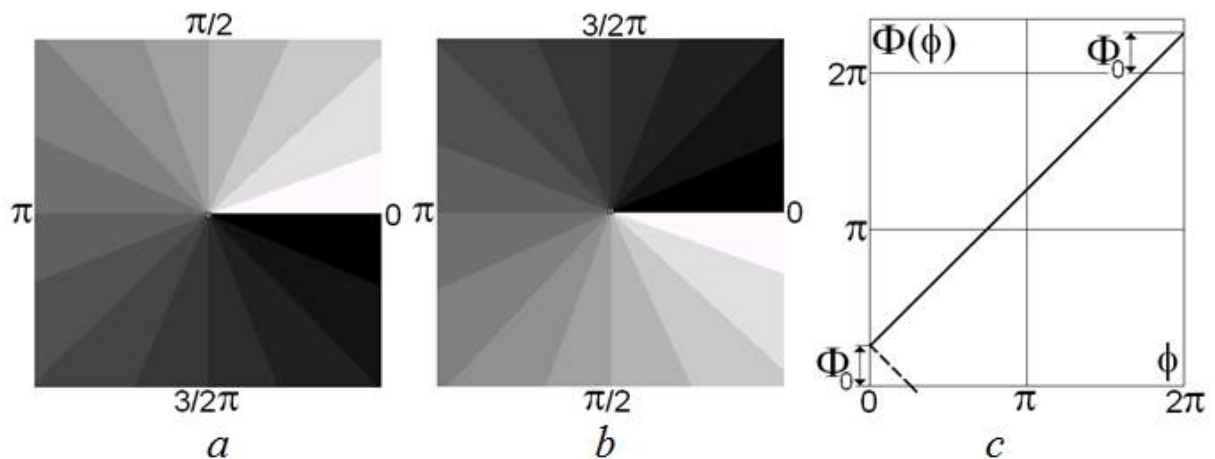
Fig. 18.5. Phase map of isotropic voric
Changing the grayscale corresponds to a phase change. a) – corresponds to the sign (+) in the equation (4.4); b) – sign (–). c) – change of phase when bypassing the vorture. Solid line in Fig. 2. (c) – positive voric (+ in expression (1.25)). Dotted - Negative.

As you can see, when bypassing the center of the vorkin in a circle, the phase grows or falls depending on the sign (+) or (–) in (1.25) linearly. In the work [51] such edema was called isotropic. In general, the equifax line corresponding to the zero phase may not coincide with the x axis of the laboratory coordinate system tied to the center of the vortices. The value of the phase shift will later be called the initial phase of the isotropic vorar. Note that the phase change (Fig. 18.5 s) can be obtained

from the distribution (Fig. 18.5 a) by simply turning the coordinate system by the angle of magnitude– $\Delta\Phi_0$.

Naturally, for a real field, the equation (1.25) is extremely rare. The area in which the phase change is described by linear approximation will be called [7] the vorar nucleus. As a rule, a change in the phase in the vorticulous nucleus is described by a nonlinear law corresponding to the appearance of (1.25) real coefficients before x and y. The most common case of vorticul phase distribution occurs with an additional rotation of the vorticul phase structure by some angle. The phase surface in the eye of the vorocation is the right or left helicoid. Only in this case is realized the increase or decline of the phase by the value of the 2π when fully bypassing the whirlwind center.

18.7.1.1. Topological charge

Special points of any magnitude are usually characterized by topological indexes of two types [7,52]. The first of these, the so-called topological charge, is introduced for a special point (for example, for a special phase field point), based on the following ratio:

$$S = \frac{1}{2\pi}\oint d\Phi, \qquad (18.6)$$

where integration is carried out over a small surface (counterclockwise) described near a special point.

It is easy to see that to change the phase (Fig. 18.5) – the topological charge is + or − 1 . The sign (+) represents the situation when. when bypassing the vortices counterclockwise, the phase builds up and (−) – if the phase decreases. In general, another phase behavior is possible, in which the topological charge for the module can be more than one and is ±1.±2.±3,.... However, it can be shown that the vortices with a topological charge modulo larger than one, topologically and physically unstable and even with a slight physical perturbation disintegrate into a system of simple single vortices. Therefore, in the future, we will assume that in the optical field only the urires with a charge S = ±1 are implemented.
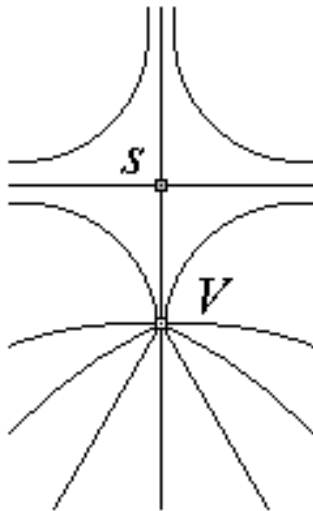
It is easy to show that for areas of the field that do not contain a singul point (including stationary points), S = 0. Figure 18.6 schematically depicts equifasive field lines in the vortices (point V) and saddle point S. Since the topological charge is inherent only in the area of the field that includes the vortices, the topological charge of the field shown in the figure is + or − 1.

Рис. 18.6.

18.7.1.2. Topological index Topological index of the second type - the so-called Poincare index (hereinafter simply an index). It is calculated as follows. When circumventing a special point, they monitor which direction the lines that characterize the field structure formed in its neighborhood (for example, equifax lines) rotate. If the direction of rotation of lines coincides with the bypass direction,

then the field structure is assigned an index with a sign (+); if the lines rotate in the opposite direction, then the index is assigned a sign (–). The index module is equal to the number of full lines revolutions, which is calculated when returning to the starting point. Thus, based on Figure 18.6, which presents the equifax lines of the field area, which includes the vortices V and saddle point s, we can conclude that both positive and negative vortices are characterized by one index N = +1, and the saddle point index N = –1. Phase extremes, like ovtores, are characterized by index N = +1.

18.7.1.3. Law of preservation of topological charge

It can be shown that for some area containing M special points, the total topological charge can be introduced $S_{tot} = \sum_{i}^{M} S_i$ and index $N_{tot} = \sum_{i}^{M} N_i$ [7]. Due to the properties of the Evclud space, the law of preservation of the total topological charge and index is carried out, which can be formulated as follows for the optical field. Any disturbance of the optical field does not lead to a change in the total topological charge and index. At the same time, if the electromagnetic wave spreads freely in a linear environment and there are no sources and completely absorbing drains on its path, then the values remain constant for any section of the field [7].

18.7.2. Principles of spatial multiplexing

Imagine that at the output of the transmitter antenna, a classic Gauss beam of zero order is formed (Fig. 18.7 a), which enters the device that introduces a certain spatial asymmetry into the field, which is formed in the far zone (Fig. 18.7 b). In other words, the main part of the beam intensity in the far zone will be concentrated in part of the Field Part2, while in part of the field Part1 radiation is practically absent. We will assume that such a bunch tolerates the signal A2. Imagine that in the same way in part1 you can form an A1 signal. Naturally, the "tail" of the signal, for example, the A1 signal in the "foreign" area will create noise for the A2 signal. However, with the appropriate signal-noise ratio, such signals will be practically orthogonal [53].

As an "assimalizing" device, you can use a simple screen that covers part of the beam in the plane of the transmitting antenna.
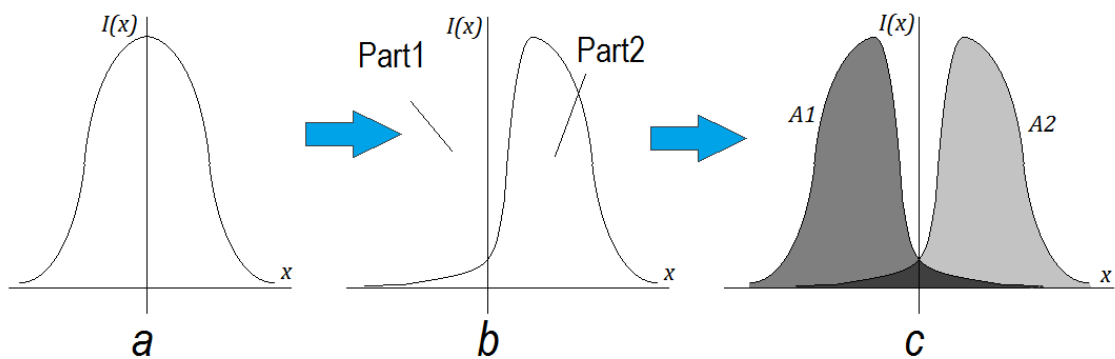
Fig. 18.7. To explain the principle of spatial multiplexing.

Let us consider in detail the diffraction of the gaussy beam of zero order on the edge of the opaque screen. The complex amplitude of the Gauss beam is determined by the ratio

$$U(x, y) \sim \exp\left(-\frac{x^2+y^2}{2\sigma_0^2}\right), \qquad (18.7)$$

where σ_0 determines the width of the beam.

We assume that in the entrance plane the screen closes exactly half a beam.

Diffrained beam at a distance of z from the screen in the plane x_1, y_1, defined by Fresnel conversion.

Then, the complex amplitude U at a distance of z can be written as

$$U(x_1, y_1) \sim \exp\left(-\frac{y_1^2}{2\sigma^2}\right) \int_0^\infty \exp\left(-\frac{x^2}{2\sigma_0^2}\right) \exp\left[j\frac{k}{2z}(x-x_1)^2\right]dx, \quad (18.8)$$

where $k = \frac{2\pi}{\lambda}$ – wave number, σ_0 – Initial width of Gauss beam, z – distance between the screen and the observation plane, the amount of σ determines the width of the beam in the direction of y_1, in which "there is no diffraction" and can be written in the form [6]

$$\sigma = \sigma_0\sqrt{1 + \frac{z^2}{k^2\sigma_0^4}}. \qquad (18.9))$$

The distribution of intensity in the diffraction field in the far diffraction zone is illustrated by Figure 18.8.
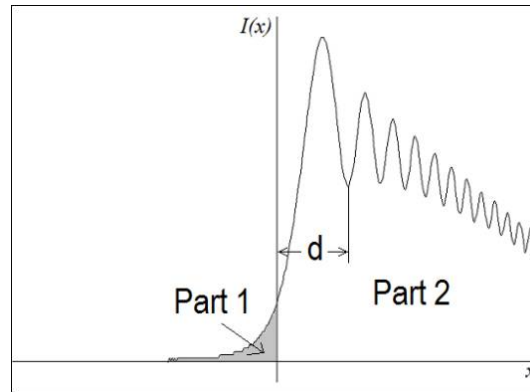
Fig.18.8. Distribution of the intensity of the Gauss beam diffraged on the edge of the screen. The value d characterizes the distance between the edge of the screen and the first additional minimum intensity.
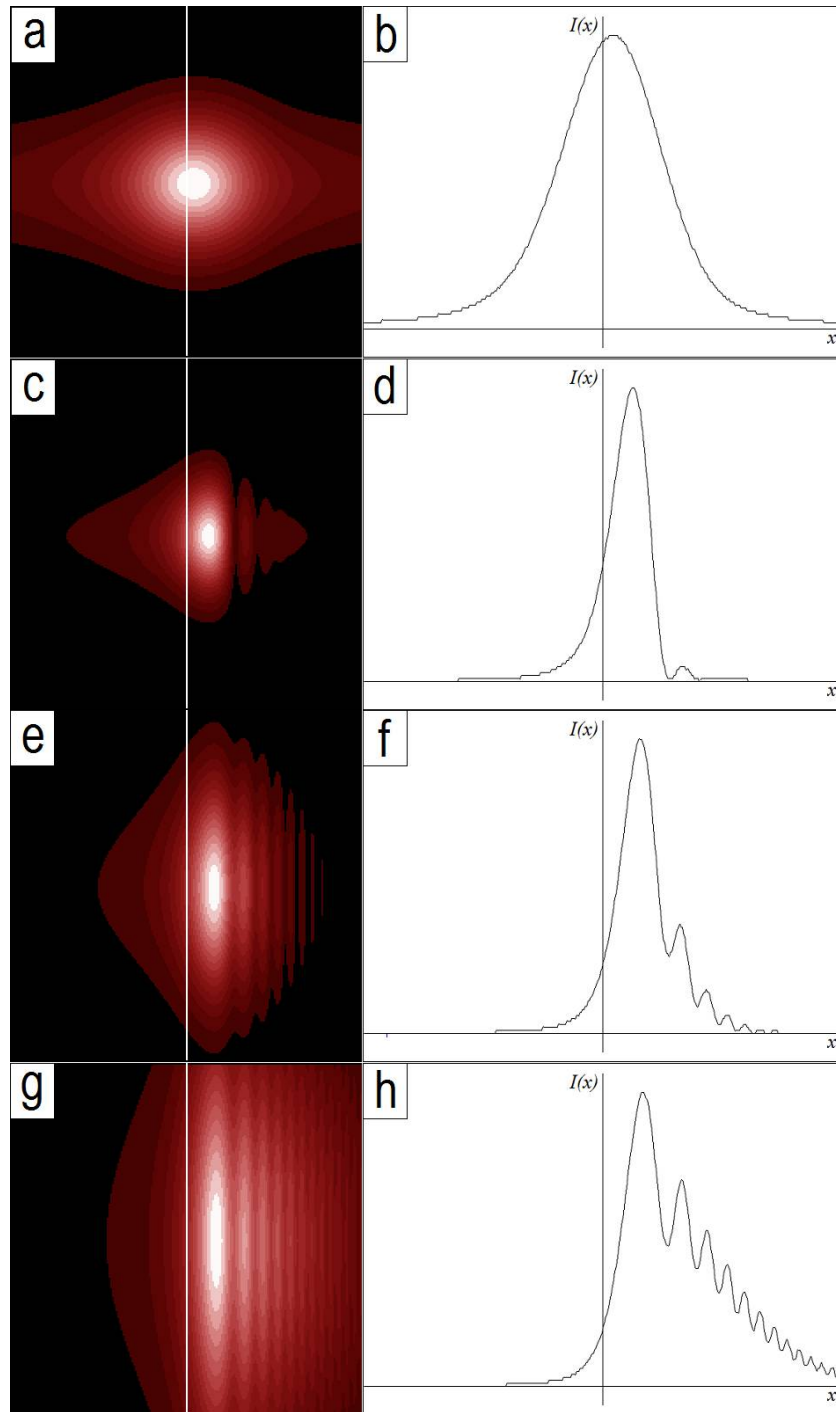
Fig. 18.7. Results of computer simulation of gauss beam diffraction on infinite screen.

String a-d - represents the value $\alpha = \dfrac{\lambda}{\sigma_0} = 2.8 \times 10^{-4}$ E-h, i-l, m-p, q-t strings counted for values $\alpha = 1.4 \times 10^{-4}, \alpha = 7 \times 10^{-5}, \ \alpha = 3.5 \times 10^{-5}$ and $\alpha = 1.7 \times 10^{-5}$ respectively. The first column illustrates the distribution of intensity in the diffraction field resulting from the diffraction of the Gauss beam of different widths on the edge of the screen. The second column corresponds to the distribution of the intensity of the resulting wave, in the central intersection of the diffraged beam. The white vertical line on the shapes indicates the position of the edge of the screen.

The part of the field that is in the space covered by the screen is marked as Part 1. Accordingly, the part of the field located in the screen-free area is marked part 2. As you can see from the picture, unlike the diffraction of a flat wave on an infinite

screen in the part of the field marked as Part 2, the average intensity gradually decreases. In this case, the rate of descending is determined by the width of the Gauss beam. The smoother the initial bundle, the faster the intensity decreases. In this case, the distance between the edge of the screen and the first additional minimum d does not depend on the width of the Gauss beam. Accordingly, we can expect that in the case when half the width of the beam $\sigma_0/2$ will be commensurate with the value d descending of medium intensity will be so fast that additional minimums in the diffraction picture will be absent.

When indented from the edge of the screen, the intensity will depend on the initial width of the Gauss beam. With a significant value σ_0 in this part of the field there will be additional modulation.

The results of computer modeling are presented in Fig. 18.9.

As you can see from the figures, the intensity distribution in part of the Part2 field is characterized by additional modulation, the nature of which depends on the initial width of the Gauss beam. This modulation practically disappears during diffraction of relatively narrow Gaussian bunches (see figure a,b). However, at the same time the asymmetry of the beam disappears and the formation of ortho-channel channels becomes impossible.

18.7.3. Use of edeable bunches for spatial multiplexing of communication channels

Let's try to use for spatial multiplexing another type of beams – edetto beams. Add that such beams are more resistant to physical disturbances, for example, turbulence. Let us consider in detail the diffraction of the edema beam on the edge of an opaque screen. The complex amplitude of the isotropic vorar in the source plane of the transmitter can be presented as [7]:

$$U_v(x,y) = \sqrt{x^2 + y^2} \exp\left(-\frac{x^2+y^2}{2\sigma^2}\right) \exp[jS\arctg\left(\frac{y}{x}\right)], \qquad (18.10)$$

where S – topological charge of the vorvore, σ –"width" beam.

If you cover part of the beam with a screen, the field in the far zone (infinity) or in the focal plane of the receiving antenna lens is described by an expression:

$$U(\omega,v) = \iint_{-\infty-\infty}^{\infty\ \infty} h(x+a)U_v(x,y)\exp[-j(\omega x + v y)]dxdy, \quad (18.11)$$

where

$$h(x) = \begin{cases} 0, & x < 0 \\ 1, & x \geq 0 \end{cases}, \qquad (18.12)$$

Heyside function [54], ω, v – normalized coordinates in the observation plane. For lens with focus f, these coordinates look like:
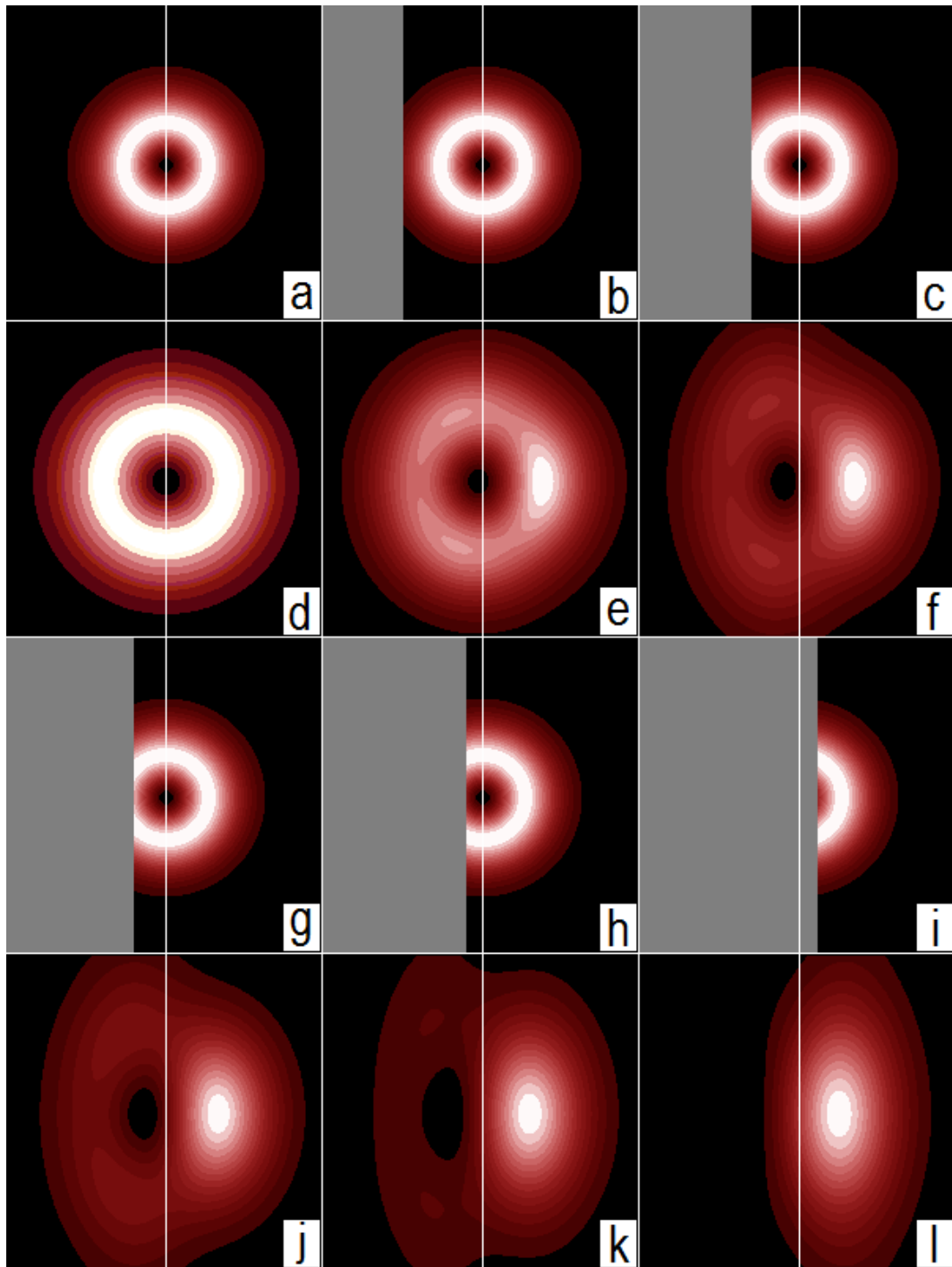
Fig. 18.8. Changing the shape of the diffraction field and shifting the center of the vortex depending on the degree of overlapping of the vorture in the input plane. The degree of overlap is determined in the shares of the width of the beam of a whirlwind σ. When walking away from the center of the whirlwind by magnitude σ the intensity of the beam is 0.37 from the maximum. The lines a-c and g-i correspond to the input field and the overlapping screen. Rows d-f and j-l diffraction result in the far zone. The white line indicates the position of the center of the vorar in the absence of a overlapping screen. a,d – input beam and diffraction field without overlapping the inlet beam; b,e – the screen is located at a distance of $s=1.3\sigma$ from the center of the vortex; c,f – $s=0.8\sigma$; g,j – $s=0.5\sigma$; h,k – $s=0.2\sigma$; i,l – $s=-0.2\sigma$, fully blocked whirlwind center in the input plane.

$$\begin{cases} \omega = \dfrac{k}{\lambda f} x_d \\ v = \dfrac{k}{\lambda f} y_d \end{cases}, \qquad (18.13)$$

where $k = \dfrac{2\pi}{\lambda}$ – wave number, x_d, y_d – coordinates in the plane of the receiver.

Then the field in the plane ω, v can be written as:

$$U(\omega, v) = \{ e^{j\omega a} H(\omega, v) \} \otimes V(\omega, v), \qquad (18.14)$$

where $H(\omega, v)$ Fourier image from The Hayside function, $V(\omega, v)$ Fourier image from the complex amplitude of the vortex [7].

The results of digital modeling by ratios (18.10) and (18.11) are shown in Figure 18.8. This picture illustrates the change in the shape of the diffraction field and the displacement of the center of the vorture, depending on the degree of overlapping of the vorture in the input plane.

The degree of overlap is determined in the shares of the width of the vorar beam σ σ. The lines of figure d-f and j-l illustrate the result of diffraction in the far zone. The white line indicates the position of the center of the vorar in the absence of a overlapping screen. Figures a,d correspond to the field in the input plane and far zone, when the diffraction field is formed without overlapping the input beam. Accordingly, all the remaining drawings characterize the situation, depending on the degree of overlapping of the incoming vortex. Figures b,e – the screen is located at a distance $s=1.3\sigma$ from center of vortex; c,f – $s=0.8\sigma$; g,j – $s=0.5\sigma$; h,k – $s=0.2\sigma$. Figures i,l – $s=-0.2\sigma$ correspond to the case when the center of the vortex in the incoming plane is completely blocked.

As you can see from the figure as the voric overlaps in the input plane:
1. Decreases the intensity in the zone corresponding to the left side of the field.
2. The center of the whirlwind shifts from the center of the picture.

This situation is additionally characterized by Figure 18.9, which shows the intensity distributions in the intersection of the diffraction field, depending on the degree of overlapping of the vorture in the input plane.

The displacement of the center of the vorage, depending on the degree of overlapping of the vorent in the entrance plane, is illustrated by Figure 18.9. Already when overlapping $s=0.5\sigma$ this bias reaches $l=0.2\sigma$.

Separately, it is necessary to analyze the case when the screen overlaps the center of the whirlwind in the input plane. As you can see from the picture when $s=-0.2\sigma$ vortex in the far zone exists and its displacement l is equal to the value 0.55σ. This situation seems to contradict the law of preservation of the topological charge, since the total topological charge of the field after the screen must be zero. However, this fact can be explained as follows. Right behind the screen in the
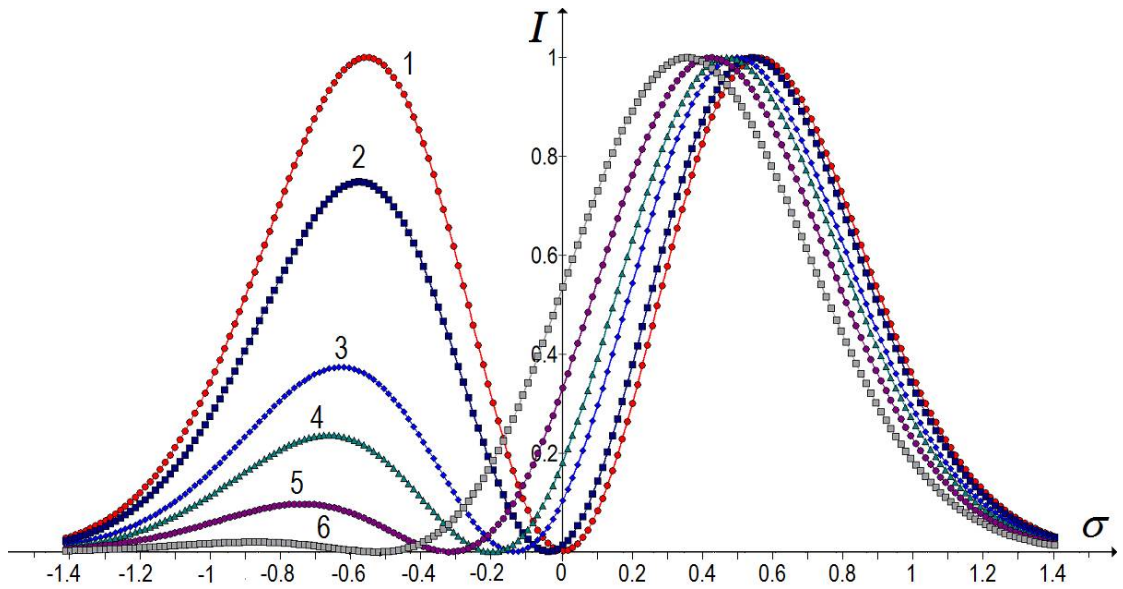
Fig. 18.9. Distribution of intensity in the intersection of the diffraction field, depending on the degree of overlapping of the vortex in the input plane.

The degree of overlap is determined in the shares of the width of the beam of the vortex σ. When walking away from the center of the whirlwind by magnitude σ the intensity of the beam is 0.37 from the maximum. 1 – entrance beam and diffraction field without overlapping the inlet beam; 2 – the screen is located at a distance of $s=1.3\sigma$ from the center of the vortex; 3 – $s=0.8\sigma$; 4 – $s=0.5\sigma$; 5 – $s=0.2\sigma$; 6 – $s=-0.2\sigma$, fully blocked whirlwind center in the input plane.
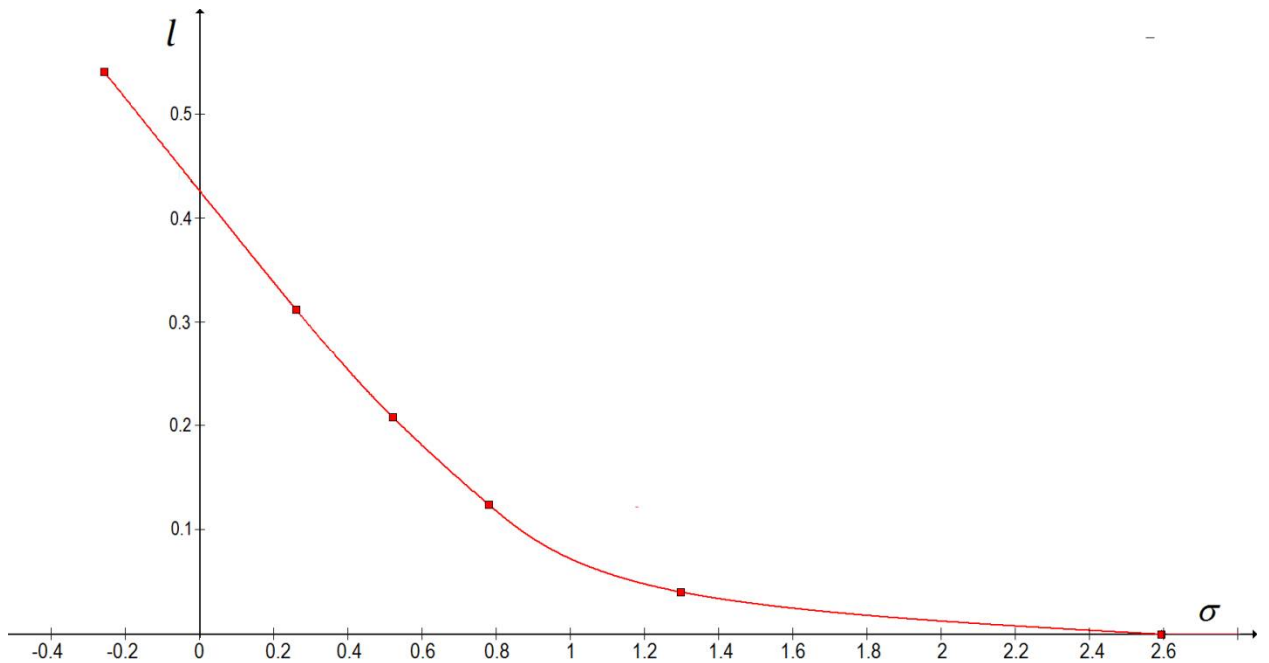
Fig. 18.10. Vortex center offset depending on the degree of overlapping vortex in the incoming plane.

The degree of overlap is determined in the shares of the width of the beam of the vortex σ. When walking away from the center of the whirlwind by magnitude σ the intensity of the beam is 0.37 from the maximum.

The diffraction field whirlwind is obviously absent. Only at a certain distance from the screen a pair of whirlwinds is born. With increasing distance to the input plane,

one of the vores moves much faster than the other. Finally, in the far zone, it shifts to the dark area of the field and ceases to be identified. However, the study of this mechanism requires additional research and is not the subject of this master's work.

So, as follows from the data of digital modeling, even a small part of the input beam is overlapping $s=0.5\sigma$ causes the intensity on the left side of the field to be much lower than in the right. In addition, since the intensity in the center of the vorar is zero, the receiver located in the vorar core zone will record the intensity corresponding only to the signal of one of the channels. In other words, it can be argued that communication channels in this case orthogonal.

18.8. Communication system equation [50]

The equation of the communication system is determined by the initial power of the emiator and various energy losses on the track in the transmission and receiving units. Consider the dependences that characterize the spread of radiation in the communication channel, losses due to the natural difference of the beam in space, the attenuation of the signal during the passage in certain tracts of the system.

Losses of energy bearing in the modulator and optical antenna are characterized by the coefficient of the transmission unit of the system

$$\tau_{\text{out}} = \frac{p_{\text{out}}}{p_{\text{LD}}}, \tag{18.15}$$

where p_{LD} – laser power, p_{out} – power output of the transmitter unit.

According to the physical model of the system, almost a parallel beam of power p_{out} reaching the receiving unit focuses the optical receiving antenna on the end of the photo receiver. Note that the size of the focused spot for the case of coherent and non-coherent radiation is different. In the first case, if neglected by the expansion of the beam due to the aberations of optics and the distortion of the beam during the passage of the atmosphere, the size of the spot is close to the size of the zero diffraction order, where about 90% of the energy is concentrated. In the second case, the size of the focused spot is primarily determined by the size of the source. As a result, when using a coherent source, the energy concentration is always higher (the size of the focused spot is smaller). However, in the case of coherent source, the size of the spot is larger than the size of the diffraction order due to random (turbulence) and deterministic (optics aberration) distortions of the flat beam.

We will assess the level of losses when spreading the beam from the transmitting unit to the receiver.

Not taking into account the attenuation of radiation on the track, we have that the losses in the plane of the inlet of the receiving unit are due only to the fact that due to the discrepancy of the beam, the area of its cross section increases as the distance between the transmitter and receiving units increases z.

передавальний блок   приймальний блок
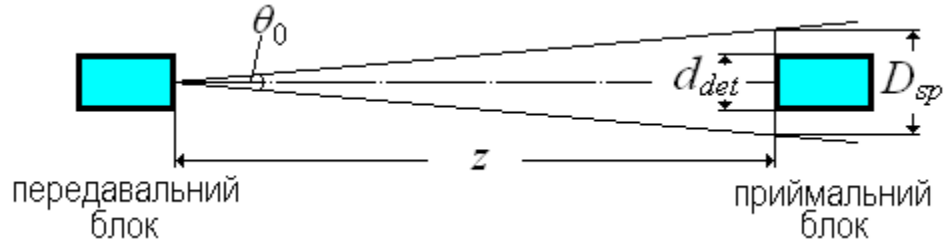
Переклад Fig. 18.11

If z is large enough, then the outlet of the transmission unit can be considered a point source. Then the area of the cross section of the beam (see Figure 18.11) is equal to

$$S_{sp} = \frac{\pi}{4}(\theta_0 z)^2. \tag{18.16}$$

Area ratio S_{sp} and the area of the inlet of the receiving unit is described by the ratio of

$$\tau_{opt} = \frac{S_{pr}}{S_{sp}} = \frac{(d_{det})^2}{(\theta_0 z)^2}, \text{ or in decibels } T_{opt} = -10\lg[\frac{(d_{det})^2}{(\theta_0 z)^2}]. \tag{18.17}$$

If we assume that the intensity of the beam is uniform along the cross section of the beam (in fact it is not), then it is this ratio in the first approximation that determines the loss of power due to the spread of the signal.

So the power that falls on the inlet of the receiving antenna is equal to

$$p_{inp} = p_{out}\tau_{opt}. \tag{18.18}$$

Naturally, not all the energy that has fallen into the inlet of the receiving unit comes to the receiver. Such losses by analogy with the transmission unit will be called the coefficient of the receiving unit of the system τ_{inp}. So given the attenuation of the signal in the τ_{atm} we can associate the radiation power taken by the receiver with the power of the laser diode

$$p_{det} = \tau_{out}\tau_{opt}\tau_{atm}\tau_{inp}p_{LD} = \tau_{out}\frac{(d_{det})^2}{(\theta_0 z)^2}\tau_{atm}\tau_{inp}p_{LD}. \tag{18.19}$$

This is the equation of the system.

If we apply the practice adopted in connection – the losses are determined in decibels, and the power in decibelmilats then the equation (18.19) will be re-written in the form of

$$\Delta P = P_{LD} - P_{det} = T_{out} + T_{inp} + T_{opt} + T_{atm} = T, \tag{18.20}$$

where ΔP – dynamic range of FSO-system in decibels, T – general losses in the communication channel in decibels.

Note that in the most rough approximal $p_{out} \approx p_{LD}$ and $p_{det} \approx p_{inp}$. Respectively $(T_{out} + T_{inp}) \to 0$ and in addition to attenuation in the atmosphere, total losses are determined only by losses of T_{opt}, called optical alignment losses

$$T_{opt} = -10\lg[\frac{(d_{det})^2}{(\theta_0 z)^2}]. \tag{18.21}$$

Naturally, for the FSO-system to work in drain mode, inequality must be

$$\Delta P > T. \tag{18.22}$$

18.9. Vtrati i zavadi in the atmospheric channel zv'yazku [36,37,43,45,55,61]
18.9.1. Vibratsiyni zavadi

Consider the consequences to which the so-called mechanical effects lead. Buildings, especially high, tend to "breathe" throughout the day. This is manifested (see Figure 18.12) in the deviation of the building from the middle position and angular deviations in the transverse plane (torsion). Sometimes the deviation of the structure from the vertical under the influence, for example, the wind, can reach tens of centimeters and even meters. For example, the Eiffel Tower deviation amplitude is close to 10 m.
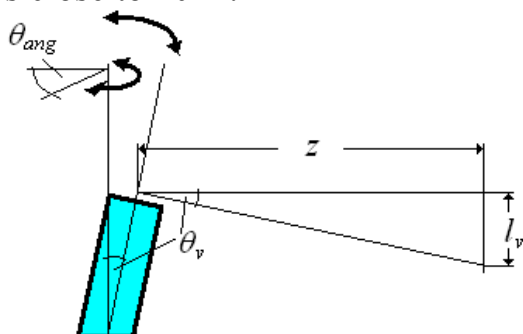
Рис. 18.12.

Accordingly, the angle of θ_v which changes the direction of distribution of the optical signal close to 0.01 councils. Approximately the same value has a torsion angle θ_{ang}. As a result, the linear displacement of the beam at a distance z close to 1 km is about 10 m. Therefore, vibrational interference significantly reduces the distance of communication.

However, the "clock" vibration frequency is much lower than the clock speed of the signal. This fact, when duplex communication allows the use of so-called adaptive technologies, transmitting next to the main signal data on the orientation of the transmitting and receiving units, which makes it possible to enter the corner correction of blocks in a timely manner.

For dynamic guidance of bunches and minimization of losses use a variety of schemes. The most optimal devices can contain two circuits of compensation of angular displacements: one – for slow changes of the second – to track changes, small and high-speed (vibrations caused by a tram or a whisper near a person).

According to Canon, the use of such systems allows for reliable communication even during hurricane wind loads and duststorms.

18.9.2. Impact of turbulence on the characteristics of the optical channel

First of all, we will introduce the concept (somewhat speculatively, but not strictly) of the scale of turbulence. Under the scale of turbulence, we will understand the transverse dimensions of heterogeneity, which is formed as a result of some physical disturbance (temperature distribution of earth-air, wind, etc.). At the same time, we will assume that within the heterogeneity of optical characteristics can be considered sustainable.

Consider 3 cases (see Figure 18.13):

- The scale of turbulence is close behind the roses with a dimemeter of the light beam $d \sim D$.
- The scale of turbulence far exceeds the diameter of the beam $d << D$.
- The scale of turbulence is much smaller than the diameter of the beam $d >> D$.
- In the first case, the disturbance of the atmosphere leads to the corresponding curvature of the wave front (the introduction of additional aberations). This in turn leads to:
- additional expansion of the beam, as a result of deterioration of the energy characteristics of the system (part of the beam does not enter the inlet of the optical receiving antenna)
- expansion of the scattering spot in the plane of the photo receiver. Additional energy losses (with appropriate sizes of FP plane) and reduced field of view of the system (reducing the adaptability of the system to mechanical interference.
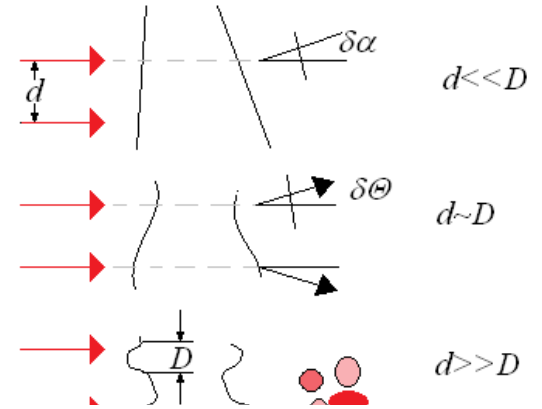
Рис. 18.13

However, the impact of turbulence of this type can in principle be neglected. From the literature [55] known ratio, which describes the increase in beam size when passing through a turbulent atmosphere:

$$\Delta d = 4.5 \cdot 10^{-6} z^{1/2} \qquad (18.23)$$

At the length of the track z=3600 m $\Delta d \sim 3$ mm.

Increasing the size of the diffusing spot in the FP plane can also be neglected. Indeed, even the extended spot has dimensions within the mm of the dos. If the transverse dimensions of the FP plane are about 10 mm, then such an increase will not lead to a significant deterioration in the characteristics of the system.
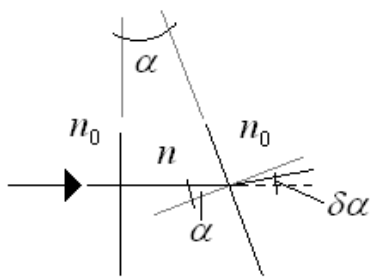
Fig. 18.14.

Exposure to the second type of turbulence (see Figure 18.14).

The beam of light that forms the communication channel will pass the "cells" of the space, the thyrization coefficient of which changes randomly. Naturally, the angle α also a random variable. Rejection sign $\delta\alpha$ is likely. Average $\delta\alpha = 0$. So we can assume that the deviation of the beam from the initial direction of distribution is due to the passage of the beam through the last meters of the track.

From the figure it follows that:

$$\delta\alpha \approx \alpha(\frac{n}{n_0} - 1). \qquad (18.24)$$

Estimated Value $\delta\alpha$.

From the literature [55] it is known that changes in the terrification rate caused by humidity (much larger than due to turbulence) do not exceed 0.5%. Let α=30º, which is also significant. Then $\delta\alpha \sim 0.0025$. In fact, this value is much smaller. So,

if the beam shift occurs on the last 10 m of the track, then the displacement of the beam does not exceed the value close to 3 mm.

Consequently, the impact of this type of turbulence can also be neglected. This is confirmed by literary data (Лаз. Навиг. Устройства) where is the value of the angular shear ~ 8-15 angle..

The impact of the third type of turbulence is the most serious. In fact, there is a scattering (diffraction) of the beam on rather small heterogeneities. In the end, this leads to the formation of a heat-picture in the plane of the receiving antenna.

At the same time, this picture changes in time due to the pulsation of the atmosphere of vibrational interference, etc. This accordingly leads to an increase in the noise component. Despite the fact that the maximum frequency characteristics of the pulsation of the atmosphere lies in the area of several Hz, this does not exclude the possibility of random atmospheric flucations during fairly small intervals of time. Taking into account the value of the coefficient BER=$10^{-12} \div 10^{-6}$, even "single" flucation can lead to disruption of the communication session.

Methods of correction of errors of this type:
- Use of multiple emitters
- Application of interference-resistant algorithms, with a high level of redundancy.

18.10. Gasped signal in the atmosphere [55-61]
18.10.1. Model of the atmosphere. Extinguished signal

As usual, the atmosphere has a locally heterogeneous structure (dust, thermal flucation of its parameters, air pollution, etc.), which leads to absorption and scattering, that is, to the weakening of radiation during its spread. As a rule, despite such local heterogeneity, the environment can be considered as homogeneous with certain integral (average) characteristics.
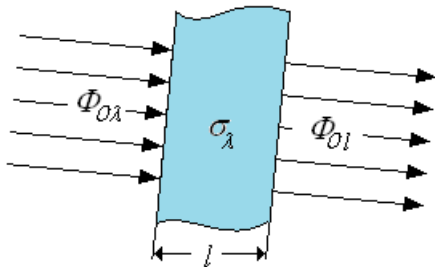
Fig. 18.15. Scheme of immediation (passage) of the atmospheric layer

Consider the main patterns of radiation weakening in such an optical environment. Let a parallel beam of monochromatic radiation stream $\Phi_{0\lambda}$ with wavelength λ enters the layer of the environment thickness l (see Figure 18.15).

We anticipate that the particles of the environment weaken the field independently of each other. Then change the flow (decrease it) when the layer is thick dl can be described by the ratio of:
$$d\Phi_{l\lambda} = -\sigma_\lambda \Phi_{0\lambda} dl, \qquad (18.25)$$
where σ_λ – attenuation coefficient (with dimension, km^{-1}), which generally depends on the properties of the environment and wavelength;
dl – thickness of the elementary layer of the medium in km.

When integrating (18.25) by l get a known expression for the Law of Booger:
$$\Phi_{l\lambda} = \Phi_{0\lambda} e^{-\sigma_\lambda l}, \qquad (18.26)$$
where $\Phi_{l\lambda}$ – monochromatic radiation stream at the output of the medium layer.

Based on (18.26) it is possible to write an expression for The Bouger Law in terms of radiation intensity:

$$J_{l\lambda} = J_{0\lambda}e^{-\sigma_\lambda l} = J_{0\lambda}\tau_{y\lambda}^l, \qquad (18.27)$$

where $J_{0\lambda}, J_{l\lambda}$ – intensity of monochromatic radiation before and after passing the medium layer (W/sterade); $\tau_{y\lambda}$ – spectral transparency coefficient of the environment with a length of 1 km (specific passing) – $\tau_{y\lambda} = e^{-\sigma_\lambda}$.

Multipliers $\sigma_\lambda l = \tau_\lambda$ is called the optical thickness of the environment layer, and the coefficient in the expression (18.27) $\tau_{y\lambda}^l = T_\lambda$ – spectral coefficient of passing (transparency) of optical environment.

It should be noted that addiction $\tau_{y\lambda}$ for the atmosphere has a selective λ character.

Thus, the expression (18.27) can be written as:

$$J_{l\lambda} = J_{0\lambda}T_\lambda. \qquad (18.28)$$

18.10.2. Atmospheric fractions that affect signal attenuation

Consider the main factors that determine the magnitude of the weakening (attenuation) of the signal in the Earth's atmosphere. Such factors are selective (per λ) molecular absorption and scattering, as well as selective scattering on particles (aerosols)).

Earth's atmosphere can be imagined as an optical medium containing a mixture of gases and water vapor and foreign solid and liquid particles weighed in it – aerosols (water droplets that occur during condensation of water vapor, gunpowder, smoke particles, etc.), the size of which ranges from $5 \cdot 10^{-6}$ to $5 \cdot 10^{-3}$ cm. Nitrogen (78%) and oxygen (21%) are the main permanent components of the squat layer of the atmosphere. The fate of other gases (carbon dioxide, hydrogen, ozone, argon, xenon, etc.) comes less than one percent of the volume
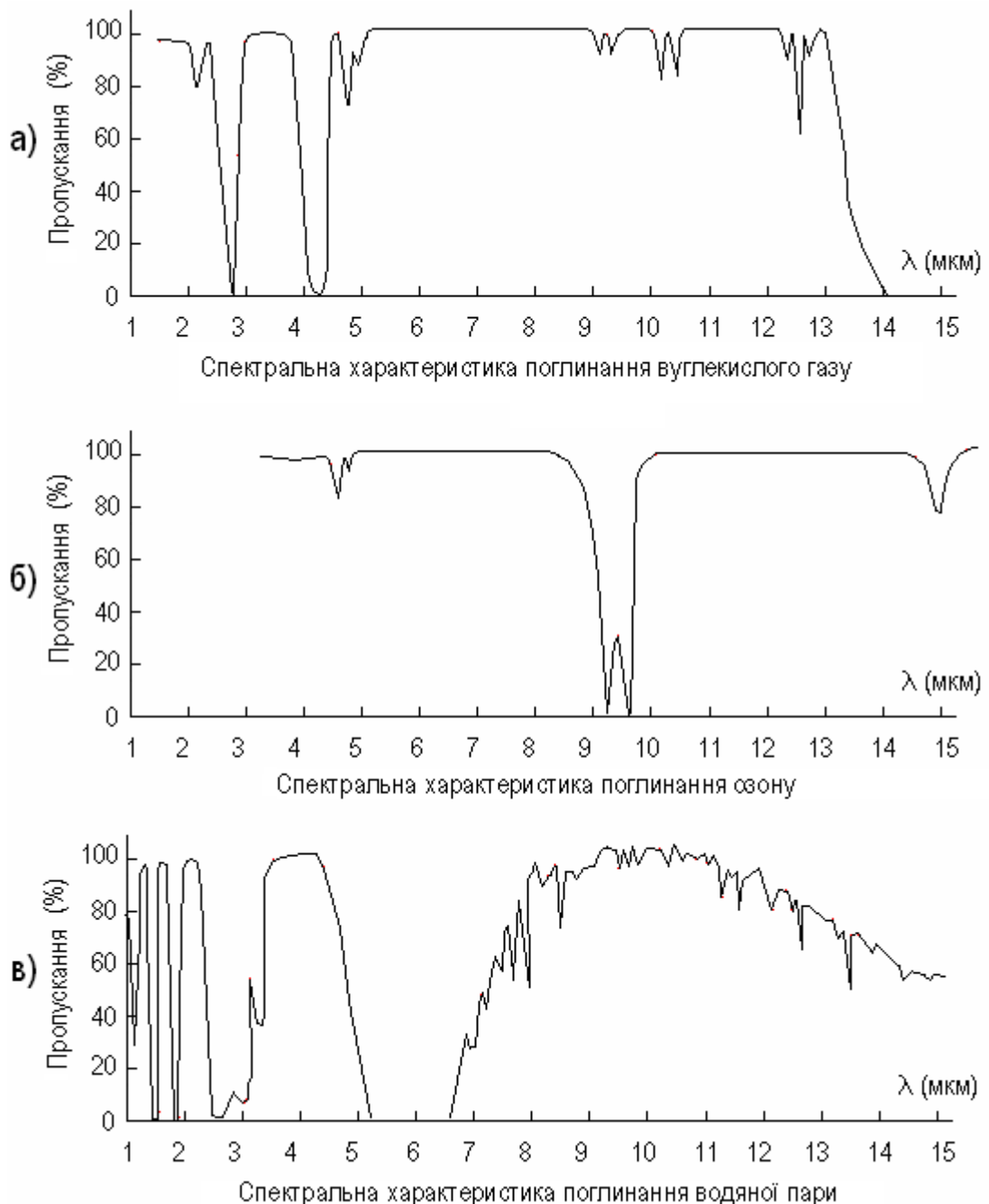
The optical properties (transparency) of the atmosphere are mainly influenced by water in gas and liquid phases, carbon dioxide, ozone, as well as aerosols. Their number in the Earth's atmosphere is different at different heights, in different geographical areas and depends on meteorological conditions. In addition, the composition of the atmosphere varies continuously due to turbulence, that is. chaotic edema movements of atmospheric layers. The concentration of water vapor in the atmosphere depends on the geographical location of the area, the time of year, the height of the atmosphere layer, local weather conditions and ranges in volume from 0.001 to 4%. The main amount of water vapor is concentrated in the lower five-kilometer layer and decreases sharply as the height increases.

The concentration of CO2 with an increase in height from 0 to 25 km is slightly

changed: from 0.03 to 0.05% by volume. The concentration of ozone in heights is uneven. Its main part is located in the atmospheric layers at an altitude of 15-40 km with a maximum concentration at an altitude of up to 25-30 km (more than 0.001%); in the lower layers of the atmosphere (height up to 20-25 km) the concentration of ozone does not exceed 10-5%. Carbon monoxide has a wavelength of 47 microns; ozone – weak absorption band at 4 microns and strong at wavelengths of 4.5 and 7.8 microns.

The attenuation caused by the main gases is illustrated by Figure 18.16.
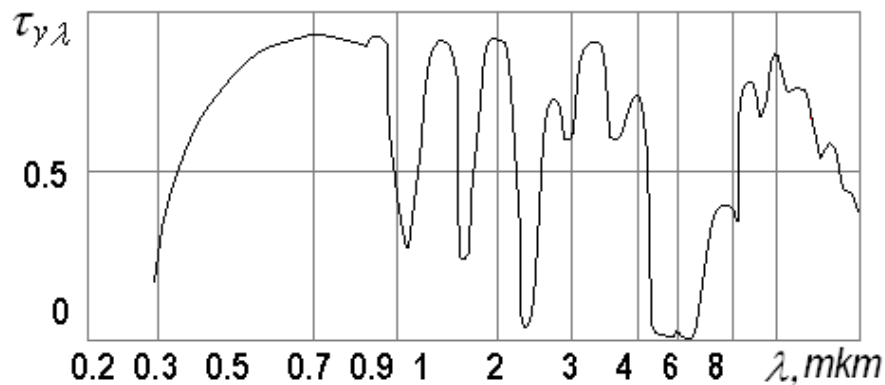
Fig. 18.17. Dependence of the spectral coefficient of passing the "clean" atmosphere on the wavelength

The dependence of the spectral coefficient of passing the "clean" atmosphere on the wavelength is shown in Figure 18.17.

The weakening of radiation in the atmosphere is due not only to its absorption, but also to scattering. Due to the optical heterogeneity of the atmosphere, thraxes, reflections and diffractions of electromagnetic oscillations occur on these heterogeneities. If the dimensions of particles weighed in the atmosphere are small compared to the wavelength of oscillations, then molecular scattering occurs, which obeys the law of the Relay. According to this law, the intensity of radiation scattering is inversely proportional to the wavelength in the fourth stage. Molecular scattering is quite large in the visible and infrared regions of the spectrum. The weakening of radiation as a result of relay scattering can be many times greater than molecular absorption. At particle sizes that are proportional in size to the wavelength of radiation, diffraction scattering is observed. This type of scattering is asymmetrical: more radiation energy dissipates forward than backwards.

If the particle size is much larger than the wavelength, then there is a geometric scattering, which is manifested mainly in the infrared region of the spectrum.

In the real atmosphere, all three types of scattering take place, since it contains the frequents of almost all the specified sizes. The greatest scattering of light flows is observed at low altitudes (up to 1000 m) especially in cities where the smoke of industrial enterprises and gunpowder greatly cloud the atmosphere, that is, in those places where the use of FSO systems is supposed to be used.

The selective nature of the absorption and dispersion of laser radiation by the atmosphere due to the presence of "transparency windows" in it, which are most

pronounced in the wavelengths of 0.38-0.9 and 9-13 microns. As the height of the atmospheric layer increases, the width of these "windows" increases.

The weakening of laser radiation by dispersion is about two orders of order more than due to absorption. For example, for λ=0,6943(ruby laser) corresponds to the "transparency window" 0,6932-0,6945 microns with $\sigma_{a\lambda}$=0,0023-0,0069 km^{-1} (coefficient of atteniation on absorption) and $\sigma_{s\lambda}$=1,19-0,29 km^{-1} (diffusing coefficient).

Therefore, for the "windows of transparency" of the atmosphere, the approximals of equality are fair:

$$\sigma_\lambda \approx \sigma_{s\lambda} \qquad (18.29)$$

and

$$T_\lambda = \exp(-\sigma_{s\lambda}l). \qquad (18.30)$$

Note that Booger's law is fair when $\sigma_\lambda \leq$15-20 км$^{-1}$. For example, when σ_λ=25 km^{-1} deviation from this law is approximately 30%.

At the same time, the power of the optical signal at the input of the receiver of the receiving module is directly proportional to the spectral coefficient of atmospheric passing:

$$P_\lambda = P_{0\lambda}T_\lambda, \qquad (18.31)$$

where $P_{0\lambda}$ – optical signal power at the receiver input when the system is in free space.

18.10.3. Meteorological range of visibility and atmospheric losses

Note that the measurement of the value σ_λ, the coefficient of flux weakening, which in the rest determines atmospheric losses at the communication distance in practice is not an easy task. At the same time, the situation is much more complicated when it comes to statistics, the receipt of which involves measuring this value for a year or even years.

Based on this, it can be argued that to obtain the value of σ_λ(its statistical distribution for a year) for an ordinary user (developer or distributor of FSO systems) in a particular area is almost impossible.

Therefore, there must be another way of calculating atmospheric losses, which should be based on meteorological data that are available to the average user.

The only data that is relatively accessible to a wide range of consumers is the data on meteorological range of visibility (MDV), which (or its analogue) is measured in almost every region, since information about it is necessary for the normal functioning of the national economy, for example, air transportation.

Let us show that the MDV value in the direct is associated with the integral losses that occur when transmitting a signal in an open communication channel in the visible and near IC ranges.

The concept of meteorological range of visibility (MDV)) S_m was introduced by the International Meteorological Conference (1929), which approved an agreed definition of this magnitude.

In these documents, the following definition of MDV is given: "The meteorological range of visibility is a conditional expression of the transparency of

the atmosphere and is equal to the distance at which, during day daytime under the influence of atmospheric conditions, the perception of a completely black surface with an angular size of at least angular minutes is lost, which is projected against the background of the sky (smoke) in the horizon. At the same time, the most reliable value V (contrast sensitivity of the eye) is 3%".

Note that the value of MDV, which is determined visually is very subjective, since the contrast sensitivity of the eye, for different people, ranges from 0.0077 to 0.06 and even 0.2.

However, today, this is practically the only value that characterizes the transparency of the atmosphere.

Consider how S_m transmitter (attainment) of the signal in the atmosphere. You can show that S_m related to the concept of brightness contrast

$$K = \frac{B_1 - B_2}{B_1}, \tag{18.32}$$

where K – brightness contrast; B_1 – object brightness (visibility guide); B_2 – brightness of the background on which the object is projected. At the same time, B_1 should be more B_2 $(B_1 > B_2)$.

According to Weber-Fechner's law, an object that has brightness B_1 can be defined against the background of B_2 when the value of K exceeds the minimum threshold for contrasting sensitivity of the eye V_{min}. Under day conditions, V_min the value of the computer does not depend on brightness and for large objects it matters close to 0.01-0.02. However, for small angular objects, it grows.

Theoretically, it has been established that the visibility range of a completely black object measuring 20 20 angular minutes corresponds to contrast *(K)*, when the observer's vision is directed along the Earth's surface and remains within the ground layer of air, which can be considered optically homogeneous. Under these conditions, the range of visibility of an object (visibility guide) projected against the background of the sky in the horizon is equal to

$$L = \frac{1}{\sigma} \ln \frac{K}{V_{min}}, \tag{18.33}$$

where L – the visibility range of an entirely black object; σ – integral attenuation rate (attenuation); K – contrast of brightness; V_{min} – threshold of contrast sensitivity of the eye.

Note that the value σ has cumulative averaged by wavelength λ character. Naturally, the corresponding spectral ating coefficient σ_λ depends on many factors and has a rather complex distribution of λ.

Переклад Fig. 18.18.

If the object is completely black, then $K=1$. The L value becomes equal to the grandeur of MDV S_m and ratio (18.33) takes the form

$$S_m = \frac{1}{\sigma}\ln\frac{1}{V_{\min}}. \quad (18.34)$$

Therefore, there is a direct link between the integral atgrium and MDW. Show that a similar connection can be established for the working wavelengths of the FSO system.

However, as we see from Figure 18.17 σ_λ almost a constant value in the visible range. Given this, and the ratio (18.25) can be considered that

$$L = \frac{1}{\sigma_{0\lambda}}\ln\frac{K}{V_{\min}}, \quad (18.35)$$

where $V_{\min}=0{,}02$ – threshold contrast sensitivity of the eye; $\lambda_0=0{,}5$ microns.

Note that the atmospheric passing for working wavelengths, which is usually 0.9 or 1.3 microns, is the same as in the visible range.

Accordingly, under such assumptions, the coefficient of signal atering in the atmosphere for the working wavelengths of the FSO system, depending on weather conditions, is equal to

$$\sigma \approx 3.91\frac{1}{S_m}. \quad (18.36)$$

Table 18.1 can be used to estimate the specific passing and the magnitude of MDV for different weather conditions.

Graphs of dependence of the coefficient of complete weakening of laser radiation in the atmosphere, depending on the meteorological range of visibility for different values of the wavelength of radiation $\sigma_\lambda = f(S_m)$ shown in Figure 18.18.

Table 18.1

Specific atmospheric consumption depending on weather conditions

Atmospheric state	Specific passing, $\tau_{y\lambda}$, км$^{-1}$	S_m, MDV, km
Fog: Very strong	Less than 10^{-34}	Less than 0.05
strong	10^{-34}-$10^{-8,5}$	0,05-0,2
noticeable	$10^{-8,5}$-$10^{-3,4}$	0,2-0,5
weak	$10^{-3,4}$-$2 \cdot 10^{-2}$	0,5-1
Smoke: Very strong	0,02-0,14	1-2
strong	0,14-0,38	2-4
noticeable	0,38-0,68	4-10
weak	0,68-0,82	10-20
Good visibility	0,82—0,92	20—50
Distinctive visibility	0,92 and more	50 and more

Therefore, for the "windows of transparency" of the atmosphere, the approximals of equality are fair:

$$\sigma \approx \sigma_{s\lambda} \tag{18.37}$$

and

$$T = \exp(-\sigma l). \tag{18.38}$$

Note that Buger's law is fair when $\sigma_\lambda \leq 15\text{-}20$ km^{-1}. For example, when $\sigma_\lambda = 25$ km^{-1} deviation from this law is approximately 30%.

Accordingly, the power of the optical signal at the input of the receiver of the receiving module is directly proportional to the spectral coefficient of atmospheric passing:

$$P = P_0 T, \tag{18.39}$$
$$P = P_0 e^{-\sigma l}. \tag{18.40}$$

where P_0 – optical signal power at the receiver input when the system is in free space; σ – attenuation coefficient (with dimension, km^{-1}), l – the thickness of the layer of the environment in km.

In practice, empirical ratio is used to determine the coefficient T when working in the "transparency windows" of the atmosphere:

$$T = \exp(-\frac{3.91 L_{zv}}{S_m}), \tag{18.41}$$

where L_{zv} – communication distance; S_m – meteorological range of visibility (MDV).

Accordingly, the loss of signal strength P_{atm} when the distance signal is received L_{zv} dB are determined by the ratio of:

$$T_{atm} = -10 \lg \left[\exp \left(-\frac{3.91 L_{zv}}{S_m} \right) \right] = 16.98 \frac{L_{zv}}{S_m}. \tag{18.42}$$

19. CALCULATION OF THE AVAILABILITY OF THE FSO-SERIES CHANNEL [63-68]

The calculation of the availability of the AOLZ channel will be carried out according to the following scheme:

- Calculation of the energy budget of the system – the value of the maximum permissible signal atering for the corresponding (specified) communication range, according to the system equation.
- Establishing compliance between permissible attainment and the corresponding minimum ILC $S_{\min}$.
- Probability calculation $P(S_k < S_{\min})$, that is, the likelihood of weather conditions when the IWD is less than $S_{\min}$.
- Calculating channel availability as a probability $P_{Dost} = 1 - P(S_k < S_{\min})$, that is, the probability of weather conditions when the IUD is greater than $S_{\min}$.

Naturally, the implementation of each stage may require additional calculations.

19.1. Calculation of the energy budget of the system – the value of the maximum permissible signal atering

The value of permissible signal atering can be determined according to the system equation (see p. 18.7):

$$\Delta P = P_{\text{per}} - P_{\text{pr}} > T_{\text{opt}} + T_{\text{atm}} = T, \tag{19.1}$$

$$\text{або } \Delta P - T_{\text{opt}} > T_{\text{atm}}, \tag{19.2}$$

where T_{opt} – loss on optical alignment, P_{per} output power of the transmitter unit, which in the first approximation is equal to the power of the laser diode P_{LD}, P_{pr} – maximum sensitivity of the receiving unit, which in the first approximation is equal to the minimum power P_{det}, which the photo receiver can fix, T – signal atering in the atmosphere in dB.

For maximum (permissible) attation, we have a ratio of:

$$T_{\text{dop}} = \Delta P - T_{\text{opt}}, \tag{19.3}$$

At the same time, in the first approximal (see p. 3.6):

$$T_{\text{opt}} = 10\lg\left[\frac{S_{\text{pr}}}{\pi(L_{zv}\theta_0)^2}\right], \tag{19.4}$$

where S_{pr} – reception lens input area, L_{zv} – communication range, θ_0 – light beam discrepancy.

Therefore, the amount of permissible atering T can be obtained taking into account the ratios 19.2 and 19.3.

On the other hand, from the previous consideration, it is known the ratio of:

$$\tau_\lambda = \exp\left[-\frac{3.91L}{S_m}\chi_\lambda\right], \tag{19.5}$$

where L – thickness of the scattering layer of the atmosphere (communication distance); $\chi_\lambda = \frac{\sigma_\lambda}{\sigma_{0\lambda}}$ (for the visible range of wavelengths (including in our case $\chi_\lambda \approx 1$), $\lambda_0 = 0.5$ microns, S_m – meteorological range visibility (MDV)).

From the preliminary review, we have established that $\tau \approx \tau_\lambda$.

Therefore, in the end, we have a ratio of:

$$\tau = \exp(-\frac{3.91 L_{zv}}{S_m}). \tag{19.6}$$

At the same time, the ateration in dB $- T = -10\lg(\tau)$. So

$$T_{atm} = -10\lg\left[\exp\left(-\frac{3.91 L_{zv}}{S_m}\right)\right] = 16.98\frac{L_{zv}}{S_m}. \tag{19.7}$$

19.2. Establishing conformity between permissible attainment and critical (minimum permissible) ILC

According to the ratio (19.7). critical (minimum) value МДВ S_{min} determined by the ratio of:

$$S_{min} = 16.98\frac{L_{zv}}{T_{dop}}. \tag{19.8}$$

19.3. Calculation of the probability of weather conditions when the IWD is less than S_{min}

It is clear that the magnitude of MDV S_m random value, depending on the time of year, day and specific terrain.

One of the methods for determining the law of $F(S_m)$ is the measurement and statistical processing of the obtained values. Such data were obtained and published in [1-5, after Figure 4.1]. Table 19.1 shows the obtained values of the average $\bar{S}_m$ and its mean quadratic deviation δ based on observations of ILC for Moscow (1972-1981) and Odessa (1969-1982) for all months of the year.

Table 19.1

Month	Moscow		Odessa	
	$\bar{S}_m$, km	δ, km	$\bar{S}_m$, km	δ, km
January	6.62	3.49	5.15	3.37
February	6.90	3.49	4.86	3.25
March	7.11	3.61	5.58	3.40
April	8.28	3.12	7.12	3.22
May	9.01	2.41	7.98	3.93
June	9.28	2.07	8.69	2.46
July	8.89	2.51	8.72	2.42
August	8.72	2.69	8.91	2.69
September	8.22	3.07	8.36	2.69
October	7.97	3.25	7.19	3.24
November	6.84	3.63	5.84	3.46
December	6.16	3.70	5.47	3.25
Mid-year	7.83	3.30	7.00	3.36

More "fresh" statistics obtained at the Russian enterprise of the Research Institute of Precision Instrumentation for the period from September 1998 to August 1999 are well coordinated with the results obtained earlier.

Probabilist dispensations (Laws of division $F(S_m)$) MDV in Moscow, obtained by means of statistical processing of measurements for the most favorable month (June) and the least favorable (December) provided in Fig. 2. 19.1.

From the analysis of data, it follows that the laws of S_m depend on many factors. Moreover, the average values of MDW differ quite strongly. So this value in Moscow differs from this value in Odessa by 12%. However, the corresponding variances differ only by 2%.
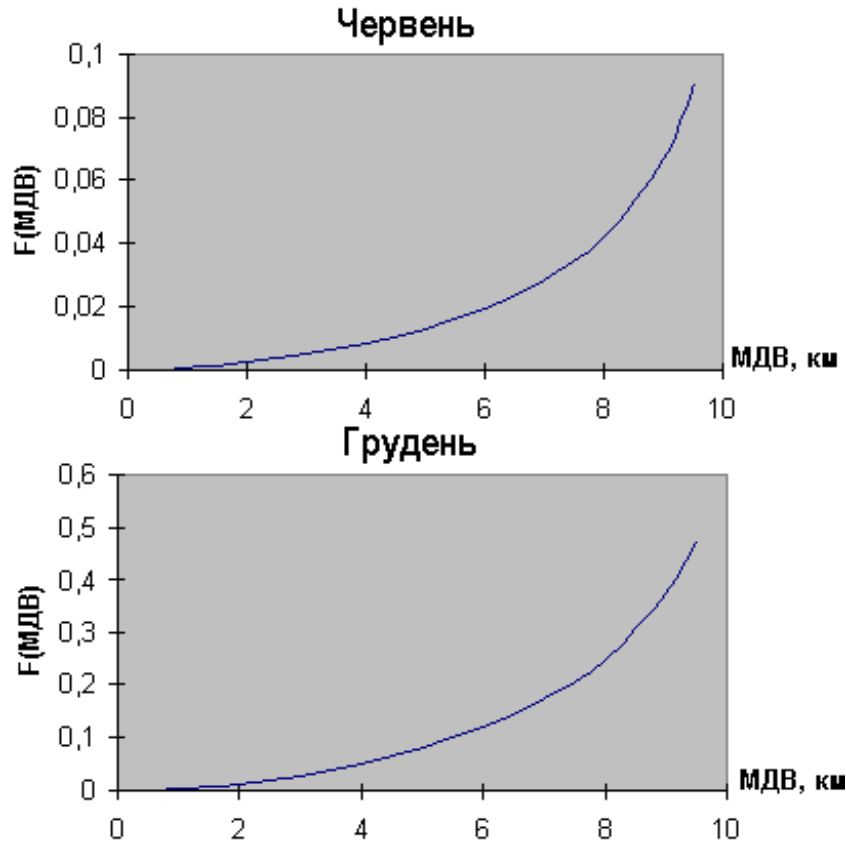
Переклад Fig. 19.1

From the analysis of data, it follows that the laws of S_m depend on many factors. Moreover, the average values of MDW differ quite strongly. So this value in Moscow differs from this value in Odessa by 12%. However, the corresponding variances differ only by 2%.

It is known that the probability that a random value x is in the interval x_1, x_2 determined by the ratio of:

$$P(x_1 < x < x_2) = \int_{x_1}^{x_2} f(x)dx = F(x_2) - F(x_1). \qquad (19.9)$$

At the same time, in our case, $F(x_1) = P(S_m = 0) = 0$, i.e. the probability of zero IUDs is zero.

Accordingly, 19.9 is transformed to the:

$$P(S_m < S_{\min}) = \int_0^{S_{\min}} f(x)dx = F(S_m). \qquad (19.10)$$

Therefore, in order to determine the appropriate probability, it is necessary to know a fully defined function of the distribution $F(S_m)$, or probability distribution density $f(S_m)$.

Note that it is also necessary to know the parameters of distribution or distribution density, such as the average MDV $\bar{S}_m$ and variance δ.

In [1-5, after Figure 5.1] established analytical laws for the distribution of ILC. Thus, the distribution of MDV (in any case for Moscow) is best approximanted by the beta distribution:

$$F(S_m) = \frac{\Gamma(a+b)}{\Gamma(a)\Gamma(b)} \int_0^{S_m} x^{a-1}(1-x)^{b-1}dx, \qquad (19.11)$$

where $\Gamma(t)$ – gamma function; $a = \frac{\bar{S}_m}{10}[\frac{\bar{S}_m(10-\bar{S}_m)}{\delta^2} - 1]$,

$b = \frac{a(10-\bar{S}_m)}{\bar{S}_m}$ – distribution options; $\bar{S}_m$ – MDW average;

δ – mean square deviation of MDV.

19.4. Assessment of weather in Chernivtsi region

Unfortunately, the full picture of the meteorological state in the region is impossible to get, at least averaged data for a long period (10 years or more) of time. The only data that is available to the general user is the data shown in Table 19.2. It presents data on the number of days in each month when fog is observed, which corresponds to the meteorological range of visibility of less than 500 m..

Table 19.2

Average number of days with fog (МДВ≤ 0.5 км)

A – the whole day

B – period from 10 to 18 hours.

No state-tion	Station	Time of day	Month												Half a year 10-3	Half a year 4-9	Year
			1	2	3	4	5	6	7	8	9	10	11	12			
677	Dankivtsi	A	7	5	4	1	0,4	0,2	0,6	0,6	2	4	7	10	38	4,8	41,8
		B	1	1	1	0,1	0	0	0	0	0,5	1	1	2	7	0,6	7,6
680	Chernivtsi AMSM	A	10	7	5	3	1	1	1	2	4	7	11	12	52	12	64
		B	2	1	1	0,7	0,1	0,1	0,1	0,5	1	1	2	2	9	2,5	11,5
690	Selyatyn	A	3	2	2	2	6	6	9	10	9	6	6	5	24	42	66
		B	0,7	0,5	0,5	0,5	1	1	1,5	2	1,5	1	1	1	4,7	7,5	12,2
691	Solonets tsivka	A	2	2	3	3	7	5	5	5	5	5	3	3	18	30	48
		B	0,5	0,5	0,7	0,7	1	1	1	1	1	1	0,7	0,7	4,1	5,7	9,8
	In general, by region	A	5,5	4	3,5	2,3	3,6	3,1	3,9	4,4	5	5,5	6,8	7,5	32,8	22,2	55
		B	1,1	0,8	0,8	0,5	0,5	0,5	0,7	0,9	0,8	1	1,2	1,4	6,2	4,1	10,3

The data are given for the plains (Chernivtsi and Dankivtsi) and mountainous (Selyatyn and Solontsivka) regions of the region. This data is radically different from each other. As we can see for flat areas, the maximum number of days when strong fogs are observed corresponds to the half year of October – March, and for mountainous the most bad weather conditions, in terms of atmospheric transparency, occur between April and August. At the same time, the average annual figures for both regions are approximately the same. The corresponding probability of fog from MDV less than 500 m is given in Table 19.3.

Table 19.3

Probability of fog with MDW≤ 0.5 km
A – the whole day
B – period from 10 to 18 hours.

Station number	Station	Time of day	Probability		
			Half-year 1 10-3 months	Half-year 2 4-9 months	Year
677	Dankivtsi	A	0,21	0,03	0,20
		B	0,04	0,003	0,02
680	Chernivtsi AMSM	A	0,29	0,07	0,18
		B	0,05	0,01	0,03
690	Selyatyn	A	0,13	0,23	0,18
		B	0,03	0,04	0,03
691	Solonets tsivka	A	0,10	0,16	0,13
		B	0,02	0,03	0,03
	In general, by region	A	0,18	0,12	0,15
		B	0,03	0,02	0,03

In order to conduct a full statistical analysis of the situation of ILC behavior in our region, it is necessary to know at least some of its statistical points, and it is better to fully function the distribution. Let's try, at least in some way, to conduct such an analysis.

Naturally, having such data set $\bar{S}_m$ and δ Impossible. Accordingly, it is also impossible to determine the beta distribution. In addition, calculating the probability of applying this type of distribution is not an easy task.

Therefore, instead of applying beta distribution, we assume that the random magnitude of MDV S_m distributed under normal law:

$$f(S_m) = \frac{1}{\sqrt{2\pi\delta}} \exp[-\frac{(S_m - \bar{S}_m)^2}{2\delta^2}], \qquad (19.12)$$

where $\bar{S}_m$ – average annual MDV, δ – the average quadratic deviation of MDV from $\bar{S}_m$. This is a pretty logical assumption. The only negative factor is that such a distribution does not reach zero when $S_m = 0$.

In the expression (19.12) unknown are values $\bar{S}_m$ and δ.

Use table data 19.3. Accordingly, the probability given by the table is determined by the ratio of:

$$P(S_m < 0.5) = 0.03 = \frac{1}{\sqrt{2\pi\delta}} \int_0^{0.5} \exp[-\frac{(S_m - \bar{S}_m)^2}{2\delta^2}] dS_m. \qquad (19.13)$$

Naturally, the magnitudes $\bar{S}_m$ and δ depend on the terrain. However, it can be predicted that δ should not be very different for the territory of Ukraine. How, it was given above the average yearly MDV $\bar{S}_m$ for Moscow and Odessa is 7.83 and 7 km, that is, they differ by 12%. At the same time, variances δ(respectively, 3.30 and 3.36 km) differ much less than 2%. Therefore, we will assume that approximately with the same accuracy δ for Chernivtsi is 3.36 km. Then from

(19.13) we find that the average meteorological range of visibility $\bar{S}_m$ for Chernivtsi region at the time of day from the 10th to the 18th is a value close to 5.5 km.

19.5. Calculation of availability of AOLZ channel in Chernivtsi region

We will calculate the availability of the channel under the following conditions:

1. The calculation will be carried out for two values of the distance of communication

L_1=0.5 km and L_2=1 and

2. We assume that the dynamic range of the FSO-system lies within 30-50 dBm. Accordingly, the ateration of the signal in the atmosphere should not exceed this value. In other words, communication will be normally established if MDV is more

3. This dynamic range corresponds to the ratio of MDV values S_m, which lie in the interval:

- for L_1=0.5 км – S_m should be more than S_{min}=0.17-0.28 km
- for L_2=1 км – S_m should be more than ніж S_{min}=0.34-0.56 km

In other words, communication will be normally established if $S_m > S_{min}$.

Now, given that $\bar{S}_m$=5.5 km and δ=3.36 km, and using the ratio of 19.13 find the probability $P(S_m < S_{min})$ for each link length and for the maximum and minimum dynamic range value.

Accordingly, the availability of the AOLZ channel can be determined by the:
$$P_{Dost} = 1 - P(S_m < S_{min}). \qquad (19.14)$$
The results of calculations are given in Table 19.4.

Table 19.4

Availability of AOLZ channel in Chernivtsi region

Communication distance, m	Dynamic range of FSO system, dBm	Availability of the AOLZ channel
500	30	0.99931
	50	0.99987
1000	30	0.99600
	50	0.99865

Thus, it can be argued that in the Chernivtsi region, with a communication distance close to 500 m, the availability of the channel is close to 0.9999 ("four nine"). With an increase in the distance of only twice (1000 m), the availability of the channel decreases by an order of magnitude (the value is close to "three nine").

19.6. Some calculated and experimental data on the impact of weather systems on the operation of FSO systems [63,64]

In the literature there are data on the study of the work of specific FSO systems in the conditions of changing the weather situation. Note that such data are "tied" to a specific area.
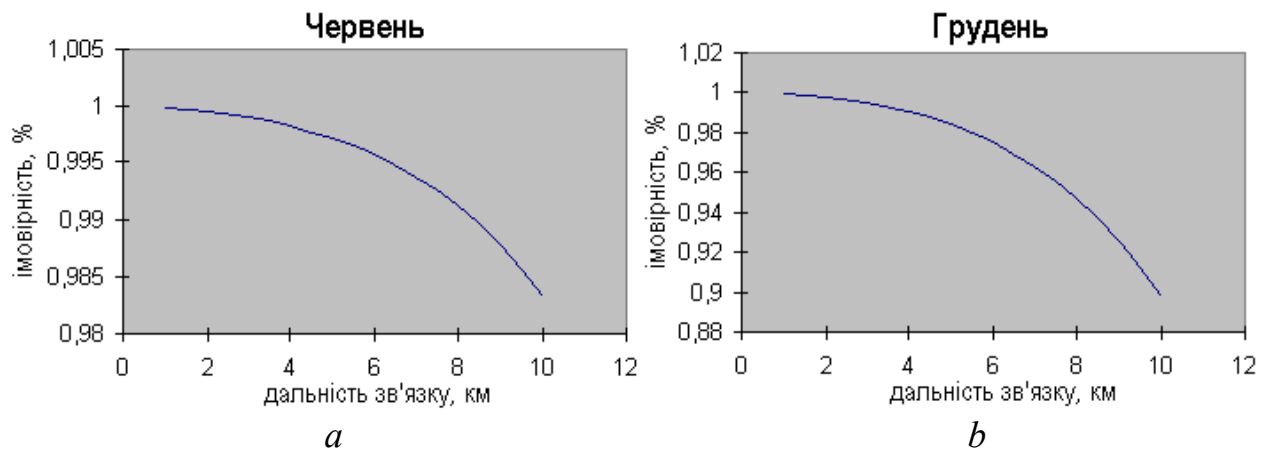
переклад Fig. 19.2

As you can see from Figure 19.1. probability that $S_m < S_{\min}$ MDV increases in December compared to June 5 or more times. Including $P(S_m < 8\text{км}) = F(8)$ for June is close to 0.04, and for December order 0.2.

In Fig. 2. 19.2 estimated dependences on the probability of AOLZ (channel availability) from the range of communication for June and December in Moscow are provided.

When calculating, the following characteristics of the terminal were used with the following parameters:

- transmitter power in pulse – 160 mW;
- receiver sensitivity – 10^{-12} W/Hz$^{1/2}$;
- diameter of the inlet of the receiving antenna – 100 мм;
- information transmission speed – 8 Mbps;
- Divergence beam – 4,1 angle. min.;
- Mistake coeff (RER) – 10^{-10}.

As follows from the figure at a distance of up to 5 km, the probability of communication even in bad weather conditions is at least 0.98.

The probability value of a relationship [62] for different distances and two terminals is shown in Table 19.5. Under the condition that the coefficient BER =10^{-6}. At terminal No. 1, the power of the transmitter in the pulse was 200 mW, the sensitivity of the receiver 5×10^{-12} W/Hz$^{1/2}$, effective diameter of receiving antenna 20 cm, transmission speed 140 Mbps. At terminal 2, these values are equal to 100 mW accordingly, $0{,}6\times10^{-12}$ W/Hz$^{1/2}$, 10 cm і 8 Mbps. From the calculations it follows that the probability of failure-free work of the track at a distance of up to 3 km at the error coefficient 10^{-6} –not lower than 0.993. This is higher than the requirements for radio relay communication lines, the probability of uptime of which should be not lower than 0.9925, which corresponds to 0.75% of the time during which the parcel coefficient does not exceed the specified value.

Table 19.5

Terminal	Communication line length, km	Probability of a relationship
№ 1	0,5	0,99985
	1,0	0,99939
	2,0	0,99729
	3,0	0,99301
№ 2	0,5	0,99988
	1,0	0,99955
	2,0	0,99818
	3,0	0,99564

In Fig. 2. 19.3 the results of calculation of the value (*1-P*), %, which can be called "inaccessibility of the channel" (*P* – availability of the communication line), depending on the distance of communication *L*, km, are provided. Calculations were made for the atmosphere of the Moscow region, for communication lines with different potential.
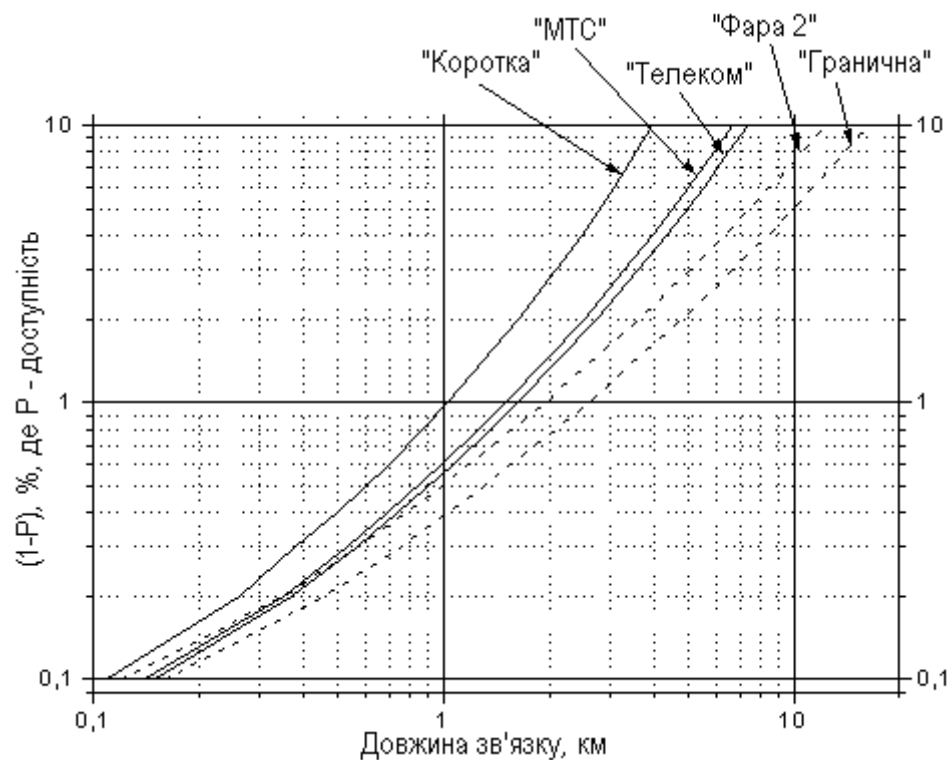
Переклад Fig. 19.3

The figure shows that for P= 0,998 (mainline lines) the reachable communication range is several hundred meters and very poorly depends on the parameters of AOLZ. Namely, from 250 m for the simplest and cheapest to 460 m for lines with maximum energy parameters, which are limited to the level of development of the modern element base (the cost of such systems is more than 50 thousand US dollars). The ratio of the communication range to the ILC is 1.85.

For the value P = 0.99, the picture is more favorable. Reachable communication range ranges from 1.0... 2.5 km for different lines. The ratio of the communication range to the ILC is exactly 2.5. For middle class lines, the reachable communication range is 1.5... 1.6 km.

And finally, with a further decrease in the permissible amount of availability, good prospects open up. For example, for P=0.95, the reachable communication range fluctuates between 2.5... 10 km. The ratio of the communication range to the ILC is exactly 4.0.

The given data corresponds to the transfer rate of 100... 140 Mbps For speeds of 2... 8 Mbps the situation is more optimistic, although the general trends noted above remain.

As a last example, we give graphs of stability of SkyCell systems (British firm PAV DATA SYSTEMS, to some extent a leader in the development, manufacture and implementation of FSO systems) to fog and rain in winter and outside megacities (to reduce the effects of impurities in the atmosphere):
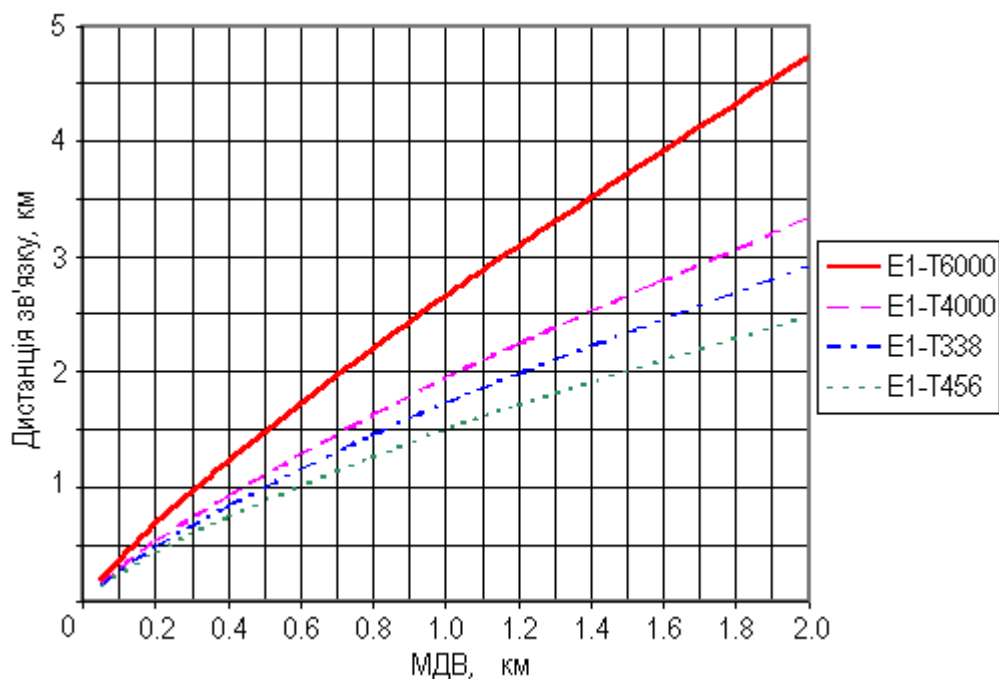
Переклад Fig. 19.4. Maximum working distances depending on meteorological visibility in fog.

Areas below the lines in the graphs determine the working areas of optical systems. The same lines mean the limit when the error rate in the channel (BER) becomes 1.0^{-9}.

With Rice. 19.4 it becomes obvious that the SkyCell E1-T6000 system installed at a distance of 2000 meters is able to work normally with meteorological visibility in the fog of about 709 meters. And how will the transmission channel behave near this boundary? If weather conditions worsen, the error rate will first increase. BER value below 1.0^{-3} will mean, in fact, the failure of the transmission channel. Further deterioration of visibility will result in complete blocking of the channel. In reality,

the channel will remain working until visibility drops to 640 meters. The behavior of SkyCell E1-T6000 systems can be illustrated with Figure 19.6.
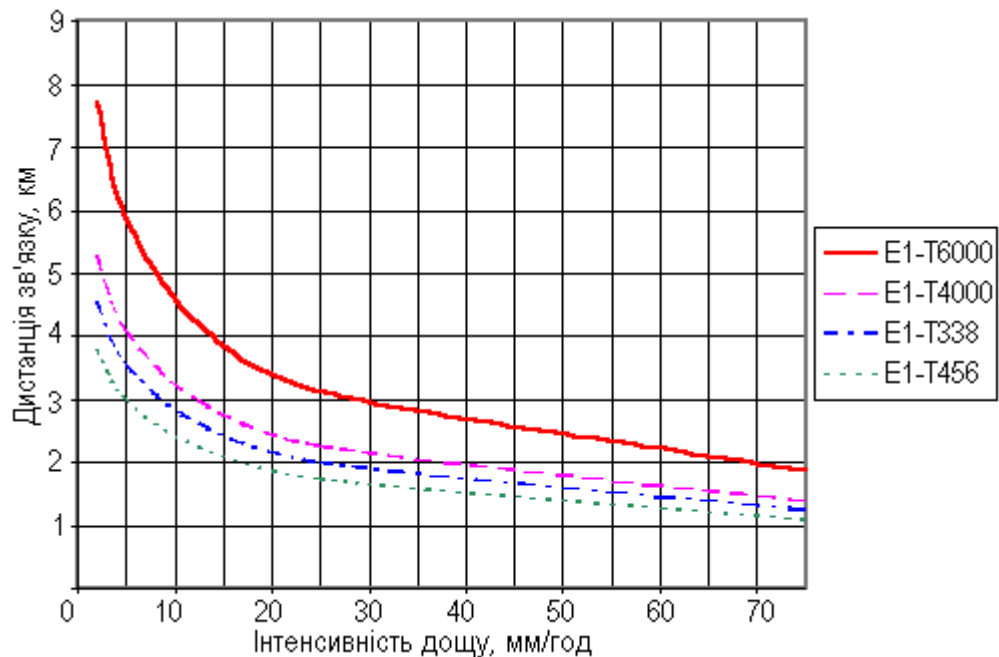
Переклад Fig. 19.5. Maximum working distances depending on rain intensity
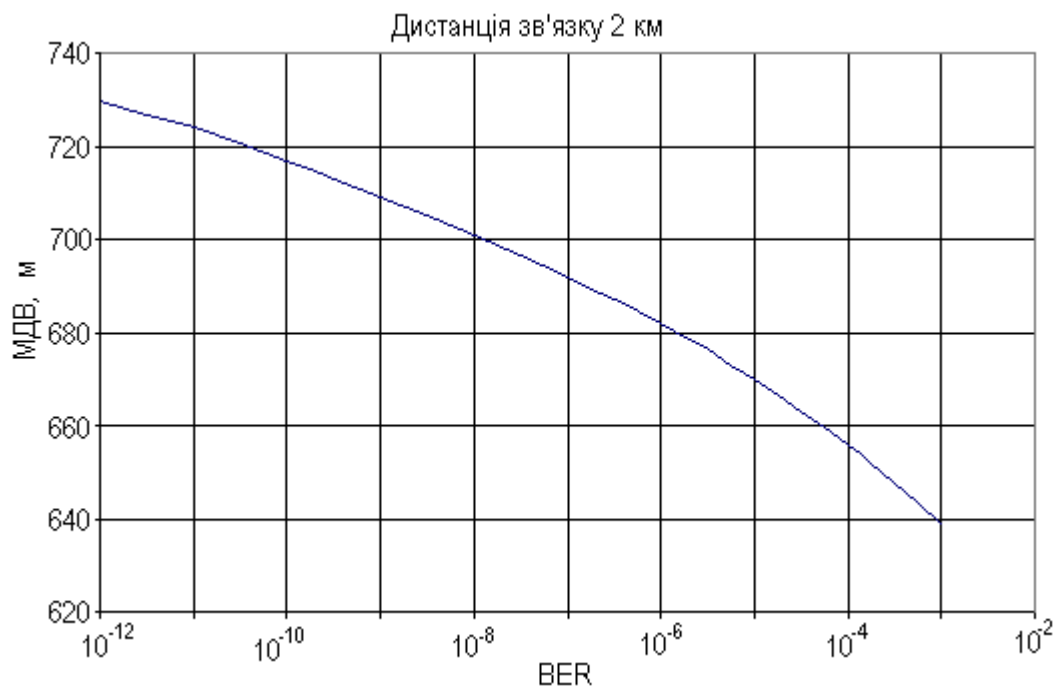
Переклад Fig. 19.6. Error level in the channel in the fog at a distance of 2 km.

The above results of calculations are confirmed by the data of testing and test operation of systems. To obtain the most "practical" parameter – channel availability factor, you must have weather statistics in a particular region. MicroMax's research shows that weather services understand similar requests and respond promptly to them. Knowing the resilience of systems to all weather systems likely to be installed

on the messenger, you can predict this parameter with high reliability and ensure the effective operation of the data transmission system. From the conducted consideration we can draw the following conclusion [69,70]– in fact, the performance of the FSO-system, the maximum communication distance (at the specified BER coefficients, and the availability of the communication channel) depends little on the dynamic range of the system (energy budget) and its cost.

This becomes clear if we take into account such facts This becomes clear if we take into account such facts:
1. Regardless of the dynamic range of the system in bad weather conditions, the communication length on average does not exceed 0.5-1 km
2. In most cases, the communication distance (due to the specifics of the use of FSO systems) does not exceed such values.

Let us turn to the following table in order to more carefully understand the specifics of FSO systems. The data in the table corresponding to the practical system correspond to the equipment, which has a relatively low cost. The cost of the "ideal" system is 2-3 orders of order higher.

Table 19.6

	Practical system		"Perfect" system	
Emitted power	30 mW	15 dBm	10 W	40 dBm
Receiver sensitivity	25 mW	-46 dBm	1 nanoWatt	-60 dBm
Guiding losses		3 dB		0
Optical losses		4		0
Stock by capacity		54 dB		100 dB
Distance in fog with at least 350 dB/km		140 Metres		286 Metres

In conclusion, we will conduct another analysis. The initial data for him is quite a practical task: the corporate user has just expanded with the help of another office located in the building nearby, and at the same time – in the conditions of direct visibility. Both offices have deployed 100 Mbps Ethernet LAN. The only channel between buildings with a capacity of 2 Mbps belongs to an operator not associated with the company. The cost of renting a line is "X" dollars. The user considers the option of purchasing FSO equipment worth "Y" dollars. It is necessary to choose between systems A and B, one of which is designed for a maximum range of 1100 meters, the other – for 4000 meters (and, accordingly, have different budgets of losses and, accordingly, different prices).

Figure 19.7. provides long-term availability coefficients for both lines (for San Francisco conditions) as a range function. As you can see, at distances within 400

meters, both lines have the same accessibility factor at the level of 99.8%. The choice in favor of a cheaper system is obvious.
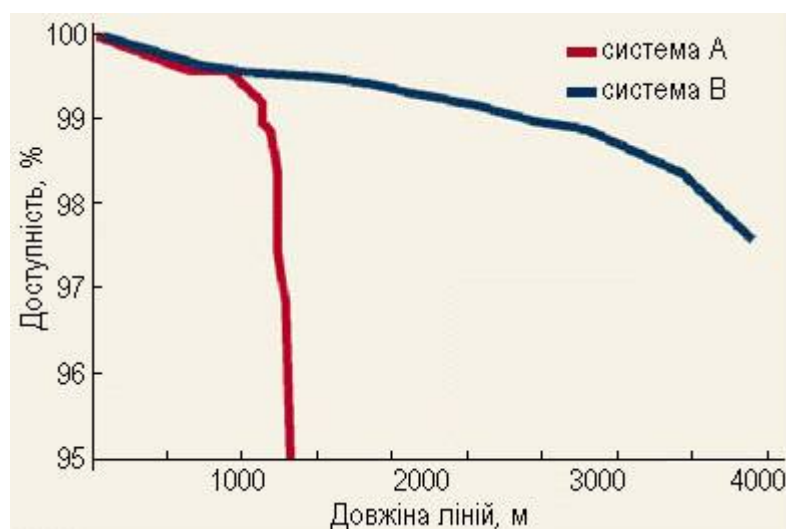
Переклад Fig. 19.7. Channel availability for systems A and B.

The difference begins to be felt at distances close to 900 meters. The availability of a cheaper system drops to 99.3%. System B availability remains close to 99.6. At distances of more than 1100 meters, the difference becomes catastrophic.

The choice in favor of system B at such distances would seem obvious. Terabeam uses a team of five meteorologists to solve such problems – weather control and modeling in the city. The obtained data and maps are used to determine the optimal power of the transmitter and the possible communication distance. However, the graph "lacks" another axis – dependence of the availability factor on the time of day. Indeed fog is usually a temporary phenomenon and is observed late in dinner and in the morning when most offices are out of work.

The general conclusion from the above example is as follows: at distances of less than one kilometer, most FSO systems have a loss budget sufficient for peaceful "coexistence" with fog.

For such communication distances, the performance of the system will be determined, first of all, by the protection of the system from the influence of mechanical factors, the vibration of buildings, and, as a result, a change in the position of the emiator (receiver) and the directions of the bunches. So, at a communication distance of more than 100-200 m, it is desirable that the FSO-system be equipped with appropriate dynamic (appropriate) guidance systems for laser beams. In some cases, the deviation of the building from the vertical under the action, for example, wind, can reach values close to 1 meter.. We will add more microvibrations and thermal heterogeneities that can cause angular deviations of the transmitter. In general, without dynamic guidance, the budget of losses will also be determined by the ratio of the area of the spot created by the transmitter on the inlet of the receiving unit to the area of this hole, the location of the spot relative to the receiving unit, the distribution of radiation power along the spot, etc. Such losses caused by mechanical factors constitute a value close to 15-30 dB. So the stock reserved "in the fog" may well be "eaten" by guiding errors!

Thus, the following conclusions can be drawn from the conducted consideration:

1. The use of atmospheric communication lines on main lines requiring availability of significantly more than 0.99 is obviously impractical. Accordingly, it is unpromising to increase the speed of data transmission, in any case more than 622 Mbps or Gigabit Ethernet.

2. On the other hand, the use of AOLZ in networks where the permissible amount of availability does not exceed 0.99 is quite promising.

3. At the same time, the maximum communication length does not exceed an average of 0.5-1 km.

4. Obviously, lower availability under other equal conditions have low-speed communication channels of 2...8 Mbps. In this area of application of AOLZ, there is a significant win in the reachable communication range (up to 4 times) with an increase in the communication line potential from 40 dB (cheap lines of 3-5 thousand US dollars) to 80 dB (expensive lines with limit parameters, more than 50 thousand US dollars). One such area where high availability is not required is Ethernet networks.

20. TECHNICAL AND ECONOMIC INDICATORS OF DIGITAL NETWORKS BASED ON AOLZ. THE CURRENT STATE OF THE MARKET [70,71]

20.1. Comparison of financial, time and other costs when building different communication lines

We will make certain estimates regarding the duration and cost of the main stages of AOLZ design and construction compared to the construction of other types of communication lines. We will compare the cost of building lines depending on their length. We will make estimates based on the data of the Russian company AO "Telecom", since there is no relevant data on Ukraine. At the same time, the specifics of the legislative, organizational framework and in the end the mentality are very close.

Once again, an important feature of AOLZ is the absence of the need to obtain permission for frequencies during the installation and operation of such systems, unlike radio relay communication lines (RSL). In other words, a long and rather expensive process of obtaining radio frequencies is excluded.

When receiving radio frequencies for the construction of the RSL, an application is first issued. On the basis of the application, the calculation and verification of electromagnetic compatibility with civilian and special purpose REM is carried out. According to the results of the electromagnetic compatibility check, the FSUP "Main Radio Frequency Center" (PIC) of the Russian Federation issues a permit for the use of the frequency range and pays for the required number of frequency points. Consideration and receipt of frequencies at specific points of location of radio relay lines usually occurs within 3-4 months. The cost of checking electromagnetic compatibility and obtaining frequencies per flight of the RSL can reach 4-5 thousand US dollars. Significant costs are also required for the calculation, measurement of levels of electromagnetic radiation and obtaining permission from the State Sanitary and Submeasive To Install the RSL.

Another advantage of AOLZ is that there is no need to receive technical conditions for construction. When laying fiber optic communication lines (FCC) in the sewer, it is necessary to obtain technical specifications for laying the cable from local communication units, which usually occurs within 1-2 months, while, as a rule, technical conditions contain a large amount of work on the laying, restoration or repair of telephone sewage and pads. Practice shows that the volume of additional robots can range from 20 to 50% of the cost of construction of the VOLZ.

Table 20.1 shows the duration and estimated cost of the main stages of design and construction of different types of communication lines.

Figure 20.1 compares the cost of building digital communication lines of different types, depending on the length of the track. Tests of AOLZ at speeds from 34 to 140 Mbps, which were carried out in Moscow and the Moscow region, showed insufficient reliability of the lines at the length of the track more than 2.5-3 km, so long tracks have relay areas with a length of 2 km.

Table 20.1

Duration and estimated cost of the main stages of design and construction of different types of communication lines

Будівництво РРЛЗ	Будівництво ВОЛЗ	Будівництво АОЛЗ
Calculation and verification of EMC with civilian REM	Obtaining technical specifications from local communication nodes	Development of a working project
Checking electromagnetic compatibility with military REM	Development of a working project	
Obtaining permission from the FSUPGRZ of the Russian Federation for the use of radio frequency bands and payment for radio frequency assignments	Coordination of the working project with local communication nodes, with The Gormost Gup and collectors	
Development of a working project (performed simultaneously with the first three points	Coordination of the volume of additional robots with local communication nodes, with The Gormost Gup and collectors	
Registration and payment of permission of the Head of the State Service of The Russian Federation for the purchase of import equipment	Conclusion of sewerage lease agreements	
Calculation of EM radiation levels and obtaining permission from the State Sanitary and Epidemiological Surveillance	Performing additional robots for local communication units, Gormost and collectors	
Obtaining permission from the Glavderzhezzdjaznadzor of the Russian Federation for the construction of the RSL	Obtaining a permit for laying FPZ	
The total duration of the project work		
3-6 months	2-4 months	Less than 1 month
The cost of design robots		
4-5 thousand rubles. $100,0 U.S. to fly	1-3 thousand rubles. $100,0 U.S. 1 km cable	1 thousand rubles. $100,0 U.S. on a flight up to 2 km
Purchase of equipment	Purchase of equipment and cable	Purchase of equipment
Construction and installation of RSL	Construction of AUSD, installation and delivery to the customer	Construction of AOLZ, installation and delivery to the customer
Obtaining a temporary permit from the FSUPGRC of the Russian Federation for the work of REM with radiation		
Delivery of RSL to the customer		
The total duration of construction works		
2-4 months	2-3 months	2-3 months
The total design and construction period of the line		
5-9 months	4-6 months	3-4 months
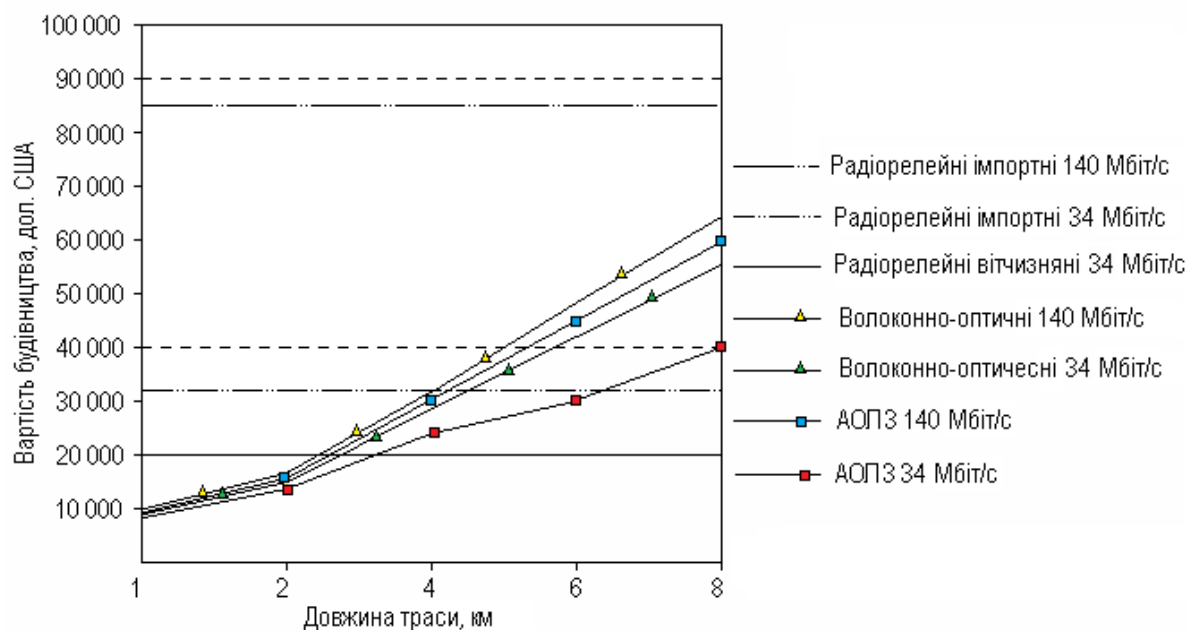
Переклад Fig. 20.1

Based on this data, you can draw the following conclusions: The cost of construction of AOLZ at speeds from 34 to 140 Mbps and the length of the track up to 2-3 km is compared with the cost of FOCLs and significantly lower in the equation with the RSL.

The cost of construction of AOLZ at speeds of 34 Mbps and distances of the track more than 4 km (relay areas of 2 km) is close to the cost of construction of FOCLs and higher in the equation with the RSL by 34 Mbps.

The cost of construction of AOLZ at speeds up to 140 Mbps and the distances of the track up to 8-10 km (relay areas of 2 km) is comparable to the cost of FOCls and lower compared to the RSL at 140 Mbps..

Unlike laying FOLZ with its need to obtain technical specifications and with a large volume of additional robots, the cost of creating communication lines based on AOLZ is reduced by 20-40%, and construction time - two to three times.

Unlike the construction of the RSL, when it is necessary to check electromagnetic compatibility and obtain frequencies, the cost of creating communication lines based on AOLZ at speeds from 34 to 140 Mbps and the lengths of the track to 2-3 km is reduced by 20-30%, and construction time - two to three times. It should be especially noted that domestic RSLs at a speed of 140 Mbps are not produced, so the cost of creating communication lines based on AOLZ is reduced by two to three times.

It is important to note that the cost of operation of AOLZ at the length of the communication line up to 4-6 km is comparable to the cost of operation of the RSL and even lower compared to FPZ due to the lack of costs for the rental of telephone sewage and cable maintenance.

Comparing the conditions for construction and installation work on communication cables that are laid in the ground or sewerage, and AOLZ, it can be argued that the construction of atmospheric lines significantly wins over time compared to laying cables in the finished sewer.

Installation of atmospheric optical terminals with a track length of up to 2.5 km, with mounting on the roof of the building and laying the necessary cables takes place by a team of three people in about 3-4 hours, with preliminary guidance to a nearby main communication unit. Accurate adjustment of special devices takes as usual 10-20 minutes.

Laying fiber optic cable up to 2.5 km long in the telephone sewer takes several days, with the need for a team of four or five people, a car with a winch and several coils with building cable lengths. After laying the cable, the couplings are mounted, the cable parameters are measured, the cross is connected, the cable is installed under excessive pressure.

During the construction of telephone sewage or laying cable in the ground, the cost of construction of FAZ can increase several times, and the laying time will stretch for 5-6 months, since laying telephone sewage or cable in the ground is carried out, as a rule, in the summer.

The use of AOLZ changes the entire course of the construction of local communication networks, as the most difficult and expensive work on the construction of telephone sewage, laying and installation of cable disappears. Installation of atmospheric optical terminals can be carried out by personnel in a few hours without performing any heavy work.

In some cases, for example, when laying communication lines through river crossings, bridges and an iron road, the construction of communication lines based on AOLZ can cost several times lower than the cost of construction of FTA.

The research of design and construction of the CSC DECT-standard on the basis of AOLZ shows that the full cycle of design, construction and delivery of the network can be carried out in 5-6 months, while the cost of construction is reduced by 20-40% compared to the implementation of the network using RSL or FOLZ..

20.2. Analysis of existing solutions and market of FSO-systems

Once again about the advantages and disadvantages of wireless communication technology – AOLZ. In favor of AOLZ technology, the following facts testify:

- data transfer speed can reach multiple Gbps;
- frequency of error bits (BER) from 10^{-10} to 10^{-9};
- no country in the world requires a license to use the frequency range used in AOLZ systems;
- almost one hundred percent protection against interference with radiodiapason (interference can only directly affect the final equipment);
- short time (close to one or several hours) installation of the system;
- lower compared to other pass-through-like technical solutions, the cost of.

The disadvantage of existing AOLZ is the high lower limit of the cost of systems. The cheapest today AOLS BOX-10ML (50 – 250m, 10Mbps) has a cost of $ 1200. UNITED STATES. If we talk about analogues that are produced in the "far" abroad, then there the prices are an order of magnitude higher. (Flight Path 20/200, up to

200m, up to 20 Mbps, $24,000). This is explained by the fact that at the moment the majority of AOLZ is positioned precisely as main means of.

Another deterrent is a certain distrust of AOLZ, which is explained by the novelty of technology and dependence on weather conditions. To overcome it, it is necessary to use various methods to improve the reliability of AOLZ, in particular, to use algorithms for data transmission interference, cryptographic protection, etc..

The general conclusion is as follows – today there is a question of developing a reliable and functional, but at the same time cheap AOLZ.

20.3. Overview of existing solutions

The construction of all infrared transmission systems is almost the same: they consist of an interface module, an emiator modulator, optical transmitter and receiver systems, a receiver demodulator and a receiver interface unit. Depending on the type of optical emitters that use distinguish laser and semiconductor infrared diod systems with different speeds and ranges of transmission. The first provide a transmission range of up to 15 km at speeds up to 155 Mbps (commercial systems) or up to 10 Gbps (research systems). It should be noted that with the increase in the requirements for the quality of the communication channel, the communication range decreases. The second type of systems provide significantly lower transmission range, although the range technology and communication speed are increasing.

The main advantage of semiconductor diodes is the time of development for failure. In addition, such channels are less sensitive to resonant absorption in the atmosphere. The shape of the beam intersection from semiconductor LEDs is almost round.

The disadvantages of LEDs and, accordingly, the advantages of laser ones, are concluded in the fact that due to the wide radiation strip there are theoretical difficulties in transmitping a high-speed signal. The transmitter must transmit as narrowly as possible a band signal with the least amount of mods. Laser diodas just have such properties, but the chim narrower signal strip, the more likely it is that the signal will enter the atmosphere in a resonant gas absorption band and the signal quality will decrease.

The shape of the beam intersection from laser diodes is elliptical. To combat this disadvantage, various methods are used: from the use of prismatic lenses to limiting the aperture of the optical system in case of loss of part of the power.

There is also an intermediate group of devices in which VCSEL laser diots (Vertical Cavity Surface Emitting Laser - laser with vertical emitted through the cavity in the surface) are used for transmitters. These devices have a narrow radiation band and a large time of development on failure, as well as a round shape of the beam intersection. However, at this level of development of the technology, their radiation power does not exceed 7 mW per diode in multimode mode, so several emitters working at the same time are used to increase the output power, which makes it difficult to synchronize between them.

It is also possible to create a backup radio channel. In this case, the transmission range increases significantly, since. there are no weather conditions that prevent the

operation of both channels at the same time, thus it is possible to use AOLZ and radio devices almost at the limit range, without creating a power reserve in case of poor weather conditions.

Today, there are a large number of foreign solutions on the market. Their disadvantages include high cost, which makes it impossible to use them to build inexpensive (and usually short) channels, in which there is a need to create district and campus networks, to connect LVM segments with a "difficult" (road, river, iron road) section between them. In other words, it should be noted that at the moment no systems are produced in the niche of inexpensive (up to 500 US dollars) ALYZ.

Another disadvantage of existing OALZs is the absence of any algorithmic systems for increasing interference in most AOLS. That is. AOLZ is a continuation of the wire channel. Although the advantage of this solution is that it provides complete transparency for network protocols of even the lowest channel level, which makes it easy to embed AOLZ in the structure of any network with serial transmission of data over the communication channel.

In conclusion, we can note the following promising areas of development of AOLZ:

- development of cheap AOLZ;
- development of algorithms for increasing interference with the preservation of transparency of the AOLZ channel for network channel protocols. Their effective implementation, taking into account the minimization of the cost of finished AOLZ.

20.4. FSO-systems presented on the market 20.4.1. FSO systems of PAV DATA SYSTEMS (UK). SkyCell and SkyNet series systems

SkyCell series

Systems of SkyCell series are designed to work in the networks of wired operators to solve the problem of the "last soap" when connecting subscribers, as well as in hundreds of communication networks to connect base stations to the controllers. Supported protocols are G.703/E1, G.703/E2, and G.703/E3. The name of the system contains an indication of the nature of the transmission flow and the optimal (maximum) communication range. For example, SkyCell E1-2000. E1 stream, range – 2km. Or SkyCell 4E1-4000. 4 streams E1, range 4km. Table 20.2 shows some characteristics of SkyCell systems.

SkyCell Systems Nomenclature

For example - SkyCell E1-2000. SkyCell E1-2000 system is designed to organize a water-free connection of the "point-to-point" type in conditions of direct visibility at distances up to 2 km using the G.703/E1 protocol.
SkyCell E1-4000. So it is for distances up to 4 km.
SkyCell 4E1-2000. So it is for distances up to 2 km and four streams G.703/E1.
SkyCell 4E1-4000. So it is for distances up to 4 km and four streams G.703/E1.
SkyCell E2-2000. So it is for distances up to 2 km and protocol G.703/E2.
SkyCell E2-4000. So it is for distances up to 4 km and protocol G.703/E2.
SkyCell E3-2000. So it is for distances up to 2 km and protocol G.703/E3.

SkyCell E3-4000. So it is for distances up to 4 km and protocol G.703/E3.

Table 20.2

Some characteristics of systems such as SkyCell

Characteristic	Тип FSO- System			
	SkyCell E1-2000	SkyCell 4E1-4000	SkyCell E3-2000	SkyCell E3-4000
Maximum length of communication distance, km	2	4	2	4
Transmitter	Laser	3 Lasers	Laser	3 Lasers
Output power, mW	100	300	100	300
Wavelength, nm	900...920	900...920	900...920	900...920
Beam divergence, mrrad	11	11	11	11
Receiver	Photodiod	Avalanche photodiode	Avalanche photodiode	Avalanche photodiode
Input power, dBm	-45...-10	-60...-20	-60...-20	-60...-20
Wavelength, nm	750...950	750...950	750...950	750...950
Acceptance zone, mm	150 x 150	150 x 150	150 x 150	150 x 150
Системний інтерфейс	G.703/E1	4 потоки G.703/E1	G.703/E3	G.703/E3
Transfer rate, Mbps	2,048	4 x 2,048	34,368	34,368
Interface	75 Ом Coax. / 120 Ом TP	75 Ом Coax. / 120 Ом TP, FO mm 1300 нм main link	75 Ом Coax., FO mm 1300 нм main link	75 Ом Coax., FO mm 1300 нм main link
Jacks	BNC / RJ-45	BNC / RJ-45/FO dual SC	BNC /FO dual SC	BNC /FO dual SC

SyNet series systems SkyNet series systems with Ethernet and Fast Ethernet interfaces are used in corporate data networks, as well as in the networks of telecom operators to provide Internet access services. SkyNet ATM series systems are used as main and backup channels in ATM networks of operators. Supported protocols: Ethernet, Fast Ethernet and ATM.

New equipment of PAV Data Systems

A novelty in the line of equipment of PAV Data Systems – PAVExpress 100 system is a new system of waterless optical communication. The equipment is designed to combine LVM Fast Ethernet in the conditions of dense construction of modern metropolises. The active networking equipment (switches, routers, servers, or network computers) is connected directly to the receiving units using standard UTP/STP category 5 cables and RJ45 connectors. Data transfer rate is 100 Mbps, maximum working distance is up to 200 m.

In the PAVExpress 100 system, a semiconductor infrared laser diode is used as a radiator, the receiver is a pin-photodiod.

According to the design implementation, the new PAVExpress equipment differs from the rest of the company's systems, therefore, for its installation, specialized mounting brackets and configuration kits are used, which are used in the initial installation of the optical communication channel and regulatory works. The PAVExpress setup kit includes an arrow meter of the signal strength in the optical receiver. In the presence of a special adapter for setting up the channel, the configuration kit used for SkyCell, SkyNet and PAVLight systems can also be used.

20.4.2. EQUIPMENT COMPANY FSONA COMMUNICATIONS (USA)

fSONA Communications was formed in 1997. for the development of information transmission systems through the optical atmospheric channel. In 1999. the development and sale of the SONAbeam 155 family was completed. S – for short distances, up to 2400 meters, M – for medium distances, from 200 to 3600 meters.

Characteristics of systems are given in Table 20.3.

20.4.3. Equipment of NFK "Katharsis" (St. Petersburg, Russia)

In early 2004 NPP "Katharsis" replaced the entire line of equipment, released into mass production new models of systems of waterless optical communication.

Their main difference from similar equipment is the use of new patented technologies: Hybrid Emission and Super Avalanche. The combination of both technologies in BOX systems made it possible to increase the energy of the channel and, as a result, the maximum range. Recommended working distances remained preliminary, which increased the stability of the channel.

Table 20.3

Model	155-S	155-M	622-S	622-M
Distance	50-2400m	200-3600 m	75-2250 m	200-3400 m
Bit rate	155 Mbps (OC-3, STM-1), 125 Mbps (Fast-E, FDDI)		622 Mbps (OC-12, STM-4)	
Wavelength	1550nm			
Emiator type	N/N Laser Diode			
Peak power emitted	320 mW	640 mW	320 mW	320 mW
Receiver aperture	100 mm	200 mm	100 mm	200 mm
Dynamic Range	58 dB	61 dB	57 dB	60 dB
Interface Type	singlemode or multimode SC 1310 nm		singlemode SC 1310 nm	
Control	SNMP, Telnet			
Execution	waterproof			
Operating temperature	-40...+60 deg. C			
Electric power supply	85-260V, 50/60Hz	110/220V, 50/60Hz, - 48 V	85-260V, 50/60 Hz	-48 V
Power consumption	not more than 255 W			
Dimensions	430 mm x 400 mm x 310 mm		410 mm x 410 mm x 430 mm	
Вага	10 Kg	20 Kg	10 Kg	20 Kg

The equipment manufactured by NPP Catharsis is designed to transmit data without the use of copper, fiber or radio, based on FSO technology. BOX systems (Wireless Optical Communication Channels) operate at distances up to 1.5 km in all weather conditions. At the same time, the recommended communication distances ensure the availability of the >99.7% channel in models intended for corporate network solutions and >99.9% in models for telecom operators.

Box-type nomenclature

SYSTEMS BOX-10-xxx. BOX-10xx series systems are designed to work in corporate data networks to unite local computer networks and to solve the problem of the "last soap" when connecting subscribers to the Internet. Can be used as main and backup channels. Ethernet protocol (10Mb/sec) 10Base-T.

SYSTEMS BOX-100M-xxx. Fast Ethernet protocol (100Mb/sec) 100Base-TX.

BOX-E1-xxx systems. BOX-E1-xxx series systems are designed to work in the networks of wired operators for supplying number capacity or connecting two PBXs. Can be used as main and backup channels. Protocol: G.703/E1.

Системи БОКС-E2-xxx. Протокол: G.703/E2. В основному використовується з мультиплексором 4xE1 – 1xE2.

SYSTEMS BOX-E1-OSH. BOX-E1-OSH series systems are designed specifically for use in networks of honeycombs and fixed-line operators. Designed to connect base stations or base stations with processing centers, for main connections. At the distances recommended by the manufacturer provides availability of 99.9% in all weather conditions. Protocol: G.703/E1.

SYSTEMS BOX-E2-OSH. Same purpose. Mainly used with multiplexer 4xE1 – E2.

20.4.4. ATMOSPHERIC OPTICAL COMMUNICATION LINES ARTOLINK. OJSC "MOSTKOM". MANUFACTURER: STATE RYAZAN INSTRUMENT PLANT

The systems of this manufacturer today best meet the criterion of price and quality. That is why we consider this type of equipment more carefully. At the same time, many different know-how and known optimal technical solutions were used in the developed AOLZ. For example, in the latest versions of the most hardware software, automatic radiation power regulation was introduced, which made it possible to get rid of the lack of previous models of equipment, when at short distances (50-200 m) due to sufficient power of laser radiation to eliminate the effect of saturation of the photodeletion was to aperture the lenses of receivers.

Before installing the equipment using the user's software, the approximate value of the length of the communication line is recorded in each receiving terminal. This is necessary so that when the equipment is turned on, the initial radiation power does not exceed the saturation threshold of the receiver of another module at this distance. After installing the equipment, the line is tuned in setup mode, after which, after synchronization of the optical channel, the equipment is transferred to operation mode. Due to the use of the built-in service channel, each terminal receives information about the level of radiation that enters another terminal and subdues the level of its own radiation to a predefined level of reception. The introduction of this automatic function made it possible to expand the dynamic range and improve the reliability of AOLZ operation in poor visibility conditions.

Fig. 20.3

As usual, when installing MOST systems, a spatial stabilization system is used, and the process of installing the system does not cause any particular problems. However, equipment manufacturers recommend signal cables, especially with a large length (more than 30 m), to shield from external electromagnetic interference. This can be done, for example, with the help of grounded armored vehicles. As practice has shown, without this operation, the main errors in the channel are due to the cables of a decrease in electromagnetic fields of atmospheric and technotrone origin. There have been cases when the equipment of both mosta and the user burned out as a result of lightning strikes. To reduce the tip (but not to protect against lightning), it is also recommended to install ferrite filters on the SC.

20.4.4.1. Some general information

There is a Certificate of Conformity NoOS/1-SP-950 according to the certification system "Communication" of the Ministry of the Russian Federation on communication and informatization. There is also a Hygienic conclusion about laser safety.

Atmospheric optical communication line Artolink is designed for wireless transmission of digital data between two points with active equipment. AOLZ is an FSO technology equipment that provides cost-effective solutions for many applications, compared to wired, fiber-optic and radiolines. The equipment can be used at distances from 0.1 to 4 kilometers or more, depending on the installation region and the requirements for the availability of the channel. It is allowed to use the system to organize a linear tract with one or more areas of regeneration.

Production is carried out on the basis of approved tues with the provision of a full range of measures to maintain high quality products and fulfill warranty obligations. Installation and operation of AOLZ does not require coordination with the GCR of the Russian Federation.

The company OJSC "MOSTKOM" (Ryazan, telephone/fax8-4912-98-66-63) is engaged in the development, support, technical support and delivery of the product. Consultations are carried out by e-mail: office@moctkom.ru. Site of OJSC "MOSTKOM": www.moctkom.ru

20.4.4.2. Application areas

Since AOLZ is an alternative solution in relation to fiber-optic and radio relay communication lines, AOLZ is successfully used in areas of use such as:

- city multiservice high-speed networks (MAN);
- distributed campus and corporate networks (LAN);
- solving the problem of the "last soap";
- connection of base stations of hundred communication (2G, 2.5G and 3G);
- prompt redundation of communication lines.

Options for the use of AOLZ Options for the use of AOLZ are shown in Figures 20.4 – 20.7.

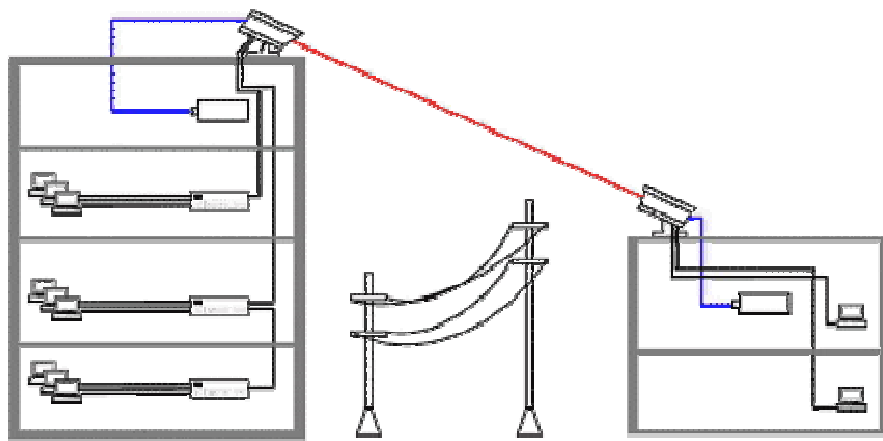| Умовні позначення	
	Receiving and transmitter module
	External interface device
	Switch
	Telephone station
	Laser communication
	Twisted pair
	Internal interface cables

Fig. 20.4. Association of LVM Fast Ethernet, separated by obstacles such as LEP motorways, railways, etc.).
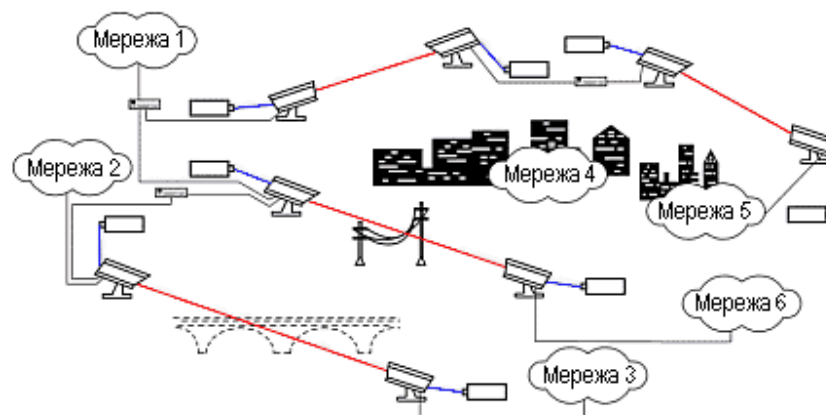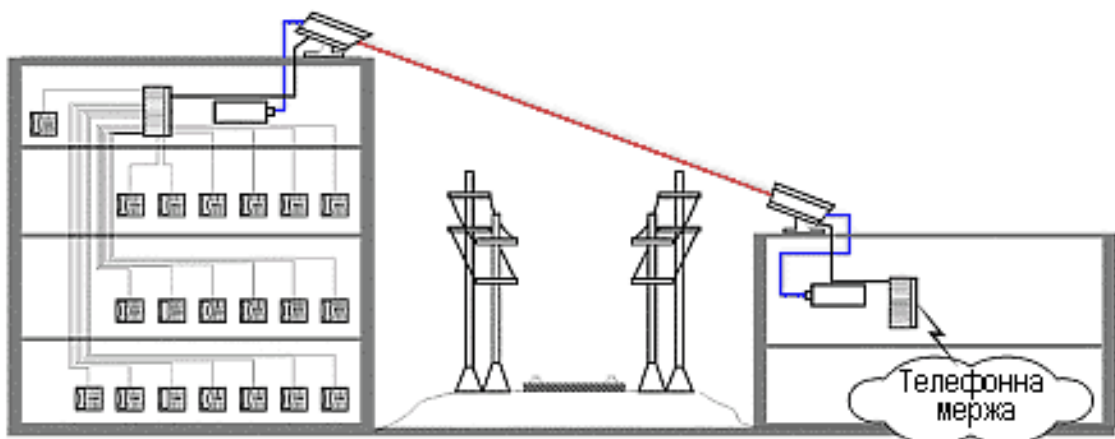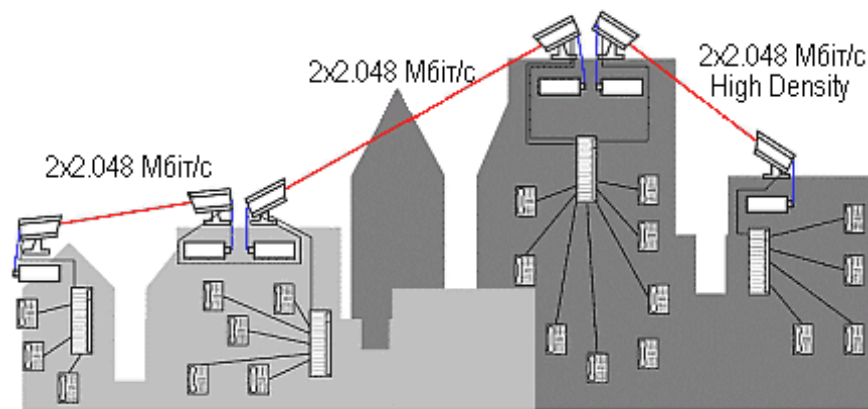

Fig. 20.5. Provision of main connections in distributed computer networks (100 Mbps).

Переклад Fig. 20.6. Telephonization of a detached living building or office without laying a cable through the exclusion zone of the railway with a stream of 2,048 Mbps High density.

Переклад Fig. 20.7. Creating a telephone network using AOLZ as a repeater and multiplexer.
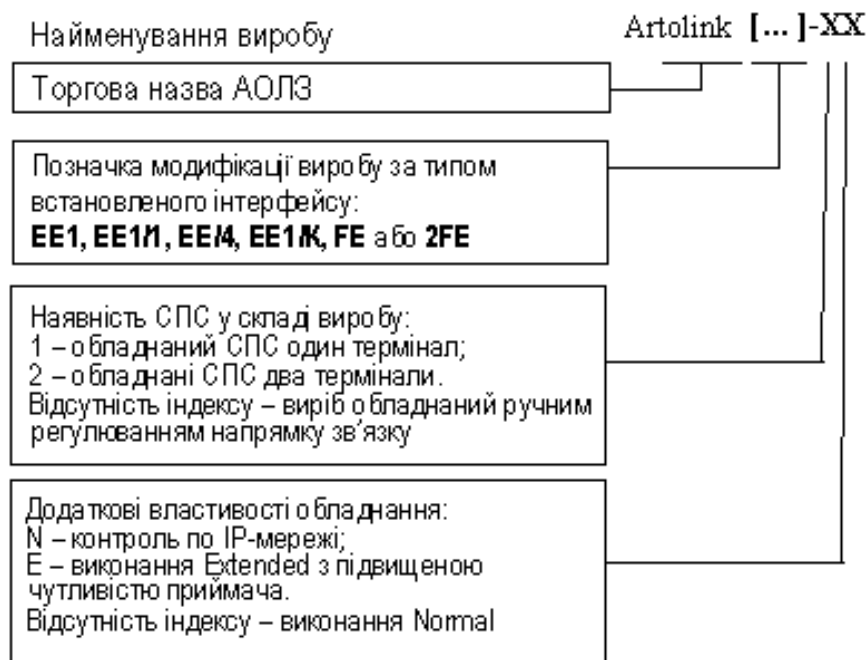
20.4.4.3. HOW THE DEVICE WORKS

All products of the series consist of two identical terminals. Each terminal contains a receiving and transmitting module (PMM), which provides the transmission and reception of optical signals in the atmospheric channel and an external interface device (UZI), which serves to provide power to the PPM and dock with external control equipment.

These units are connected to each other by an internal interface cable (KVI). The information signal is fed directly to the PFM through the connecting signal cable (WSC) (standard pair output). SSC is not included in the delivery kit and is supplied by a separate order, or manufactured and laid by the user from the PPM to the appropriate equipment in accordance with the number of digital streams. Length of cable connections – up to 150 m.

The power supply of the product is carried out from ac power 220V 50 Hz or a DC source 48V +/-20%.

The delivery kit includes a remote control program that allows you to control the parameters of the PMM operation on a personal computer connected to UZI via a communication cable with a computer (KSK). The product is programmed for a limited time (about 50 hours), sufficient for its installation and configuration. After setting up the product, it is necessary to load your license file (provided by the supplier) in each PMP, which allows it to work within the time specified by the delivery contract (including indefinite). Downloading the license file is carried out from a personal computer using remote control programs.

The type of installed interface determines the modification of the product, and specific executions depend on the presence in its composition of the spatial stabilization system, the type of photo receiver, the device of remote monitoring over the IP network. The system of marks of the product is as follows (Fig. 20.8)

Найменування виробу

Artolink [...]-XX

Торгова назва АОЛЗ

Позначка модифікації виробу за типом встановленого інтерфейсу: **EE1, EE1/1, EE/4, EE1/K, FE** або **2FE**

Наявність СПС у складі виробу: 1 – обладнаний СПС один термінал; 2 – обладнані СПС два термінали. Відсутність індексу – виріб обладнаний ручним регулюванням напрямку зв'язку

Додаткові властивості обладнання: N – контроль по IP-мережі; E – виконання Extended з підвищеною чутливістю приймача. Відсутність індексу – виконання Normal

Перекласти Fig. 20.8.

The principle of operation of the product is based on the transmission of a digital signal through the atmosphere by modulation of infrared radiation and then its thyroid by optical photo-reception device (FSO-technology).

Figure 20.9 shows the connection scheme of the product, which allows you to organize the transmission of four channels E1 between two PBXs.

When transmitping digital signals from communication equipment in the HDB3 code via SSC, they enter the linear digital joints of the PPM (ports 1-4 of Fig. 5.9) and through the RS4 connectors enter the device of the line interface. Here they are regenerated, if necessary, multiplexed and converted into a consistent self-synchronizing transport code. The digital flow prepared in this way is directed to sinphasnos-configured laser transmitters.

As a source of radiation serves as a semiconductor laser diode, which converts "current-light". The radiation of the laser diud is formed by collimental optics in a bundle of small discrepancies and rushed to another terminal.

The presence of two transmitters, increasing the reliability of the product, increases the output power and reduces the influence of interference instability of the wave front of the coherent laser radiation due to heterogeneities in the atmosphere, which increases the reliability and range of communication.
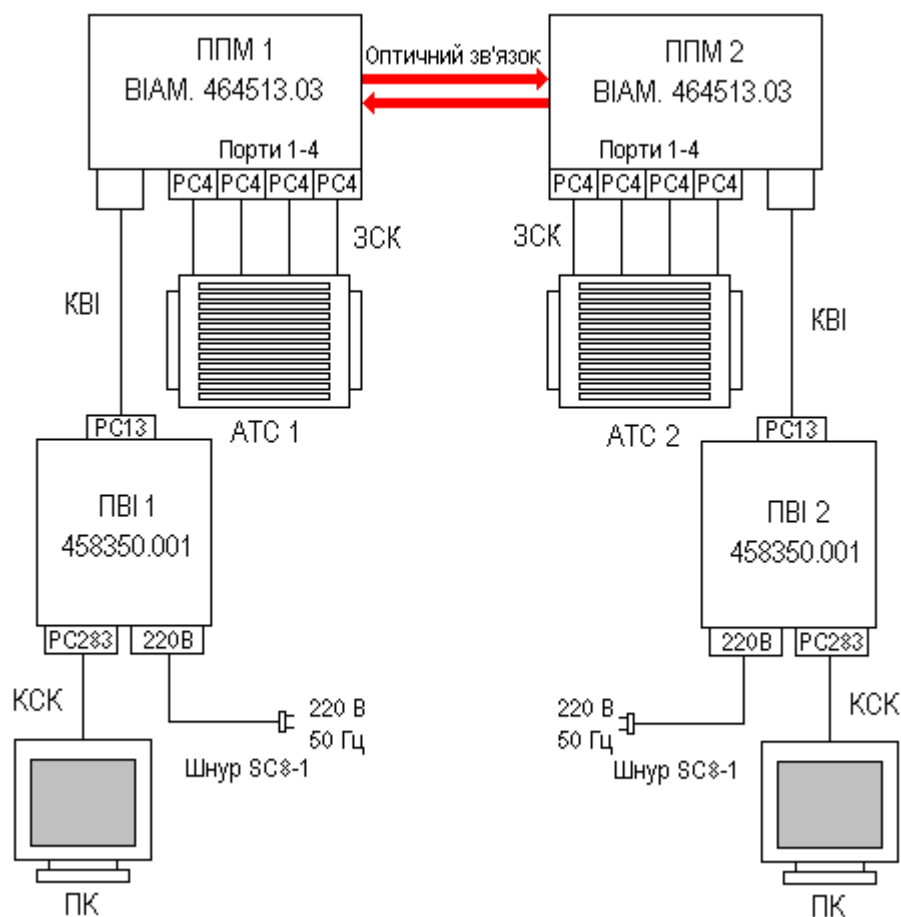
Переклад Fig. 20.9

The approximate shape of the beams (directional diagram) of the PPM laser radiation is shown in Figure 20.10.
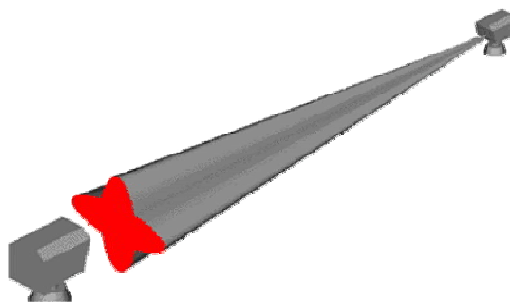

Fig. 20.10. Diagram of direction of beams of laser radiation

When receiving laser radiation from another terminal, it is collected by three lenses and with the help of unifying optics focuses on the photo-sensitive platform of a high-speed PIN diode. Part of the radiation before the photodiode is directed to the coordinate sensor, which determines the deviation of the axis of the receiving system from the direction to another terminal. With the ideal axis of laser beams in the direction should coincide with the line connecting both terminals.

The ampled and filtered electrical signal in the photo-reception device is directed to the device of the line interface. Here is the signal transcoding and the formation

of linear code HDB3 in accordance with the requirements of G.703 to linear digital signals communication equipment.

20.4.4.4. SIGNAL TRANSMISSION QUALITY AND RELIABILITY

It is believed that the quality of the water-free connection provided by AOLZ is determined mainly by one parameter – the size of the reserve, which overlaps the attenuation, is applied by natural aerosols (fog, snow, rain) at a given distance, usually 1 km. However, the harmful effects of hydrometeorologicals and other environmental factors of operation are not exhausted by the phenomenon of weakening of the optical signal in the atmospheric channel. The accumulated research of equipment operation in various climatic zones showed that the cumulative impact of these factors without taking special measures suggests a much greater (compared to the attenuation of the signal), the impact on the reliability of the FSO system. The developer and manufacturer of AOLZ believe that the true quality of products is achieved only if special measures are taken to eliminate the negative effects of these factors, increasing the time of inaccessibility of the channel, sometimes tenfold.

The punculation and trembling of the bunches in the atmospheric channel make errors in the transmitted signal, which greatly exaggerate the er ber 10-9, which is especially manifested at long distances and in clear weather. In AOLZ, this phenomenon is compensated by the use of a multi-aperture optical system containing three transmitting and two receiving channels, as well as unique interfaces that provide special transport coding of optical signals..

Solar and other parasitic lighting leads to overloading of the photo receiver and interruption of communication. In AOLZ, their influence is minimized (the probability of interruption of communication is less than 0.01%) due to powerful optical selection using two spectral, two spatial and one polarization filter in the receiving channel, as well as a small angular field of view of the optical receiver.

Guiding errors caused by the instability of the supports on which the equipment is installed, under the influence of temperature gradients, wind load and other factors, lead to additional, even up to 100%, power losses due to angular displacements of the transmitter bunches. In Artolink products, this effect is completely absent, since they include a system of stabilization of the direction of communication (autotracking). It contains a highly sensitive sensor of angular deviations of the optical axis with the original integrated-variation algorithm of goal selection and a high-precision positioning system.

Position errors caused by the coordination of optical axes of the receiver and transmitter under the influence of temperature changes and solar radiation, make an additional, up to 10 dB, weakening in the optical channel. This effect is especially acute when using equipment with a spread-out receiver and transmitter. In AOLZ, these phenomena are practically excluded (less than 1 dB) due to the implementation of the receiving and transmitter module in the form of a thick-left cast monoblock of the original design, which ensures the alignment of temperature gradients and the thermal solution of internal optical elements. Additionally, the monoblock is surrounded by a protective casing that protects it from wind and radiation load.

Icing and contamination of the external optical elements of the receiver and transmitter, which are caused by sudden changes in temperature and humidity, as well as the operation of equipment in the conditions of sedimentation and dusty atmosphere, lead to communication disruption. In AOLZ, guaranteed measures were taken to exclude such a case by using a system of original screens, which, due to aerodynamic effects, ensure the purity of optics. In particularly difficult operating conditions, an additional thermal protection system of optical joint is used, which has in comparison with traditional solutions 2-5 times less power consumed at the same efficiency.
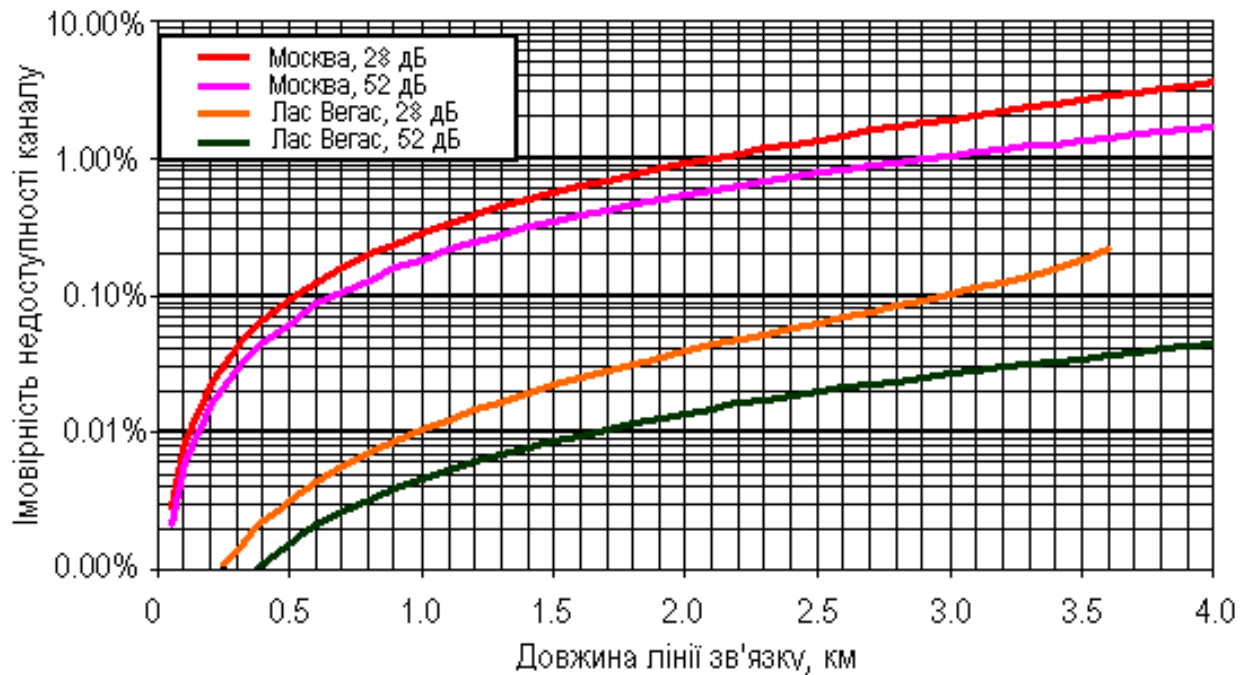
Переклад Fig. 20.11

Interference with inverse scattering, which is caused by inverse reflection of light from sedimentation, especially when the line is operating during snowfall, leads to a decrease in the real sensitivity of the receiver by 20 or more dB. In AOLZ due to narrow angular diagrams of the direction of the transmitter radiation and the field of view of the receiver, as well as the use of the original scheme of selection of signal photons on the principle of "own alien", which ensures the constant sensitivity of the receiver under all operating conditions.

The whole set of implemented technical solutions guarantees the receipt of *a real operational reserve* for the reinsurance of AOLZ from 28 to 52 dB with a communication line length of 1 kilometer. Its specific value depends on the speed of information transmission and the configuration of the product. In this case, the main operational parameter of the product is the availability time of the channel for the quality of signal transmission from BER not worse than 10^{-9} is really determined only by the geography of its installation and the length of the communication line.

Figure 21.11 shows that in the case of nomination to the line of requirements of a high degree of availability of the channel in regions with bad "optical weather", it is necessary to reduce the length of the optical connection. At the same time, the

value of the energy reserve is not of fundamental importance. A more important factor is meteorological conditions at the point of installation of equipment. In the southern regions, AOLZ can ensure the reliability of communication at the level of 99.9% and better with a connection length of several kilometers.

20.4.4.5. Basic models and some specifications

The ability to connect the optical channel to the user's equipment is determined by a set of available digital joints. Different models of AOLZ on the line support electrical connections with both plesiohronous digital hierarchy networks and Ethernet – packet data networks. The types of serially manufactured interfaces and equipment are shown in Table 20.4.

Other types of interfaces can be manufactured and delivered by order, including fiber-optic connection.

20.4.4.6. Differences and features of equipment

1. AOLZ is serially manufactured at the State Ryazan Instrument Plant, one of the largest and more successful enterprises certified according to ISO 9001. Production is carried out on the basis of approved TU with the provision of a full range of measures to maintain high quality products and fulfill warranty obligations.

2. AOLZ is one of the world's few serial models of FSO equipment, which has a system of spatial stabilization of the communication line (SVP) with a highly sensitive axis deviation sensor. The combination of this system, a unique multi-aperture optical circuit of PFM and specially designed optical interfaces for the atmospheric channel, provides a higher quality seamless connection compared to most other FSO solutions. Depending on the conditions and geography of operation, the equipment can ensure the level of availability of the communication channel up to 99.99%.

3. The equipment is focused on the simple installation and operation of it by the user. AOLZ terminals are fixed on any supports, including pipe-resistant, with the help of a universal mounting set of the original design. Built-in channel visual guidance and control tools, including communication line direction monitoring, multi-level installation of loops and test alarm systems, avoid additional costs for the services of specialized installation organizations.

Table 20.4.

Type of inter-face	Bit rate, protocol	Network joins	Features
EE1	2,048 Mbps, G.703 (E1) +10 Mb, IEEE802.3 (Ethernet)	Симетрична лінія 120 Оми10BASE-T	Simultaneous and independent transmission of E1 and Ethernet streams, a built-in service channel.
EE1/4	4 x 2,048 Mbps,G.703, (4xE1)	Симетричні лінії 120 Ом, 4 порти	Built-in multiplexer for 4 E1 streams, independent synchronization
FE	100 Mbps IEEE 802.3u (Fast Ethernet)	100BASE-TX	Fast Ethernet full-duplex transmission (analogue of VOLZ))
FE/К	N x 2,048 Mbps, G.703 (E1) + Fast Ethernet (до 50 Мбіт/с)	Симетричні лінії 120 Ом, N портів, 100BASE-TX	External multiplexer of Fast Ethernet and NH1 streams (N < 16), routing of service data.
2FE	To 2 x 100 Mbps IEEE802.3u, (Fast Ethernet)	2 x 100BASE-TX	Simultaneous and independent transmission of 2-stream Fast Ethernet
2FE/G	800 Mbps IEEE802.3z, (Gigabit Ethernet)	1000 BASE-FX	4 parallel channels, switch for 24 ports 10/100 Mbps

4. Extensive service capabilities in terms of various types of monitoring (RS232, UDP, HTTP, SNMP and SMTP alarms) allow minimizing the cost of operation of the product. The manufacturer and supplier provide technical support to users, including remote monitoring and diagnostics of equipment, as well as provide warranty and post-warranty service. The warranty period of the product is 2 years.

5. AOLZ equipment is #1 in the world in terms of price-quality-service ratio. The cost of its purchase, installation and operation is 3-5 times less than for products of other manufacturers of comparative quality. Combined with versatility, high quality and low costs, AOLZ provides a high degree of investment protection and a minimum return period.

20.4.4.7. Installing and installing hardware

The equipment is focused on simple installation and operation by the user, which avoids additional costs for the services of specialized installation organizations. AOLZ has in its composition all the necessary components for its independent installation and quick commissioning. The equipment is fixed on any supports,

including pipe-resistant, with the help of a universal mounting set of the original design.

For prompt and convenient guidance and justation of the line, each PFM includes:

- reference-rotating device;
- spatial stabilization system (SPS), or mechanism of fine adjustment;
- diopthrium storage device;
- Control indicator bar with direction indicator.

A set of these tools allows you to establish a connection within 5-10 minutes after installation of AOLZ. For testing the communication line, the possibilities of multi-level installation of loops, error control in the optical channel and service channel, implemented with the help of specialized software included in the delivery kit, are provided..

20.4.4.8. REMOTE CONTROL

Remote control of the equipment during operation is carried out either through the junction RS-232 or through the Ethernet port 10/100 Mbps over the IP network with an unlimited number of connections to the product network. In the latter case, the embedded software provides remote control of AOLZ using the following technologies:

- based on UDP packages using specialized software;
- using an Internet browser (built-in WWW server);
- sending emergency SNMP messages;
- sending emergency e-mail messages.

The choice of one or more control technologies and its (their) parameters are determined by the user.

20.4.5. EQUIPMENT OF THE COMPANY "GRANCH"

Another Russian manufacturer, Novosibirsk company Granch, in early 2003 released the Granch SBAL-2/3 laser system, which is designed to transmit at a speed of 2048 Kbit/c and is equipped with a linear G.703 interface. If necessary, the system can be equipped with additional network endings in the form of PCI adapters G.703 SBNI14-G.703 PCI (there is a wide range of drivers for different OS) or external bridges /routers G.703<=>Ethernet. The cable descent range from the optical emiator to the power point when using the modem can reach 1500 m.